Proceedings

Seminar on

RECENT DEVELOPMENT

WITHIN OFFSHORE DESIGN AND SYSTEMS

Copenhagen, February 11, 1988

DANSK VANDBYGNINGSTEKNISK SELSKAB
DANISH SOCIETY OF HYDRAULIC ENGINEERING
v/ H. F. Burcharth, AUC, Sohngårdsholmsvej 57, 9000 Aalborg. Tlf. 08 - 142333

Proceedings

Seminar on

RECENT DEVELOPMENT

WITHIN OFFSHORE DESIGN AND SYSTEMS

Copenhagen, February 11, 1988

DANSK VANDBYGNINGSTEKNISK SELSKAB

DANISH SOCIETY OF HYDRAULIC ENGINEERING

v/ H. F. Burcharth, AUC, Sohngårdsholmsvej 57, 9000 Aalborg. Tlf. 08 - 142333

INTRODUCTION

The present publication contains the contributions of invited speakers to a seminar arranged by The Danish Society of Hydraulic Engineering.

Members of Danish Society of Naval Architecture and Marine Engineering and the Hydrocarbon Committee under the Danish Society of Civil Engineers were invited to join the seminar.

The organisation is most gratefull to the speakers for their valuable contributions to the seminar.

Danish Society of Hydraulic Engineering

Helge Gravesen
Secretary

LIST OF CONTENTS

danop

DRIFT FORCES AND MOTIONS

OF

FLOATING STRUCTURES

by

STIG E. SAND

MARCH 1989

danop

1. INTRODUCTION

The attached paper for the BOSS '82 conference gives an overview of the terms involved in the mathematical description of drift forces and damping of moored, floating structures.

The first few pages here deals with an alternative simplified way of describing the physics of drift forces and motions.

To illustrate the importance of the slow drift motions Fig. 1 shows the mooring load of a 30,000 t semisub with 8 mooring chains in 180 m water depth. The significant wave height is 8.8 m and the period 12.3 s. It appears that a typical short period load (same frequency as the waves) is about 90 t whereas the max. drift force is 290 t. It is obviously important to take into account the drift force in designing mooring arrangements for floating structures.

In calculating and designing for these drift forces the question is to which key parameters this low frequency phenomenon relate and how the form of dependence is.

Fig. 1

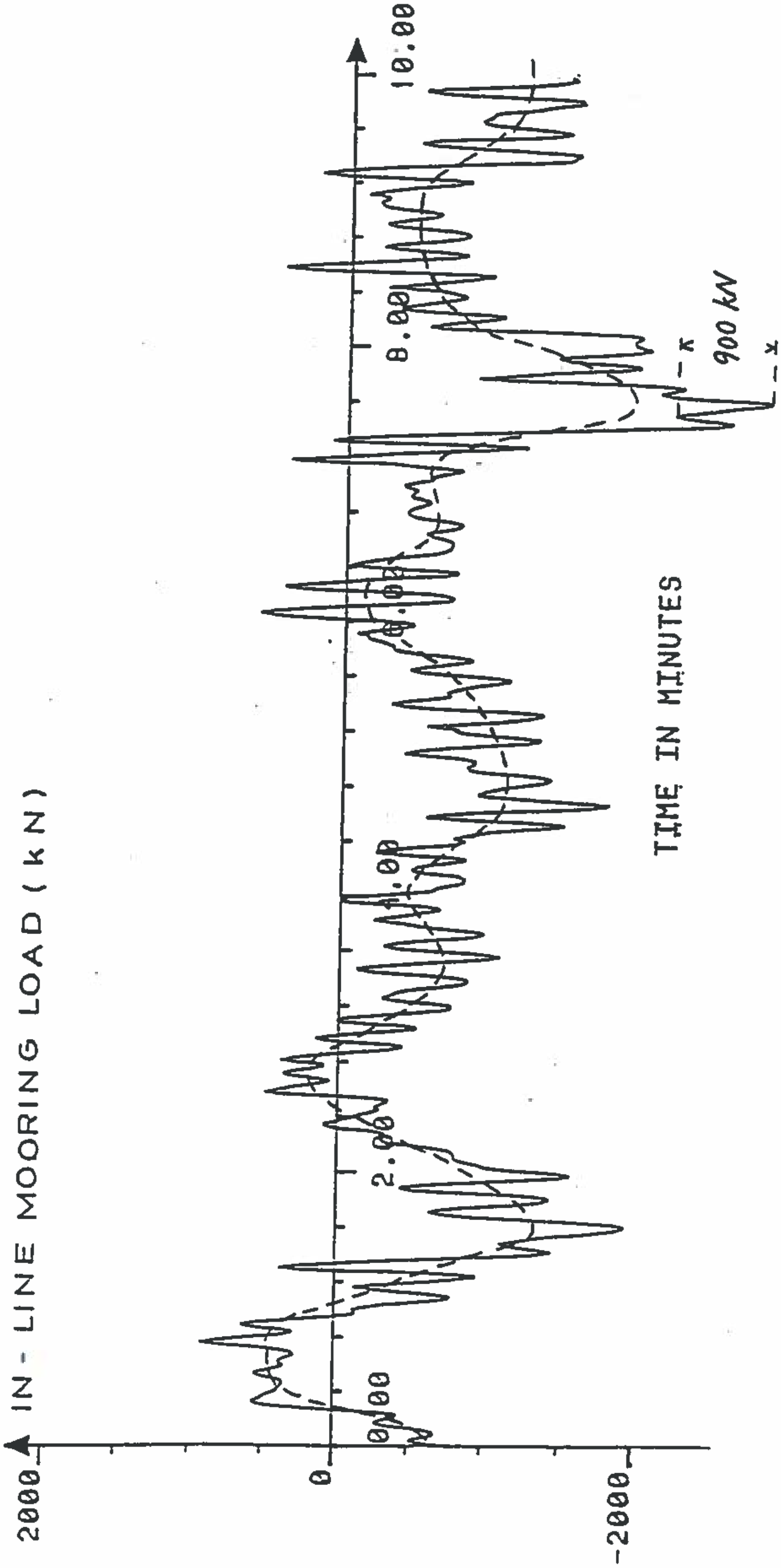
IN - LINE MOORING LOAD (k N)
TIME IN MINUTES
2000
0
-2000
0.00
2.00
4.00
6.00
8.00
10.00
900 kN

danop

2. WAVES AND DRIFT FORCES

The missing direct relation between waves and drift forces is illustrated in Fig. 2. This shows the spectra of waves and in-line mooring (chain) forces from Fig. 1. The upper one is wave energy as function of frequency and the lower one is the mooring force energy also as function of frequency. It appears that the strong reaction takes place in the region w < 0.25 rad/s, i.e. well below the wave frequencies.

To illustrate how the low frequency terms appear a simple explanation of one of the drift terms is given below. Consider a ship exposed to waves as shown in Fig. 3. In the case of linear waves (upper figure) the integral of the elevations (only up to the MWL) around the ship will equal zero over one wave period. However, to second order (lower figure) the part above MWL will give a non-vanishing contribution, i.e. drift force term number one is proportional to the integral of elevations squared. That this will also be of low frequency can be seen by taking the elevations as:

$$\eta(t) = \sum_{n=1}^{N} \cos(\omega t + \epsilon)$$

then the squared elevations will contain a low frequency part, viz.:

$$\eta^2 \sim \sum_{n} \sum_{m} a_n a_m \cos((\omega_m - \omega_n)t + \epsilon_m - \epsilon_n)$$

At least six other second order terms can be derived mathematically.

Fig. 2

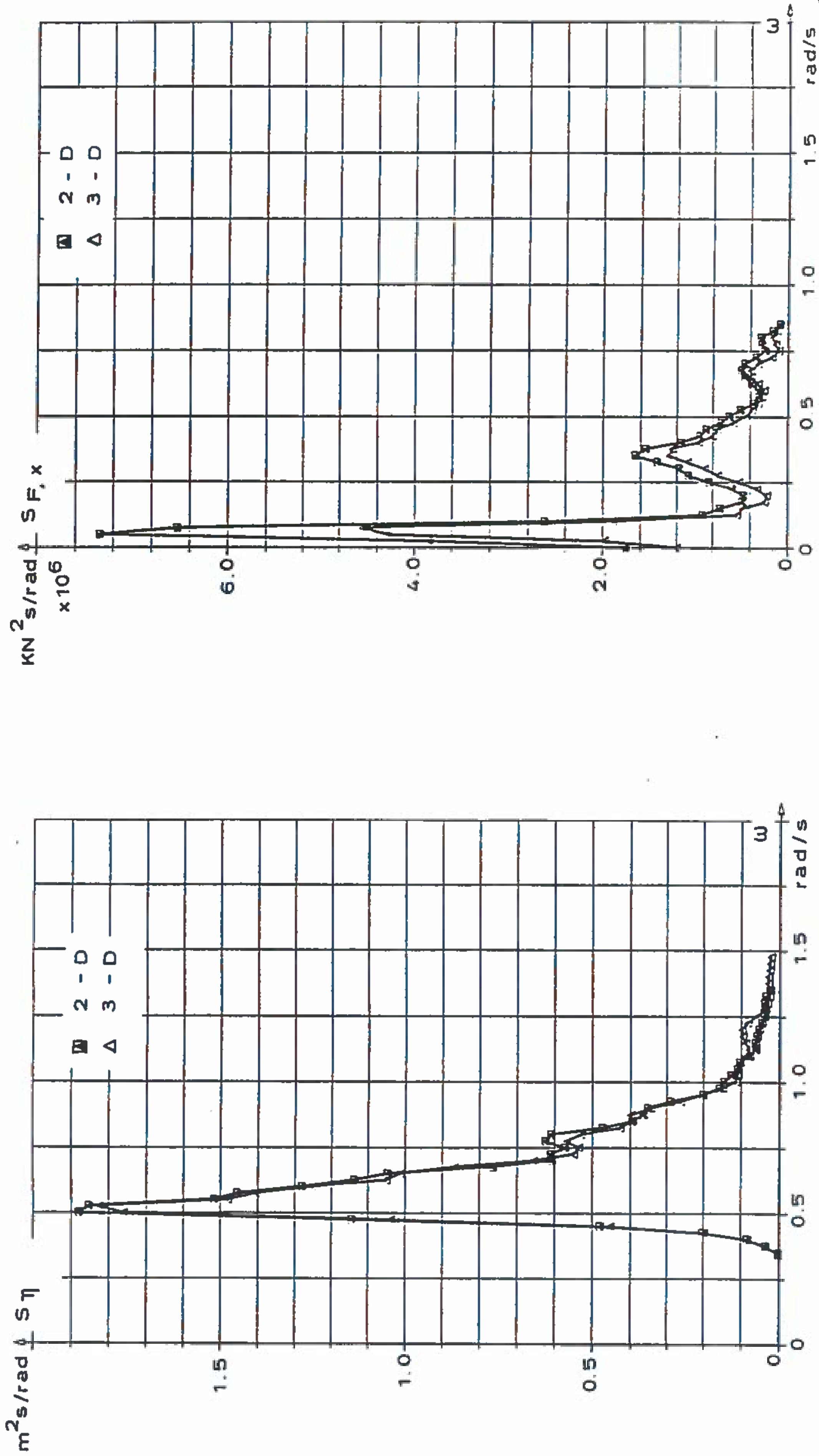
KN²s/rad
x10⁶
S F, x
6.0
4.0
2.0
0
0.5
1.0
1.5
rad/s
ω
2 - D
3 - D
m²s/rad
Sη
1.5
1.0
0.5
0
0.5
1.0
1.5
rad/s
ω
2 - D
3 - D

Fig. 3 **DRIFT FORCES**

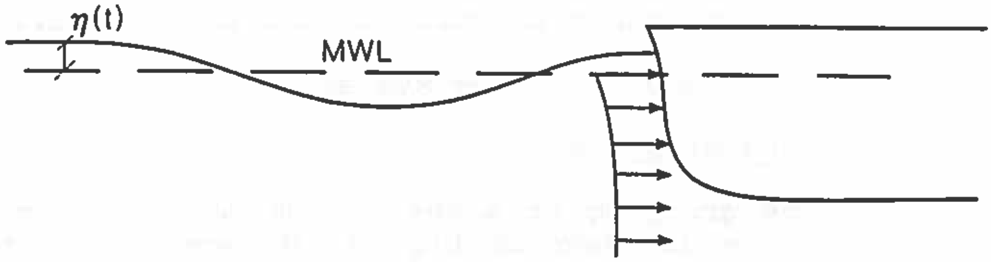

2nd order force:

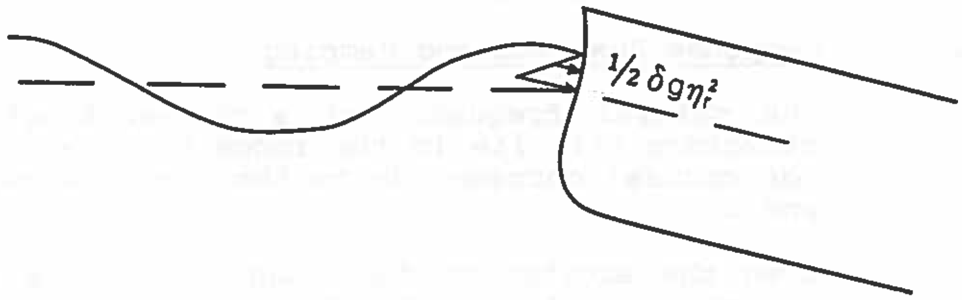

$$F_1 = -\tfrac{1}{2}\delta g \int \eta_r^2 \vec{n}\, dl$$

danop

3. KEY ELEMENTS IN DRIFT FORCES

To describe the physics of the drift force phenomenon three important elements have to be dealt with, viz.:

- wave grouping
- response function of moored structure
- damping of the system.

3.1 Wave Grouping

The grouping of waves can be described in several ways - one is seen in Fig. 4. By smoothing the elevations squared a low frequency curve following the grouping pattern appears. The spectrum of this is shown by a formula and illustrated by a curve in the low frequency end of the spectrum.

That the wave grouping is one of the three important elements in drift force description can be seen from Fig. 5 which compares measured surge and sway forces with a wave grouping curve such as that in Fig. 4.

3.2 Response Function and Damping

The natural frequency of a moored floating offshore structure will lie in the range 0.005 - 0.02 Hz, which (of course) corresponds to the response seen in Fig. 1 and 2.

When the excitation force approaches the natural frequency, f_N, of a system Fig. 6 shows how the response is amplified for various values of the damping.

The point is that dependent on actual response function and damping conditions the excitation force (waves) does not have to be large in itself to produce a serious situation for the floating system.

Fig. 4

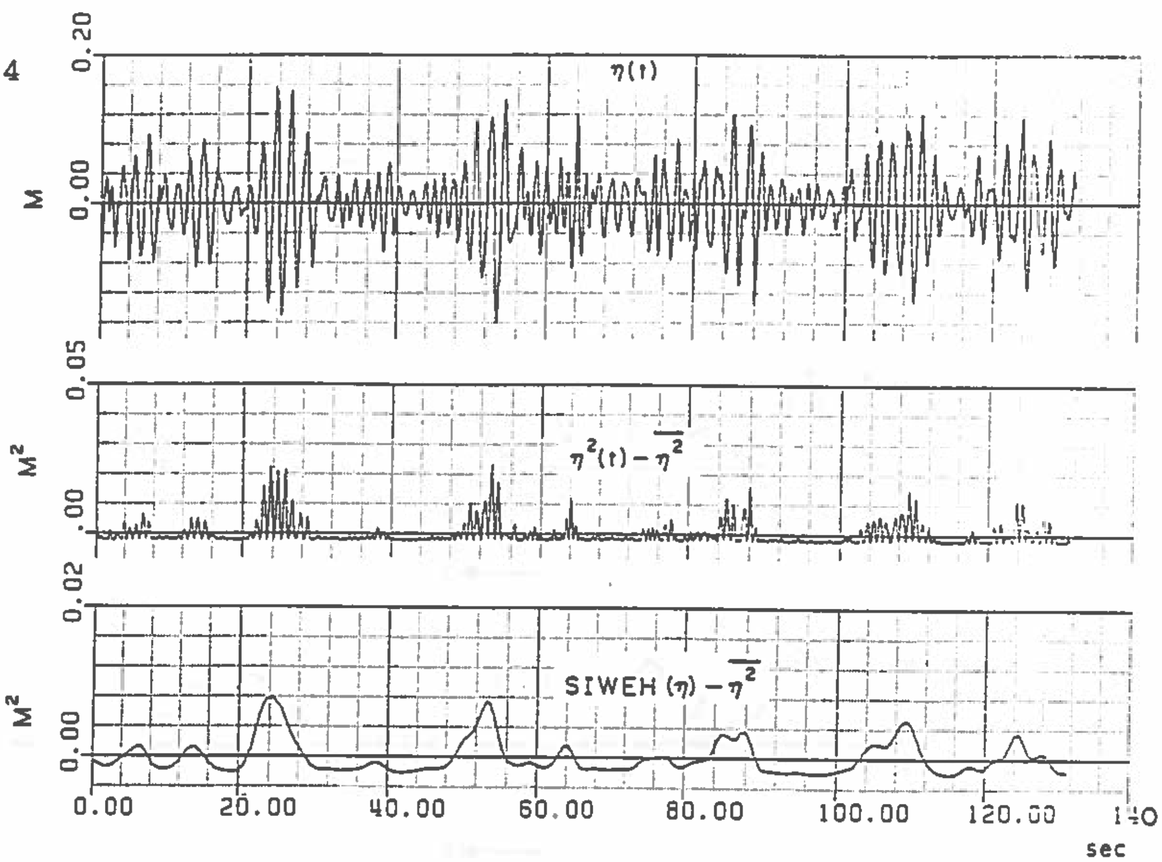

$$S\eta^2(\Delta\omega) = 2\int_0^\infty S\eta(\omega)\, S\eta(\omega+\Delta)\, d\omega$$

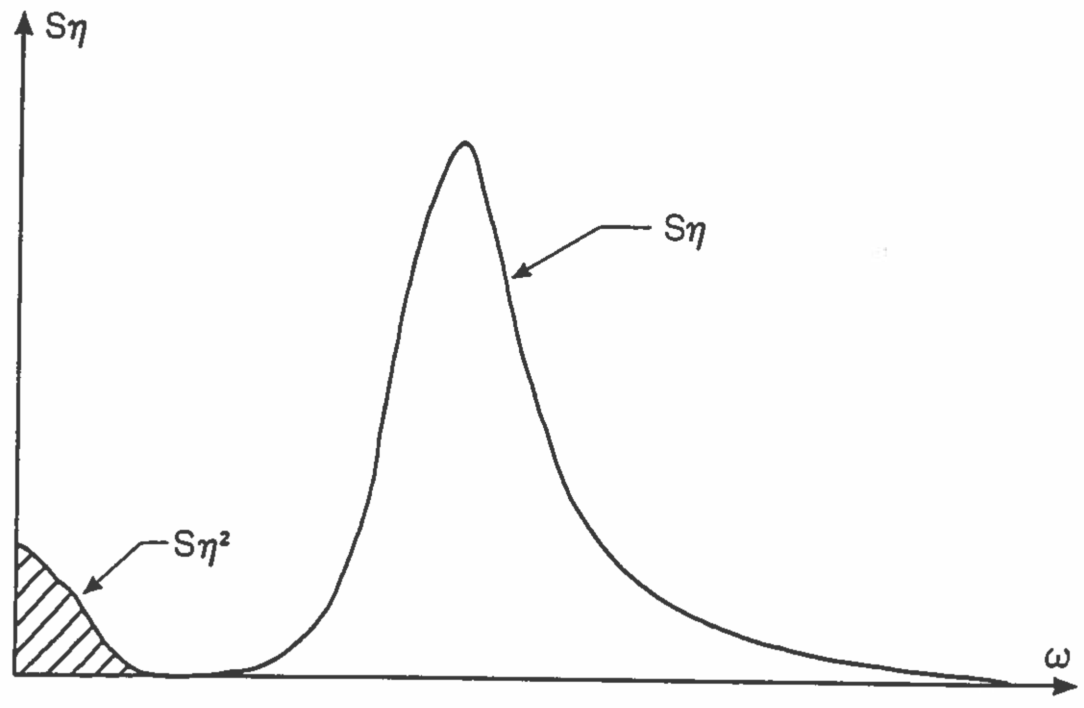

Fig. 5

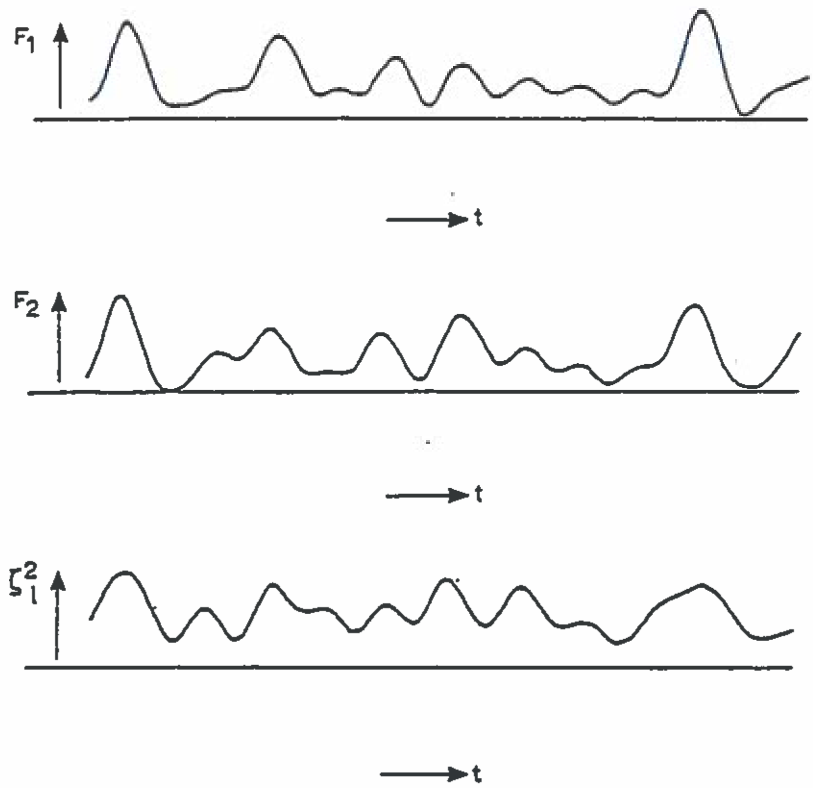

Examples of measured low frequency surge and sway drifting forces on a tanker and low frequency part of wave height squared

Fig. 6

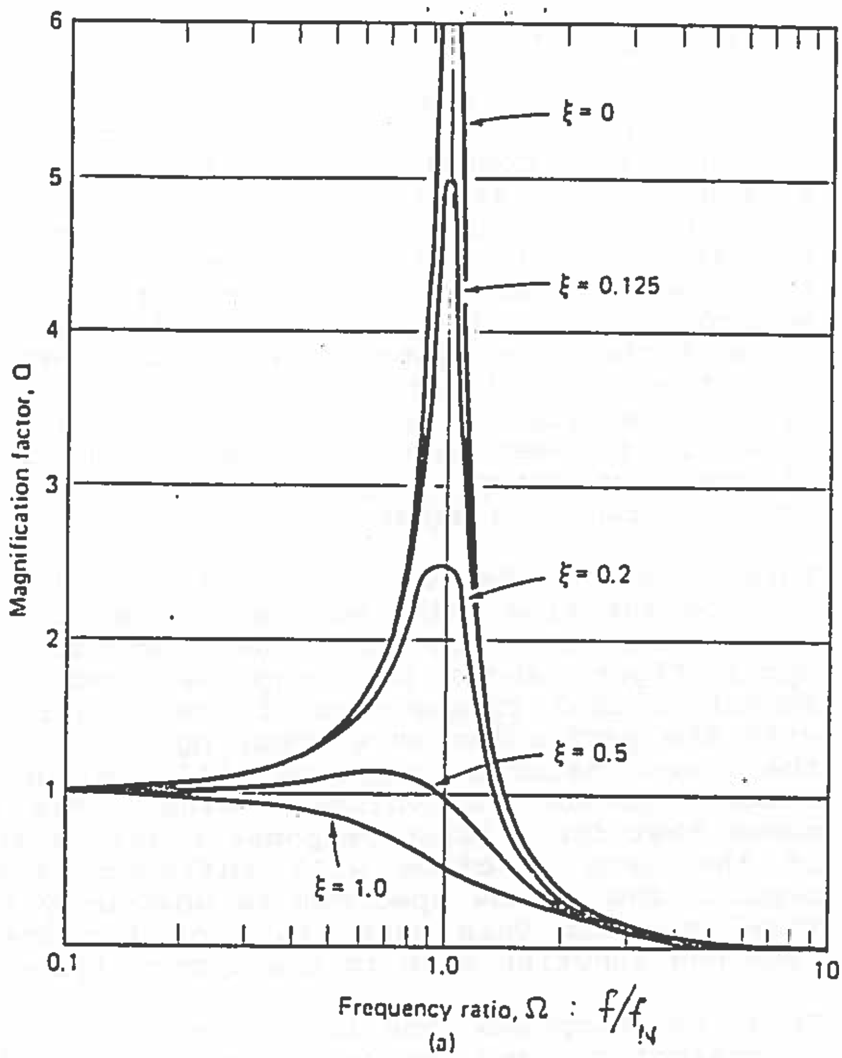

Magnification factor, Q
6
5
4
3
2
1
ξ = 0
ξ = 0.125
ξ = 0.2
ξ = 0.5
ξ = 1.0
0.1
1.0
10
Frequency ratio, Ω : f/f_N

(a)

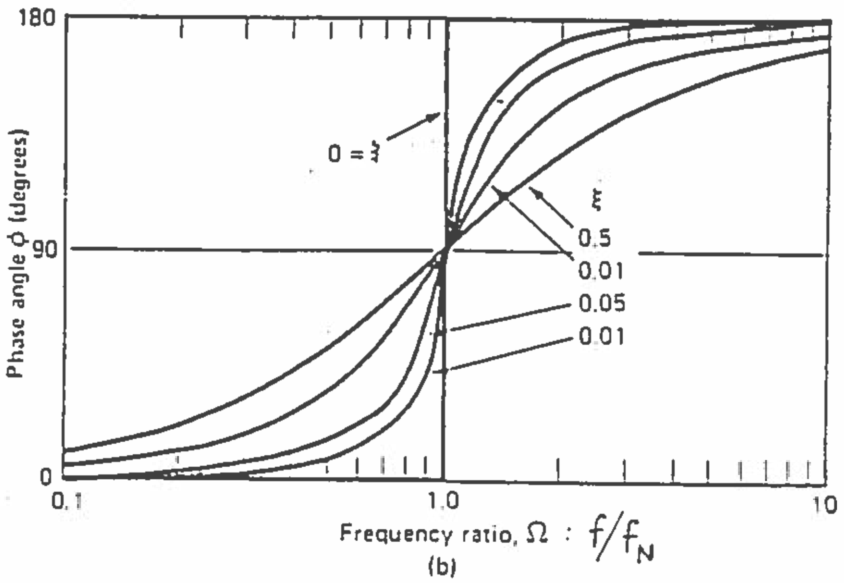

Phase angle ϕ (degrees)
180
90
0
ξ = 0
ξ
0.5
0.01
0.05
0.01
0.1
1.0
10
Frequency ratio, Ω : f/f_N

(b)

danop

4. SIMPLIFIED DRIFT MOTION DESCRIPTION

To show how wave grouping and response function (incl. damping) interact in principle to produce a slow drift motion Fig. 7 comprises basic ship characteristics and a simplified drift response function H. In Fig. 8 it is shown that the surge motion spectrum can be written as the integral of the wave spectrum and the response function squared. To find the variance of the surge motion another integral has to be taken, and if it assumed that the response H is only dependent on the wave frequency differences and the peak frequency of the spectrum (in addition to pure ship characteristics) it is seen that variance ends up in an integral of the wave grouping spectrum - cf. Fig. 4 - and the response function squared.

This is all condensed in Fig. 9. To obtain an impression of the slow drift motion one has to convolute the wave group spectrum with the response function. The upper figure shows two response functions with different natural frequencies of the floating system, and with the particular wave grouping spectrum in question the lowest natural frequency will obviously create the largest motion (convoluted value). The lower figure shows that for a given response function also the shape of the wave spectrum will influence the convoluted result. The narrow spectrum is obviously the most critical one for this case, but not for the alternative response function seen in the upper figure!

Thus, the simplied case illutrates the physics of drift forces/motions and the key parameters involved.

danop

Fig. 7 RESPONSE OF FLOATING STRUCTURE

M : Added mass

C : Coefficient of restoring force

b : Damping coefficient

δ : Logarithmic decrement

$$\delta = b\pi/\sqrt{MC} \qquad T_N = 1/f_N = 2\pi/\sqrt{C/M}$$

Simplified case:

Drift forces 1, 2 and 6 $\Rightarrow$

$$H^2(\Delta\omega) = \frac{2g^2}{L_s^2 D_s^2 \left[(C/M - \Delta\omega^2)^2 + \Delta\omega^2 b^2/M^2\right]}$$

$$\left[(1-D_s/h)\, \mathrm{SIN}\left\{\frac{L_s}{2}(k(\omega+\Delta\omega) - k(\omega))\right\}\right]^2$$

Ship : L_s, D_s, M

Mooring : C, b

Waves : ω, k

Depth : h

danop

Fig. 8 Surge response function:

$$H^2(\Delta\omega) = f(L_S D_S, \delta\omega_N, \omega_P h)$$

Surge motion spectrum:

$$S_x(\Delta\omega) = \int_0^\infty S\eta(\omega)\, S\eta(\omega+\Delta\omega)\, H^2(\omega, \omega+\Delta\omega)\, d\omega$$

Variance of surge motion:

$$X^2 = 2\int_0^\infty \int_0^\infty S\eta(\omega)\, S\eta(\omega+\Delta\omega)\, H^2(\omega, \omega+\Delta\omega)\, d\omega\, d\Delta\omega$$

Simple case: $H^2(\Delta\omega, \omega_P) \Rightarrow$

$$\overline{X^2} = 2\int_0^\infty H^2(\Delta\omega, \omega_P) \int_0^\infty S\eta(\omega)\, S\eta(\omega+\Delta\omega)\, d\omega\, d\Delta\omega$$

$$= \int_0^\infty S\eta^2(\Delta\omega)\, H^2(\Delta\omega, \omega_P)\, d\Delta\omega$$

$\overline{X^2} \sim$ Convolute $\{$Wave Grouping, Response$\}$

danop

Fig. 9

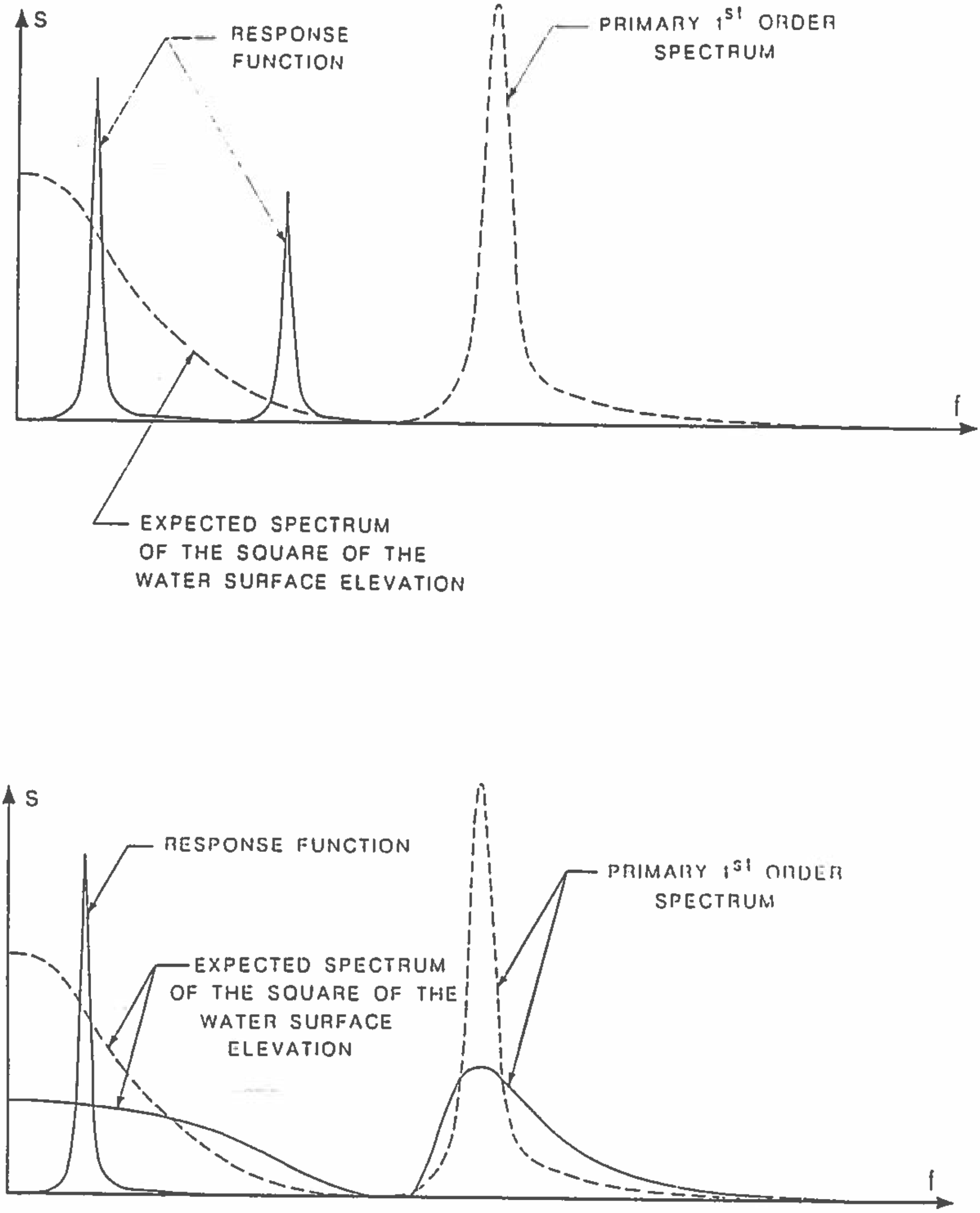

SES/lkj
08.03.1989

DRIFT FORCES AND DAMPING

IN

NATURAL SEA STATES

BY

H. LUNDGREN, TECHNICAL UNIVERSITY OF DENMARK & DANISH HYDRAULIC INSTITUTE
STIG E. SAND, TECHNICAL UNIVERSITY OF DENMARK
J. KIRKEGAARD, DANISH HYDRAULIC INSTITUTE

BOSS '82
MIT, Cambridge, Mass - August 1982

Preprint

DRIFT FORCES AND DAMPING IN NATURAL SEA STATES

A CRITICAL REVIEW OF THE HYDRODYNAMICS OF FLOATING STRUCTURES

H. LUNDGREN
Technical University of Denmark
& Danish Hydraulic Institute

STIG E. SAND
Technical University of Denmark

J. KIRKEGAARD
Danish Hydraulic Institute
Denmark

SUMMARY

1. Drift and damping forces are of paramount importance to the design of large floating structures (TLPs, semisubmersibles, etc.). A scrutiny of recent literature shows that the determination of these forces still may need *clarification*.

2. Since the drift forces depend so much on wave directionality and grouping, there is a great need for *three-dimensional recordings of natural sea states* in various locations. These recordings should include the determination of the phases. It is not safe to assume that the phases are random.

3. The first order description of recorded *sea states in the North Sea* is mentioned in Sec. 2. The recordings cover frequencies, directions and phases.

4. The *second order description*, as derived from the first order description, is discussed in Sec. 3, including frequencies, directions and phases. These low frequency waves are of significance for the drift forces.

5. For the determination of drift and damping forces one should always observe the *basic principle* of f i r s t combining the various flow components, i.e. waves, currents and body motions.

6. A survey of the physics of *drift forces*, involving 8 different types and their relative importance, is given in Sec. 4.

7. A survey of *damping forces*, involving 7 different types, is given in Sec. 5.

8. A discussion in Sec. 6 of the *Mathieu instability* problem results in the conclusion that wave directionality and grouping are of great significance.

9. *Model testing techniques* are mentioned in Sec. 7. Tests with offshore structures should be made in 3-D reproduced natural sea states. With an oscillating carriage, forces from irregular waves and currents can be studied at greater scale in 2-D flow. In this connection it is possible to compensate for dominant inertial pressures.

1. INTRODUCTION

It is well known that drift and damping forces are decisive for the design of slowly osc lating systems with low damping, such as a vessel connected to a single point mooring (SPM), a moored semisubmersible or a tension leg platform (TLP).

While the developments of SPMs and semisubmersibles have been gradual, so that it has be possible to utilize previous experience for each step into deeper water or worse environmental conditions, the application of TLPs will represent a rather *discontinuous development* into a te nologically virginal area. As a consequence of this, and in order to reduce the risk of failu extensive efforts have been spent, and are being spent, by the offshore industry and by hydrod namic institutions, on investigations of many kinds, including numerical and physical models, hydrodynamic theories, etc.

A perusal of recent literature reveals, however, that there still exist considerable *di culties* in:

(1) The description of the environmental factors.

(2) The relative role, as well as the magnitude, of the various hydrodynamic forces.

These difficulties are discussed below.

The *conclusion* is that a large amount of investigation is still needed in order to elim nate the uncertainties inherent in the design of large floating structures, which could otherw be in a risky situation or require excessive costs.

1.1 Environmental Factors

The *wind velocity profile and turbulence* during extreme gales are reasonably well known The local distributions above the troughs and the crests of a natural sea state, however, requ further studies, in as much as the gusts contribute to the slow drift forces. These local dis butions may be accounted for in a physical model, if a natural, gusty wind is superimposed upo the waves in the area around the structure.

The *tidal currents* at a given location are known with good accuracy from numerical mode of the oceans. The turbulence characteristics, which influence the drift forces, may require cal measurements because of stratification.

The *wind-driven currents* in fairly shallow areas like the North Sea may be predicted wi good accuracy from simple numerical models, cf. for example, the design forces for the Danish North Sea gas pipeline (Brink-Kjær, et al, 1982). For wind-driven oceanic currents the develo ment of a satisfactory numerical model is needed.

In a given situation the drift forces from winds and currents are stochastically indepe ent and may be added accordingly (Wichers, 1979).

The most important, and least known, drift forces originate from the *waves*. The diffic ties encountered are due to deficient descriptions of the natural sea states.

Historically, sea states have been described on the following levels:

1. Periodic, 2-D design waves.
2. Irregular, 2-D waves with a certain spectrum (infinitely wide fronts).
3. Irregular, 3-D waves with a certain directional spectrum (short-crested waves).

It is not until recently that physical and numerical models have moved onto Level 3.

A number of numerical models have been developed for the forecast or hindcast of the wa motion on Level 3 (see, for example, Brink-Kjær, et al, 1982).

It is evident that the *wave directionality* has great influence on the low frequency mot of moored structures (surge, sway, yaw). This has been demonstrated by model tests with a bul carrier exposed to a deterministic reproduction of storm waves recorded in nature (Kirkegaard, al, 1980).

It has often been assumed that natural waves have random phases. This is most unlikely cause of the high order, nonlinear interactions. In 2-D tests it has been demonstrated, as co be expected, that the *wave grouping* has great influence on the surge motions (Spangenberg and Kofoed Jacobsen, 1981).

The *grouping of waves over varying directions* has a particular influence on the yaw mot which could be critical for the stability of a TLP, cf. Sec. 6 below. Such grouping is availa from a storm in the Danish sector of the North Sea, based on a 3-D recording system (see Secs. 2 and 3 below). There is a great need, however, for many more 3-D records from various areas, before it may become possible to extract some 'typical' natural sea states.

The influence of the 3-D structure of waves on the *Mathieu instability* problem is described in Sec. 6 below.

The directional spread of wave energy observed at one point has its counterpart in a *directional concentration*, which is known to generate 3-D plungers in the middle of the ocean. Though such plungers have limited influence on the low frequency motions, they may be important for the survival.

1.2 Hydrodynamic Forces

The difficulties inherent in numerical and physical models may be illustrated as follows:

(a) Some numerical models consider only *potential flow* for the determination of drift and damping forces, neglecting the viscous effects.

(b) Other numerical models consider only *viscous forces*, neglecting the potential flow forces.

(c) The value of the Morison *drag coefficient*, C_d, is often taken from hydrodynamic conditions that differ widely from the situation considered.

(d) The drift and damping forces should always de determined a f t e r proper *superposition* of the various flow components, i.e. wave motion (including wave flow separation), current, and body motion. If one does not adhere to this principle, the result may be off by orders of magnitude.

(e) The *scale effects* in physical models are mainly due to the low values of Reynolds number when drag or friction is involved. This applies to both waves and currents.

The difficulties concerning the drift and damping forces will be discussed in Secs. 4 and 5 below. In some cases the scale effects, which exaggerate drag and friction in physical models, increase the damping forces more than the drift forces, which is likely to lead to results on the unsafe side.

2. NATURAL SEAS - FIRST ORDER DESCRIPTION

It is generally recognized that the directionality of natural waves is important for the design of offshore structures. The three-dimensional character of ocean waves can be described by two fundamentally different methods. One is *stochastic* and based on the application of a spectrum with random phases and a parameterized spreading function. The other is *deterministic* and utilizes all information - also the phases - from site wave records. Here emphasis is placed on analyses attached to the latter method.

The directional measurements have been obtained by means of an echo sounder giving the surface elevations, η, and an electromagnetic current meter giving the two horizontal components of orbital velocities, u and v. The necessary information could as well have been obtained by means of a pitch and roll buoy measuring the elevations, η, and the slopes η_x and η_y. Application of the deterministic theory is, however, demonstrated for the η, u and v records taken in one vertical.

It is assumed that the wave motion in the natural sea is linear and composed of a large number of sinusoidal waves having infinitely wide fronts. When the three simultaneous time series η, u and v are decomposed into Fourier series, it is possible to utilize the fact that u and v form a velocity vector while η reveals whether the component considered has a crest or a trough attached to this vector. Thus, in narrow frequency bands it is possible to determine the directional distributions. The mathematical principles applied to obtain such results are described in Sand, 1979. When the large number of directional components are determined, and the phases have been stored, the wave field can be calculated in an area around the point of recording. In this respect the theory has been checked by measuring also the velocities u_1, v_1 at another point 1.3 $\bar{\lambda}$ away, $\bar{\lambda}$ being the mean wavelength. Satisfactory agreement was obtained between measured and calculated quantities.

In order to compare directional distributions obtained under different conditions, the spread is often fitted to a functional form. This has mostly in the literature been $\cos^{2s}((\theta-\theta_m)/2)$ with s(f), or a normal distribution, $N(\mu,\sigma^2)$. It has been shown how well the empirical variations of the spreading parameter, s(f), agree for measurements in the Baltic Sea, the Atlantic Ocean, and in the Gulf of Mexico (Sand, 1982b). However, the mean direction as a function of frequency, $\theta_m(f)$, (around which the waves are spread with parameter s(f)) shows very different variations, depending on the type of storm, fetch, etc.

It is easier to fit and to visualize the directional distributions when they are represented by *normal distributions*, $N(\theta_m(f), \sigma^2(f))$. For illustration, two normal distributions with $\theta_m = 0$ and σ^2 equal to 0.1 rad^2 and 1 rad^2, respectively, are shown in Fig. 1. The corresponding standard deviations in degrees are also given.

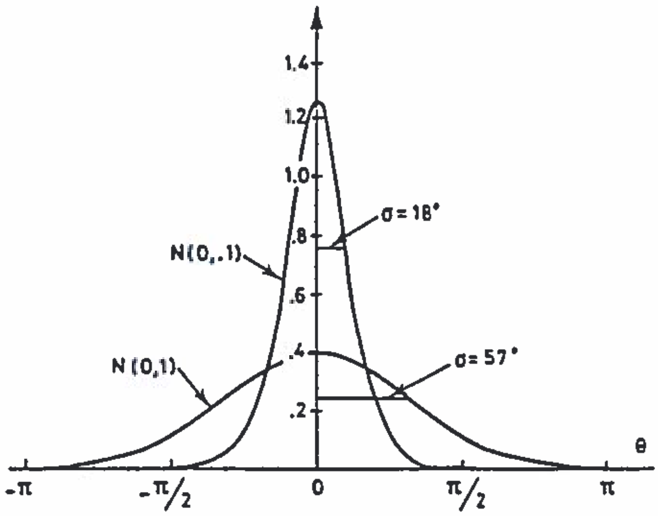

Fig. 1
Normal distributions with standard deviations given in degrees.

Normal distributions have been applied to *directional measurements* taken during storms in the North Sea and in the Baltic Sea. For narrow frequency intervals the distribution is fitted to the actual spreading. This results in series of frequency dependent mean directions, $\theta_m(f)$, and angular variances, $\sigma^2(f)$. Fig. 2 shows, like the comparisons referred to above, a striking agreement between the variances obtained in different locations and under quite different conditions. The frequencies are normalized by the frequency $f_{1,-1} = \sqrt{m_1/m_{-1}}$, where m_n is the n'th moment of the one-dimensional spectrum, $S_{\eta\eta}(f)$. The well-known tendency is seen, viz. the variance increases with frequency, except at the lowest wave frequencies.

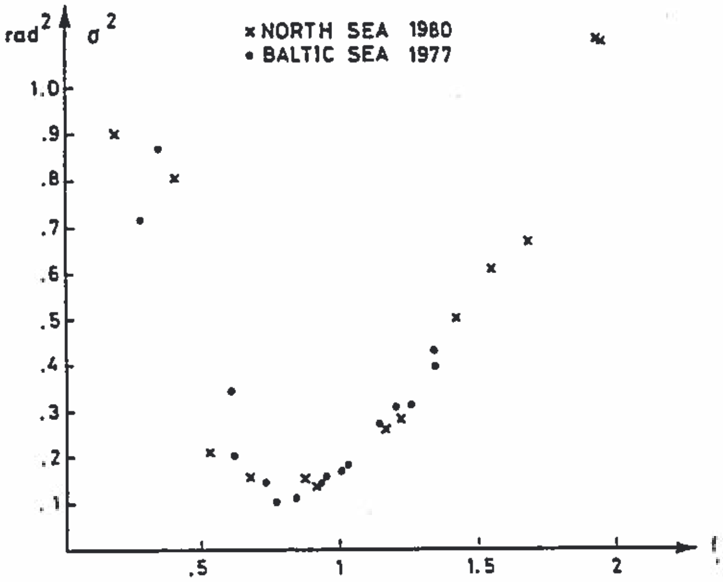

Fig. 2
Angular variance σ^2 as a function of dimensionless frequency $f/f_{1,-1}$ for two storms.

The records were taken during a storm from SE in the Baltic Sea and one from NNW in the North Sea. The significant wave heights were 2.4 m and 6.2 m, respectively. The *mean direction* as a function of frequency, $\theta_m(f)$, is shown in Fig. 3, which also reflects the development of the history of the storms.

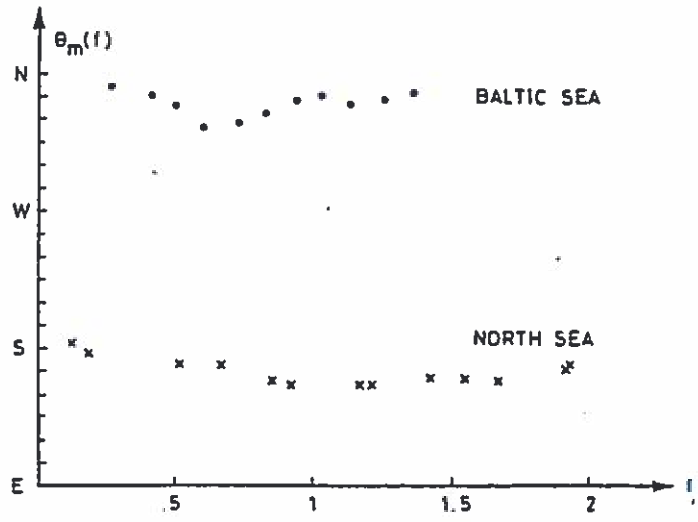

Fig. 3
Mean direction θ_m as a function of dimensionless frequency $f/f_{1,-1}$ for storms from SE (Baltic Sea) and NNW (North Sea), respectively.

The normal distribution used for the directional spread is on the usual form

$$N(\theta_m,\sigma^2) = \frac{1}{\sigma\sqrt{2\pi}} \exp\{-(\theta-\theta_m)^2/2\sigma^2\} \quad (2.1)$$

Furthermore, in the range of frequencies where essential energy is present, cf. Fig. 2, the following linear relationship is found

$$\sigma^2(f) = 0.72\, f/f_{1,-1} - 0.54 \quad (2.2)$$

Hence, so far as a linear description of natural seas is concerned the directional spectrum is given by

$$S_{\eta\eta}(f,\theta) = S_{\eta\eta}(f)\; N\big(\theta_m(f),\sigma^2(f)\big) \quad (2.3)$$

Of course, for a deterministic description the phase information obtained from the site wave records has to be applied. Apart from this, however, a *natural sea state* is defined by

(i) The one-dimensional spectrum, $S_{\eta\eta}(f)$.

(ii) The mean direction as a function of frequency, $\theta_m(f)$.

(iii) The variance, $\sigma^2(f)$, of the energy around θ_m as a function of frequency, cf. for instance (2.2).

An attempt to illustrate the directional spectrum is made in Fig. 4, in which some of the angular standard deviations from Fig. 2 are indicated along the one-dimensional spectrum from the North Sea measurements. The lowest frequency part of this spectrum is discussed in the following section.

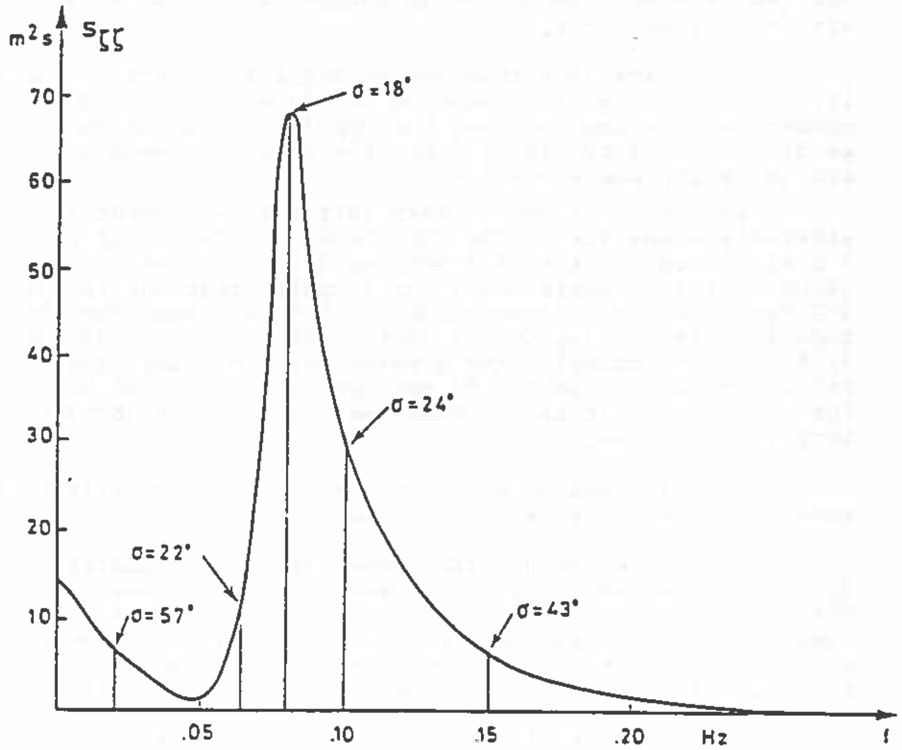

Fig. 4
Spectrum measured in the North Sea with indication of angular standard deviation σ at various frequencies. The second order low frequency part has been exaggerated by a factor 4 for clarity.

3. NATURAL SEAS - SECOND ORDER DESCRIPTION

In a second order description of a natural sea state two types of additional terms, both solutions to the Laplace equation, have to be introduced in order to satisfy the nonlinear surface conditions. So, in addition to the well-known linear solution expressed in regular sine components of wavenumber vectors $\bar{k}$, terms with wavenumbers $\bar{k}_n + \bar{k}_m$ and $\bar{k}_n - \bar{k}_m$ occur, cf. Fig. 5. Obviously, the $\bar{k}_n + \bar{k}_m$ components have very short wavelengths (corresponding to second harmonic waves). The practical importance of these components is in the wave shapes. With a view to the drift forces, the discussion may be confined to the long wave components $\bar{k}_n - \bar{k}_m$.

The *low frequency* part, $S_{\zeta\zeta}$, of the total directional spectrum, $S_{\zeta\zeta}(f,\theta)$, is shown schematically in Fig. 6. A measured second order low frequency spectrum from the North Sea is seen in Fig. 4. From radiation stress considerations it can be deduced that the second order components

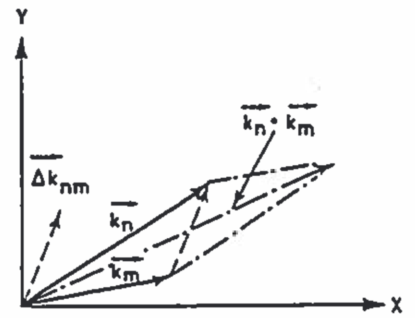

Fig. 5
Second order solution to the Laplace equation: a short wave component $\vec{k}_n + \vec{k}_m$, and a long one $\overrightarrow{\Delta k}_{nm} = \vec{k}_n - \vec{k}_m$.

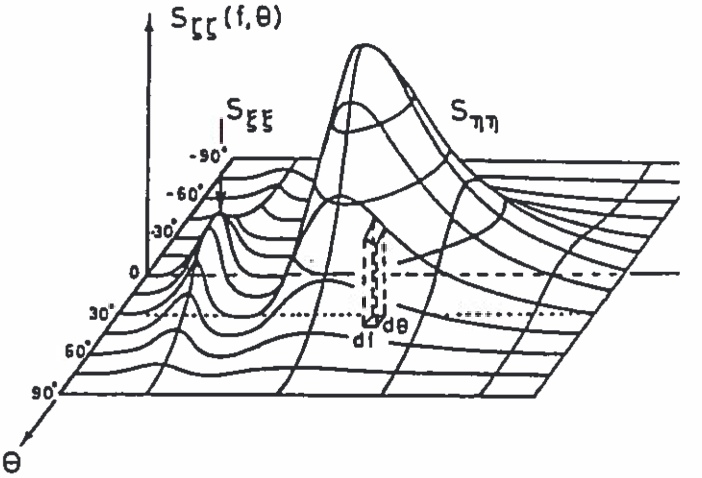

Fig. 6
Directional spectrum containing both the wave frequencies, $S_{\eta\eta}$, and the low frequencies, $S_{\xi\xi}$, with $S_{\zeta\zeta} = S_{\eta\eta} + S_{\xi\xi}$.

follow the groups, with troughs beneath the higher waves and crests in between. Thus, the lo frequency waves are a group-induced phenomenon, and, for a group composed of two waves, f_n an the low frequency component is determined by the difference $f_n - f_m$, while direction and waven are found from $\vec{k}_n - \vec{k}_m$.

There are some interesting characteristics of the second order low frequency waves. F ly, the fact that the direction of travel is determined by the difference of two first order number vectors implies that the *angular spread* is much larger than that of the first order wa as demonstrated by Fig. 5. For the North Sea measurements, Fig. 4, a typical value of the st ard deviation was $\sigma = 57^\circ$.

Secondly, it can be seen that the 3-D character of the first order waves results in a siderable *reduction of the amplitudes* of the second order low frequency waves, as compared wi 2-D situation. Transfer functions from the first to the second order waves have been derived (Sand, 1982a). These show, for example, that the low frequency waves are smaller in the (nat 3-D case than in a (theoretical) 2-D case. Consider, for example, two components each of amp tude 5 m, travelling in the directions $+15^\circ$ and -15° with the frequencies $f_n = 1/14$ Hz and f 1/19 Hz, respectively, and a water depth of, say, 450 m. Such a simple wave field induces a ond order wave of period 53 seconds, travelling in the direction 42° with a wave height of 0. For comparison, it can be mentioned that in the corresponding 2-D situation the height would larger by a factor of 3.

Finally, due to the vectorial wavenumber difference the 3-D low frequency waves have l wavenumbers and, hence, *smaller wavelengths* than corresponding 2-D waves.

Since the second order waves can be calculated, by means of transfer functions, from t first order waves it is also possible to determine the *low frequency spectrum*, $S_{\xi\xi}$. However, previously described (Sand, 1982b) it is important to note that the *phases are needed* for thi computation. As mentioned earlier, the phases (attached to $S_{\eta\eta}(f,\theta)$) can either be obtained f site wave records or they can be randomly selected. Naturally, this ambiguity leads directly the present intense debate about stochastic and deterministic approaches.

In principle, it is possible to attach an infinity of phase combinations to a given fi order spectrum, $S_{\eta\eta}(f,\theta)$. Each combination will give its own wave grouping and, hence, drift forces. If, therefore, a time series is produced on the basis of the spectrum and a random p ess for the phases, the result is just one of many possibilities. In addition, it has never proved that the natural sea state that we want to simulate is characterized by a random phase tribution. Thus, it may be feared that some of the important, but as yet unrevealed *features nature* could be *eliminated* by the random phase concept.

Out of such fear the Danish Hydraulic Institute has for ten years worked on a determin basis from *site wave records*. Thereby it is assumed that important properties of natural wave are retained. Hopefully, essential properties are also preserved when site records are scale in time and amplitudes in order to represent, for example, a 100 year situation. Since the di cussion of the phase distribution in nature has not come to a final conclusion, the present p losophy is that a reproduction based on information from nature by no means could be inferior just o n e arbitrary realization of a stochastic process. Incidentally, the deterministic c cept has been supported by vertical breakwater tests, where the application of time series wit randomly selected phases implied no shock forces, whereas natural wave records (with an identical spectrum) gave reasonable shock force distributions, independent of the length of the wave flume.

It should be noted that the emphasis in this paper on the deterministic approach is related to the present *state of the art* with respect to wave grouping, etc. It would be highly desirable in the years to come if the probability distribution of phases could be determined, perhaps as a function of water depth, fetch, etc. When such profound knowledge become available, time series might be produced from the directional spectrum combined with the phase distribution. In the necessary future research two *recently developed concepts* may be involved. One is the group spectrum derived from η^2, called SIWEH (Funke and Mansard, 1979 and 1981). The other is the low frequency, second order wave spectrum, $S_{\zeta\zeta}(f)$, described above (Sand, 1982a).

4. DRIFT FORCES

4.1 Wave Related Drift Forces

In contrast to the first order wave forces, which oscillate between large positive and negative values at the wave frequencies, the wave related drift forces are *characterized by*:

(a) having small values,

(b) having mostly a mean value different from zero,

(c) varying with much lower frequencies than the wave frequencies, and

(d) giving rise to horizontal motions (of moored structures) much larger than the first order motions.

The most *important drift forces* are:

I. Viscous flow forces:

A. Wave drag drift.
B. Current-wave drag.
C. Current-wave friction.

II. Potential flow forces:

D. Wave elevation drift.
E. Velocity head drift.
F. Body translation drift.
G. Body rotation drift.
H. Second-order-wave drift.

The physics of these 8 drift forces will be explained below. A *common feature* of these forces is that they are of second or higher order. A second order term is defined as a term that contains the product of two first order terms. As first order terms are understood:

(1) Wave elevations, velocities, and pressures.
(2) Current velocity.
(3) Body displacements due to first order waves.

4.2 Wave Drag Drift

Though the Morison formula gives an imperfect picture of the hydrodynamic situation in connection with wave drag, it will be used for illustration, applied to a vertical cylinder of diameter d and draught D placed in a small wave with horizontal velocities u:

$$F_d = \frac{1}{2} \rho C_d d u |u| \cdot D \quad (4.1)$$

For a small sine wave the mean value of u |u| over the period T vanishes. Hence, there is no essential drift.

For a *large wave*, however, it is necessary to take the variation, $\eta(t)$ of the wave elevation into consideration. Consider, for example, one of the columns in a TLP, where the heave is negligible compared with the wave heights. Then, the factor D in (4.1) must be replaced by D + η, giving

$$F_d = - \rho C_d d u |u| \cdot (D + \eta) \quad (4.2)$$

Now, the mean value of F_d over the period is positive because positive values of u are accompanied by positive values of η, and negative values of u by negative η.

As will be seen below, the mean value of (4.2) over the period is the *dominant drift force* on a TLP (and a semisubmersible). This has been stated by Ferretti and Berta, 1981 (without indicating the C_d value applied).

The wave drag drift has been applied in several *numerical models*:

(i) Pijfers and Brink, 1977, where the C_d-value has been chosen as a weighted average between the Reynolds dependent steady-flow value, C_d(Re), involving the sum of the

current velocity and the wave (Stokes) drift velocity, and the Keulegan-Carpente
dependent, but Reynolds independent, wave flow value, $C_d(KC)$, involving the hori
zontal velocity.

(ii) Denise and Heaf, 1979 (without indicating the C_d-value used).

(iii) Sebastiani, et al, 1981, where reference is made to Ferretti and Berta, 1981, mentioned above.

Other numerical models exclude the wave drag drift on the grounds that it is a cubic te
(u^2, η). Indeed, it seems to be a *quartic term*, because C_d is approximately proportional to th
wave height (see below).

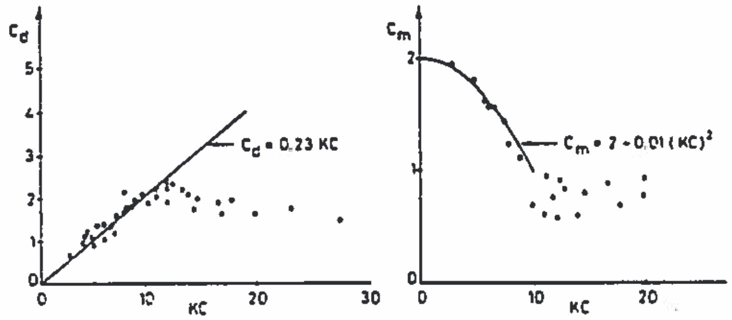

Fig. 7
Subcritical C_d- and C_m-values found in an oscillating water tunnel (from Bearman and Graham, 1979).

As an illustrative *example*, one of the columns in the TLP discussed by Gie and de Boom,
1981, has been considered (with the significant wave as a regular wave):

$$d = 16.9 \text{ m}, \; D = 35 \text{ m}, \; H = H_s = 18.1 \text{ m}, \; \bar{T} = 16.7 \text{ s} \qquad ($$

For this wave, KC = 3.36 and, according to Fig. 7, the subcritical C_d-value is about 0.67. A s
critical value of 0.35 has been chosen as a rough estimate. Fig. 8 shows the variation of the

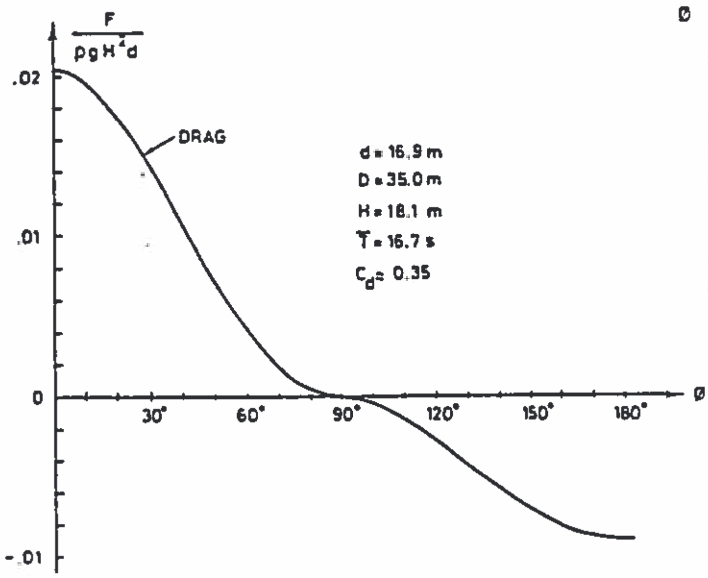

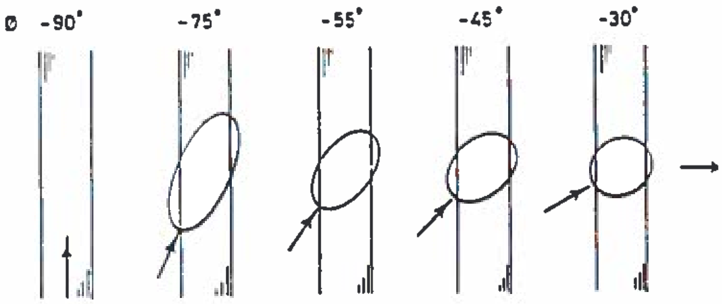

Fig. 9
The 'effective' cross sec
of a circular cylinder e
tered by wave motion wit
circular orbit.

Fig. 8
Wave drag on a column as a function of wave phase.

drag (integrated from z = - 35 m to z = η) for a sine wave. After integration over the perio
mean value is found to be

$$F_{dr,A} = 0.0024 \; \rho \; g \; H^2 \; d$$

(If the second order wave profile is used, the increase is only 1%.) Originally, the Morison
mula was tentatively proposed for application in shallow water, where the wave orbits are ver
long ellipses. To use it in deep water where the orbits are circles, is most questionable, c
Fig. 9, which demonstrate that the 'effective' cross sections encountered by a wave with cres
$\phi = 0°$ are elliptic most of the time. Hence, it is possible that the actual C_d-values are le
than indicated in Fig. 7. Anyway, it is likely that $C_d \approx 0$ at the beginning of the wave cres
$(\phi = -90°)$, where separation starts along the rear generatrix of the cylinder.

At the *stern of a ship* exposed to head waves there is also a wave drag drift because of the wave flow separation in connection with the (elevated) crest, as compared with the nearly potential flow in the (depressed) trough.

Further studies are required in order to determine the C_d-values for a column in the prototype, where the flow is *supercritical*. In addition, there are great difficulties in determining the *low frequency wave drag drift* in a natural sea state with its changing groups and directions, particularly because the development of the 'drag coefficient' depends upon the wave height, the wave period, etc.

4.3 Current-Wave Drifts

If a small current velocity (or Stokes drift), V_c, is added to u in (4.1), the *current-wave drag* is found as the mean value over the period:

$$F_{dr,B} = \frac{1}{2}\,\rho\, C_d\, d\, \frac{4}{\pi}\, u_m\, V_c\, D \qquad (4.5)$$

where, for simplicity, the maximum horizontal orbital velocity, u_m, has been assumed to be constant over the draught D, as in (4.1). If the variation of the wetted surface is considered, there will be a minor change of the drift force.

The *current-wave friction* has some influence on large ships in head waves because the wave friction factor, f_w, is much larger than the current friction factor. For small currents the resulting friction drift is proportional to f_w, u_m and V_c, and it is active along the sides and the bottom of the ship. The force is analogous to the wave friction damping; reference is made to Fig. 11 and pertaining text.

4.4 Potential Flow Drift Forces

The most *thorough discussion* of the 5 types of potential flow drift forces on floating bodies has been given by Pinkster, 1980, to which reference is made for all details.

The forces may be divided into 3 groups:

(i) 'D. Wave elevation drift' and 'E. Velocity head drift' may, roughly, be said to originate from the reflection of the first order waves from the body. This is illustrated by Fig. 10, where the drift force on a restrained ship in beam sea is seen to diminish as the wavelength λ increases relatively to the ship length L_{pp}.

(ii) 'F. Body translation drift' and G. Body rotation drift' originate from the displacements of the body in combination with the pressures on the body from the first order waves.

(iii) 'H. Second-order-wave drift' is the force exerted on a (fixed) body by the low frequency, second order waves discussed in Sec. 3 above.

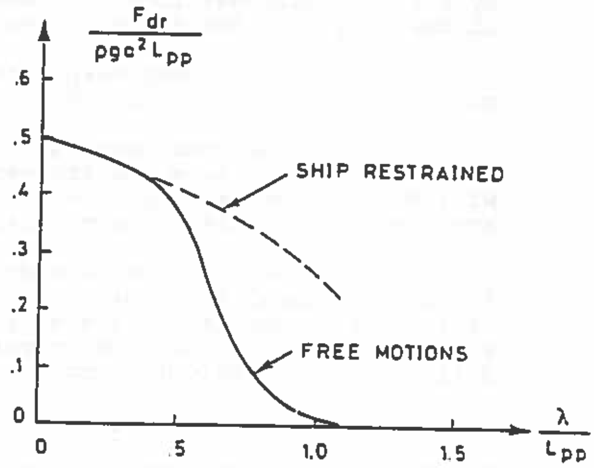

Fig. 10
Mean wave drift forces on loaded 130,000 dwt tanker in beam sea (from Løken and Olsen, 1979).

For uni-directional irregular waves a considerable amount of work has been done in order to determine the *quadratic transfer function* from first order waves to drift forces (Newman, 1975; Faltinsen and Løken, 1979). Seemingly, only random phases have been considered. Hence, the influence of natural phases remains to be seen. This also applies to the influence of directional sea states.

The *wave elevation drift* on a body is the integral around its waterline of the force $\frac{1}{2}\rho g \eta^2$, where η is the first order wave elevation. This expression represents for a first order pressure distribution the excess triangular force at still water level that does not vanish when averaged over time. The force is taken as a horizontal pressure force perpendicular to the waterline. (For a sloping side of the body there is also a vertical force; this is without interest for the drift forces.) The diffracted waves are included in η.

The *velocity head drift* on a body is the integral over its wetted surface of the pressure $p_V = -\frac{1}{2}\rho V^2$, where V is the velocity vector at the body surface due to the first order wave motion, including the waves diffracted around the body. p_V is the pressure drop corresponding to the velocity term in the Bernouilli equation.

As an *example* will be taken the column given by Eq. (4.3). The exact determination of drift forces requires the application of the 3-dimensional, potential flow source method. Inst an approximate approach is used because it gives a simpler picture of the problem. To begin w the draught is assumed to be infinite. Then there is an explicit solution along the following lines (cf., for example, Isaacson, 1977 or Skovgaard and Jonsson, 1981): The incoming wave, p: gating in the direction $\theta = 0$, is developed in a series of Bessel functions. Because the inte is in the drift force in the wave direction, only the terms involving $J_0(kr)$ and $J_1(kr) \cdot \cos\theta$ tribute, where k is the wavenumber and $r = a = d/2$ is the surface of the cylinder. In the reflected wave the corresponding Hankel functions are involved.

Since the diameter of the cylinder is small compared with the wavelength, it suffices t take the first terms in the power series of the Bessel and Hankel functions. The result is a elevation drift

$$F_{dr,D} \approx \frac{\pi^2}{16} (ka)^3 \rho g H^2 d \qquad ($$

The velocity head drift is $F_{dr,E} = -\frac{1}{2} F_{dr,D}$, thus reducing the total drift on a fixed cylinder 50% of (4.6). If, as a rough estimate, the limited draught, D = 35 m, is taken into considera by a reduction factor, $[1 - \exp(-2kD)] = 0.64$, a potential flow drift force of

$$F_{dr,D+E} = 0.00036 \rho g H^2 d \qquad ($$

results. It will be noted that this is only 15% of the wave drag drift in (4.4), the latter b based on an estimate of the supercritical C_d-value.

The *body translation drift* is associated with the 3 translational displacements x_i (i = 1 that will shift the body into a slightly different pressure field because of the pressure grad $\partial p/\partial X_i$, due to the first order wave motion, including the diffracted waves. Hence, the produc $x_i \cdot \partial p/\partial X_i$ has to be integrated over the wetted surface as an additional pressure.

The *body rotation drift* is associated with the 3 angular displacements x_j (j = 4,5,6) tha will shift the directions of the pressures on the sides of the body due to the first order wav motion, including diffraction. For example, a roll angle, x_4, will tilt the bottom of a ship that the total wave pressure, P_3, on the bottom will give a sway force component, $F_2 = - x_4 \cdot P$ in the X_2-direction. Since the wave pressures integrated over the body surface can be express by the body accelerations, the body rotation drift is found to be $x_j \times (M \ddot{x}_i)$, where M is the m of the body, and the summation extends over all i and j.

Usually, the body displacement drifts contribute to a reduction of the total drift forc cf. the two curves in Fig. 10.

The *second-order-wave drift* is due to the pressure gradient in the second order waves. Since these waves have low frequencies and, hence, very long wavelengths, the pressure gradien will normally correspond to the surface slope of the second order wave, unless the body dimens are very large. The pressure gradient has to be applied to the body plus added mass.

As an *example*, the second-order-wave drift has been calculated for the column in Eq. (4 for a directional sea state with a significant wave height, $H_s = 18.1$ m, and a mean period, $\bar{T}$ 16.7 s, corresponding to a peak period, $T_p = 18.0$ s. The sea state used has been scaled up fr a natural sea state recorded three-dimensionally in the North Sea. The result is a significan drift force (corresponding roughly to second order waves with $H_s \approx 0.15$ m and $\lambda \approx 1500$ m)

$$F_{dr,H} \approx 0.0008 \rho g H_s^2 d \qquad ($$

determined from the transfer functions (Sand, 1982a). This force is about twice the mean drift

5. DAMPING FORCES

5.1 Hydrodynamic Damping Forces

The most *important damping forces* are:

I. Wave-related, viscous flow forces:
- L. Wave drag damping.
- M. Wave friction damping.

II. Current-related, viscous flow forces:
- N. Current drag damping.
- O. Current friction damping.

III. Other viscous flow forces:
- P. Pure drag damping.
- Q. Pure friction damping.

IV. Potential flow forces:
- R. Radiation damping.

The physics of these damping forces will be explained below. Most of the damping forces are, least approximately, proportional to the drift velocity, V_{dr}. In Groups I and II they increase, in addition, with some other velocity (wave orbital velocity or current velocity). Only in Group III the damping force is quadratic in the sense that it is proportional to V_{dr}^2. These forces occur in still water.

Theoretical considerations, as well as experiments (Wichers and van Sluijs, 1979), show that the wave-related, viscous damping dominates. Next comes the current-related, viscous damping. The potential flow damping is often negligible.

5.2 Wave-Related Damping Forces

For a regular wave the *wave drag damping*, F_L, may be found from a formula similar to (4.5), replacing V_c by V_{dr}. Thus the damping coefficient becomes

$$b_L = \frac{2}{\pi}\,\rho\, C_d\, d \cdot (u_m D) \tag{5.1}$$

assuming u_m constant over the draught D. In this connection it should be remembered that C_d increases with KC (Fig. 7).

Wave friction damping, F_M, is of importance along the sides and bottom of a ship moored to an SPM, as illustrated by Fig. 11. Assuming a circular orbital motion, the water particle motion relative to the ship will exhibit an orbit opened by the amount $\Delta X = V_{dr} T$ after the wave period T.

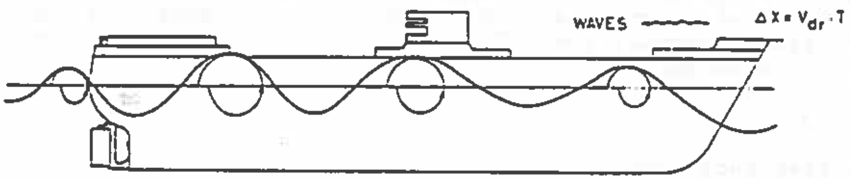

Fig. 11
Wave friction damping along the sides of a ship.

If V_{dr} is small compared with the orbital velocity, the friction will be dominated by the wave friction coefficient, f_w. For a smooth wall and fully turbulent flow, the friction factor to be applied to the orbital velocity is (Fredsøe, 1981b, Fig. 4):

$$f_w = 0.032\; RE^{-0.15} \quad \text{with} \quad RE = u_m\, a/\nu \tag{5.2}$$

where a = orbital radius (orbital amplitude under ship's bottom). Thus, along the ship's side, the damping coefficient becomes

$$b_M = \pi\, \rho\, f_w \cdot (a\, u_m D) \tag{5.3}$$

assuming a and u_m constant over the draught D. A similar formula may be derived for the ship's bottom.

For the combination of waves and currents reference is made to Fredsøe, 1981a, and for rough walls to Fredsøe, 1981b, and Jonsson, 1980.

5.3 Other Damping Forces

If the current drag is $\frac{1}{2}\rho\, C_d\, A_d\, V_c^2$, where A_d is the cross-sectional area, and V_c is much larger than V_{dr}, the *current drag damping* coefficient becomes

$$b_N = \rho\, C_d\, A_d\, V_c \tag{5.4}$$

Similarly, for the *current friction damping* with a friction coefficient, f_c, and a surface area, A_s,

$$b_O = \rho\, f_c\, A_s\, V_c \tag{5.5}$$

The *pure drag damping* force $F_P = \frac{1}{2}\rho\, C_d\, A_d\, |V_{dr}|\, V_{dr}$ and the *pure friction damping* force $F_Q = \frac{1}{2}\rho\, f_c\, A_s\, |V_{dr}|\, V_{dr}$ are, in contrast to the other damping forces, quadratic in the drift velocity. Some numerical models have taken only the quadratic damping forces into consideration. However, since these forces correspond to still water, they are without significance for structures in waves or currents.

For a given frequency of an oscillating structure the *radiation damping* force is linear in V_{dr}. The energy loss corresponds to the energy flux in the waves generated by the oscillating structure and radiated towards infinity. If the drift forces originate from waves or currents, the radiation damping coefficient may often be neglected. An exception is a ship that is exposed to waves other than head waves.

6. MATHIEU INSTABILITIES

In the equation of motion of compliant offshore structures, e.g. a TLP, a *time varying stiffness* term can occur due to the wave forces. For simple harmonic stiffness variations the system is characterized by Mathieu's equation, which under certain conditions produces unstabl solutions. Reference is made to Rainey, 1978 and 1981, to Richardson, 1979, and to Jefferys a Patel, 1981. The analysis for natural sea states requires either a time-domain numerical or a physical model.

An instability is a constantly growing oscillation as a result of energy steadily being into the system faster than it can be dissipated. In the Mathieu case the time varying stiffn term may do net work on the system faster than it can be dissipated by a linear damping. As m tioned below, three sources may lead to varying stiffness of the system and thereby to the pos bility of instabilities.

Consider, for example, the constant part of the stiffness for the surge motion, althoug the phenomenon discussed could as well appear in the sway or yaw modes. The stiffness is dete mined as the sum of the tether tensions, T, divided by the tether length, ℓ. The *first*, obvio time-varying *contribution* is due to the heave force introducing the term $(F_3/\ell)\cos\omega t$. With a surge force F_1 the equation of motion for the TLP is

$$(M + M_a^1)\,\ddot{x}_1 + b\,\dot{x}_1 + \frac{1}{\ell}(T + F_3\cos\omega t)\,x_1 = F_1\sin\omega t \qquad (}$$

where M_a^1 is the added mass in the surge mode. The interesting solutions, as far as instabilit are concerned, are the transients, i.e. terms that decay under the influence of a relatively s damping. These are found for zero horizontal load, $F_1 = 0$, in (6.1). The substitution $r = x$ with $a = \frac{1}{2}b/(M + M_a^1)$ leads to the equation

$$\ddot{r} + \omega_1^2\,(1 + Q\cos\omega t)\,r = 0 \qquad (}$$

where ω_1 is the natural surge frequency with

$$\omega_1^2 = \frac{T}{\ell\,(M + M_a^1)} - a^2 \qquad \text{and} \qquad Q = \frac{F_3}{\ell\,(M + M_a^1)\,\omega_1^2} \qquad (}$$

This is Mathieu's equation and, by means of tabulated solutions, Fig. 12 can be drawn. It giv as a function of the ratio, ω/ω_1, between the wave frequency and the natural frequency. It ap pears that twice the natural surge frequency is a very critical wave frequency.

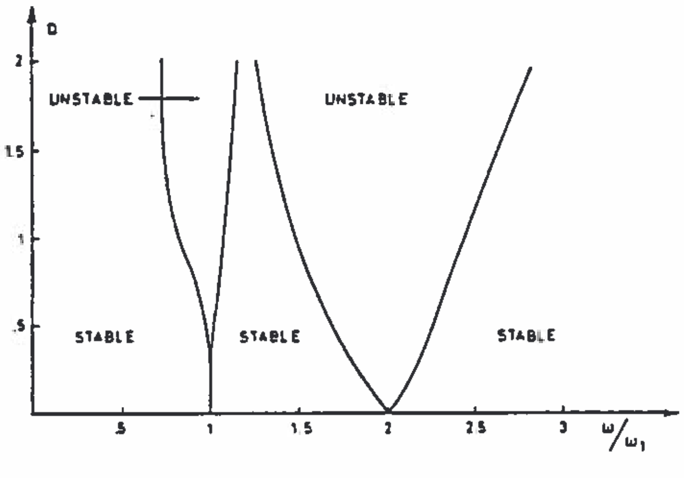

Fig. 12
Regions of instability of Mathieu type
(from Richardson's discussion, p. 74 in Rainey, 1978).

A *second contribution* to the time varyin stiffness is found from the change of the surge force due to the displacement x_1 of the structu Since this force varies in the x_1-direction, th platform is exposed to the force $F_1^1 = F_1\sin(\omega t - k$ Taking into account that $kx_1 \ll 1$, allows the li arized version $F_1^1 = F_1\sin\omega t - k\,F_1\,x_1\cos\omega t$ to b introduced. The cos-term may be included in th stiffness term in (6.1) because the two terms a in phase with each other. This will again lead the Mathieu equation (6.2) but for the value of to be used in Fig. 12:

$$Q = \frac{F_3 + k\,\ell\,F_1}{\ell\,(M + M_a^1)\,\omega_1^2} \qquad (}$$

The unstable solutions grow with an expo tial time constant, which decreases with increa Q. Thus, the stability of the structure depend the damping coefficient b in such a fashion tha the oscillations will continue to grow until su cient damping is mobilized by the motion of the platform. The wave frequencies in the unstable regions of Fig. 12 are very low, e.g. around twice the natural frequency ω_1, and the instabili depends, of course, on the extent to which such low frequency waves occur in natural seas.

Using the example of the TLP in Gie and de Boom, 1981, the surge period is 106 s, corre sponding to low frequency wave periods around 53 s for the most critical instability region. is just a typical period for the group-induced second order waves. With 3 - 5 waves in a group wave period should lie in the interval 10 - 18 s, which is reasonable for a natural sea state. Hence, it seems worthwhile to consider the second order waves. It was earlier found that a ty cal amplitude is of the order of 0.1 m. In principle, this should be sufficient to trigger th instability since the instability region in Fig. 12 extends down to Q = 0 for $\omega/\omega_1 = 2$. However, a definite answer will require further investigations.

The *third source* of instability appears when two wave trains, with a frequency difference equal to the natural frequency of the structure, are considered. In this case the equations will produce what Rainey, 1978, has called subharmonic resonance. It is, indeed, a resonance situation although the oscillations are still governed by damping as in the former instability cases. From the equations it is possible to conclude that the worst resonance appears in a cross-sea, i.e. the situation where the two wave trains travel at right angles to each other. In uni-directional waves the phenomenon is found to vanish. Thus, with regard to this third kind of instability, obviously, the directionality of the natural sea becomes important.

Because of the stiffness variations occurring for a TLP, some potential sources of instability have been discussed above. Evidently, the next problem is to evaluate the damping in order to determine the behaviour of the structure, and to assess to which extent the transients of the possible instabilities will grow. It is well-known that physical model tests with a TLP require special precautions since the hydrodynamic damping increases with decreasing model scale, and the instability phenomena are highly dependent on the damping coefficients. However, in order to obtain realistic results it can be *concluded* that the model tests should reproduce the natural, directional sea, as well as the correct second order, group-induced waves (cf. Ottesen Hansen, et al, 1981).

7. MODEL TESTING

In offshore research *numerical and physical models* are expected to supplement each other for the next decade or two. It has previously been demonstrated that a satisfactory deterministic reproduction of a natural sea state may be obtained by means of only seven, vertically hinged wave generators (Sand, 1979, Lundgren, et al, 1979 or Sand and Lundgren, 1981).

A new *wave basin* (Fig. 13) with 60 wave generators for the 3-D *reproduction of natural sea states* (including approximate reproduction of second order waves) is being planned at the Danish Hydraulic Institute for the study of offshore structures. It is designed for scales 1:80 to 1:100 with a maximum wave height in the model of 0.4 m. With a width of 0.5 m of each flap the system is capable of generating a wide range of sea states. The limiting direction of essential energy at wave frequencies has been chosen as 60° with a minimum period of 0.76 s (λ = 0.89 m). The design and the software of the control system are based on the experience with the pilot system described in the above references.

For thorough studies of 2-D wave forces on individual cylinders, riser bundles, hydroelasticity, etc. the technique of the *oscillating carriage* has been gradually improved over the last seven years in close cooperation between the Institute of Hydrodynamics and Hydraulic Engineering (Technical University of Denmark) and the Danish Hydraulic Institute. The carriage shown in Fig. 14 is installed at the former institute and has been used in a number of basic and applied projects.

As seen in Sec. 4, the wave drag is a dominant drift force on the columns of a TLP, a semisubmersible, etc. At the same time the KC-values are so low that the drag may be 5% or less of the inertia force.

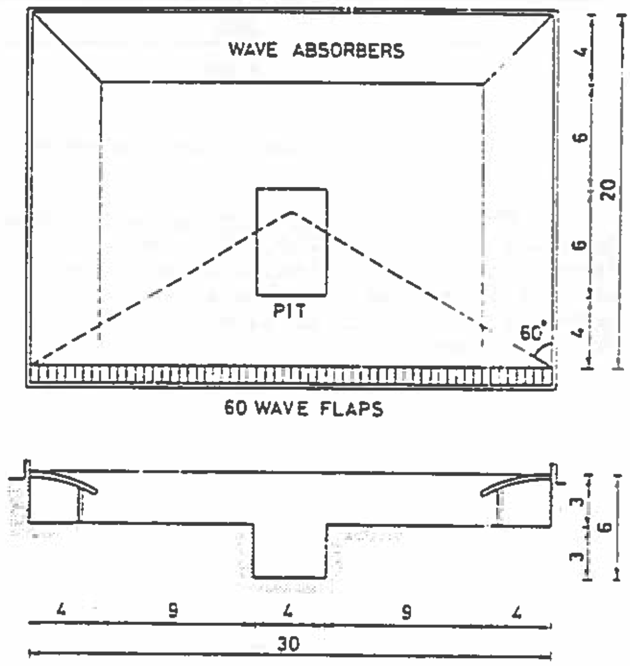

Fig. 13
Wave basin for 3-D reproduction of natural sea states.

With the *arrangement of pressure transducers*, T, shown in Fig. 15, there is complete compensation for the inertia pressure corresponding to C_m = 2. Hence, the range of the transducers can be fully utilized for recording the drag only. In this connection it is natural to consider any difference between the total pressure and the inertial pressure for C_m = 2 as being due to separation and vortex shedding in accordance with the flow history (Maull and Milliner, 1978, and Lundgren, et al, 1979).

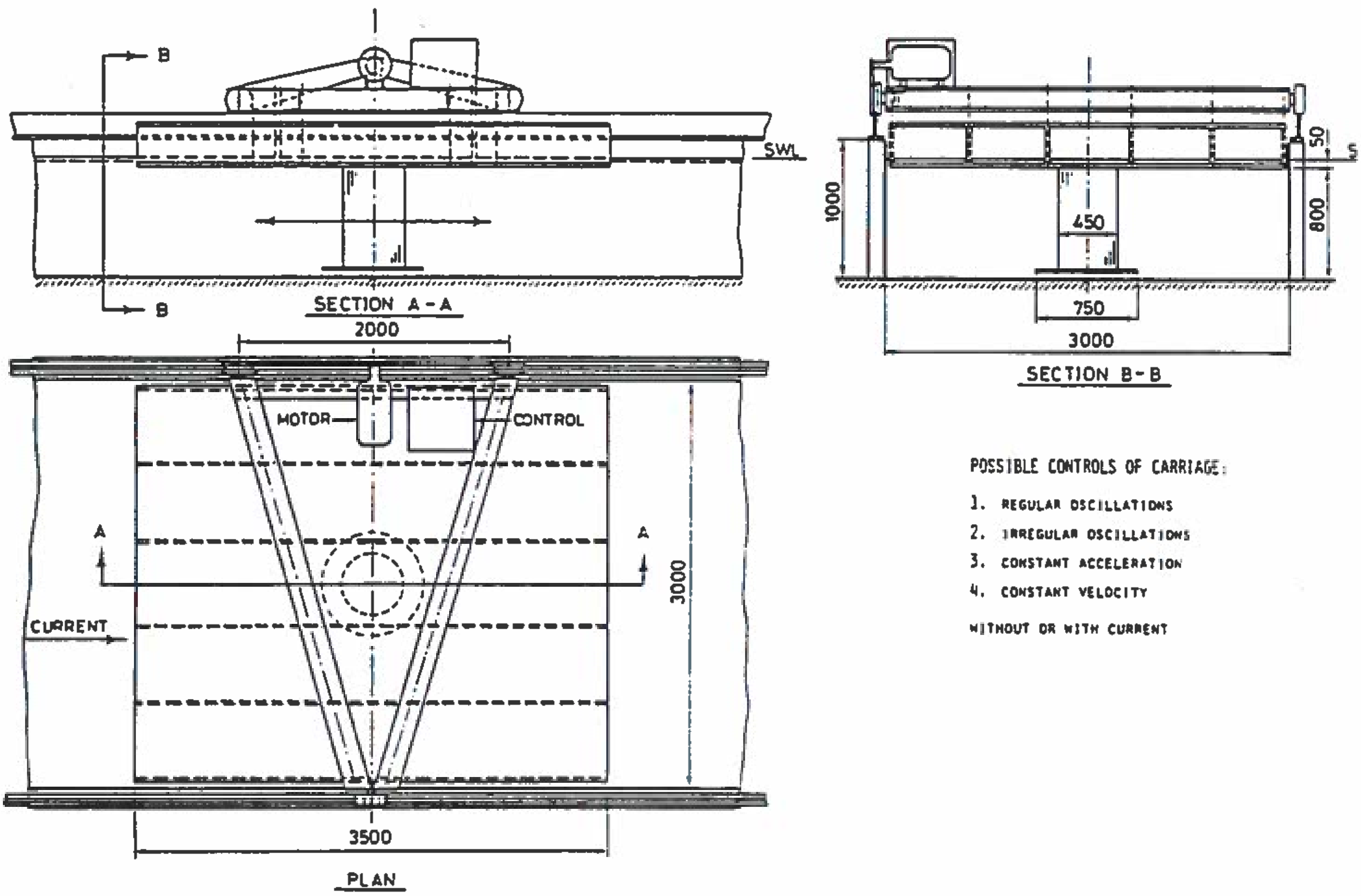

Fig. 14
Oscillating carriage for the study of wave and current forces in 2-D flow.

The oscillating carriage will allow *Reynolds numbers* of 200,000 or more. Compared with the oscillating water tunnel it has the advantage of being able to simulate irregular wave motion, also in combination with a current.

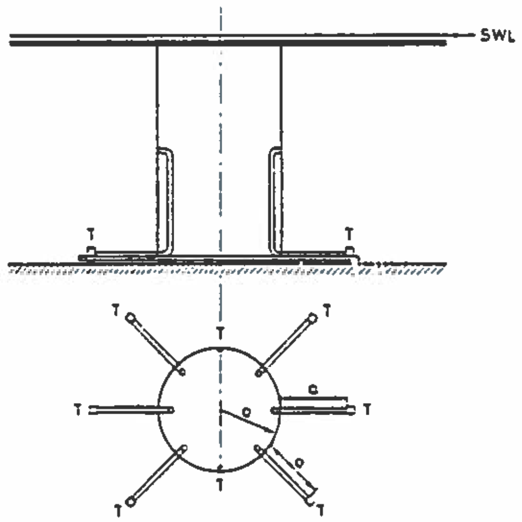

Fig. 15
Arrangement of pressure transducers, T, with compensation for the inertial pressure.

8. REFERENCES

BEARMAN, P. W. and J. M. R. GRAHAM, 1979, "Hydrodynamic Forces on Cylindrical Bodies in Oscillatory Flow," *Proceedings, 2nd International Conference on the Behaviour of Off-Shore Structures*, London, England, 1979, Volume 1, Paper 24, pp. 309-322. Cranfield, Bedford, England: BHRA Fluid Engineering.

BRINK-KJÆR, O., J. DIETRICH and K. MANGOR, 1982, "Wave and Current Study for the Danish North Sea Gas Pipeline," *Proceedings, ASCE & ECOR International Symposium Directional Wave Spectra Applications '81*, Berkeley, California, 1981.

DENISE, J.-P. F. and N. J. HEAF, 1979, "A Comparison Between Linear and Non-Linear Response of a Proposed Tension Leg Production Platform," *Proceedings, 11th Annual Offshore Technology Conference*, Houston, Texas, 1979, Volume III, Paper OTC 3555, pp. 1743-1754.

FALTINSEN, O. M. and A. E. LØKEN, 1979, "Slow Drift Oscillations of a Ship in Irregular Waves," *Applied Ocean Research*, Volume 1, Number 1, pp. 21-31.

FALTINSEN, O. M. and F. C. MICHELSEN, 1975, "Motions of Large Structures in Waves at Zero Froude Number," *International Symposium on The Dynamics of Marine Vehicles and Structures in Waves*, London, England, 1974, Paper 11, pp. 91-106. London, England: The Institution of Mechanical Engineers.

FERRETTI, C. and M. BERTA, 1981, "Viscous Effect Contribution to the Drift Forces on Floating Structures," *Proceedings, International Symposium on Ocean Engineering-Ship Handling*, Gothenburg, Sweden, 1980, Paper 9, pp. 1-10. Gothenburg, Sweden: Swedish Maritime Research Centre, SSPA.

FREDSØE, J., 1981a, "Mean Current Velocity Distribution in Combined Waves and Current," *Institute of Hydrodynamics and Hydraulic Engineering, Technical University of Denmark*, Lyngby, Denmark, Progress Report 53, pp. 21-26.

FREDSØE, J., 1981b, "A Simple Model for the Wave Boundary Layer," *Institute of Hydrodynamics and Hydraulic Engineering, Technical University of Denmark*, Lyngby, Denmark, Progress Report 54, pp. 21-28.

FUNKE, E. R. and E. P. D. MANSARD, 1979, *On the Synthesis of Realistic Sea States in a Laboratory Flume*, National Research Council Canada, Report LTR HY 66.

FUNKE, E. R. and E. P. D. MANSARD, 1981, "On the Meaning of Phase Spectra," *Proceedings, International Symposium on Hydrodynamics in Ocean Engineering*, Trondheim, Norway, 1981, Volume 1, pp. 49-69. Trondheim, Norway: The Norwegian Institute of Technology.

GIE, T. S. and W. C. DE BOOM, 1981, "The Wave Induced Motions of a Tension Leg Platform in Deep Water," *Proceedings, 13th Annual Offshore Technology Conference*, Houston, Texas, 1981, Volume III Paper OTC 4074, pp. 89-98.

ISAACSON, M. DE ST. Q., 1977, "Shallow Wave Diffraction Around Large Cylinder," *Journal of the Waterway, Port, Coastal and Ocean Division*, Volume 103, Number WW1, pp. 69-82. New York: American Society of Civil Engineers.

JEFFERYS, E. R. and M. H. PATEL, 1981, "Dynamic Analysis Models of the Tension Leg Platform," *Proceedings, 13th Annual Offshore Technology Conference*, Houston, Texas, 1981, Volume III, Paper OTC 4075, pp. 99-107.

JONSSON, I.G., 1980, "A New Approach to Oscillatory Rough Turbulent Boundary Layers," *Ocean Engineering*, Volume 7, Number 1, pp. 109-152 plus Tables in Number 4, pp. 567-570.

KIRKEGAARD, J., S. E. SAND, N.-E. OTTESEN HANSEN and M. HVIDBERG-KNUDSEN, 1980, "Effects of Directional Sea in Model Testing," *Proceedings, Ports '80*, Norfolk, Virginia, pp. 597-613. New York: American Society of Civil Engineers.

LUNDGREN, H., O. BRINK-KJÆR, S. E. Sand and V. JACOBSEN, 1979, "Improved Physical Basis of Wave Forces," *Proceedings of the Specialty Conference Civil Engineering in the Oceans IV*, San Francisco, California, 1979, Volume 1, pp. 1-16. New York: American Society of Civil Engineers.

LØKEN, A. E. and O. A. OLSEN, 1979, "The Influence of Slowly Varying Wave Forces on Mooring Systems," *Proceedings, 11th Annual Offshore Technology Conference*, Houston, Texas, 1979, Volume IV, Paper OTC 3626, pp. 2325-2335.

MAULL, D. J. and M. G. MILLINER, 1978, "Sinusoidal Flow Past a Circular Cylinder," *Coastal Engineering*, Volume 2, Number 2, pp. 149-168.

NEWMAN, J. N., 1975, "Second-order, Slowly-varying Forces on Vessels in Irregular Waves," *International Symposium on The Dynamics of Marine Vehicles and Structures in Waves*, London, England, 1974, Paper 19, pp. 182-186. London, England: The Institution of Mechanical Engineers.

OTTESEN HANSEN, N.-E., S. E. SAND, H. LUNDGREN, T. SORENSEN and H. GRAVESEN, 1981, "Correct Reproduction of Group-Induced Long Waves," *Proceedings, 17th Coastal Engineering Conference*, Sydney, Australia, 1980, Volume I, Chapter 48, pp. 784-800. New York: American Society of Civil Engineers.

PIJFERS, J. G. L. and A. W. BRINK, 1977, "Calculated Drift Forces of Two Semisubmersible Platfo Types in Regular and Irregular Waves," *Proceedings, 9th Annual Offshore Technology Conference*, Houston, Texas, 1977, Volume IV, Paper OTC 2977, pp. 155-164.

PINKSTER, J. A., 1980, *Low Frequency Second Order Wave Exciting Forces on Floating Structures*, Netherlands Ship Model Basin, Wageningen, Netherlands, Publication Number 650.

RAINEY, R. C. T., 1978, "The Dynamics of Tethered Platforms," *Transactions of The Royal Institution of Naval Architects*, Meeting, Royal Institution of Naval Architects, 1977, Volume 120, pp. 59-80.

RAINEY, R. C. T., 1981, "Parasitic Motions of Offshore Structures," *The Royal Institution of Naval Architects*, Volume 123, pp. 177-194.

RICHARDSON, J. R., 1979, *Mathieu Instabilities and Response of Compliant Offshore Structures*, National Maritime Institute, Feltham, England, Report NMI R49.

SAND, S. E., 1979, *Three-Dimensional Deterministic Structure of Ocean Waves*, PhD Thesis, Instit of Hydrodynamics and Hydraulic Engineering, Technical University of Denmark, Series Paper 24.

SAND, S. E., 1982a, "Long Waves in Directional Seas," *Coastal Engineering*, in press.

SAND, S. E., 1982b, "Short and Long Wave Directional Spectra," *Proceedings, ASCE & ECOR Internc tional Symposium Directional Wave Spectra Applications '81*, Berkeley, California, 12 pp.

SAND, S. E., 1982c, "Long Wave Problems in Laboratory Models," Submitted to *Journal of the Wate way, Port, Coastal and Ocean Division*. New York: American Society of Civil Engineers.

SAND, S. E. and H. LUNDGREN, 1981, "Selection and Three-Dimensional Reproduction of Wave Record that give Maximum Ship Motions," *Proceedings, International Symposium on Hydrodynamics in Ocea Engineering*, Trondheim, Norway, 1981, Volume 1, pp. 101-120. Trondheim, Norway: The Norwegian Institute of Technology.

SEBASTIANI, G., A. D. GRECA and G. BUCANEVE, 1981, "Characteristics and Dynamic Behaviour of Technomare's Tension Leg Platform," *Proceedings, International Symposium on Hydrodynamics in Ocean Engineering*, Trondheim, Norway, 1981, Volume 2, pp. 947-961. Trondheim, Norway: The Nor wegian Institute of Technology.

SKOVGAARD, O. and I. G. JONSSON, 1981, "Computation of Wave Fields in the Ocean Around an Islan *International Journal for Numerical Methods in Fluids*, Volume 1, pp. 237-272.

SPANGENBERG, S. and B. KOFOED JACOBSEN, 1981, "The Effect of Wave Grouping on Slow Drift Oscill tions of an Offshore Structure," *Proceedings, International Symposium on Ocean Engineering-Shi Handling*, Gothenburg, Sweden, 1980, Paper 8, pp. 1-14. Gothenburg, Sweden: Swedish Maritime Research Centre, SSPA.

WICHERS, J. E. W., 1979, "Slowly Oscillating Mooring Forces in Single Point Mooring Systems," *Proceedings, 2nd International Conference on Behaviour of Off-Shore Structures*, London, England 1979, Volume 3, Paper 27, pp. 661-692. Cranfield, Bedford, England: BHRA Fluid Engineering.

WICHERS, J. E. W. and M. F. VAN SLUIJS, 1979, "The Influence of Waves on the Low-Frequency Hydr dynamic Coefficients of Moored Vessels," *Proceedings, 11th Annual Offshore Technology Conferen* Houston, Texas, 1979, Volume IV, Paper OTC 3625, pp. 2313-2324.

Danish Society of Hydraulic Engineering

Seminar on Recent Development within Offshore Design and Systems

Copenhagen, 11th February 1988

FREAK WAVES AND FREAK WAVE GROUPS

by Helge Gravesen, Dansk Geoteknik as, Carl Bro Group
Granskoven 6, DK 2600 Glostrup.

and Per Klinting, Danish Hydraulic Institute
Agern Alle 5, DK 2570 Hørsholm.

LIST OF CONTENTS

1. INTRODUCTION

The present paper gives a brief status of the results of recent years research on natural 3 dimensional waves with emphasis on the consequences on important design aspects for fixed and floating structures.

2. 2D/3D WAVES

2.1 2-dimensional design waves

Stokes 5 order wave

Below an example of the tradional used stokes 5 order waves is shown. The assumed maximum wave and current induced design velocity is shown on fig. 2.1 and 2.2 for a wave heigth H=20.5 m and an associated wave period T=14.5 sec. for a structure of a water depth of h=42 m.

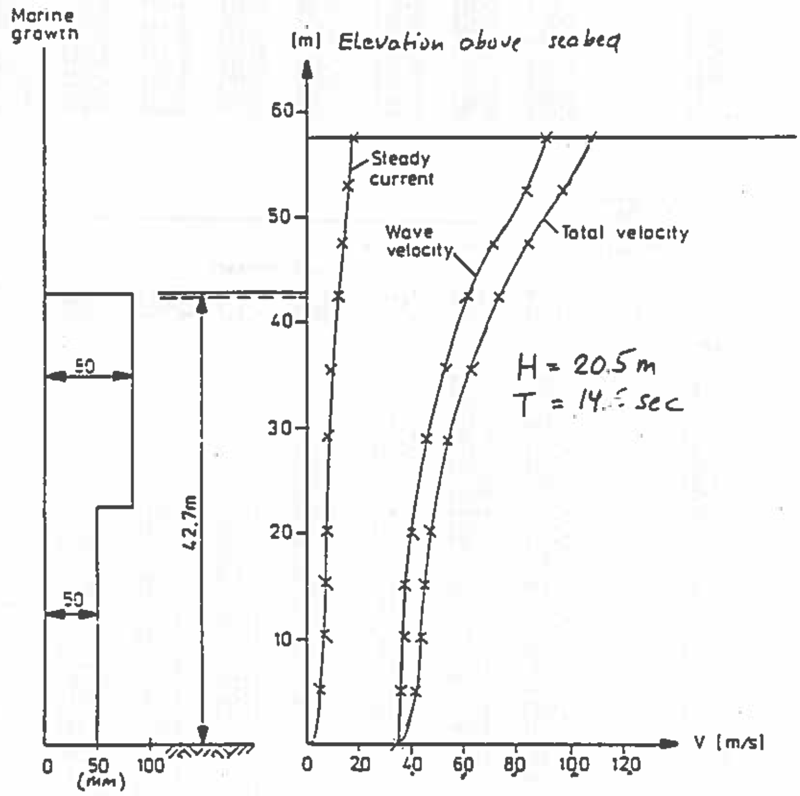

Fig. 2.1 Design Velocities and Marine Growth.

RAMBOLL & HANNEMANN
PROGRAM POSA
2-JUL-
KL. 10:

WAVE HEIGHT=20.5 M   WAVE PERIOD=14.5 S

V E R T I C A L   V E L O C I T Y   (EXCLUDE CURRENT)

X-COORD. (M)	0.00	11.61	23.23	34.84	46.45	58.06	69.68	81.29	92.90	104.51	116.13	127.74
SURFACE (M)	13.46	12.23	9.13	5.60	2.06	-0.57	-2.40	-4.16	-5.27	-6.01	-6.53	-6.90
SUR.VEL. (M/S)	0.000	2.646	4.300	4.795	4.530	3.691	3.124	2.384	1.746	1.217	0.760	0.372
Z-COORD. (M)												
13.46												
12.21	0.000	[illegible]										
10.96	0.000	[illegible]										
9.71	0.000	[illegible]										
8.47	0.000	[illegible]	4.195									
7.22	0.000	[illegible]	4.005									
5.97	0.000	[illegible]	3.823									
4.72	0.000	[illegible]	[illegible]	4.478								
3.47	0.000	[illegible]	[illegible]	4.470								
2.23	0.000	[illegible]	[illegible]	4.271								
0.98	0.000	[illegible]	[illegible]	4.079	4.363							
-0.27	0.000	[illegible]	[illegible]	[illegible]	4.177							
-1.52	0.000	[illegible]	[illegible]	[illegible]	[illegible]	[illegible]						
-2.77	0.000	[illegible]	[illegible]	[illegible]	[illegible]	[illegible]	[illegible]					
-4.01	0.000	[illegible]	[illegible]	[illegible]	[illegible]	[illegible]	[illegible]					
-5.26	0.000	[illegible]	[illegible]	[illegible]	[illegible]	[illegible]	[illegible]	[illegible]				
-6.51	0.000	[illegible]	[illegible]	[illegible]	[illegible]	[illegible]	[illegible]	[illegible]	[illegible]	[illegible]		
-7.76	0.000	[illegible]	[illegible]	[illegible]	[illegible]	[illegible]	[illegible]	[illegible]	[illegible]	[illegible]	[illegible]	[illegible]
-9.01	0.000	[illegible]	[illegible]	[illegible]	[illegible]	[illegible]	[illegible]	[illegible]	[illegible]	[illegible]	[illegible]	[illegible]
-10.25	0.000	[illegible]	[illegible]	[illegible]	[illegible]	[illegible]	[illegible]	[illegible]	[illegible]	[illegible]	[illegible]	[illegible]
-11.50	0.000	[illegible]	[illegible]	[illegible]	[illegible]	[illegible]	[illegible]	[illegible]	[illegible]	[illegible]	[illegible]	[illegible]
-12.75	0.000	[illegible]	[illegible]	[illegible]	[illegible]	[illegible]	[illegible]	[illegible]	[illegible]	[illegible]	[illegible]	[illegible]
-14.00	0.000	[illegible]	[illegible]	[illegible]	[illegible]	[illegible]	[illegible]	[illegible]	[illegible]	[illegible]	[illegible]	[illegible]
-15.25	0.000	[illegible]	[illegible]	[illegible]	[illegible]	[illegible]	[illegible]	[illegible]	[illegible]	[illegible]	[illegible]	[illegible]
-16.49	0.000	[illegible]	[illegible]	[illegible]	[illegible]	[illegible]	[illegible]	[illegible]	[illegible]	[illegible]	[illegible]	[illegible]
-17.74	0.000	[illegible]	[illegible]	[illegible]	[illegible]	[illegible]	[illegible]	[illegible]	[illegible]	[illegible]	[illegible]	[illegible]
-18.99	0.000	[illegible]	[illegible]	[illegible]	[illegible]	[illegible]	[illegible]	[illegible]	[illegible]	[illegible]	[illegible]	[illegible]
-20.24	0.000	[illegible]	[illegible]	[illegible]	[illegible]	[illegible]	[illegible]	[illegible]	[illegible]	[illegible]	[illegible]	[illegible]
-21.49	0.000	[illegible]	[illegible]	[illegible]	[illegible]	[illegible]	[illegible]	[illegible]	[illegible]	[illegible]	[illegible]	[illegible]
-22.73	0.000	[illegible]	[illegible]	[illegible]	[illegible]	[illegible]	[illegible]	[illegible]	[illegible]	[illegible]	[illegible]	[illegible]
-23.98	0.000	[illegible]	[illegible]	[illegible]	[illegible]	[illegible]	[illegible]	[illegible]	[illegible]	[illegible]	[illegible]	[illegible]
-25.23	0.000	[illegible]	[illegible]	[illegible]	[illegible]	[illegible]	[illegible]	[illegible]	[illegible]	[illegible]	[illegible]	[illegible]
-26.48	0.000	[illegible]	[illegible]	[illegible]	[illegible]	[illegible]	[illegible]	[illegible]	[illegible]	[illegible]	[illegible]	[illegible]
-27.73	0.000	[illegible]	[illegible]	[illegible]	[illegible]	[illegible]	[illegible]	[illegible]	[illegible]	[illegible]	[illegible]	[illegible]
-28.97	0.000	[illegible]	[illegible]	[illegible]	[illegible]	[illegible]	[illegible]	[illegible]	[illegible]	[illegible]	[illegible]	[illegible]
-30.22	0.000	[illegible]	[illegible]	[illegible]	[illegible]	[illegible]	[illegible]	[illegible]	[illegible]	[illegible]	[illegible]	[illegible]
-31.47	0.000	[illegible]	[illegible]	[illegible]	[illegible]	[illegible]	[illegible]	[illegible]	[illegible]	[illegible]	[illegible]	[illegible]
-32.72	0.000	[illegible]	[illegible]	[illegible]	[illegible]	[illegible]	[illegible]	[illegible]	[illegible]	[illegible]	[illegible]	[illegible]
-33.96	0.000	[illegible]	[illegible]	[illegible]	[illegible]	[illegible]	[illegible]	[illegible]	[illegible]	[illegible]	[illegible]	[illegible]
-35.21	0.000	[illegible]	[illegible]	[illegible]	[illegible]	[illegible]	[illegible]	[illegible]	[illegible]	[illegible]	[illegible]	[illegible]
-36.46	0.000	[illegible]	[illegible]	[illegible]	[illegible]	[illegible]	[illegible]	[illegible]	[illegible]	[illegible]	[illegible]	[illegible]
-37.71	0.000	[illegible]	[illegible]	[illegible]	[illegible]	[illegible]	[illegible]	[illegible]	[illegible]	[illegible]	[illegible]	[illegible]
-38.96	0.000	0.105	0.196	0.259	[illegible]	[illegible]	0.264	0.226	0.177	0.130	0.084	[illegible]
-40.20	0.000	0.070	0.130	0.172	0.195	0.192	0.176	0.149	0.118	0.086	0.056	0.028
-41.45	0.000	0.035	0.065	0.086	0.098	0.096	0.084	0.075	0.059	0.043	0.028	0.014
-42.70	0.000	0.000	0.000	0.000	0.000	0.000	0.000	0.000	0.000	0.000	0.000	0.000

RAMBOLL & HANNEMANN
PROGRAM POSA
2-JUL-
KL. 10:

WAVE HEIGHT=20.5 M   WAVE PERIOD=14.5 S

H O R I Z O N T A L   V E L O C I T Y   (EXCLUDE CURRENT)

X-COORD. (M)	0.00	11.61	23.23	34.84	46.45	58.06	69.68	81.29	92.90	104.51	116.13	127.74
SURFACE (M)	13.46	12.23	9.13	5.60	2.06	-0.57	-2.40	-4.16	-5.27	-6.01	-6.53	-6.70
SUR.VEL. (M/S)	8.867	7.996	5.606	3.565	1.537	-0.047	-1.209	-2.022	-2.383	-2.768	-3.221	-3.365
Z-COORD. (M)												
13.46												
12.21	8.368	7.989										
10.96	8.282	7.728										
9.71	8.009	7.479										
8.47	7.748	7.241	5.812									
7.22	7.500	7.014	5.647									
5.97	7.263	6.797	5.489									
4.72	7.036	6.591	5.338	3.526								
3.47	[illegible]	[illegible]	[illegible]	[illegible]								
2.23	[illegible]	[illegible]	[illegible]	[illegible]								
0.98	[illegible]	[illegible]	[illegible]	[illegible]	1.540							
-0.27	[illegible]	[illegible]	[illegible]	[illegible]	[illegible]							
-1.52	[illegible]	[illegible]	[illegible]	[illegible]	[illegible]	-0.012						
-2.77	[illegible]	[illegible]	[illegible]	[illegible]	[illegible]	[illegible]	-1.200					
-4.01	[illegible]	[illegible]	[illegible]	[illegible]	[illegible]	[illegible]	[illegible]					
-5.26	[illegible]	[illegible]	[illegible]	[illegible]	[illegible]	[illegible]	[illegible]	-1.944				
-6.51	[illegible]	[illegible]	[illegible]	[illegible]	[illegible]	[illegible]	[illegible]	[illegible]	-2.526	-2.968		
-7.76	[illegible]	[illegible]	[illegible]	[illegible]	[illegible]	[illegible]	[illegible]	[illegible]	[illegible]	[illegible]	-3.178	-3.337
-9.01	[illegible]	[illegible]	[illegible]	[illegible]	[illegible]	[illegible]	[illegible]	[illegible]	[illegible]	[illegible]	[illegible]	[illegible]
-10.25	[illegible]	[illegible]	[illegible]	[illegible]	[illegible]	[illegible]	[illegible]	[illegible]	[illegible]	[illegible]	[illegible]	[illegible]
-11.50	[illegible]	[illegible]	[illegible]	[illegible]	[illegible]	[illegible]	[illegible]	[illegible]	[illegible]	[illegible]	[illegible]	[illegible]
-12.75	[illegible]	[illegible]	[illegible]	[illegible]	[illegible]	[illegible]	[illegible]	[illegible]	[illegible]	[illegible]	[illegible]	[illegible]
-14.00	[illegible]	[illegible]	[illegible]	[illegible]	[illegible]	[illegible]	[illegible]	[illegible]	[illegible]	[illegible]	[illegible]	[illegible]
-15.25	[illegible]	[illegible]	[illegible]	[illegible]	[illegible]	[illegible]	[illegible]	[illegible]	[illegible]	[illegible]	[illegible]	[illegible]
-16.49	[illegible]	[illegible]	[illegible]	[illegible]	[illegible]	[illegible]	[illegible]	[illegible]	[illegible]	[illegible]	[illegible]	[illegible]
-17.74	[illegible]	[illegible]	[illegible]	[illegible]	[illegible]	[illegible]	[illegible]	[illegible]	[illegible]	[illegible]	[illegible]	[illegible]
-18.99	[illegible]	[illegible]	[illegible]	[illegible]	[illegible]	[illegible]	[illegible]	[illegible]	[illegible]	[illegible]	[illegible]	[illegible]
-20.24	[illegible]	[illegible]	[illegible]	[illegible]	[illegible]	[illegible]	[illegible]	[illegible]	[illegible]	[illegible]	[illegible]	[illegible]
-21.49	[illegible]	[illegible]	[illegible]	[illegible]	[illegible]	[illegible]	[illegible]	[illegible]	[illegible]	[illegible]	[illegible]	[illegible]
-22.73	[illegible]	[illegible]	[illegible]	[illegible]	[illegible]	[illegible]	[illegible]	[illegible]	[illegible]	[illegible]	[illegible]	[illegible]
-23.98	[illegible]	[illegible]	[illegible]	[illegible]	[illegible]	[illegible]	[illegible]	[illegible]	[illegible]	[illegible]	[illegible]	[illegible]
-25.23	[illegible]	[illegible]	[illegible]	[illegible]	[illegible]	[illegible]	[illegible]	[illegible]	[illegible]	[illegible]	[illegible]	[illegible]
-26.48	[illegible]	[illegible]	[illegible]	[illegible]	[illegible]	[illegible]	[illegible]	[illegible]	[illegible]	[illegible]	[illegible]	[illegible]
-27.73	[illegible]	[illegible]	[illegible]	[illegible]	[illegible]	[illegible]	[illegible]	[illegible]	[illegible]	[illegible]	[illegible]	[illegible]
-28.97	[illegible]	[illegible]	[illegible]	[illegible]	[illegible]	[illegible]	[illegible]	[illegible]	[illegible]	[illegible]	[illegible]	[illegible]
-30.22	[illegible]	[illegible]	[illegible]	[illegible]	[illegible]	[illegible]	[illegible]	[illegible]	[illegible]	[illegible]	[illegible]	[illegible]
-31.47	[illegible]	[illegible]	[illegible]	[illegible]	[illegible]	[illegible]	[illegible]	[illegible]	[illegible]	[illegible]	[illegible]	[illegible]
-32.72	[illegible]	[illegible]	[illegible]	[illegible]	[illegible]	[illegible]	[illegible]	[illegible]	[illegible]	[illegible]	[illegible]	[illegible]
-33.96	[illegible]	[illegible]	[illegible]	[illegible]	[illegible]	[illegible]	[illegible]	[illegible]	[illegible]	[illegible]	[illegible]	[illegible]
-35.21	[illegible]	[illegible]	[illegible]	[illegible]	[illegible]	[illegible]	[illegible]	[illegible]	[illegible]	[illegible]	[illegible]	[illegible]
-36.46	[illegible]	[illegible]	[illegible]	[illegible]	[illegible]	[illegible]	[illegible]	[illegible]	[illegible]	[illegible]	[illegible]	[illegible]
-37.71	[illegible]	[illegible]	[illegible]	[illegible]	[illegible]	[illegible]	[illegible]	[illegible]	[illegible]	[illegible]	[illegible]	[illegible]
-38.96	[illegible]	[illegible]	[illegible]	[illegible]	[illegible]	[illegible]	[illegible]	[illegible]	[illegible]	[illegible]	[illegible]	[illegible]
-40.20	[illegible]	[illegible]	[illegible]	[illegible]	[illegible]	[illegible]	[illegible]	[illegible]	[illegible]	[illegible]	[illegible]	[illegible]
-41.45	[illegible]	[illegible]	[illegible]	[illegible]	[illegible]	[illegible]	[illegible]	[illegible]	[illegible]	[illegible]	[illegible]	[illegible]
-42.70	[illegible]	3.421	2.950	2.239	1.382	[illegible]	-0.381	-1.139	[illegible]	[illegible]	[illegible]	[illegible]

Fig. 2.2 Design Velocities, stokes 5 order theory.

But the velocity fixed is not 2-dimensional but 3-dimensional as it can be seen on fig. 2.3.

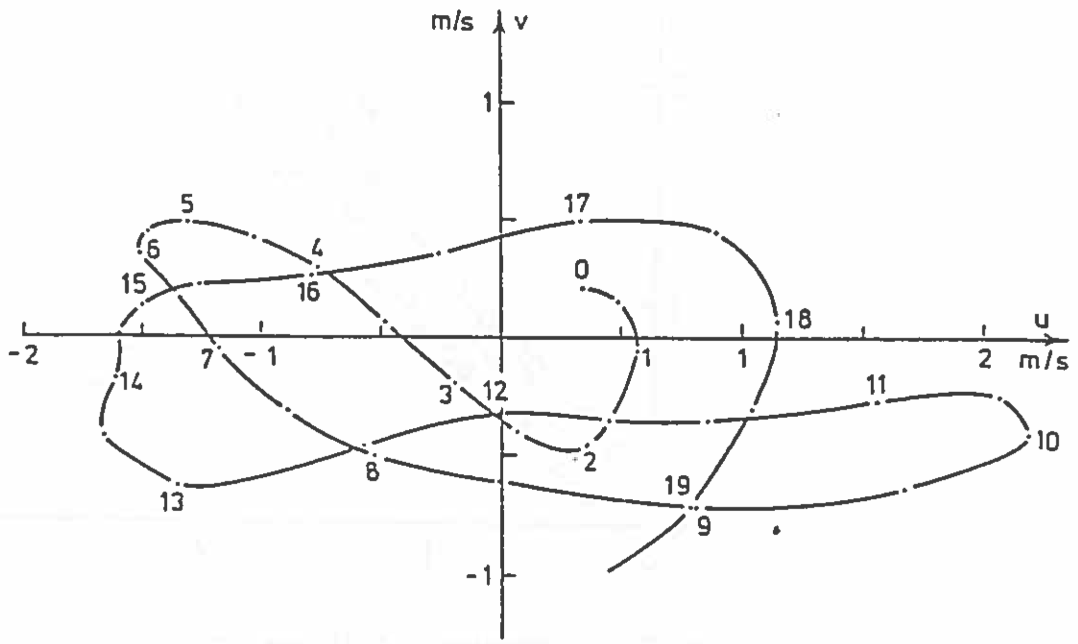

Fig. 2.3 Time history of the horizontal velocity vector measured at the top current meter the largest wave (Forristall et al.)

Fig. 2.4 and 2.5 show a comparison between the measured 3D wave velocities and the corresponding theoretical values obtained by using Stokes 5 order theory on the determined single maximum waves and corresponding period. The comparison shows a significant tendensy to overestimate at the wave crest by using Stokes 5 order theory. But the overestimate is reduced above still water level.

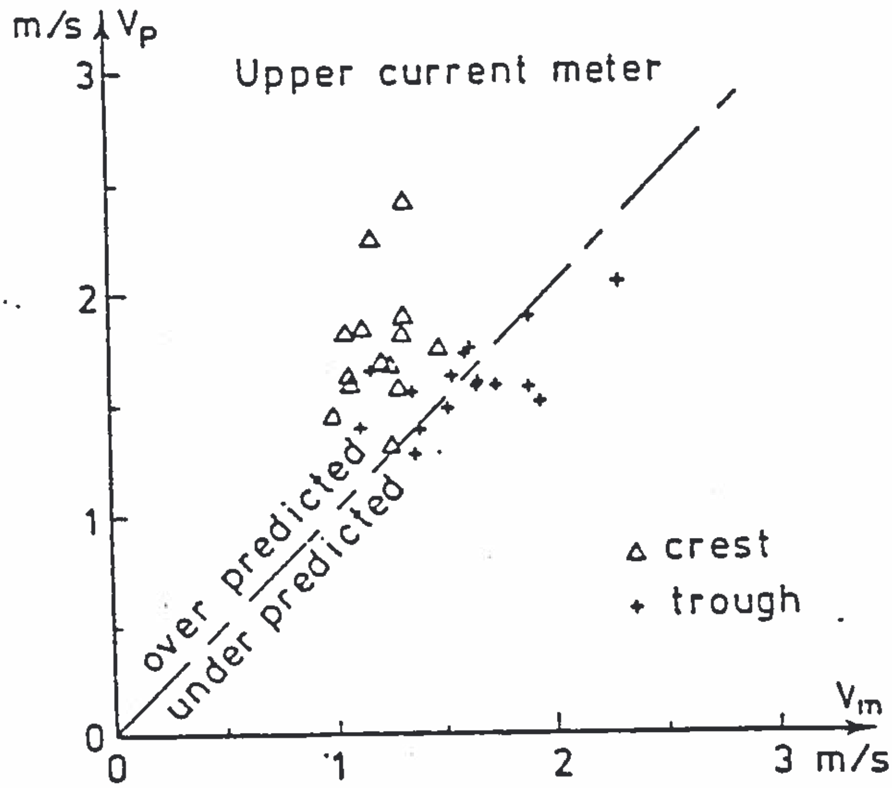

Fig. 2.4 Comparison of Stokes' fifth order to measured maximum velocities during the largest waves for top current meter (Forristall et al.).

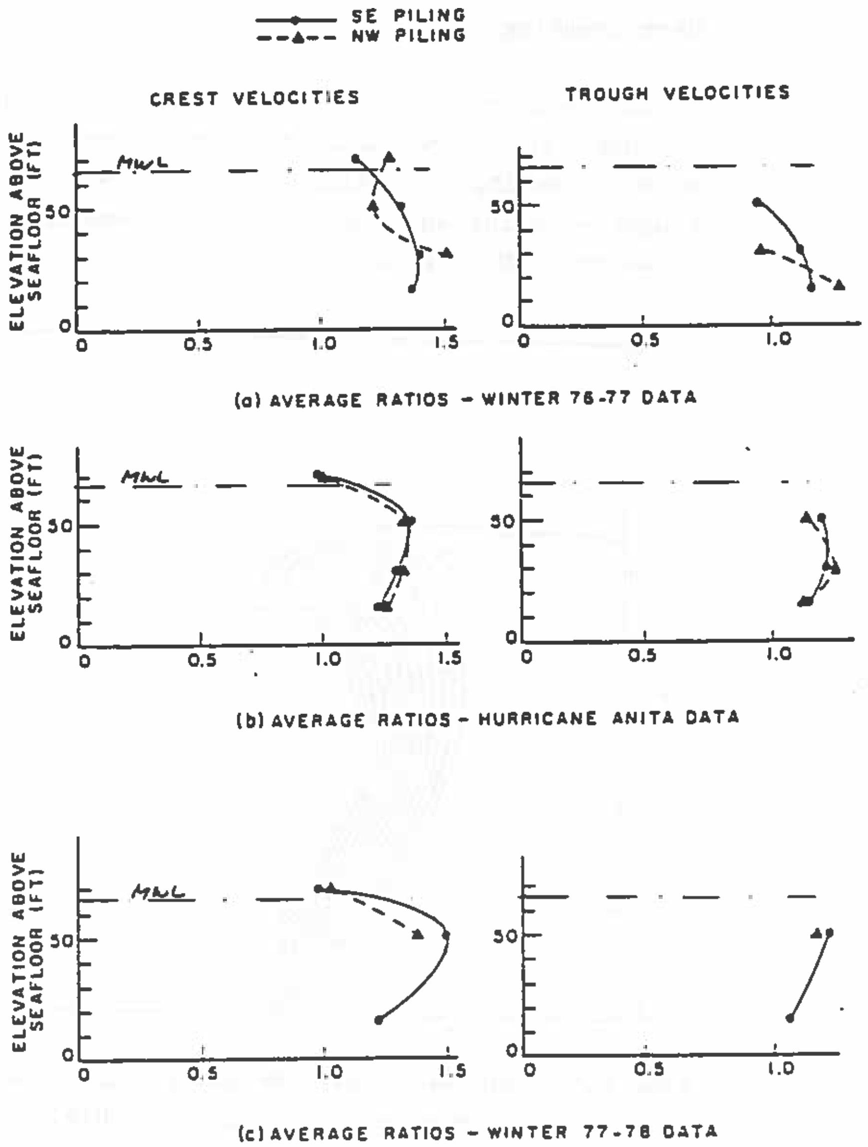

Fig. 2.5 Average of Ratios for Stokes to Measured In-line Velocities under Crest and Though. OTS (1976-78).

2.2 Wave Breaking

At intermidiate and deep water it has not been usual to design offshore structures with account to the risk of deep water wave breaking. Allready in 1976 some researh by Longest-Higgins and Cokelet showed example of deep water wave breaking (2-D)(fig. 2.6).

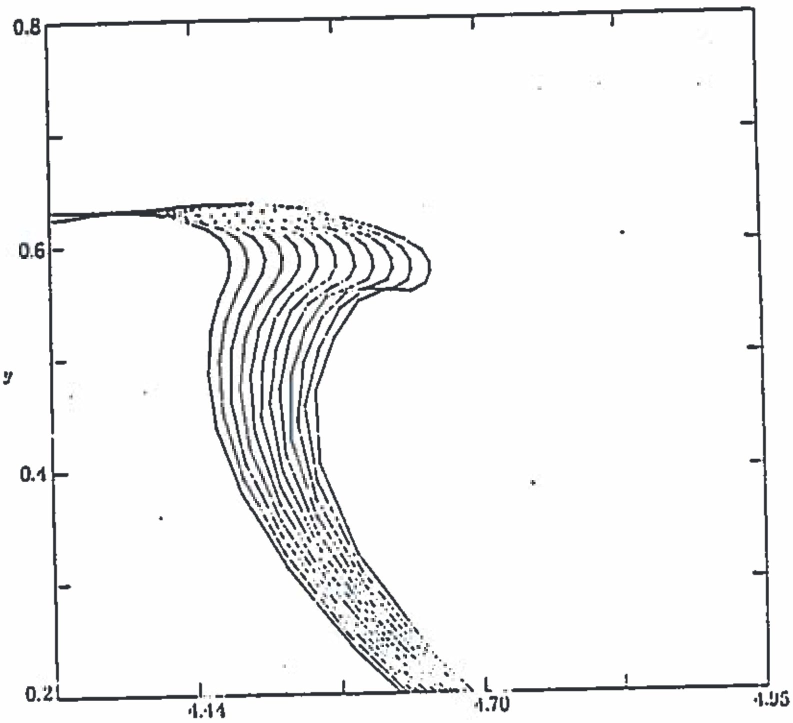

Fig. 2.6 Deep water wave breaking. Details of the wave crest trajetories. (Longuet-Higgings and Cokelet (1976)).

Fig. 2.7 and 2.8 show two examples of velocity and acceleration vector fields with maximum velocity equal to 1.24 $(g/k)^{1/2}$ and maximum acceleration equal to 0.89 g (Peregrine (1978).

Other reseach have shown examples of surface jets with even larger acceleration (up to 3 g).

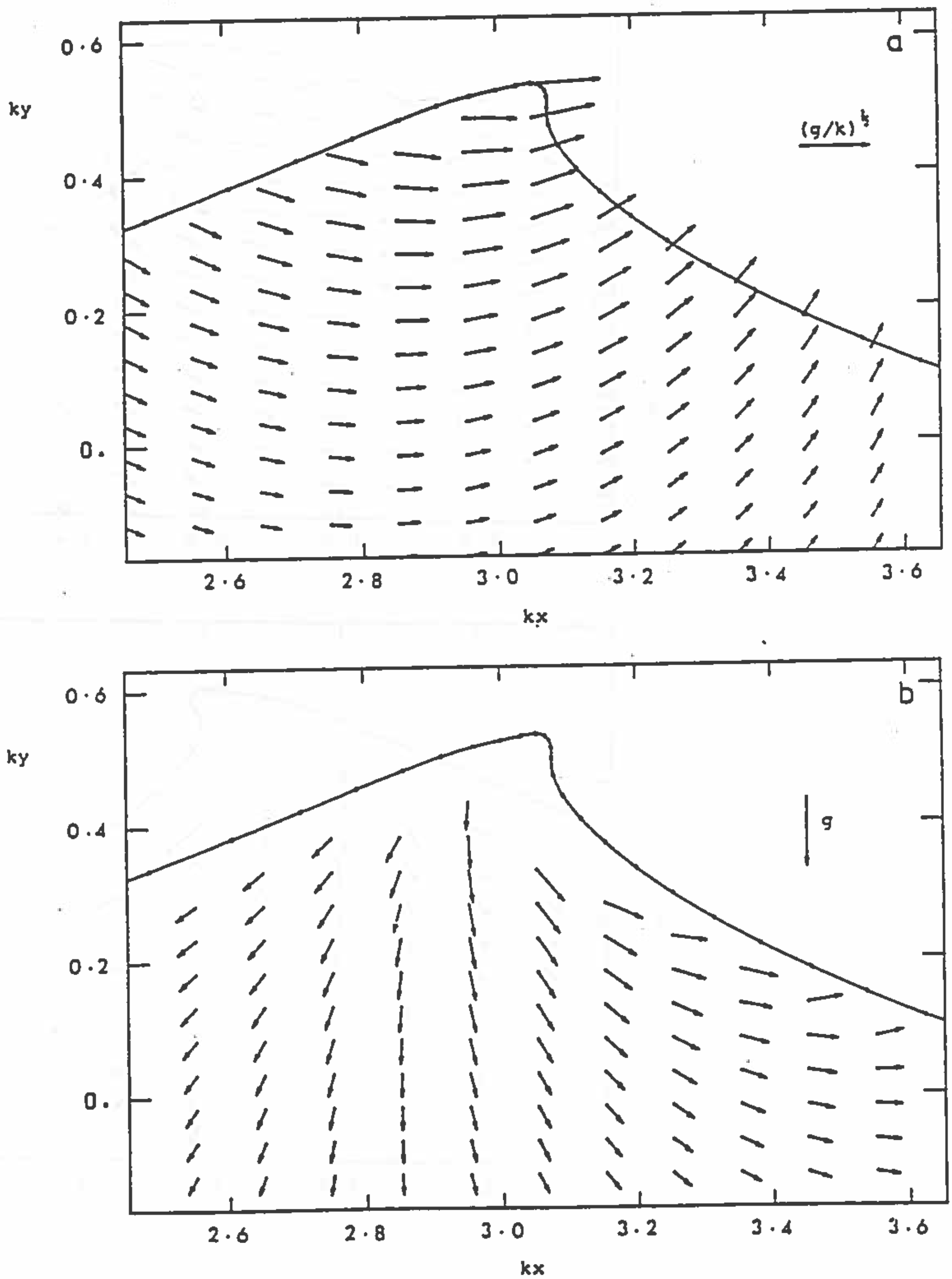

Fig. 2.7 Wave breaking (wave initiated as steep sinus wave). (Cokelet (1978), H/L ~ 0.10).

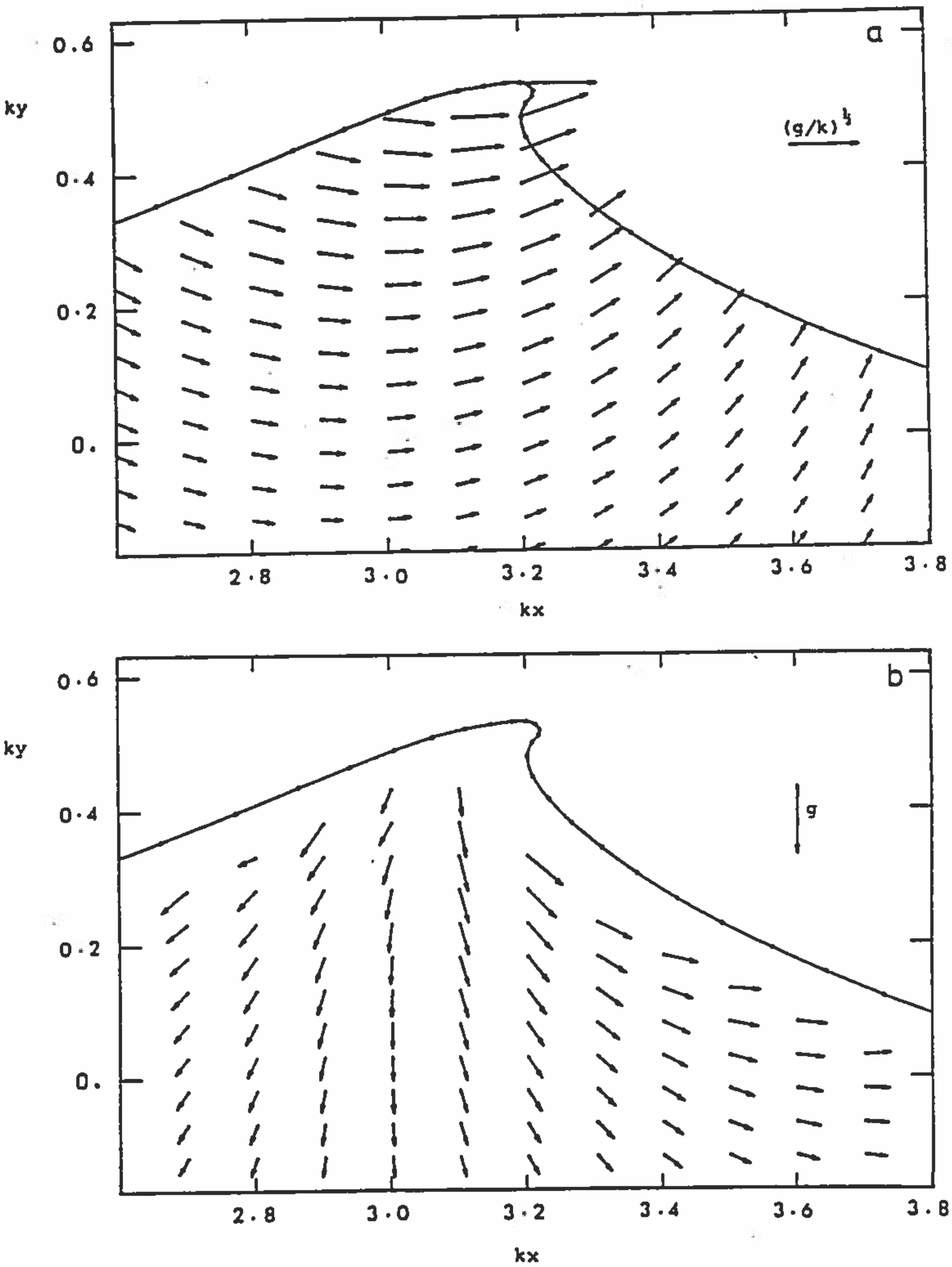

Fig. 2.8 Like fig. 2.7 but a moment later.

2.3 Pilot investigations on freak waves (by Lundgren 1984)

Freak wave are defined as waves having significant larger crest elevation than they were expected to have based upon the corresponding significant wave height.

Fig. 2.9 originates from a record in the North Sea taken by means of a radar on a fixed platform.

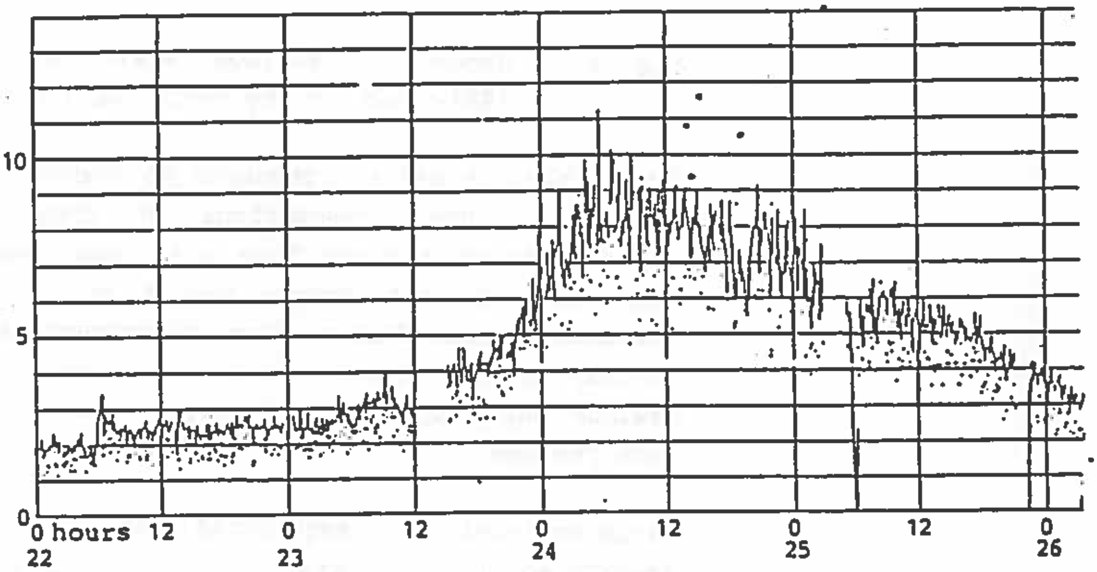

Fig. 2.9 Storm in the North Sea (Gorm Field), Nov. 22-26, 1981. The line indicates H_s (in metres). The dots represent the maximum crest elevations.

Fig. 2.9 shows the variation of H_s (computed for short intervals), as well as the maximum crest elevations. Generally, the latter were less than the H_s-values. After the culmination of the storm during November 24, however, some crest elevations exceeded H_s. The extreme crest, which exceeded 14 m, appeared at 2.31 a.m. on November 25, when $H_s \sim$ 6.5 m, cf. fig. 2.10. This 17 m high wave was a freak wave with 75% of its height above MWL (at about +1.5 m).

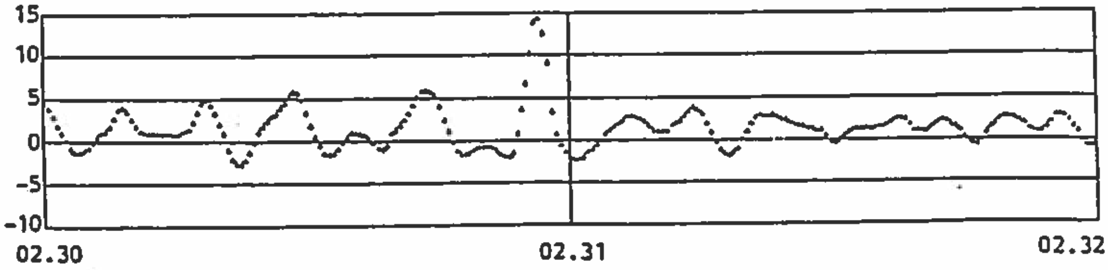

Fig. 2.10 Record of surface elevation during the storm 1981-11-25 in the North Sea (Gorm Field).

Presumably, it had a pronounced 3D character, i.e. very short crested. Other obsrvations of freak waves after the culmination of a storm have also been reported. Since the components in the longer period part of the short wave spectrum travel faster than contributions around the peak period, it is possible that such components from the storm maximum catch up with each other and form a freak wave by interference.

Large uncertainty is associated with the question: .ow is the associated velocity distribution for freak waves since an extreme large wave height may easily be generated by crossing wave field but withoutimplying that the extreme velocity obtain corresponding high values.

3. 2D/3D WAVE FORCES ON VERTICAL CYLINDER

This section mainly describes results from research project carried out supported by the Ministry of Energy (EFP 1980) by ISH, R&H, SL and DHI.

The instrumented cylinder used in the project is shown on fig. 3.1.

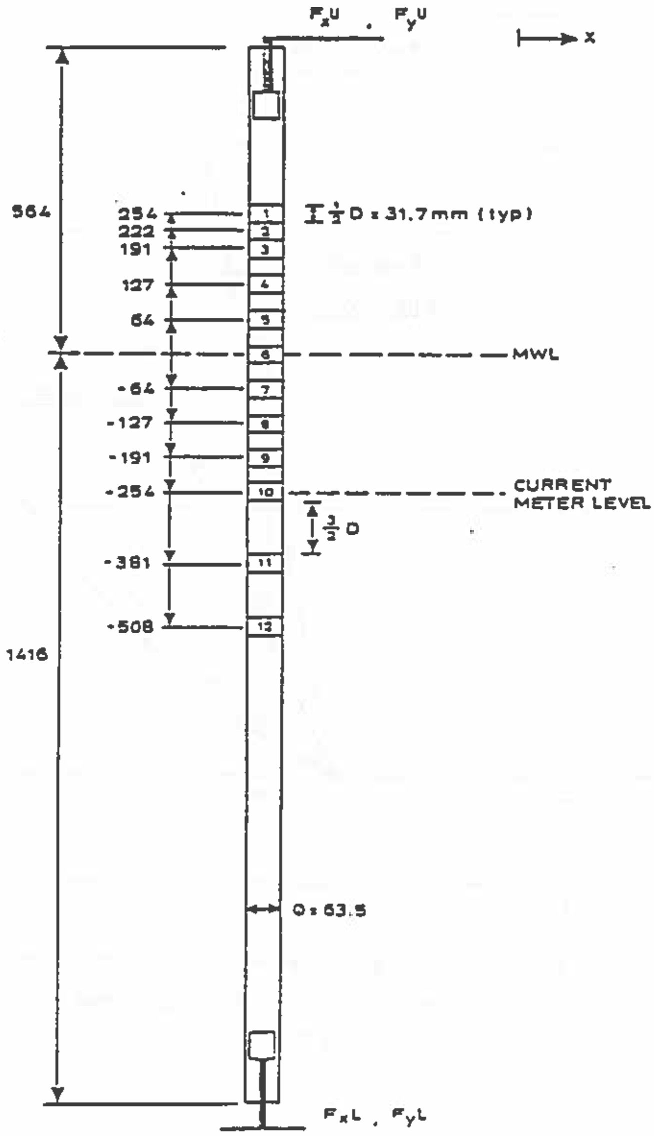

Fig. 3.1 Instrumented cylinder (Measures in mm).

The results are of cause influenced by scale effects, but a relative comparison between 2D and 3D waves is less influenced by scale effects. Fig. 3.2 show the cummulated distribution of maximum wave loads.

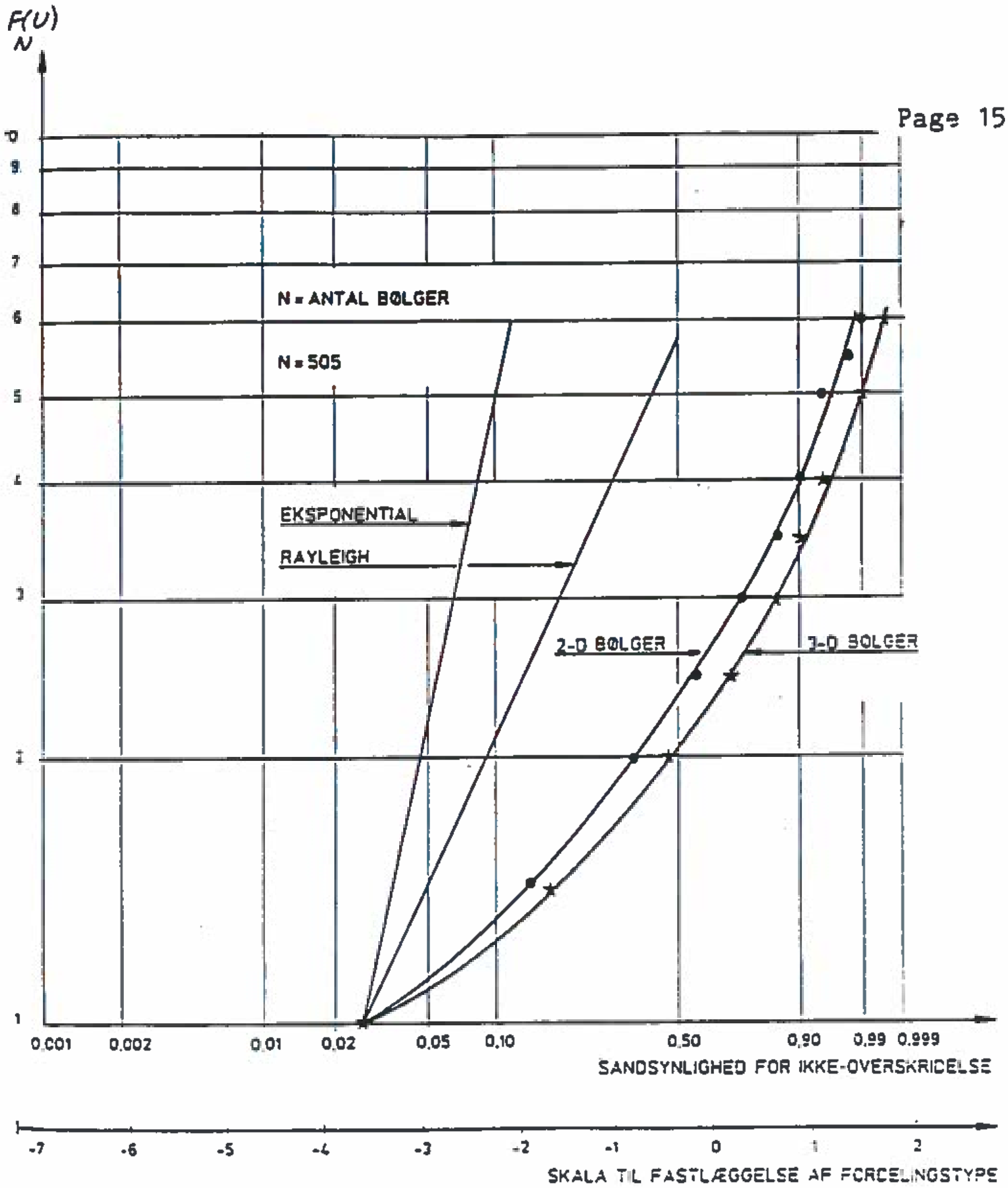

Fig. 3.2 Cumulated distributions for maximum wave loads for respectively 2D and 3D waves.
H_s = 0.25 m T_p = 2.2 s, JONSWAP Spektrum.

The significant loads are compared as shown in tabel 3.1

Model wave condition			F_xU RMS (N)		Ratio between 3D and 2D
H_s (m)	T_p (s)	Spectrum	2D	3D	
0.25	2.2	JONSWAP	1.46	1.23	0.84
0.25	2.2	PM	1.46	1.27	0.87
0.20	1.5	JONSWAP	1.41	1.22	0.87
0.20	1.7	PM	1.33	1.18	0.88

Tabel 3.1 Ratio between significant wave loads for respectively 2D and 3D wave (total forces) in wave direction.

The study report concludes that with respect to fatigue loads it is confirmed that the 2D design load is 15% larger than the more realistic 3D load.

With respect to the extreme design load the report recommend further studies because sufficient accurate theories do not exist and because visual observations offshore have indicated risk for even extreme nearly 2D long crested waves (see fig. 3.3).

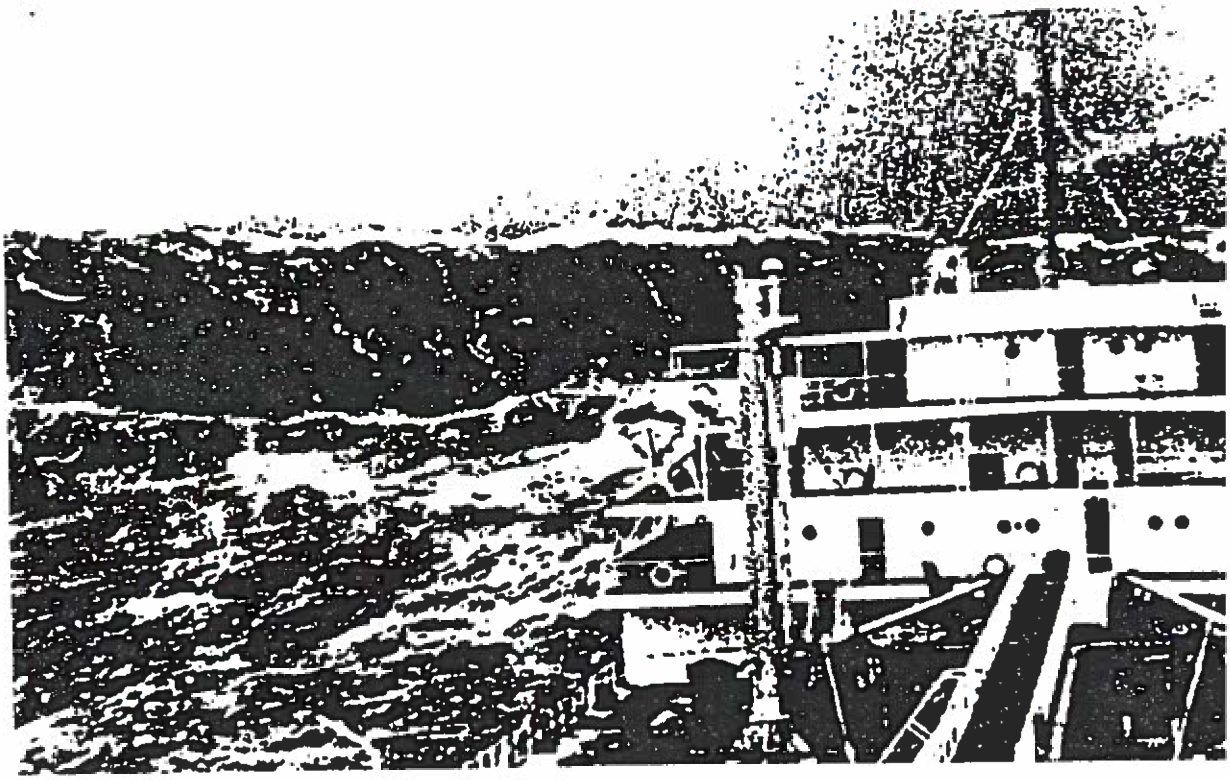

Fig. 3.3 Extreme large and steep longcrested wave seen from unidentified ship Publisched in "Surveyor" May 1968.

4. 2D/3D WAVES: FLOATING STRUCTURES

4.1 Semisubmersible (from Sand at al. (1987))

Heave, Pitch, Roll in Operational Condition

The tests in operational condition generally confirmed the expectation that the in-line motions (surge and pitch in head seas) decrease in 3D waves, and that the transverse motions (sway and roll) increase.

A closer look at the response spectra for heave, roll and pitch reveals that the major part of the difference between 2D and 3D waves is concentrated around the natural frequencies of the vertical motions. This is illustrated in Figs. 4.1, 4.2 and 4.3 which show the heave, roll and pitch response spectra in 2D/3D operationel condition for head sea.

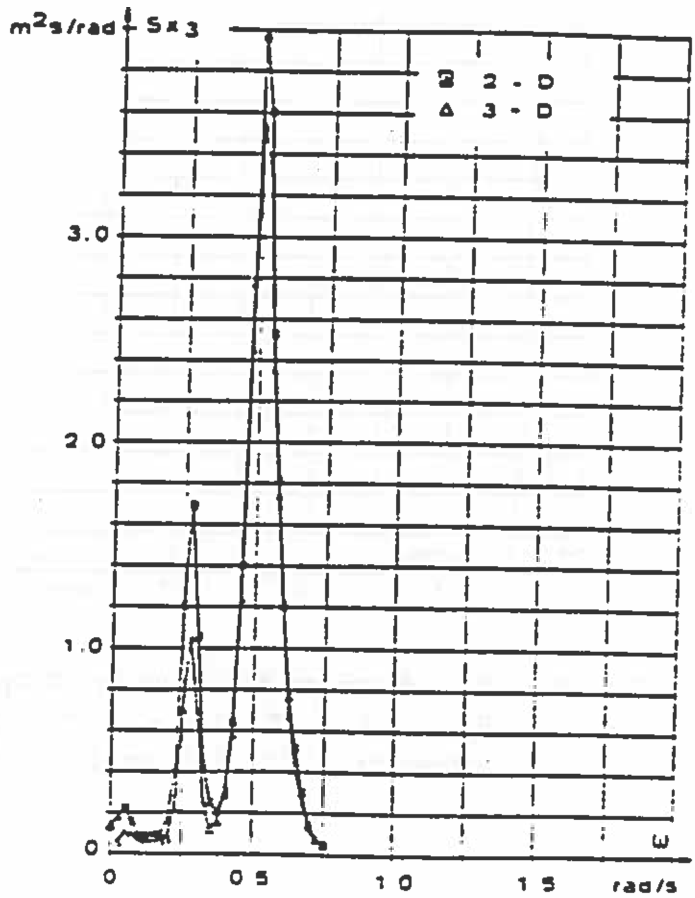

Fig. 4.1 Heave Response Spectra in 2D/3D Operational Condition, H_s = 8.8, T_p = 12.3 s. Head Seas.

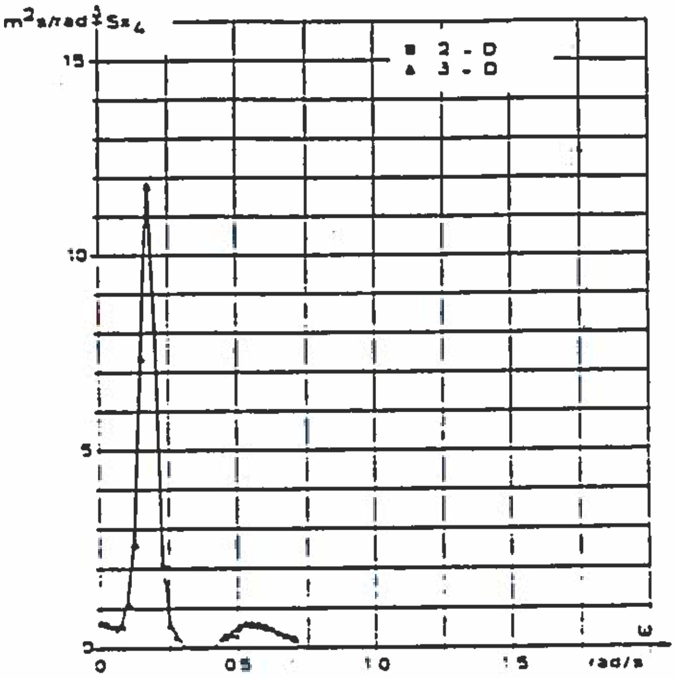

Fig. 4.2 Roll Response Spectrum in 3D Operational Condition, H_s = 8.8 m, T 12.3 s. (The 2D response does not appear at all in this scale). Head Seas.

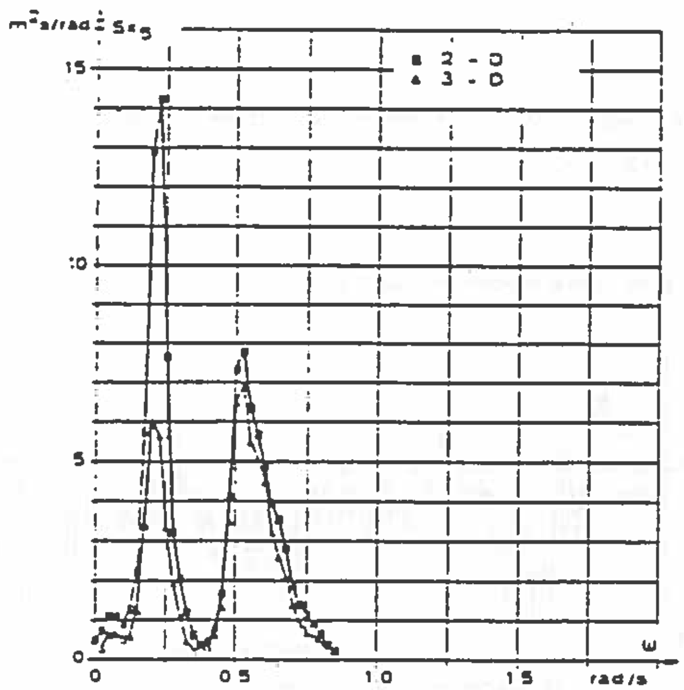

Fig. 4.3 Pitch Response Spectra in 2D/3D Operational Condition, H_s = 8.8 m, T_p = 12.3 s. Head Seas.

The sensitivity of mooring force to 2D/3D wave is illustrated on fig. 4.4.

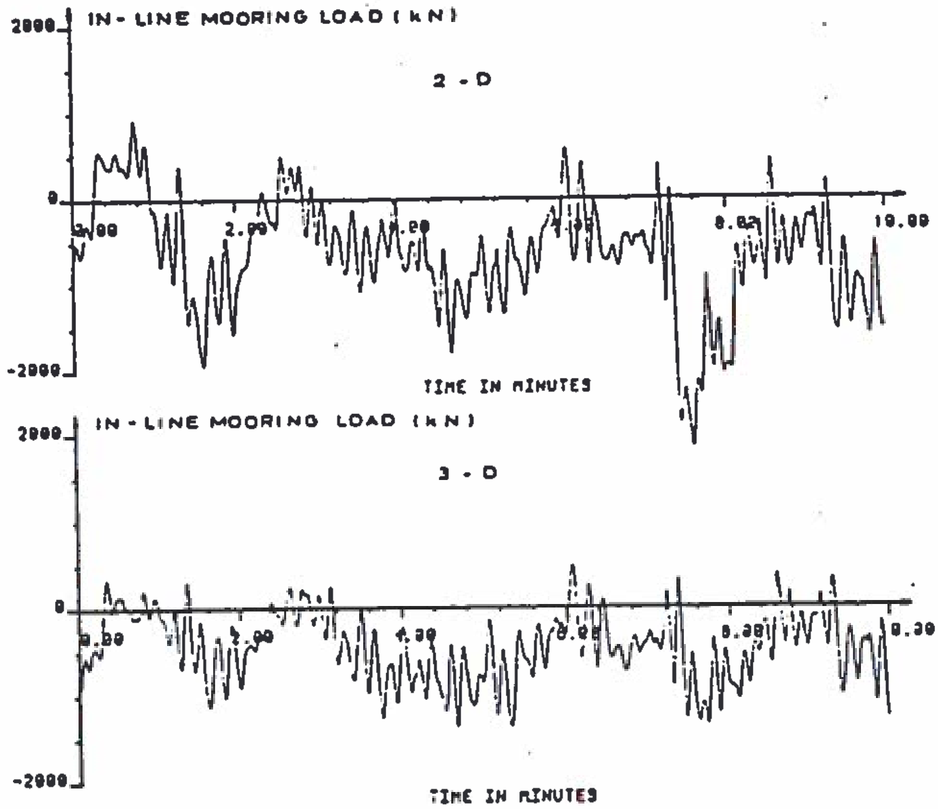

Fig. 4.4 Illustration fo Synchronized Mooring Loads in 2D and 3D waves due to the Deterministic Wave Reproduction Technique (operational condition H_s = 8.8 m, T_p = 12.3 s).

4.2 Floating production barge (Compass)

(See Kirkegaard, Sand and Denise (1986))

Another example is a floating production barge, fig. 4.5. The reference gives a detailed comparision on the effect of 3 D waves tc 2 D waves.

This case is specially interesting because the force response here is found to be extreme sensitive to the combination of current, wind and wave direction. A small direction change (see Y-component of velocity in fig. 4.7 and 4.8) result in a significant change in the maximum force experienced. Note that the direction of wave 2 is towards the vessel while wave 1 travels more along the vessel. The forces are dominated by a combination of long period motion effect superimposed by wave frequency dominated snap loads. The long period motion gives rise to varying stiffness of the mooring system. This because that the mooring force for a certain wave will be higher when the vessel is in an extreme position (when wave 2 hits the vessel)

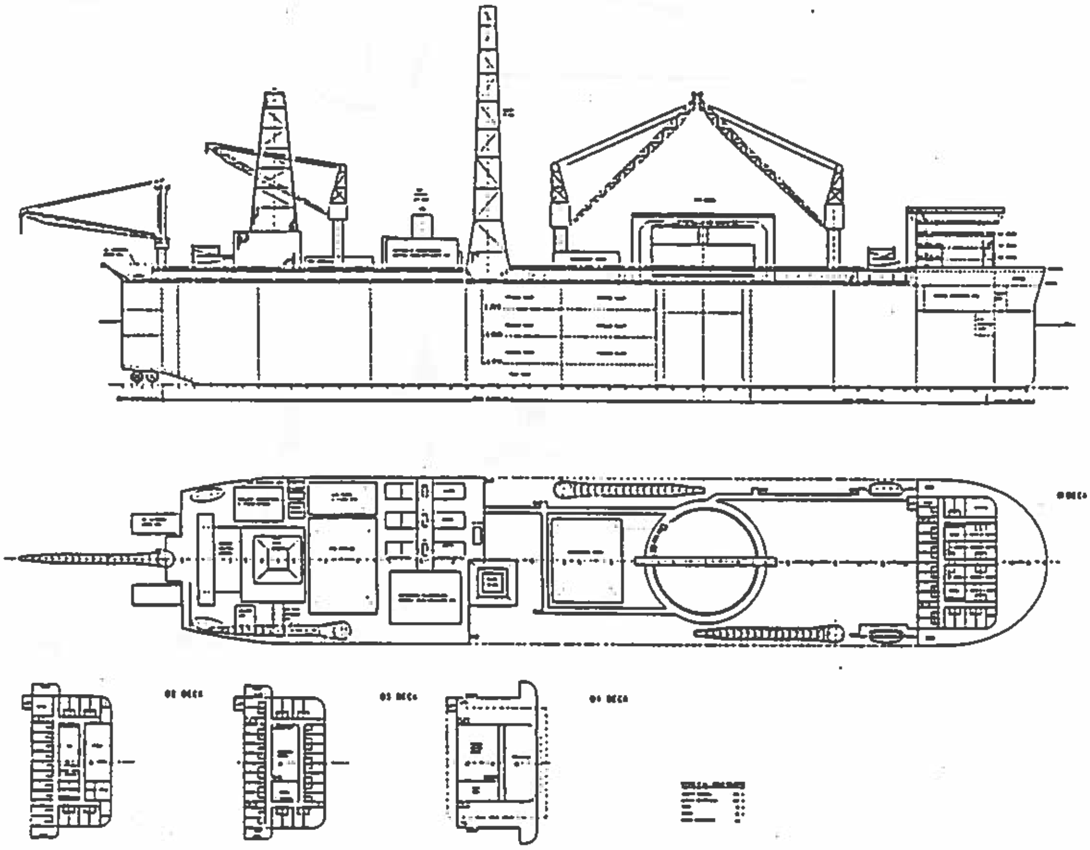

Fig. 4.5 Layout of COMPASS 230 barge.

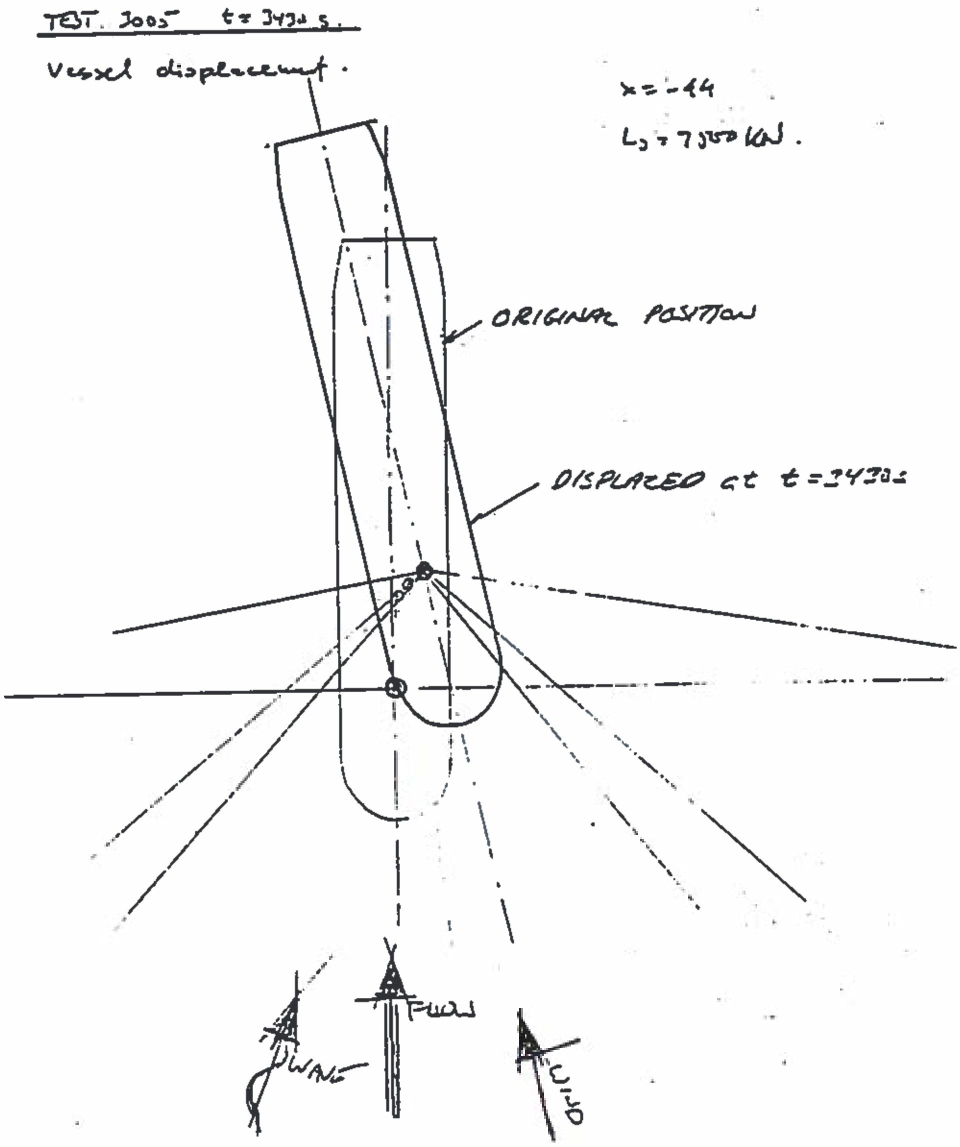

Fig. 4.6 Wave, current and wind directions.

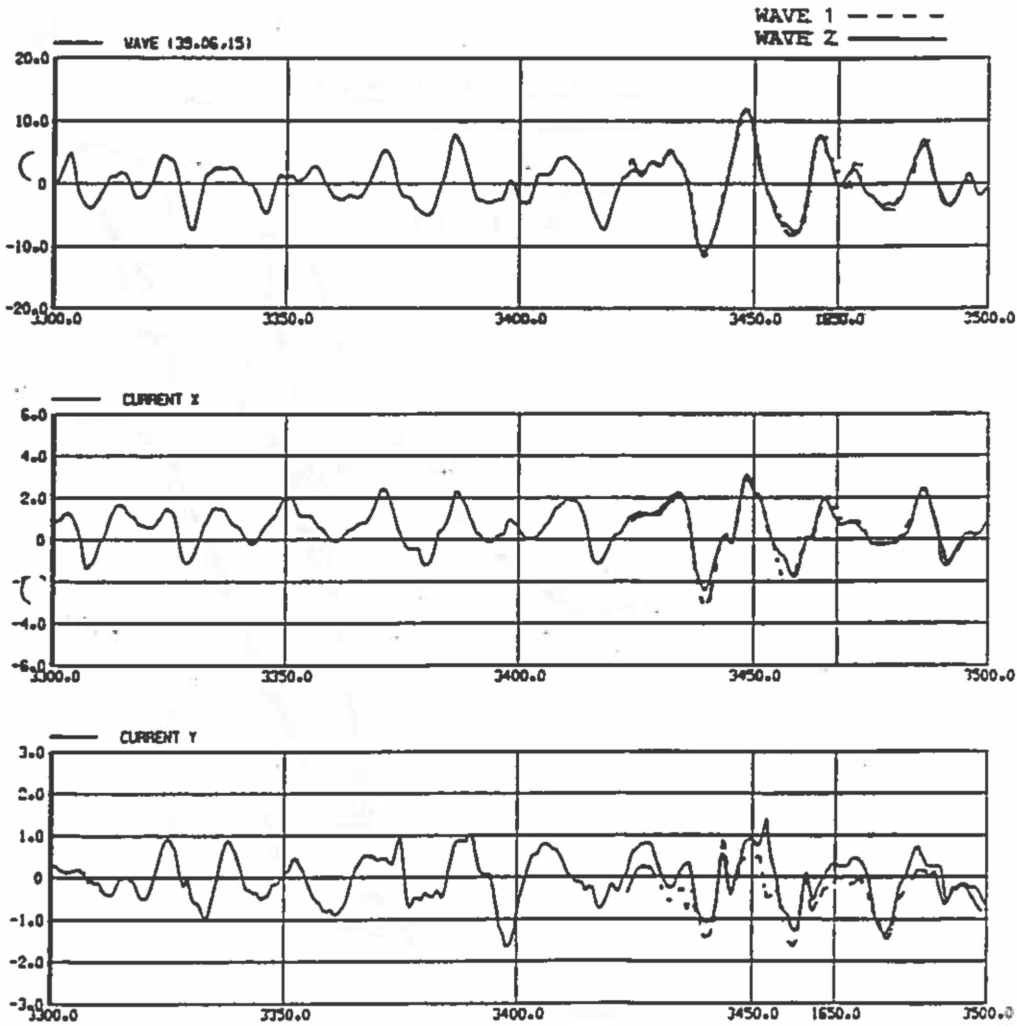

Fig. 4.7 Record of wave elevation and wave induced velocities during a test condition repeated twice.

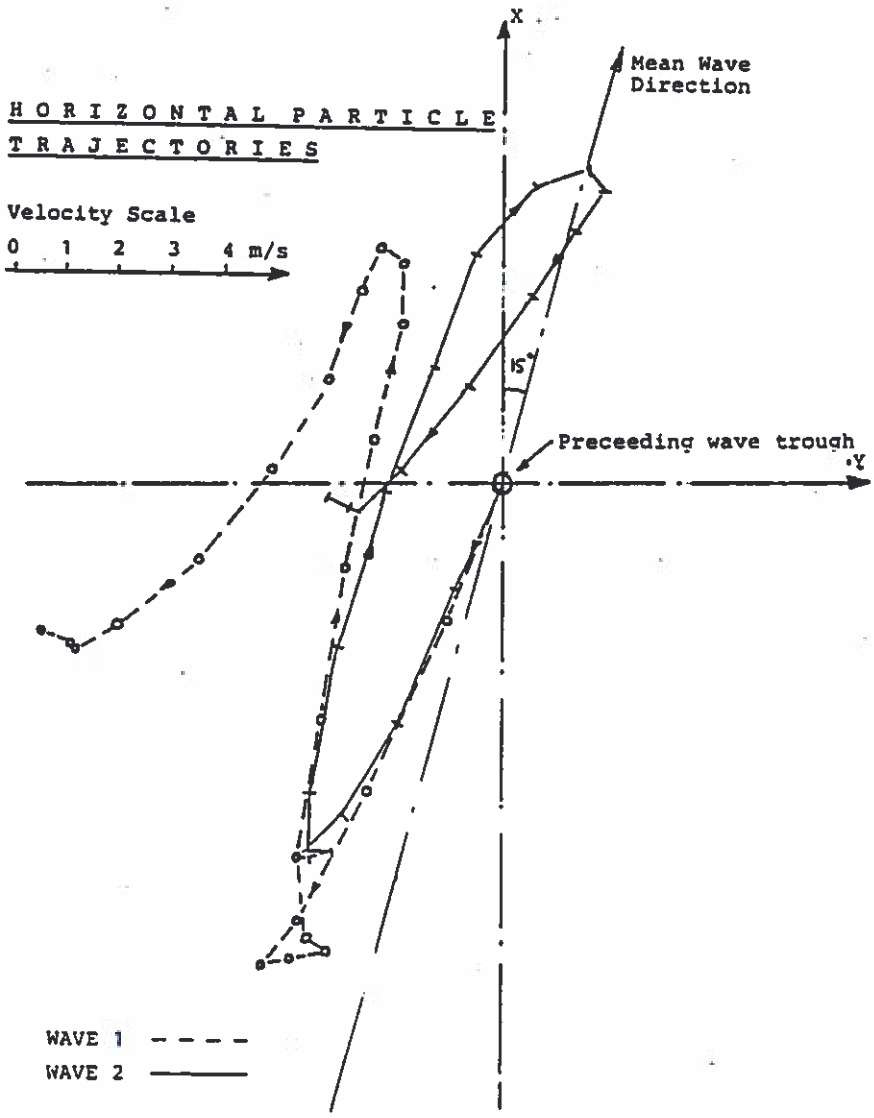

Fig. 4.8 Horisontal particle trajetories during the same wave repeated twice.

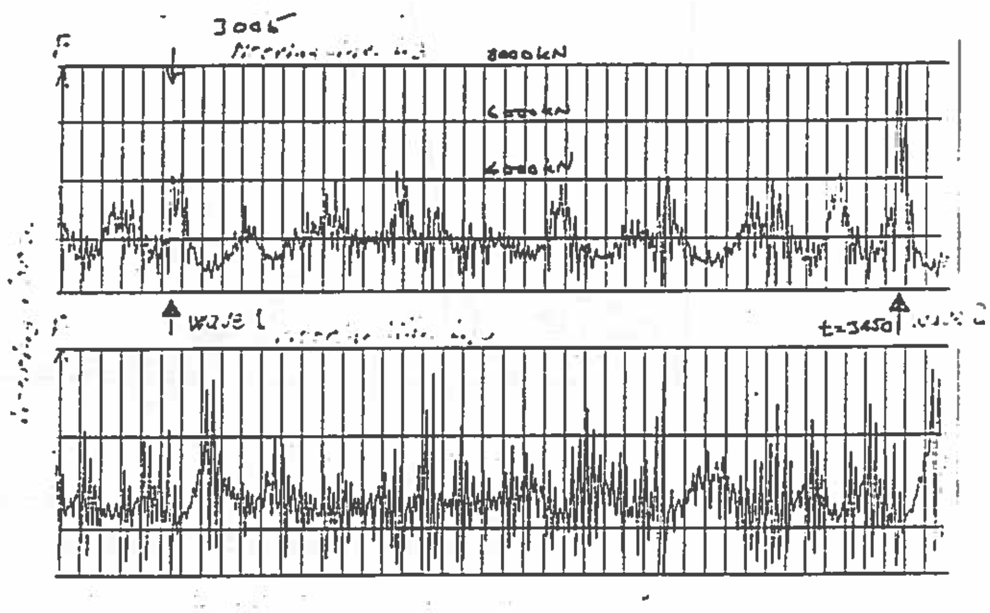

Fig. 4.9 Mooring forces for respectively wave 1 and wave 2.

5. 2D WAVES, NON LINEAR THEORY

(Mansand, Sand and Klinting (1987)).

Today it is possible in 2D waves to take account to non-linearities induced by interaction between wave with frequencies close to each other, fig. 5.1 and 5.2.

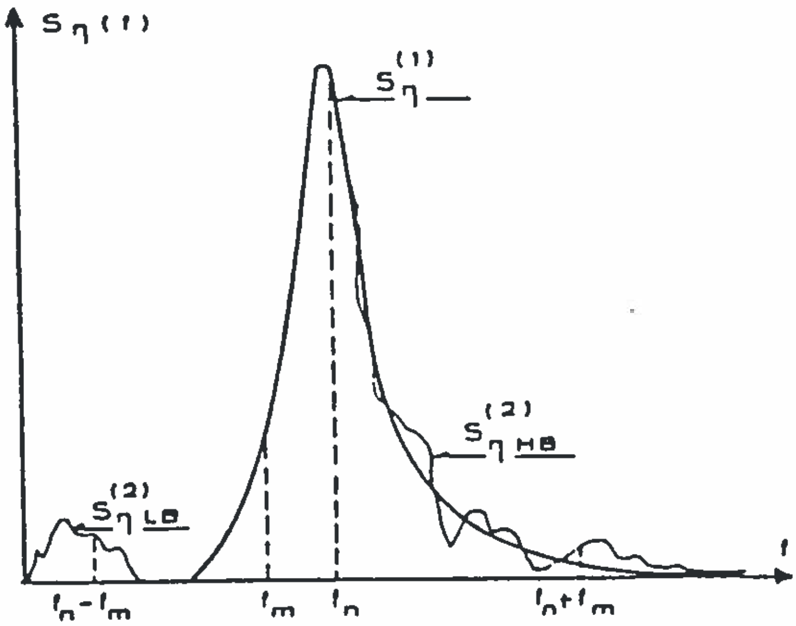

Fig. 5.1 Spectral domains of sub- and super-harmonics relative to primary 1st-order spectrum.

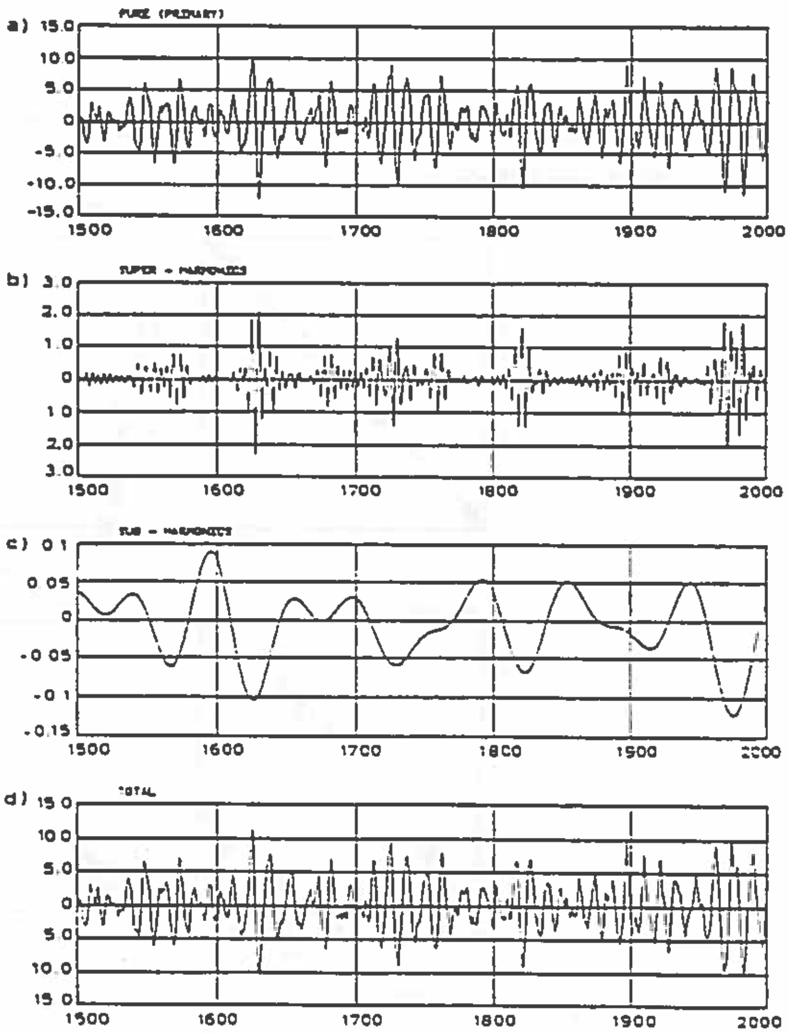

Fig. 5.2 Sample output of analysis of Camille storm, 248 m depth.

a) Pure 1st-order wave train

b) and c) 2nd-order super-and sub-harmonics, respectively.

d) Total 2nd order wave train.

In intermediate water depths the 2nd-order effects become predominant. For instance, in the Gorm Field (h/L_0 = 0.12) a net increase of 1 m in crest level is obtained by the 2nd-order formulation although the primary waves are smaller than those of Camille.

Fig. 5.3 showes the results of a 2nd order analysis for some wave parameters.

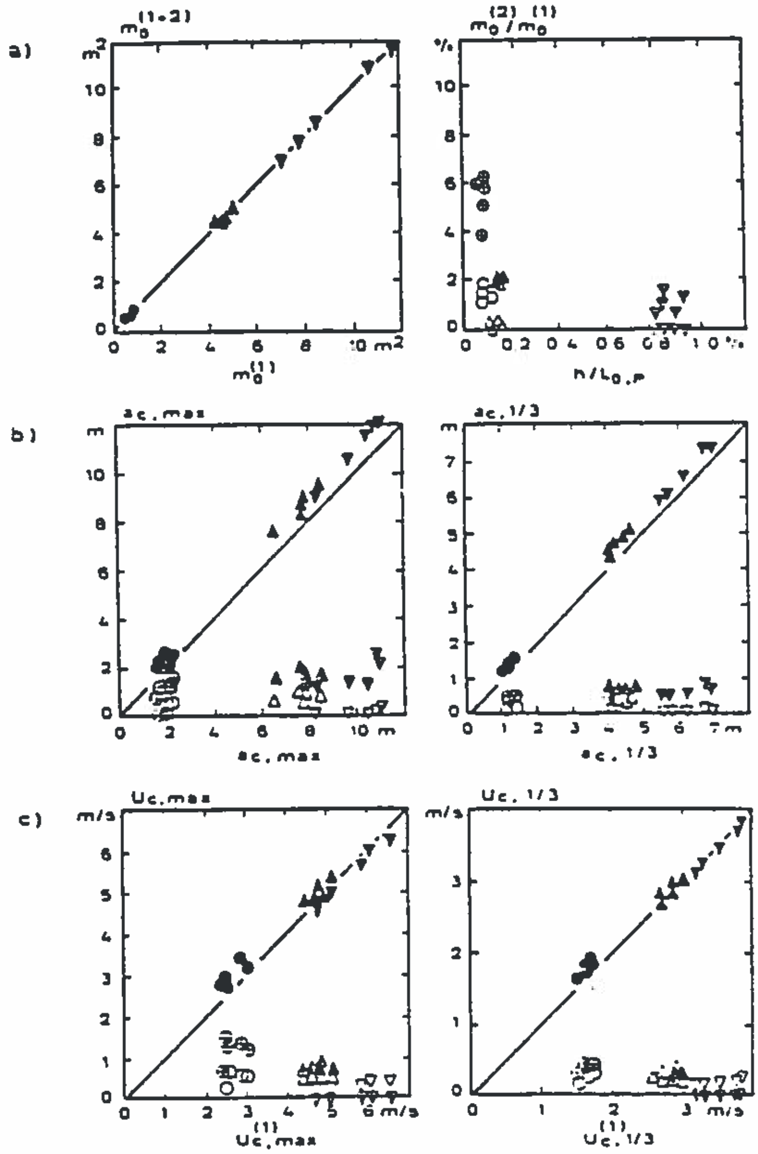

Fig. 5.3 1st- and 2nd-order statistics of records from Gulf of Mexico, North Sea, and Baltic Sea:

a) Zeroth moments

b) Crest levels

c) horizontal velocities at MWL.

6. FREAK WAVES

(See Klinting and Sand (1987))

At Danish Hydraulic Institute (DHI) the main field recordings of freak waves has been obtained for the instrumented platform in the Gorm Field, fig. 6.1.

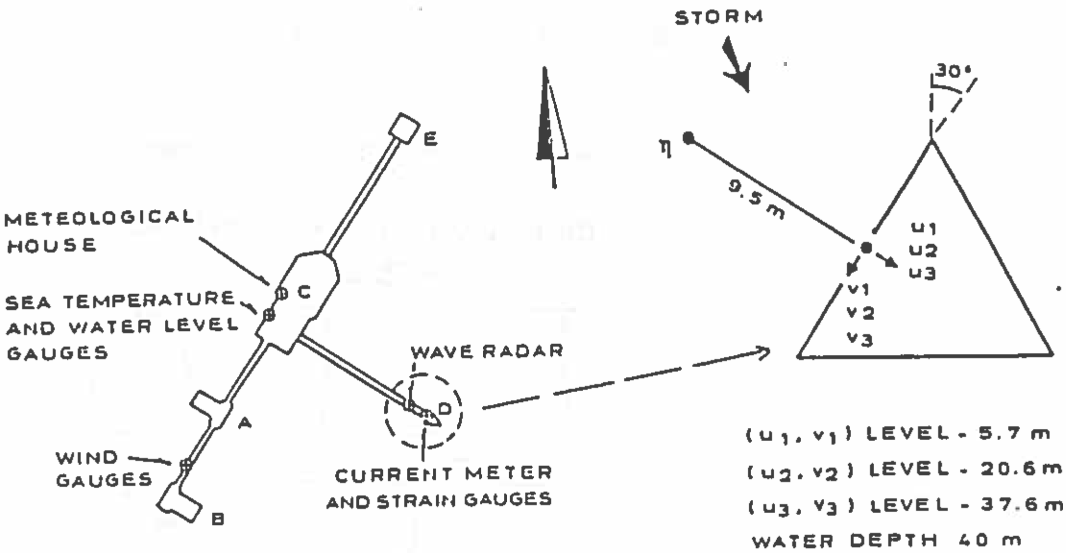

Fig. 6.1 Instrumentation on platforms in the Gorm Field.

A record form November 1981 showed a wave profile as indicated on fig. 6.2. This high wave is typically characterized as a freak wave, because it is single - not part of a smooth wave group pattern - and because the crest height clearly exceeds that of its neighbours.

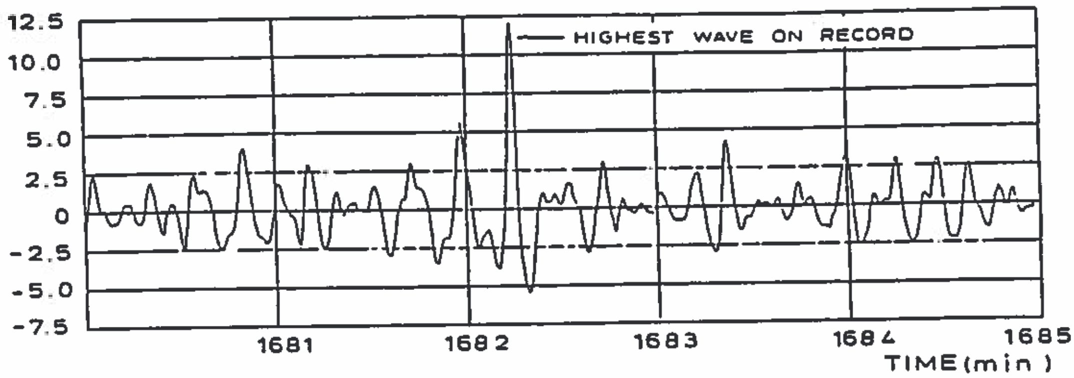

Fig. 6.2 Freak wave recorded in the North Sea on 23. Nov. 1981.

Definitions fo steepness and assymmetry are given in fig. 6.3.

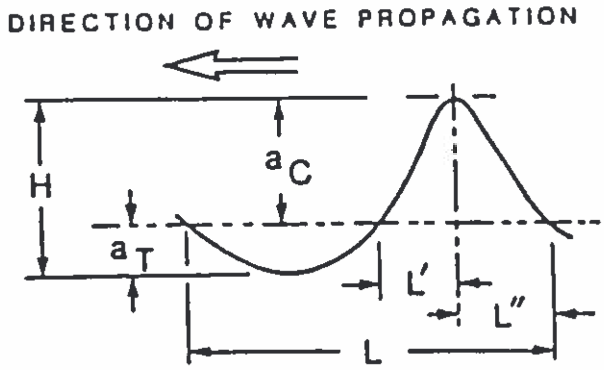

WAVE STEEPNESS: $Sz = H/L$

CREST FRONT STEEPNESS: $S'_C = a_C/L'$

CREST REAR STEEPNESS: $S''_C = a_C/L''$

VERTICAL ASYMMETRY: $\mu_V = L''/L'$

HORIZONTAL ASYMMETRY: $\mu_H = a_C/H$

Fig. 6.3 Definition of steepness and asymmetry, IAHR (1986).

An attempt was made to see if the extraordinary high crest elevations could be explained by non-linear 2D wave theories (se section 5).

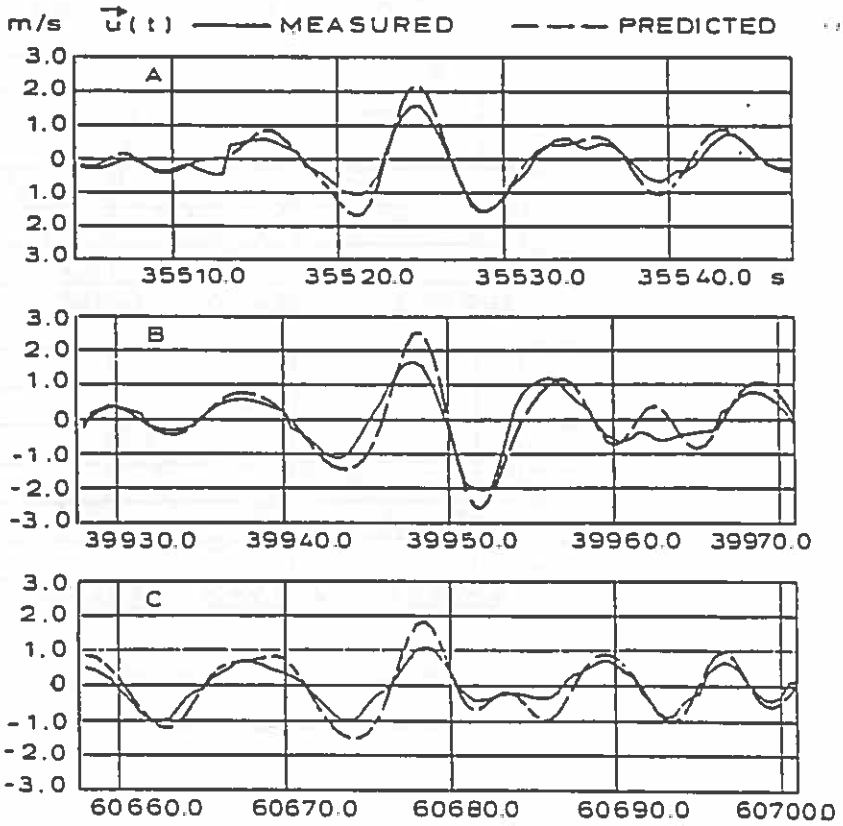

Fig. 6.5 Comparison of predicted second-order velocity with the measured velocity vector at z = -5.7 m for wave A, B and C.

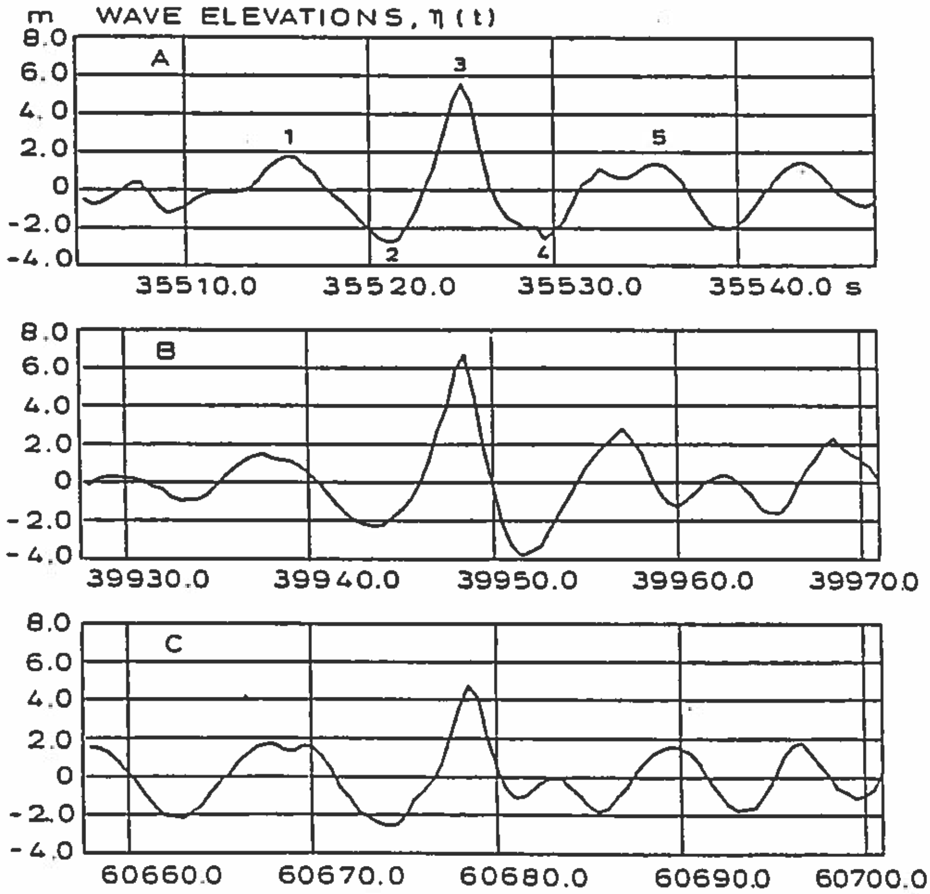

Fig. 6.4 Time series plot of the freak waves A, B and C listed in table 6.1.

Measured		2-D theory					
Wave no.	$\vec{u}_{max}$ m/s	$u^{(1)}$ m/s	Δ %	$u^{(2)}$ m/s	Δ %	$u^{(5)}$ m/s	Δ %
A	1.56	2.26	+45	2.28	+46	2.37	+52
B	1.86	2.46	+32	2.70	+45	2.51	+35
C	1.12	2.08	+86	1.92	+71	2.11	+88

Table 6.1 Comparison between measured velocity vector and horizontal velocities predicted by linear (design) wave theory, second-order irregular wave theory and Stokes fifth-order theory (regular wave).

The significant over-prediction by all the 2D theories -especially under the freak waves - leads to the preliminary conclusion that the phenomenon cannot be characterized as being two-dimensional.

This may be confirmed by considering the polar plot of horizontal velocities (fig. 6.7). Remark the difference in direction between the characteristic velocity trajectories.

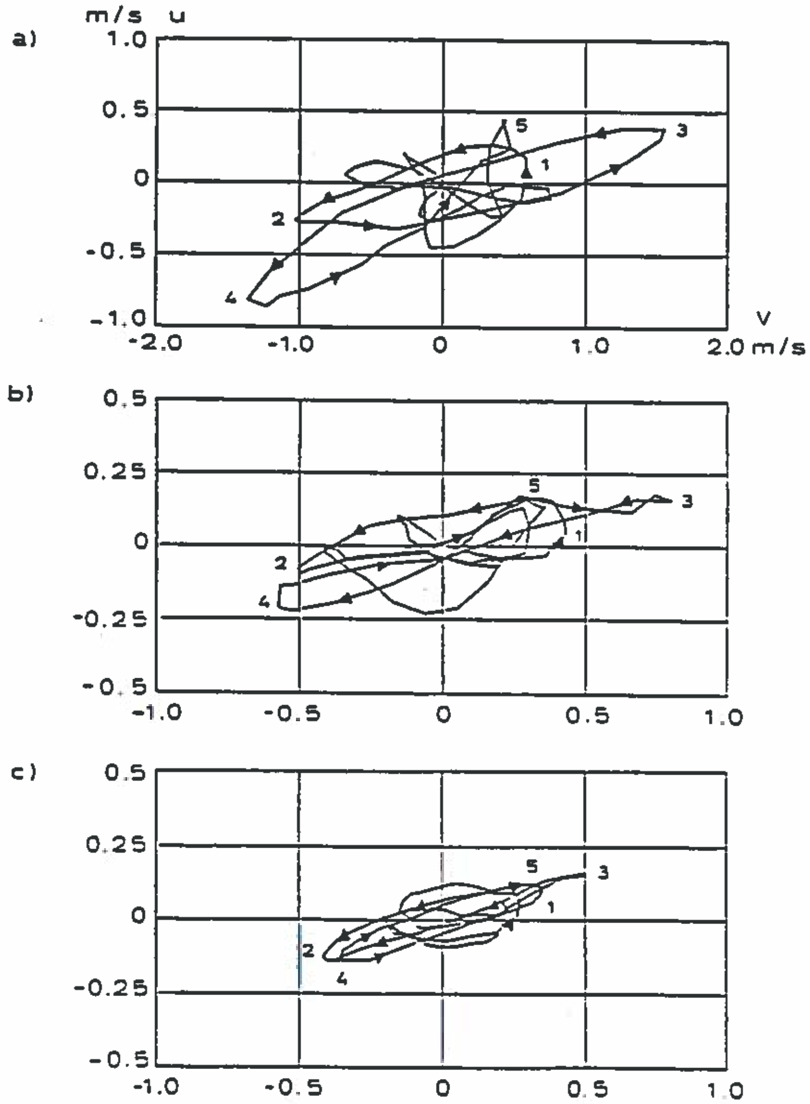

Fig. 6.7 Polar plot of horizontal velocities in the three current meter levels a) -5.7 m, b) -20.6 m and c) -37.6 m for freak wave A.

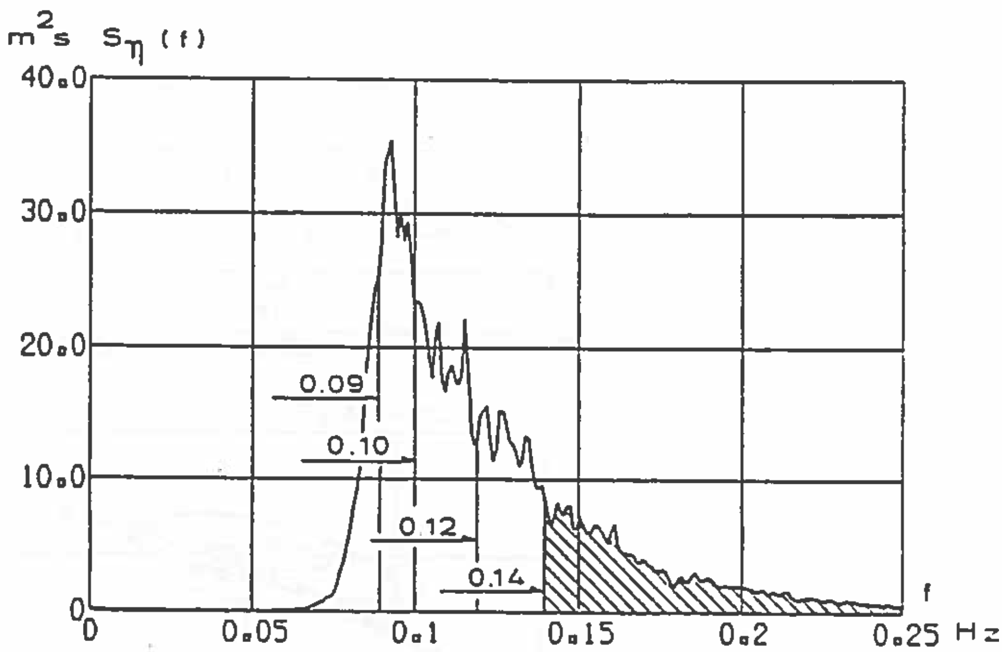

Fig. 6.8 Wave spectrum with indication of four low-pass filter cut-off frequencies.

To analyse the observed freak waves further, the time series were filtered as can be seen on fig 6.8 and 6.9. From these analyses follow that the longer period wave components correspond to 70-80% of the wave energy but only to 50-60% of the crest height. The shorter period components correspond to 20-30% of the wave energy but cause 40-50% of the crest height. This shows that the abnormal crest elevtion mainly is due to strong 3-D phase interaction between the higher frequency wave components.

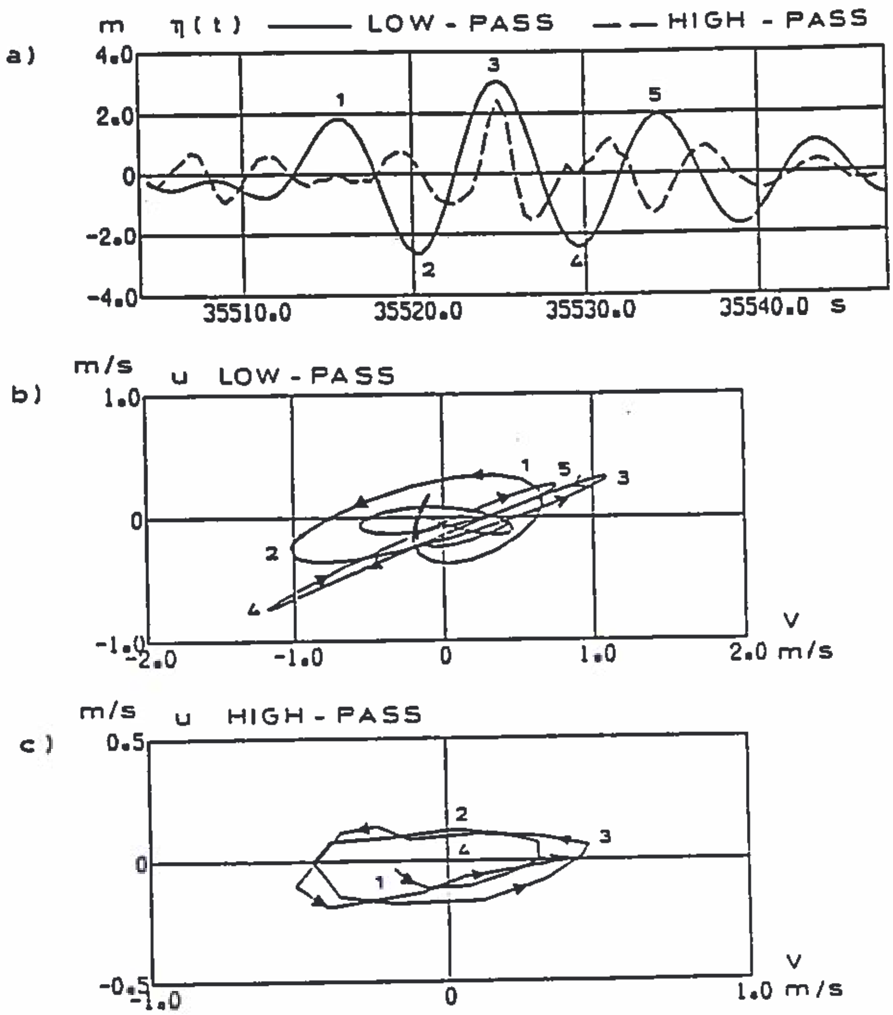

fig. 6.9 High and low-pass filtered freak wave A; a) elevations, b) low-pass filtered velocity vector (f < 0.14 Hz), and c) high-pass filtered velocity vector (f > 0.14 Hz); z = -5.7 m.

7. WAVE VELOCITIES ABOVE STILL WATER LEVEL

A growing number of field recording of wave induced velocities have been carried out the recent year. But although the most interesting is the extreme wave induced velocities above still water level, there still exist very few recordings due to practical problems of instruments been located partly in water and partly in air.

In order to improve the knowledge of this important design aspect a research program has been carried out supported by the Ministry of Energy (EFP 88). The project includes model tank recordings in 2-D and 3-D waves with a special developed feed back system making it possible to measure velocities at a certain distance below the instantaneous water surface.

Examples of the recordings are shown in fig. 7.7.

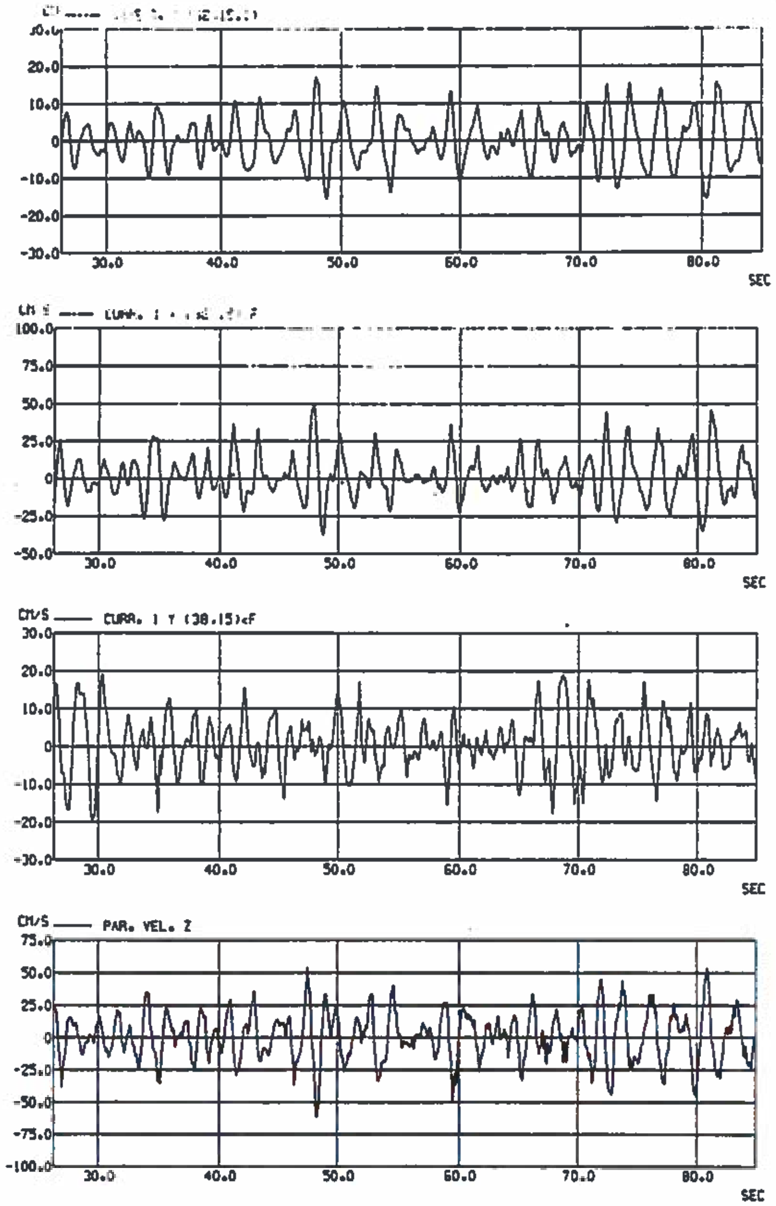

Fig. 7.1 Time Series of Wave Elevation and Water Velocities (x,y,z), Recorded 9 cm below Instantaneous Water Surface.

Only very preliminary results from the 2D tests are available (see fig. 7.2). It will be interesting to see the results from 3-D waves including freak waves.

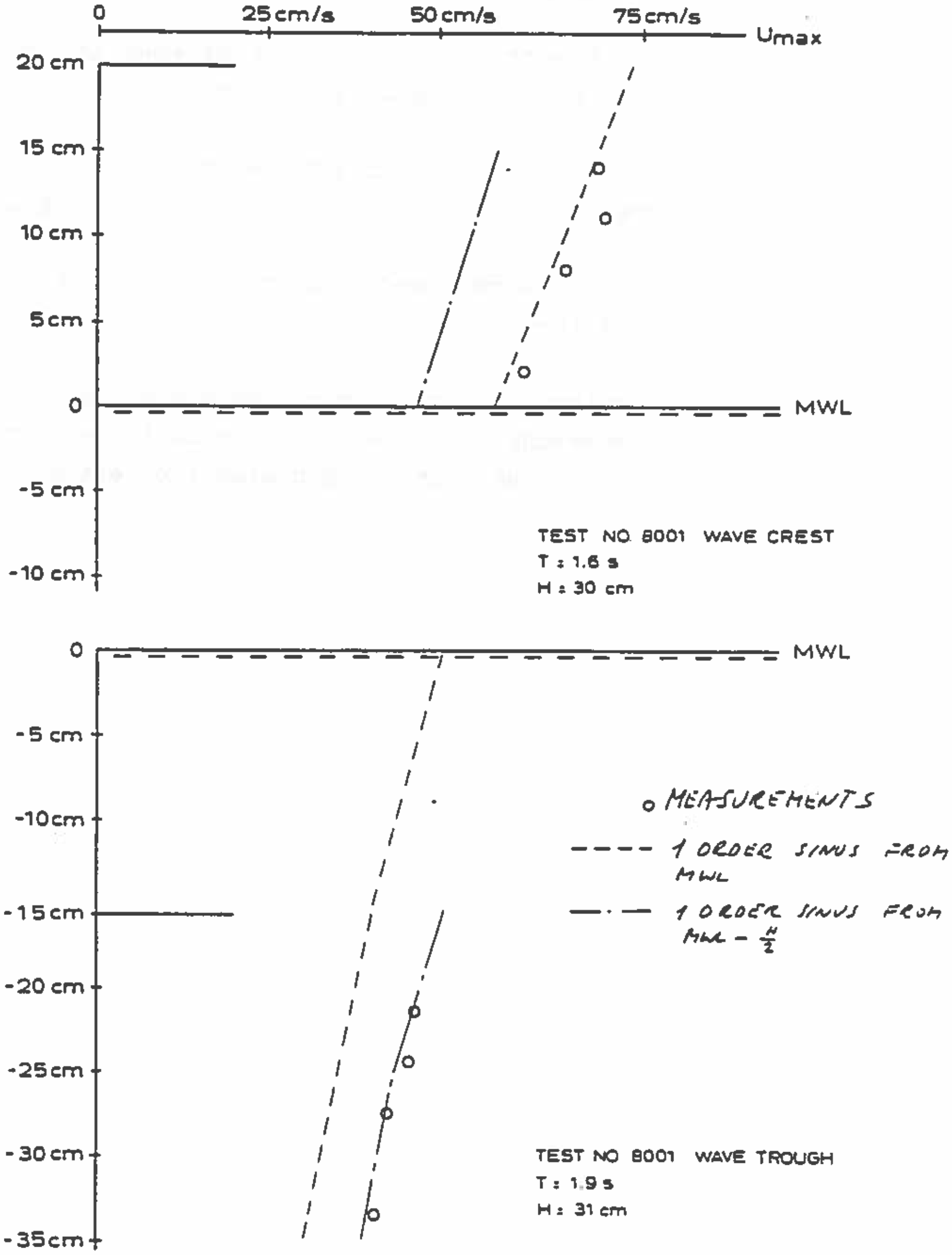

Fig. 7.2 Wave velocities determined at selected distances below the instantaneous water surface during 2-D waves.

8. FREAK WAVE GROUPS

This section describes on attempt to improve the quality of the selected design situation.

Fig. 8.1 show this problem presented as a part of a improved rational approach for design of floating structures.

The required feed back from results to input selection is a key item.

Another and much more expensive way of solving this very important principal question is to increase the number of test conditions selected and also the test duration see fig. 8.2.

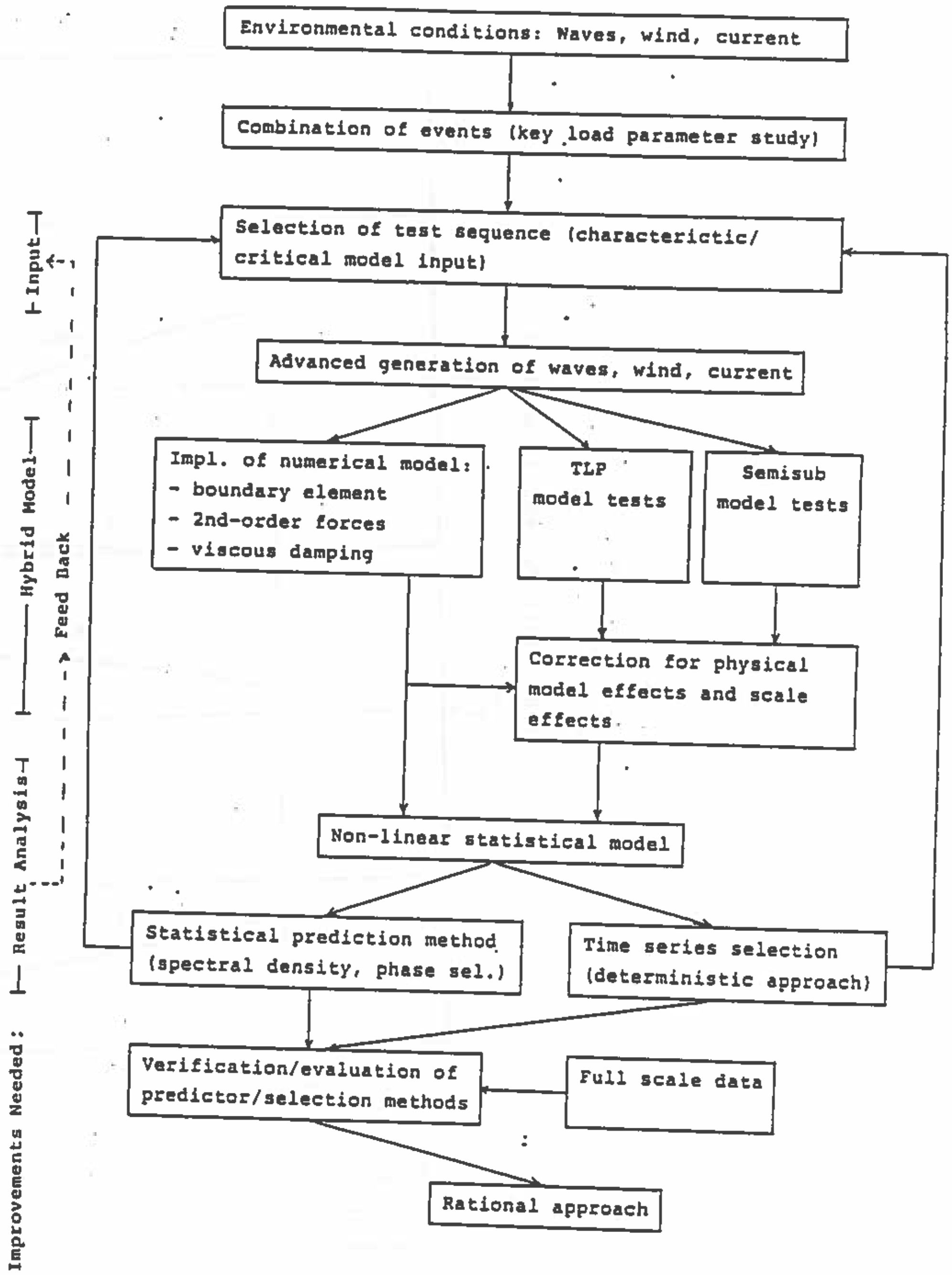

Fig.8.1 Illustraton of Elements in Rational Approach to the Description of Forces and Motions of Floating Structures.

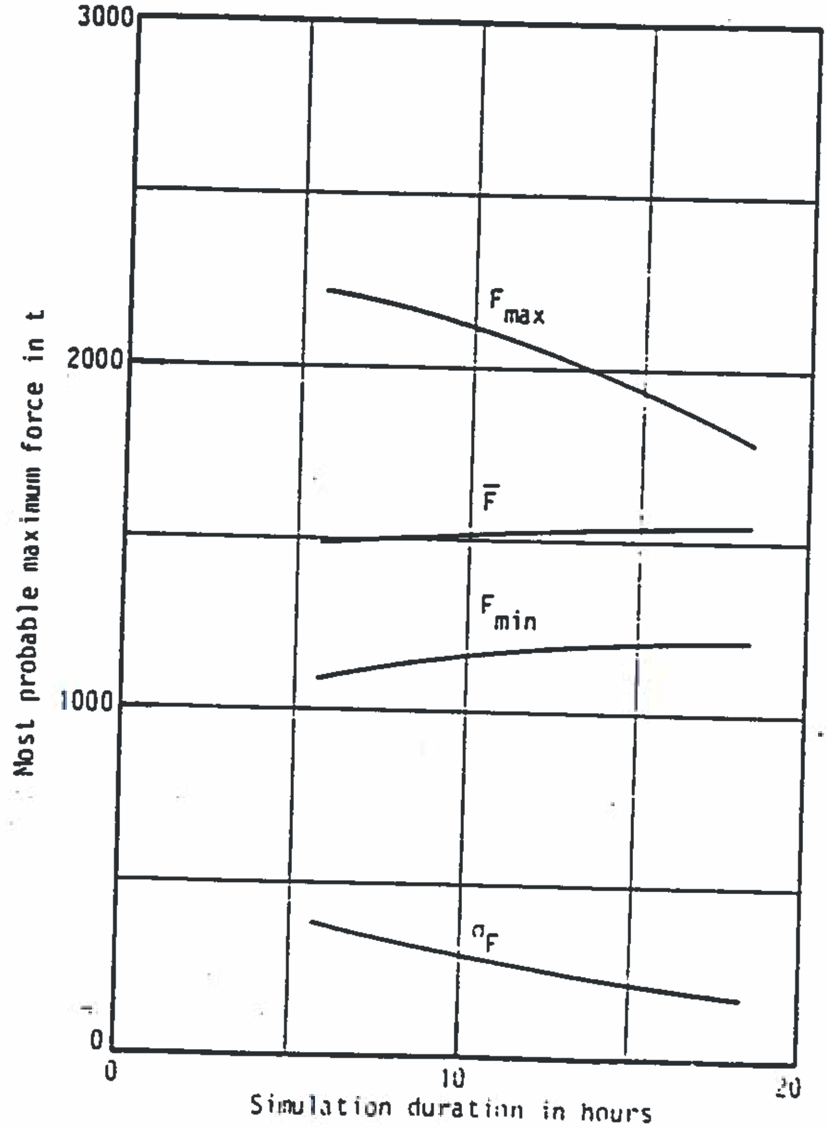

Fig. 8.2 Influence of simulation duration on variability of most probable maximum mooring force in 3 hours. Pinkster (1987).

The basic problem may be illustrated by fig. 8.3 (from Pinkster (1987)) which show that the distribution of the extreme motions may include a significant scatter and also significant consistent deviations from traditional used assumptions.

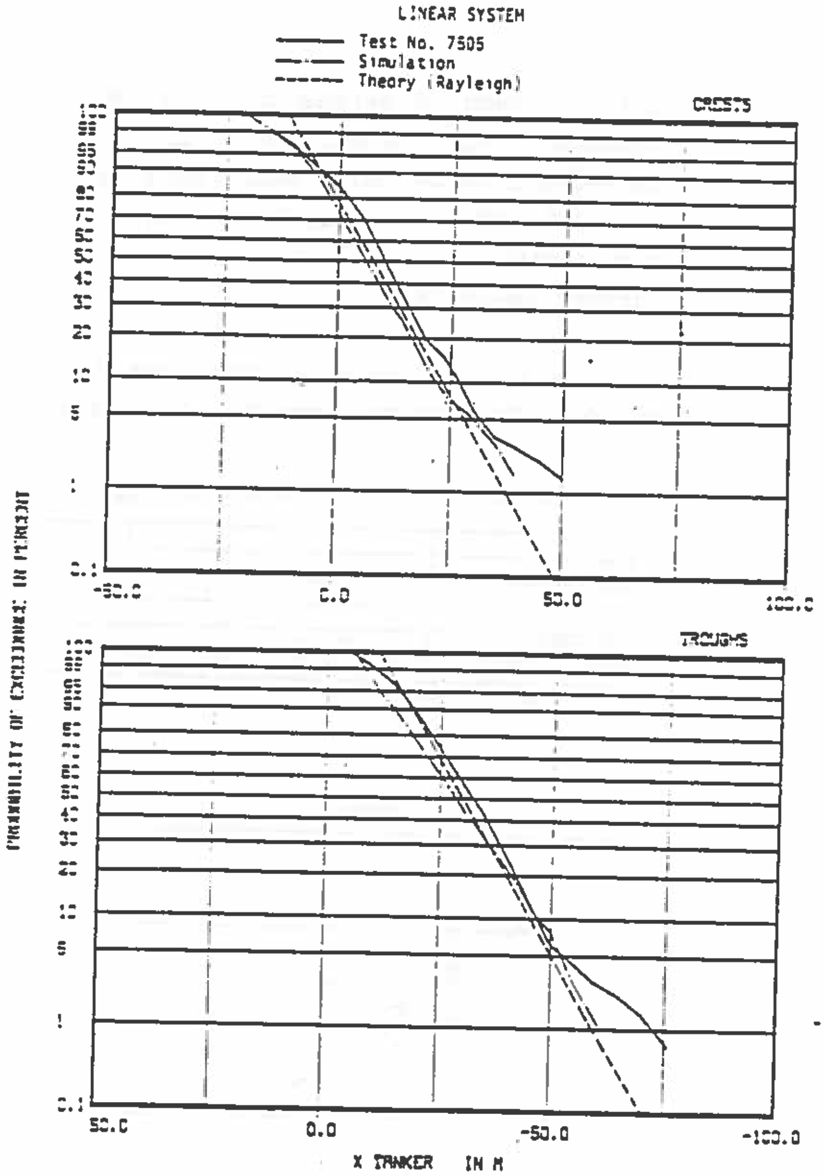

Fig. 8.3 Distribution of surge motion extremes. (Pinkster (1987)).

This has recently as discussed by Gravesen and Klinting (1987) shown to be even more important as a preliminary freak wave analysis of field recordings showed surprising results.

The continuous records were divided into 40 minutes subseries and for each subseries the rms value was used to find the expected crest elevation. If the actual crest elevaton exceeded a value which would only occur with less probability than 10% (corresponding to the expected level of 1 to 2 maximum events during 24 hours) those waves were selected for further analysis.

This selection procedure resulted in 6 extreme events being found instead of the expected 1-2 events.

One of these events is shown in Fig. 8.4.

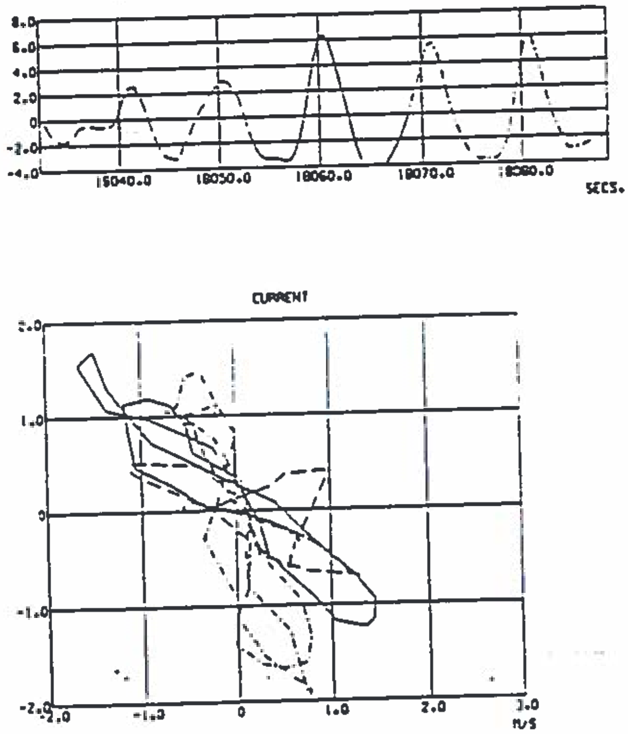

Fig. 8.4 Freak Wave Elevation and 2-Directional Velocity in el. -5.7 m.

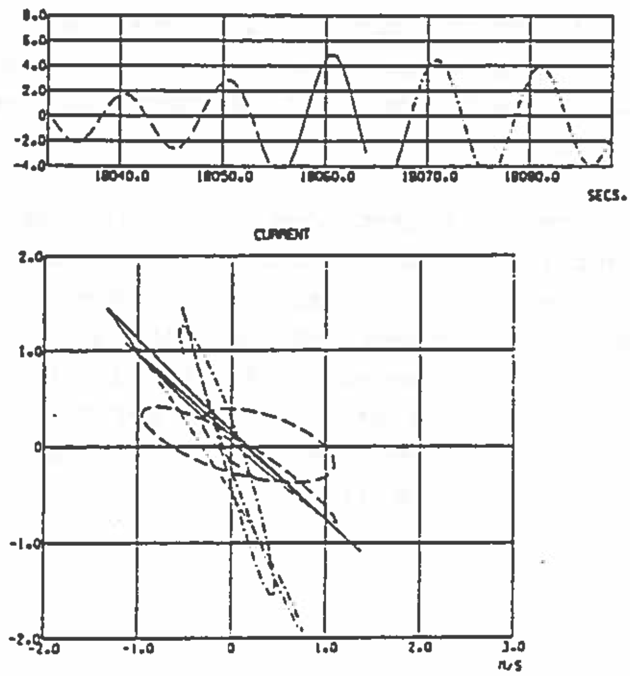

Fig. 8.5 Freak Wave Elevation and 2-Directional Velocity in el. -5.7, low pass filtered.

By introducing a filtering the same record is shown in fig. 8.5 which shows a scaring picture. There is not just one large freak wave but a group of waves with approximately the same direction and an average height exceeding very much what could be expected.

With an analogy to the single freak wave we may name this a <u>freak wave group.</u>

This brings high attention to the requirement of more detailed analysis of prototype wave recordings.

It seems that a lot of information is lost by only utilizing H_s and T_p and possible the spectrum of the prototype recordings.

Another important aspect is to consider the input selection as an integrated part of the modelling. Initial results and growing physical understanding of the most critical problem should be reflected in improved input selection as schetched on fig. 8.1.

The required last step is finally that the basic prototype data should be analysed by the same procedures that have created the input selection. Hereby it may be possible to avoid the present indirect link through traditional average prototype parameters. A more direct connection between the prototype wave data and the critical contents of the test input could lead to improve accuracy in the estimates of absolute probabilities.

9. REFERENCES

Barthel, V., Mansard, E.P.D., Sand, S.E., and Vis, F.C. (1983). Group Bounded Long Waves in Physical Models. Published in the Ocean Engineering, Vol. 10, No. 4, 1983.

Cokelet, E.D. (1978) Breaking waves - the plunging jet and interior flow-field. IAHR-symposium on mechanics of wave-induced forces on cylinders, Bristol.

Danish Hydraulic Institute and Danish Maritime Institute (1983). Comparative Model Testing in 3-D and 2-D Waves with Tripod Tower Platform. Catenary Anchored Semi-Submerskible Moored Tanker.

Forristall, G.Z., Ward, E.G., Gardone, V.J., and Borgman, L.E. (1978). The directional spectra and kinematics of surface gravity waves in tropical storm Delia. Journ. Phys. Oceanography, Vol. 8, pp. 888-909.

Gravesen, H. and Klinting, P. (1987). Determination of Critical Wave Sequences for Moored Floating Structures. Proc. Workshop on Floating Structures and Offshore Operations, Wageningen, Elsevier.

Hansen, N.E.O., Sand, S.E., Lundgren, H., Sørensen, T., and Gravesen, H. (1980). Correct Reproduction of Long Group Induced Waves. Presented at the 17th International Conference on Coastal Engineering, Sydney, Australia, March.

Kirkegaard, J., Sand, S.E., Hansen, N.E.O., and Hvidberg-Knudsen, M. (1980). Effects of Directional Sea in Model Testing. Presented at the Ports '80 Conference, ASCE, Norfolk, Virginia, USA.

Kirkegaard, J., Sand, S.E. and Denise J.-P. (1986). Modelling the Behaviour of Floating Production Concepts in 3-Dimensinal Waves. Presented in Conf. Way Forward for Floating Production Systems, London.

Klinting, P. and Sand, S.E. (1987). Analysis of Prototype Freak Waves. proc. ASCE Spec. conference Nearshore Hydrodynamics, Univ. of Delaware.

Longuet-Higgins, M.S. & E.D. Cokelet (1976). The deformation of steep surface waves: I, A numerical method of computation. Proc. Roy.Soc.Lond., A 350, 1660, pp. 1-26.

Lundgren, H., Brink-Kjær, O., Sand, S.E., and Jacobsen, V. (1979). Improved Physical Basis of Wave Forces. Presented at the 4th Conference on Civil Engineering in the Oceans, San Fransisco, USA.

Lundgren H., Davidsen E., Frederiksen E.W., and Sand, S.E. (1984). Decription of Natural Sea States, 19th Intern. Conf. Coastal Engng., Houston.

Lundgren, H., Sand, S.E., and Kirkegaard, J. (1981). Drift Forces and Damping in Natural Sea States (BOSS' 82). Behaviour of Offshore Structures. Proceedings of the Third Conference, Cambridge, Mass. USA.

Mansard, E.P.D., S.E. Sand and Per Klinting (1987). Sub- and Super-Harmonics in Natural Waves. Presented at the Sixth (1987) International Symposium & Exhibit on Off-shore Mechanics and Arctic Engineering, Houston, Texas.

Peregrine, D.H. (1978) Analysis of motion as a wave commences to break. Research Note, Private communication, Bristol, Dec.. 1978.

Pinkster (1987): On the determination of the statistical properties of the behaviour of moored tankers. Proc. Workshop on Floating Structures and Off-shore Operations, Wageningen. Elsevier.

Sand, S.E. (1982). Wave Group Described by Bounded Long Waves. Published in the Ocean Engineering, Vo. 9, No. 6, pp. 567-580.

Sand, S.E. and Arthur E. Mynett (1987). Directional Wave Generation and Analysis. AIRH-SEMINAR-IAHR, Lausanne, 1987.

Sand, S.E., J. Rõmeling and J. Kirkegaard (1987). Influence of Wave directionality on Response of Semisubmersible. Presented at the Sixth (1987) International Symposium & Exhibit on Offshore Mechanics and Arctic Engineering, Houston, Texas.

Svendsen I.A., (1979). Bølgebrydning. Notat til forelæsning, ISVA.

4 SHIELDING

4A Shielding in Wellheas Platforms
by LIC Engineering

4B Shielding in Pipe Arrays in Waves and Current
by Niels-Erik Ottesen Hansen, LIC Engineering
Peter Justesen, ISVA, Technical University of Denmark

4C Reserve Strength of Wellhead Platforms in the North Sea
by Henrik Nedergaard and Niels-Erik Ottesen Hansen
LIC Engineering

SHIELDING

SHIELDING IN WELLHEAD PLATFORMS

LIC ENGINEERING A/S

EHLERSVEJ 24
DK-2900 HELLERUP
PHONE: + 45 1 62 16 42
TELEFAX: + 45 1 62 54 80
TELEX: 21437 LICENG DK

INTRODUCTION

Dense spacing of members in platforms will influence the free flow by breaking up the waves and by changing the flow-field around the members. These effects result in a decrease in force on the lee-ward. The effect is in general referred to as shielding.

The shielding effect is well known in wind engineering. However, it has until recently not been widely used in offshore structures. One of the reasons are the complications in connection with waves. Here the shielding effect has to be developed during the passage of the wave. This means that the water particles shall be accelerated from the velocity field undisturbed by the structure to a velocity field as depicted in the figure opposite. Such an acceleration takes time so in the short period of the passage of a wave the shielding will only be partially developed. This is opposed to steady current where there will always be sufficient time to develope the shielding completely.

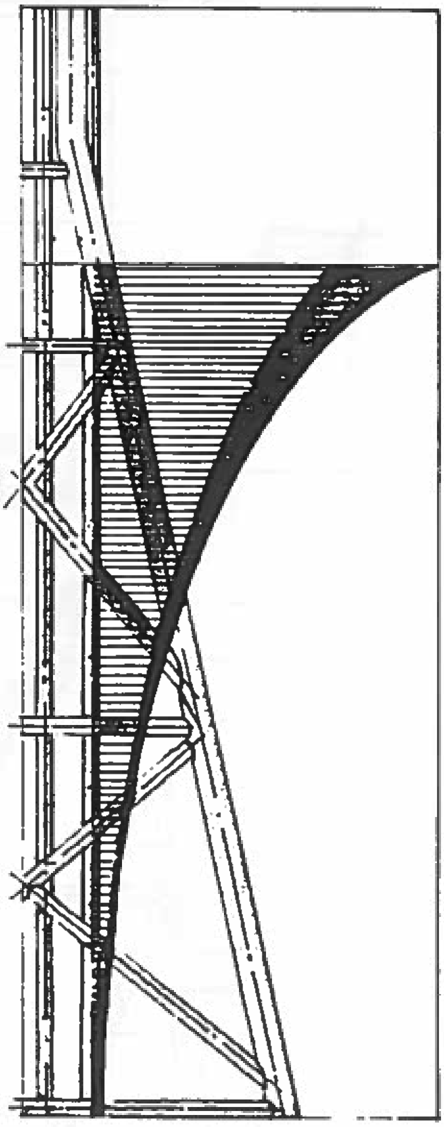

CALCULATION METHOD

LICengineering has a couple of years ago developed methods for calculating the shielding effect. The original work was made as a joint industry project of "Hydrodyanmic Forces on Well Conductor Arrays", conducted by LICengineering and sponsored by

Mobil Development Corporation
Mærsk Olie og Gas A/S
Norsk Hydro
Statoil
Texaco Inc.

The above method has been extensively tested on a large number of different conductor arrays. In addition, the method is supported by the results of the tests with twenty different configurations of production risers tested in the JIP-Kongsberg Riser Development Project (sponsored by 10 oil companies). Lately the method has been developed further in a project sponsored by Norsk Hydro. The method has further been verified by tests with complex arrays and high Reynolds number

Finally the calculation method for shielding effect has been approved by Lloyds in London and DnV in Norway.

GORM WATER INJECTION

SHIELDING, VORTEX SHEDDING AND WHIRLING ANALYSIS FOR GORM 'A'

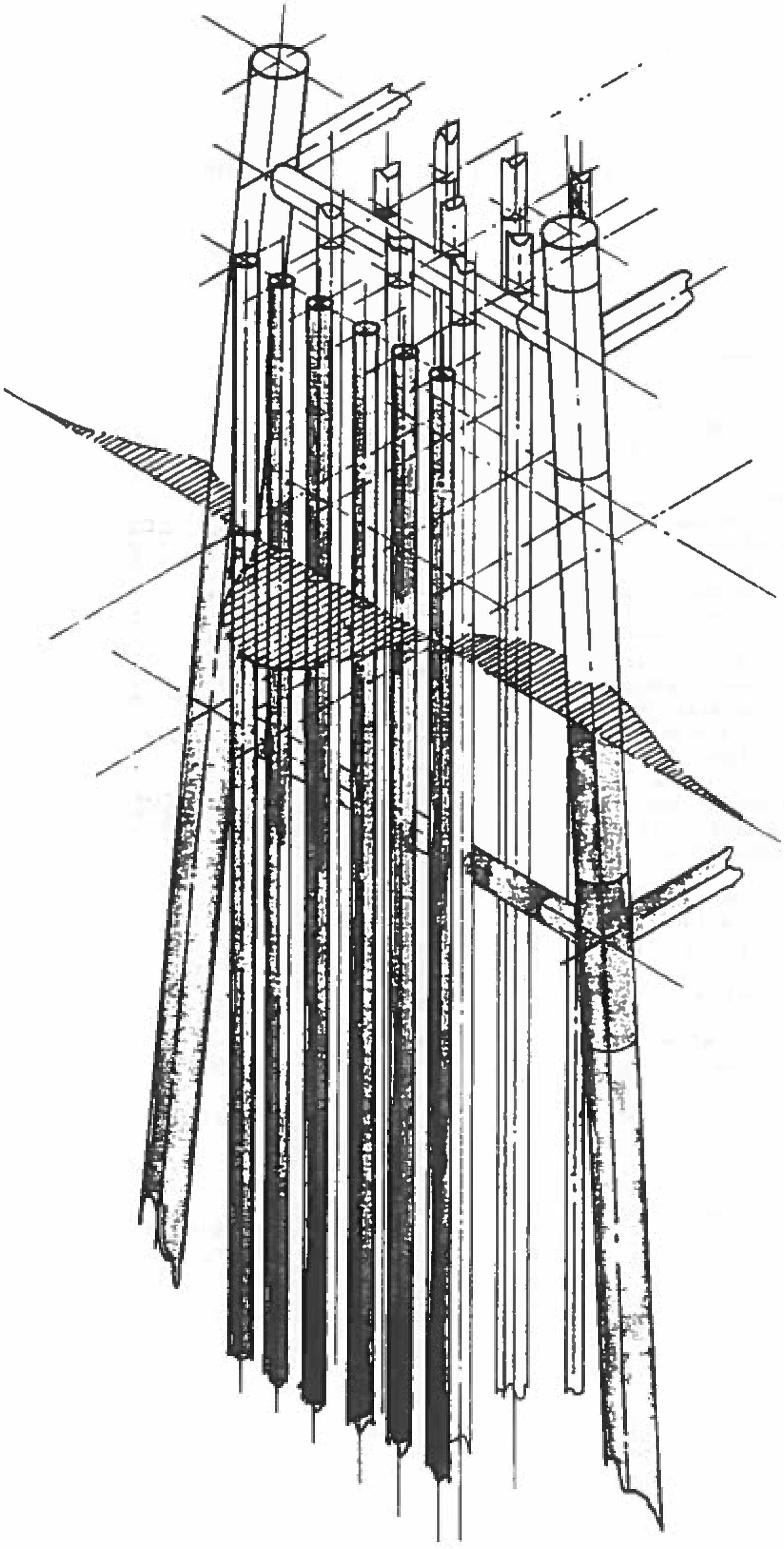

The project was carried out by LICengineering in November-December 1987 for Mærsk Olie og Gas A/S.

The Gorm 'A' platform is an existing wellhead platform in 40 m water depth approx. 230 km west of Esbjerg in the Danish North Sea Sector.

The report comprised the results of a total shielding analysis on the Gorm 'A' wellhead platform with 6 additional conductors. Furthermore it included a vortex shedding and whirling analysis for the 6 additional conductors. The method of calculation adopted enabled the installation of the extra conductors to be carried out using only one underwater clamp.

The report conclusions simplified installation of the additional risers and proved through the shielding re-analysis that the existing structure was adequately strong to withstand the increased loading, this in turn gave the client substantial savings.

LIC ENGINEERING A/S

EHLERSVEJ 24
DK-2900 HELLERUP
PHONE: + 45 1 62 16 42
TELEFAX: + 45 1 62 54 80
TELEX: 21437 LICENG DK

SHIELDING IN PIPE ARRAYS IN WAVES AND CURRENT

by

Niels-Erik Ottesen Hansen, LICengineering A/S, Copenhagen

Peter Justesen, ISVA, Technical University of Denmark, Lyngby

ABSTRACT

In recent years many experiments have been performed to assess the effect of shielding in pipe arrays. They clearly show that there can be a substantial change in forces and in hydrodynamic damping due to the modified flow field within the array.

In steady current the flow will be fully developed leading to reduced drag forces. In waves the inertia forces on the array are increased whereas the drag forces are decreased. The flow field causing the shielding is developing in each half period of the oscillation. Therefore the shielding will depend on the KC-number. It will decrease with increasing KC-numbers. It can be negative for low KC-numbers. In addition, phase differences between the maximum ambient undisturbed velocity and the local maximum drag force are introduced. This is very important for the dynamic response of a pipe bundle. A description of the shielding phenomenon and its implications as to the design of offshore structures and experimental results from a joint industry project are presented. It is shown that the change in response for pipe arrays can be substantial - up to 30-40%.

A theory for calculating shielding in pipe arrays in oscillatory flow is presented. The theory is valid both in the subcritical and in the supercritical range. The theoretical results are compared with the experimental data and good agreement is observed.

It is concluded from the present study that the added accuracy gained by including the effect of shielding can be important for the hydrodynamic forces on pipe arrays. This applies to riser arrays or to wellhead jacket platforms with a dense member spacing.

NOMENCLATURE

c : Spacing between pipes (center to center)
C_D : Drag coefficient
C_{Dp} : Drag coefficient based on pitch diameter
$\bar{C}_D$: Typical drag coefficient
C_M : Mass coefficient
c_1 : Constant
c_2 : Constant
D : Diameter of pipes
D_p : Pitch diameter of riser (diameter of outer ring)
F : Force
F_D : Drag force
F_I : Inertia force
g : Gravititional acceleration
H : Wave height
j : Index
H_s : Significant wave height
k : Index for eigenmodes
k : Nikuradse equivalent sand roughness
K : Generalised stiffness
KC : Keulegan-Carpenter number
m : Vertical mass
M : Moment
M_o : Moment without shielding
$o(\ )$ To the order of
p : Pressure
Q : Constant
Re : Reynolds number (based on pitch diameter)
S : Shielding
S_D : Shielding on drag force
S_{Do} : Steady state shielding
t : Time
T_z : Zero crossing wave period
u : Velocity
u' : Velocity in connection with shielding
v : Typical velocity
U_s : Significant velocity in waves
U : Undisturbed velocity
x : Deflection of riser parallel with flow
β : The structural damping ratio
δ : Half width of flow affected by shielding
ρ : Density of water
τ : Degree of shielding developed

τ	:	Time
ω	:	Cyclic frequency
Ω	:	Enclosed volume
•	:	Differentiation with respect to time
~	:	Dimensionless parameter
o	:	Without shielding (index)

DESCRIPTION OF PHENOMENON

It is well known that a pipe bundle with closely spaced pipes exposed to steady flow will experience less total force than if the pipes in the bundle were more openly spaced. This effect is normally referred to as shielding.

The shielding in circular riser bundles has been investigated in Refs. /1/,/4/,/6/,/7/,and /10/ for both high and low Reynolds numbers and for steady and unsteady flow. Investigating the measured total forces on a typical riser bundle as shown in Fig. 1, the following features can be observed if the surrounding current is gradually increased.

The most interesting feature is the drop in the drag coefficient for the total force when the Reynolds number based on the pitch diameter is increased beyond $2 \cdot 10^6$, Fig. 2. The pitch diameter is in this context defined as the diameter of the outer ring of pipes and the drag coefficient is based on the undisturbed flow velocity. The drop can be attributed to the drop in the force coefficients on the front pipes, see Fig. 3, in which the force coefficients based on the undisturbed outer flow is depicted. No such effect is seen on the lee pipes on which only small drag coefficients are measured. This does not mean that the local drag coefficients are low. On the contrary it is reasonable to assume that the drag coefficients have the same value as if the pipes were standing isolated in the flow. It reflects that the local velocities are small. The mechanism causing these small values is a deflection of the flow outwards resulting in a smaller local velocity around the rearward (lee) pipes.

The effect is pronounced at the lower Reynolds numbers. Increasing the velocity the flow enters the transcritical regime and the drag coefficients on the front pipes are reduced such that they are carrying a smaller part of the total load. This results in a smaller deflection of the flow outwards and the flow is therefore running more directly through the riser. In the end the drag coefficients reach their minimum (at a Reynolds number of $5 \cdot 10^6$) and the flow is running virtually directly through the riser resulting in an almost equal load on all the outer pipes. This development is highly interesting, because it suggests, that for a relatively open riser geometry the forces on the individual pipes are determined by the local velocity, which again is determined by the deflection of the flow caused by the resistance of the front pipes. The flow picture is shown in Fig. 4a for a riser with high resistance on the front pipes and the corresponding picture for a riser with lower resistance on the front pipes is shown in Fig. 4b. If the pipes in the riser have rough surfaces the drag coefficients will be relatively high for each individual pipe for all Reynolds numbers. Therefore no changes in flow pattern takes place over the Reynolds number range. This feature is depicted in Fig. 5 where it is seen that the high flow resistance on the front pipes and the central pipe deflect the flow such that only smaller forces and hereby velocities, are experienced on the lee pipes. The picture is in this case obscured a little in the rear part of the configuration because a jet phenomenon exist too. The phenomenon is depicted on the figure and is caused by a large suction behind the front pipes compared with the outer pressure. However, as an average the forces on the rear pipes much smaller than on the front pipes, because of the general deflection of the flow.

The deflection of the flow has an impact on the inertial forces too. Considering an experiment in which the flow is accelerating from rest, the flow around the individual riser pipes is local in the first few instants after the start of the movement. Measuring the hydrodynamic mass coefficient at this stage, it will be equal to the coefficients found in ideal flow (for a cylinder ≃1 plus a contribution from the interference between the pipes). Gaining speed, the flow begins to adjust itself to a flow more looking like the flow field from a steady state current. To reach such a deflected flow field it is necessary to accelerate the flow outwards from the riser. The excess pressure needed for this acceleration can be expressed as an added contribution to the hydrodynamic mass.

The arguments presented can be applied on oscillatory flow, too. For small Keulegan-Carpenter numbers the excursions of the water particles are small compared with the spacing. In this case the normal non-viscuous hydrodynamic mass will result. Increasing the KC-number the outwards acceleration of water will gradually start to develop, resulting in an apparent increase in hydrodynamic mass.

In order to calculate the shielding effect it is therefore necessary to calculate the change in flow field which is a result of the forces on the individual cylinders.

Recent advances have been done in this field and methods have been presented in Ref. /4/ and later improved in Ref. /5/ both for steady flow and unsteady flow. In the following a summary of the method suggested in Ref. /5/ will be presented.

THEORY FOR CALCULATION OF SHIELDING

Assume that pipes in a riser configuration give rise to changes in the velocity field. Let us assume that the changes compared with undisturbed flow, U, is given by u' and that they take place in an area which typically is of an order of magnitude 2-3 times the extend of the configuration. The velocity u is then given by

$$u = U + u'(x,y) \qquad (1)$$

Assuming no shielding, then the total force on the configuration is given by

$$F = F_{Do} = \frac{1}{2} \rho U|U| \sum_{j=1}^{N} C_{Dj} D_j \qquad (2)$$

Let us instead include the shielding. Then the total force over N pipes, F, per unit length is given by

$$F = F_D = \frac{1}{2}\rho \sum_{j=1}^{N} C_{Dj} D_j (U+u'(x,y)) |U+u'(x_j,y_j)| \qquad (3)$$

in which the drag coefficients for each pipe are assumed to be a function of the Reynolds number. The spacing between the pipes are assumed to be so large that it does not influence the local drag coefficients. This is an important assumption for the problem. It simply means that the pipes have so large a spacing that the local flow around each individual pipe has decayed sufficiently to be negligible at the locations of the other pipes.

The shielding in the riser bundle is defined by

$$S_{Do} = 1 - \frac{F_D}{F_{Do}} \qquad (4)$$

Assuming small shielding, then the square velocity terms in Eq. 3 can be linearized. Inserting into Eq. 4 this gives

$$S_{Do} = -2 \sum_{j=1}^{N} C_{Dj} D_j \frac{u'(x,y)}{U} / \sum_{j=1}^{N} C_{Dj} D_j \qquad (5)$$

Methods for calculating the shielding analytically by determining the velocity $u'(x,y)$ have been developed, see Ref. /5/.

It can be shown that the velocity distribution $u'(x,y)$ has the following order, Ref. /5/

$$\frac{u'(x,y)}{U} \sim o\left(C_D \frac{D}{c}\right) \qquad (6)$$

in which c is the typical spacing between the pipes. Considering Eq. 5 this means that the shielding must have the same order. Hence the shielding is small for small drag coefficients and large spacings.

In the special case where the local drag coefficients are the same on all pipes (these are the drag coefficients based on the local flow and not the drag coefficients based on the outer flow as in Figs. 3 and 5) the shielding can be expressed as:

$$S_{Do} = -\frac{\overline{u'}}{U} Q \qquad (7)$$

in which $\overline{u'}$ is a weighted average value of all the $u'(x_j,y_j)$ and Q is a constant typical for the configuration with an order of $Q \sim o(1)$. It is important to note that the drag coefficient enters the equation as a basic parameter. This means that the method is valid for both subcritical flow and supercritical flow. If the drag coefficients are different on the different pipes, Q will vary.

In the case of oscillatory flow, it is necessary to take into account the timelag between the flow inside and outside the structure. This is done by expressing the equation of momentum for the flow area depicted in Fig. 6. The equation only has to be expressed for the shielding.

Using the arguments from the chapter with the description of the phenomenon there is an unbalance in force due to the time lag in developing the shielding.

If the flow has reached an outer velocity of $U = U(t)$ then the steady state shielding is given by Eq. 7.

However, due to the time lag the velocity has not reached the final velocity associated with shielding $u'(x,y)$.

The instantaneous velocity under development is called $u''(x,y,t)$, the instantaneous shielding, S, is simply expressed by:

$$S = -\frac{u''(t)}{UQ} \qquad (8)$$

Expressing the momentum equation for the area defined in Fig. 6 for the flow associated with shielding we can express that the unbalance in force due to the shielding is simply used to accelerate the flow associated with shielding, i.e.

$$\rho \int_{-\infty}^{\infty} \int_{-\delta}^{\delta} \frac{\partial u''}{\partial t} dy dx = (S_{Do} - S_D) F_{Do}$$

in which δ is the half width of the flow. In the above equation it is an inherent assumption that the drag coefficients on all the pipes are the same or remain unchanged in the cycle. It is seen that it has the same form as an oscillating boundary layer equation.

Assuming that the velocity profiles $u'(x,y)$ and $u''(x,y)$ are similar with the same flow width δ and with a length scale for variation in the x-direction of δ the left hand side of Eq. 9 can be expressed as

$$\int_{-\infty}^{\infty} \int_{-\delta}^{\delta} \frac{\partial u''}{\partial t} dy dx \sim \delta^2 \frac{\partial \overline{u''}}{\partial t} = \frac{\delta^2}{Q} \frac{\partial}{\partial t} (US) \qquad (10)$$

~ means proportional with. Inserting Eqs. 2 and 10 into 9 the following equation appears:

$$\frac{-\rho \delta^2 I_1}{Q} \frac{\partial}{\partial t} (US) = (S_{Do} - S) \frac{1}{2} \rho U|U| \sum_{j=1}^{N} C_{Dj} D_j \qquad (11)$$

in which Q is given in Eq. 7. I_1 is a constant only dependant on the velocity profile, i.e. knowing the velocity profile it can be calculated. Introducing that $S = \gamma S_{Do}$, Eq. 11 can be expressed as:

$$\frac{\partial}{\partial \tilde{t}} (\gamma \tilde{U}) = (\gamma - 1) C_1 \tilde{U}|\tilde{U}| \qquad (12)$$

in which $\tilde{t} = \frac{t}{T_z}$ and $\tilde{U} = \frac{U}{U_s}$ are the dimensionless parameters for time and velocity and C_1 is given by

$$C_1 = Q \frac{T}{\delta^2} I_1 U_s D \bar{C}_D \sum_{j=1}^{N} \left(\frac{C_{Dj} D}{\bar{C}_D D}\right) = C_2 \left(\frac{\bar{C}_D D^2}{c^2}\right) KC \qquad (13)$$

When the velocity distribution $u'(x,y)$ is known C_1 and C_2 can be calculated directly. If an analytical expression is not available C_2 can simply be determined from experimental results in the literature, e.g. Refs. /1/, /6/ and /7/.

In this case Eq. 12 shall be solved in order to find the ratios between the steady state shielding and the unsteady shielding. With a sine variation of $\tilde{U}$ this is easily done numerically. So long as the flow around the pipes are completely subcritical or completely supercritical C_2 is only a function of the geometry (for instance = 0.05 for the riser configuration shown in Fig. 1).

In Fig. 7 measured total drag coefficients are compared with computed coefficients. The solution is found for sinusoidal flow for different riser geometries, Refs. /1/ and /6/. The drag coefficient is based on the pitch diameter i.e.

$$C_D = \sum_{j=1}^{N} C_{Dj} \frac{D_j}{D_p} (1 + 2u'(x_j, y_j))/U \qquad (14)$$

It is seen that there is a reasonably good fit between measured and calculated values. The geometries are rather open.

A number of shielding investigations have been made over the years. Several of them have been made in quite narrow flumes. These results shall be applied with great care. Recent investigations, Ref. /5/, have demonstrated that the results are very sensitive to flume width due to blocking effects.

APPLICATION TO BUNDLE RISER SYSTEMS

In order to illustrate the importance of the shielding phenomenon in practical applications it is shown in this section how the effect of shielding can be included in the calculation of the dynamic response of a deep sea bundle riser.

The method for calculation of the dynamic response of the riser system, which is depicted in Fig. 1, is almost identical with the method described by Justesen et al /3/. Here the response is found as the total response of a series of eigenmodes. Coupling between the eigenmodes due to the nonlinear drag force is fully accounted for. The equation of motion for the k'th eigenmode reads

$$m_k \frac{\partial^2 x}{\partial t^2} + c_k \frac{\partial x}{\partial t} + K_k x = F_{Dk} + F_{Ik} \tag{15}$$

Subscript k denotes generalized quantities. This equation is solved by a convolution integral given by

$$x_k(t) = \frac{1}{m_k \omega_k} \int_0^t \exp(-\beta_k \omega_k (t-\tau)) \sin(\omega_{ok}(t-\tau)) \left[F_{Dk}(\tau)+F_{Ik}(\tau)\right] d\tau \tag{16}$$

In the unshielded case, the drag force is described as

$$F_{D,o} = \frac{1}{2} \rho D C_D (u-\frac{\partial x}{\partial t}) |u-\frac{\partial x}{\partial t}| \tag{17}$$

in which u is the local undisturbed particle velocity and x is the deflection of the structure. We shall write the shielded drag force as

$$F_{D,} = F_{D,o}(1-\tau S) \tag{18}$$

S denotes the shielding in steady state flow for the particular pipe configuration. τ is the ratio between the shielding and the fully developed shielding in steady flow S_{Do}. The values of S_{Do} and τ are obtained as described earlier in this paper.

The inertia force has to be modified as well. The unshielded inertia term is

$$F_{I,o} = m_v \frac{\partial x_s}{\partial t} \tag{19}$$

in which m_v is the virtual mass and x_s is the static displacement of the riser due to the floater motion. The inertia force from the vibration of the riser is accounted for in the acceleration term in the equation of motion. The shielding of the inertia force can be derived from the change in acceleration. The mean-velocities are affected as

$$u \simeq U\ (1-\frac{1}{2} \tau S_{Do}) \tag{20}$$

Therefore the accelerations are modified through

$$\frac{\partial u}{\partial t} \simeq \dot{U} - \frac{1}{2} S_{Do} \frac{\partial}{\partial t} \left[u_{unshielded}\right] \tag{21}$$

By introducing eq. 12 we obtain

$$\frac{\partial u}{\partial t} \simeq \dot{U} - \frac{1}{2} S_{Do} U_s C_1 \frac{1}{T_z} |\tilde{U}(0)| \tilde{U}(0)\ (1-\tau)$$

U_s is the significant velocity $\left(\pi \frac{H_s}{T_z}\right)$ used to normalize $\tilde{U}(0)$ and T_z is the zero crossing wave period. Hence the shielded inertia force is given by

$$F_I = F_{Io} - \rho C_M \Omega\ S_{Do}\ U_s\ C_1 \frac{1}{T_z} |\tilde{U}(0)| \tilde{U}(0)\ (1-\tau) \tag{23}$$

In this equation $C_M \Omega$ is the sum, $\Sigma\, C_{Mi} \Omega_i$ for all pipes. Ω is the enclosed volume.

In the calculation procedure these new forcing terms have been introduced. Further, τ is calculated as a function of time as derived previously.

In the wave-active zone the moments are calculated by the procedure outlined in Ref. /3/.

$$M = M_o(1-\tau S_{Do}) \tag{24}$$

The moments can be assumed to originate from the drag forces mainly.

EXAMPLES

Two calculation examples have been carried out. A vertical circular bundle type riser in 200 m of water with 12 Ø 3 1/2" satellite flowlines surrounding a central Ø 10 3/4" main header has been considered. As depicted in Fig. 1 it is attached to a flexjoint at the sea bed and suspended from a floating vessel at 20 m above MSL. The characteristics of the riser correspond to those for the similar bundle riser system in Ref. /3/. Two environmental conditions have been considered. A one year operational condition with regular wave motion of H = 12 m and T = 14 s and an irregular wave train generated from a Pierson Moskowitz spectrum of H_s = 10 m and T_z = 7 s.

The vessel motion is assumed to be in phase with the horizontal water particle motion at the surface with an amplitude of half that of the water particles.

To elucidate the effect of shielding on the force as outlined in the previous section, the temporal variation of the force intensity at z = -100 m, i.e. at middepth, is depicted in Fig. 8. It is seen how the force amplitude is reduced due to shielding. The largest relative force reduction occurs later than the maximum force. This is due to the fact that the flow field develops more and more during the half period. The r.m.s. value of the response at z = -100 m is depicted in Fig. 9. The static motion has been removed for this signal, so it is the response about the static position. Due to the force reduction it is seen that the dynamic response is in fact increased. The reason for this is of course that the reduced force is a damping force.

In irregular wave motion the situation may be somewhat different. In Fig. 11, we have shown the force intensity variation at z = -100 m when the riser system is exposed to the irregular wave train as depicted in Fig. 10. There are in general only minor differences between the shielded and the unshielded force intensities. The force varies at a higher frequency than in the case of regular waves. Therefore the development of shielding is reduced drastically except in situation with a large transient impact. This is highly important because this suggests that there will be increased responses in cases of transients.

In Fig. 12 the response as a function of time at z = -100 m is depicted. The deviations between the two signals are very small except in case of the large transient.

In the wave active zone it is not the dynamic response of the riser system but the direct loads from the wave motion which are important. As the shielding effect is also present in this region the calculated moments in this region should be reduced according to the decrease in forces. This is illustrated in Fig. 13 in which the moment envelope in the wave active zone is shown for the irregular wave situation. Here the shielding is 25% in this case Often this reduction will be of the order of 30 to 40 per cent. This is important and especially applicable for densely spaced structures as wellhead platforms.

CONCLUSIONS

A method for calculation of the development of shielding in openly spaced pipe arrays in steady and unsteady flow has been presented. It has been checked against measurements and the comparison shows reasonable agreement.

The method has been used for calculation of the dynamic response of a deep-sea riser systems. The results show that the shielding effect developes when the exciting forces are of low frequency or when they are very large. On the other hand the shielding does not develop for high frequency force excitations.

It is concluded from the present study that the added accuracy gained by including the effect of shielding can be important for the hydrodynamic forces on pipe arrays. This applies to riser arrays or to wellhead jacket platforms with a dense member spacing.

REFERENCES

/1/ Demirbilek, Z., Halvorsen, T.: "Hydrodynamic Forces on Multitube Production Risers Exposed to Currents and Waves". Proceedings of the Fourth International Offshore Mechanics and Arctic Engineering (OMAE) Symposium, Dallas, 1985, pp. 363-370.

/2/ Heideman, J.C., Sarpkaya, T.:" Hydrodynamic Forces on Dense Arrays of Cylinders". OTC Paper 5008, Houston, Texas, 1985.

/3/ Justesen, P., Ottesen Hansen, N.-E., Lyngberg, B.: "The Role of Hydroelastic Vibrations in Risers". Proceedings of the Fifth (1986) International Offshore Mechanics and Arctic Engineering (OMAE) Symposium, Vol III, Tokyo 1986. pp. 417-425.

/4/ Kongsberg Våpenfabrikk A/S: "Production Riser Development Project Reports no. 1 and 2 JIP-Development Project, Phase V", sponsored by AGIP, ARCO, Conoco, Chevron, Elf, Getty, Mobil, Norsk Hydro, Statoil and Texaco. Norway 1982.

/5/ LICengineering A/S: "Hydrodynamic Forces on Well Conductor Arrays",Vol. I-III, JIP-Development Project, sponsored by Mobil, Mærsk Olie og Gas A/S, Norsk Hydro, Statoil and Texaco. Denmark 1985 (Propriatory Information).

/6/ Løken, A.E., Torset, O.P., Mathiassen, S., Arnesen,T.: "Aspects of Hydrodynamic Loadi... Design of Production Risers". OTC Paper 3... Houston, Texas, 1979.

/7/ Ottesen Hansen, N.-E., Jacobsen V., and Lundgren,H.: "Hydrodynamic Forces on Composite Risers and Individual Cylinders". OTC paper 3541, Houston, Texas, 1979, pp. 1607-1621.

/8/ Pearcey, H.H., Cash, R.F., and Salter, I.J.: "Flow past Circular Cylinders. Simulation of Full Scale Flows at Model Scale". National Maritime Institute, Report NMI R131, March 1982.

/9/ Pearcey, H.H., Cash.R.F., and Salter, I.J.: "Interference Effects on the Drag Loadings for Groups of Cylinders in Uni-directional Flow". National Maritime Institute, Report NMI R130, September 1982.

/10/ Sarpkaya, T.: "Hydrodynamic Forces on Various Multiple-Tube Riser Configurations". OTC paper 3539, Houston, Texas, 1979.

/11/ Schlichting, H.: "Boundary Layer Theory", McGraw-Hill, New York, 1960.

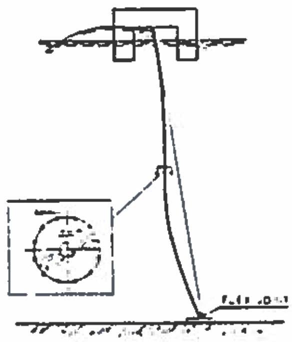

Fig. 1 Typical multibore riser configuration (KV2).

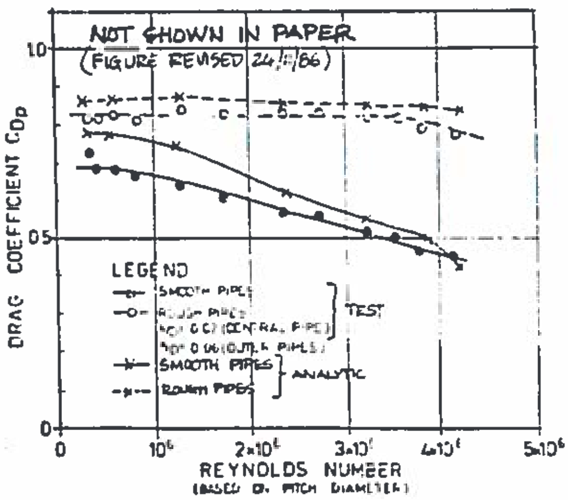

Fig. 2 Drag force on riser configuration KV2.

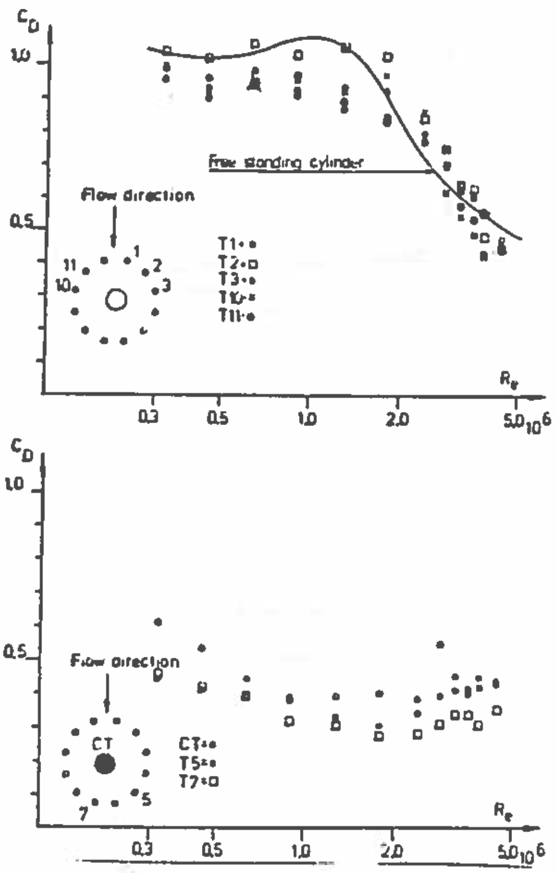

Fig. 3 Forces on the individual pipes of KV2.

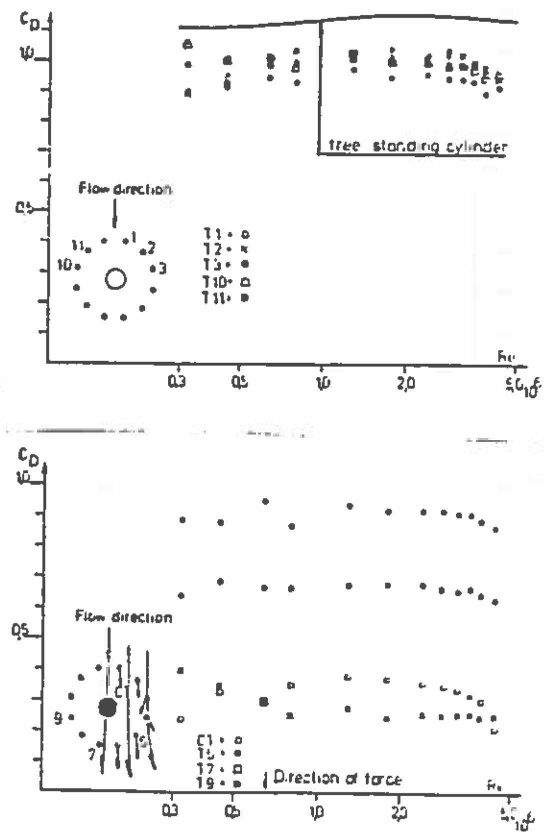

Fig. 5 Forces on individual pipes of KV2 for rough cylinder, k/D = 200

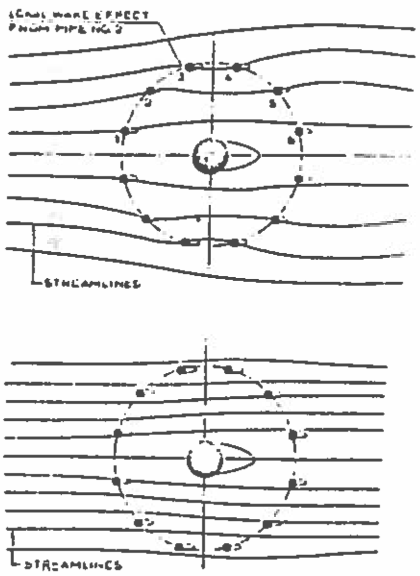

Fig. 4 a) Flow field at a riser with high resistance on the front pipes. b) Flow field at a riser with lower resistance on the front pipes.

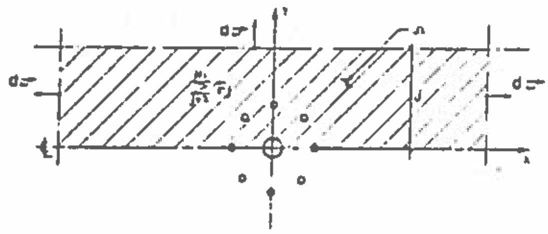

Fig. 6 Force equilibrium in oscillatory flow.

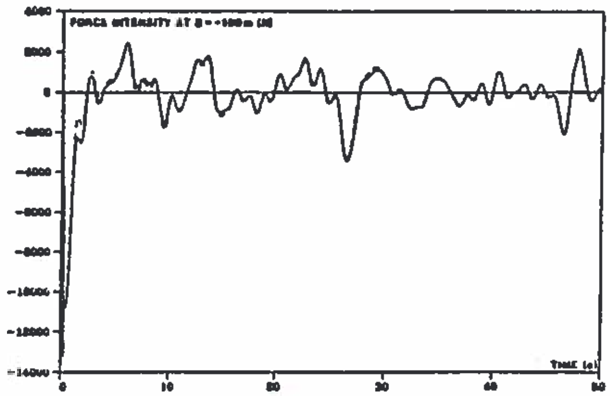

Fig. 11 Calculated force variation at z = -100 m as a function of time, irregular waves. ——: unshielded; ----: shielded.

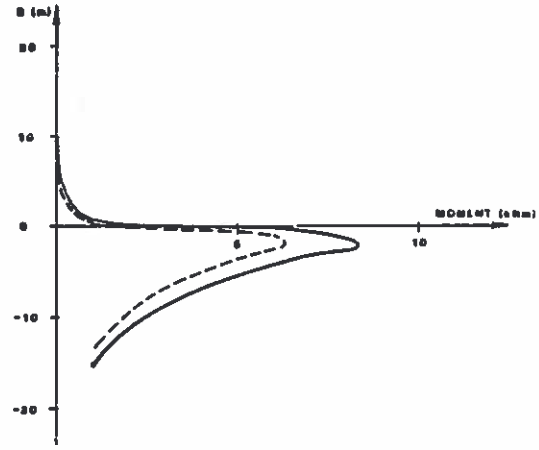

Fig. 13 Calculated moment envelope in wave active zone, irregular waves. ——: unshielded; ----: shielded.

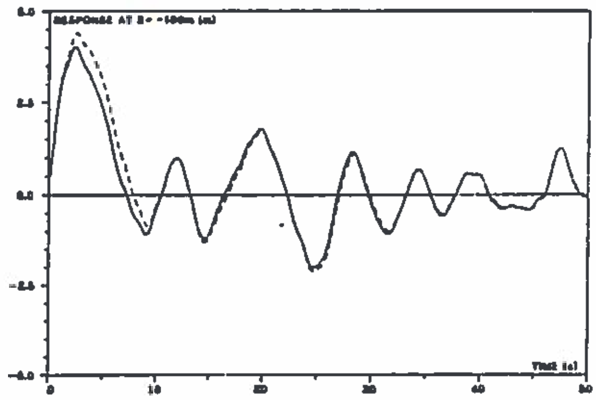

Fig. 12 Calculated response at z = -100 m, irregular waves. ——: unshielded; -----: shielded.

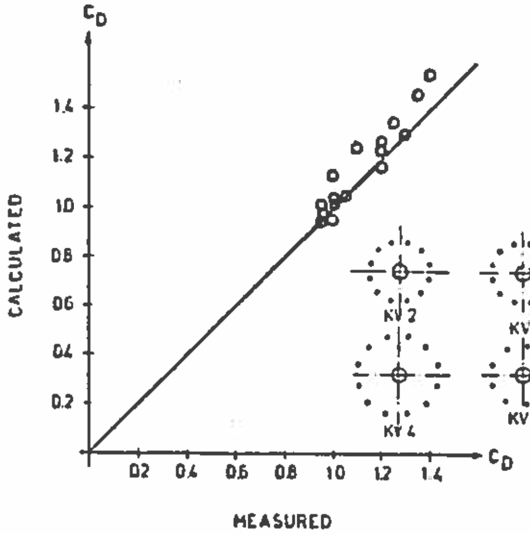

Fig. 7 Comparison between measured and calculated drag coefficients for different riser configurations in oscillatory flow. The drag coefficients are based on pitch diameter.

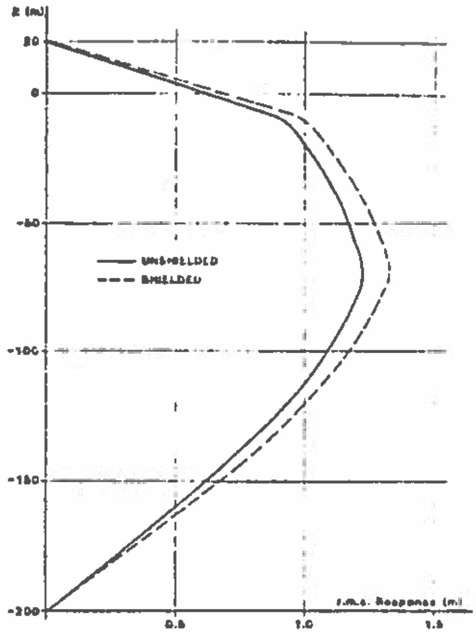

Fig. 9 Calculated r.m.s. value of response with the static component removed. Regular waves, H = 12 m and T = 14 s.——: unshielded; -----: shielded.

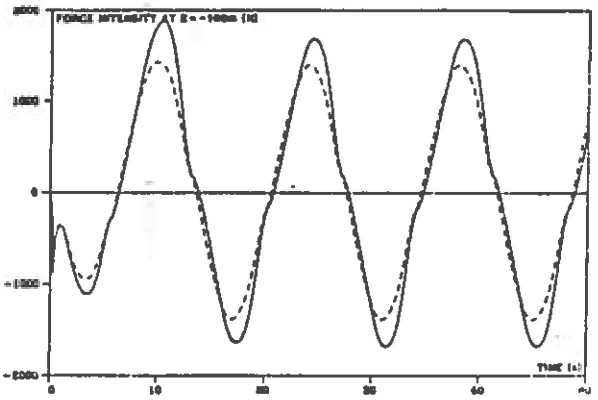

Fig. 8 Calculated variation of the total force intensity at z = -100 m as a function of time. Regular waves, H = 12 m and T = 14 s. ——: unshielded; ------: shielded.

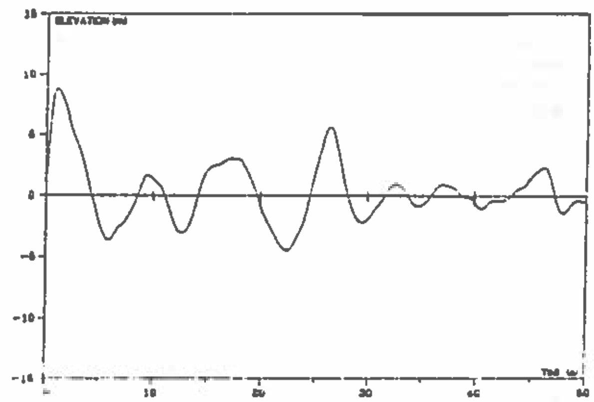

Fig. 10 Surface elevation as calculated from Pierson Moskowitz spectrum. H_s = 10 m and T_z = 7 s.

RESERVE STRENGTH OF WELLHEAD PLATFORMS IN THE NORTH SEA

by

Henrik Nedergaard, LICengineering A/S

N.-E. Ottesen Hansen, LICengineering A/S

ABSTRACT

The reserve against global collapse of jacket platforms due to wave loads in 40m of water in the North Sea is investigated. The effect of elastic/plastic stability of the members are considered and the effect of shielding in the hydrodynamic loads are estimated. The structural analysis procedure is a finite element model in which a plastic hinge method is used. The effect of gradual plastification of the beam cross sections is included and the method is verified against a number of tests. Good agreement is found. It turns out that there is a sufficient safety against wave causing collapse when using the normal design practice. If the shielding effect is included in the analysis the probability of wave causing collapse is found to decrease with a factor 34.

NOMENCLATURE

C_D : Drag coefficient
C_M : Mass coefficient
D : Diameter of member
F : Cumulative probability function
F : Force
F_o : Force without shielding
H : Wave height
$\underline{\underline{k}}$: Stiffness matrix
$\underline{\underline{k}}_e$: Stiffness matrix for normal force
$\underline{\underline{k}}_{g1}$: Stiffness matrix for coupling between axial
$\underline{\underline{k}}_{g2}$ and lateral deformations
$\underline{\underline{k}}_p$: Plastic reduction matrix
S : Shielding
T : Wave period
T : Return period
U : Velocity perpendicular to member axis
$\dot{U}$: Acceleration perpenducular to member axis
α : Parameter in the Weibull distribution
β : Parameter in the Weibull distribution
γ : Parameter in the Weibull distribution
Γ : Yield surface
ρ : Density of sea water
λ : Average number of extreme stroms per year
$\hat{}$: Maximum likelihood estimate

STATEMENT OF PROBLEM

The safety level for steel jacket wellhead platforms has long been debated. Several elements enter this problem for instance ultimate loads, fatigue damage, and damage due to ship impact. This makes the problem of determining risk rather complicated.

A simpler problem will be the one where only one of the above effects is present. An example of this is a North Sea wellhead platform in shallow water. The safety of such platforms is assumed to be governed by the ultimate loads, i.e. the highest waves.

The design practice for offshore platforms varies from country to country but in general the platforms are designed to sustain 50 yrs to 100 yrs waves with associated current with suitable safety coefficients on materials, on geometrical parameters and on the hydrodynamic loads. These safety coefficients are selected such that the platform in principle obtains the same safety as a normal building on land. The question is whether this is sufficient especially in the light of the fact that design for instance in Denmark is made for waves with 50 yrs recurrence interval which means that there is a 33% probability of this event taking place within a 20 yrs lifetime of the structure.

In shallow water the waves will be limited to o.69 times the water depth. If a shallow water platform can sustain such ultimate, near breaking waves with sufficiently small permanent deformations to allow further use then the safety level must be large and the safety level of the platform is not likely to be governed by waves.

The inherent conservatism in the design practice is not usually taken into account. An additional reserve is given to the platform when the shielding on well conductor arrays and dense areas are considered. For very open platforms such as flare platforms this effect will not mean very much. For wellhead platforms with dense conductor arrays a large conservatism is included into the design. In this paper this conservatism is determined for one particular platform - a typical Danish wellhead platform. The conservatism is simply determined by comparing the probabilities of occurrence of waves which will cause the same deformations in the platform with or without shielding taken into account.

Possible ways to optimize future platforms is pointed out if it is decided to include the shielding effects in the design.

STRUCTURAL REPRESENTATION

In order to determine the reserve strength in platforms the large scale deflections due to yield must be taken into account, because they form the real reserve. Therefore the structural model must consider both material and geometrical non-linearities. The beam element used in the model is shown in Fig. 1.

The calculation procedure in the structural model is incremental and an updated Lagrange (co-rotational) formulation is used for each increment step. This means that the local x-axis of the element is assumed to be joining the two end nodes. Interpolation functions associated with the linear Timoshenko beam theory in deriving the geometric non-linear beam element stiffness matrix is used. Using the Green's strain tensor and the principle of virtual work the basic member force-deformation relation is derived. The elastic tangent element stiffness matrix is achieved in a straight forward way, Eq. 1.

$$\bar{\bar{k}}_{te} = \bar{\bar{k}}_e + \bar{\bar{k}}_{g1} + \bar{\bar{k}}_{g2} \qquad (1)$$

in which $\bar{\bar{k}}_e$ is the standard element stiffness matrix for a Timoshenko beam. $\bar{\bar{k}}_{g1}$ is a matrix which depends on the normal force acting on the beam element. It contains the eigenvalues for buckling (Refs 1 and 2). The $\bar{\bar{k}}_{g2}$ matrix is a function of the deformation of the element and gives the coupling between axial and lateral deformation. It is the inclusion of this matrix which makes it possible to model each prismatic beam element as only one element, even in the post-buckled region.

The introduction of yielding of the beam element is mathematically described by the plastic node concept (Ref 15). By use of this concept plasticity can only be introduced in the element ends. In the present model an extra node is introduced at midspan of the element if plasticity occurs there. The extra ode is then condensed out of the equation system before assembling the global stiffness matrix.

The plastic reduction matrix $\bar{\bar{k}}_p$ is based on the assumption that the material is ideal elastic/plastic and furthermore that:

- The plastic incremental deformation is perpendicular to the tangent of the yield surface Γ_p.
- The incremental change in generalized forces in the beam cross-section is parallel with the tangent of the yield surface Γ_p.

These two assumptions are derived from Drucker's postulate from the theory of plasticity.

The present plastic reduction matrix is further expanded to include gradual plastification of the cross-section between the initial yield surface Γ_e and the yield surface Γ_p. In Fig. 2 the yield surfaces are shown for a circular hollow cross-section.

The total incremental tangent element stiffness matrix $\bar{\bar{k}}_t$ is then:

$$\bar{\bar{k}}_t = \bar{\bar{k}}_e + \bar{\bar{k}}_{g1} + \bar{\bar{k}}_{g2} + \bar{\bar{k}}_p \qquad (2)$$

This element stiffness matrix is used in an incremental calculation procedure, where forces and displacements are summed after each increment. Also the element geometry is updated.

Two test examples are presented. First the example shown in Fig. 3 has been solved analytically and tested experimentally (Ref 17). This particular example has been used to test several non-linear elastic solution procedures (Refs 9 and 18).

The elastic solution (Ref 17) takes into account large deformations, the influence of the axial forces on the flexural stiffness and the axial shortening due to lateral bending. The present calculation procedure has been tested by modelling each of the two beams as one element. As seen in Fig. 4 the present results are in close agreement with the analytic solution.

As a second example which includes the effect of plasticity we have chosen the K-brace shown in Fig. 5. This frame has been analysed numerically using the program FENRIS, and tested experimentally by Moan et al, 1985. In the FENRIS model each beam is divided into 8 elements whereas in the present model only one element is used for modelling each beam. Further, in the FENRIS model a material strain-hardening law is used, whereas an ideal elastic-plastic material is used in the present model. The results are shown in Fig. 6. It turns out that the ultimate loads are overestimated slightly by both methods. This fact can probably be explained by the fact that local changes in cross-section have not been taken into account in either of the procedures. The experiment shows a considerable loss in strength just after the ultimate load has been reached. This behaviour is apparently represented satisfactorily by the present procedure.

HYDRODYNAMIC FORCES

The hydrodynamic forces are represented by the Morison equation. Expressing the force intensity per unit length:

$$F_o = \tfrac{1}{2}\rho\, DC_D U|U| + \rho D^2 \frac{2\pi}{4} C_M \dot{U} \qquad (3)$$

For calculating the wave kinematics the stream function theory is used, because it is the most stable method to describe high and near breaking waves. The wave kinematics have been combined with a 50 yr current. The hydrodynamic coefficients C_D=0.7 and C_M=2.0 have been used. Measurements have shown that the uncertainty on the coefficients are reasonably small (10-20%), but that the uncertainty on the wave may be large. This is especially the case for near breaking waves.

In the case of dense grouping of member there may be a shielding effect where the downstream members stand in lee of u stream members.

The shielding can be expressed as a percentage reduction in force, S, such that

$$F = (1-S)F_o \qquad (4)$$

in which F_o is the hydrodynamic force without shielding and F is the hydrodynamic force taking into account the shielding.

The shielding will be an average figure on how the individual members are influenced. Some elements will experience a very large reduction whereas other elements in fact may experience an increase in force. The reason for this is that the shielding is caused by a change in the flow field reducing the velocities at lee pipes but due to continuity in the flow it is of course necessary to have increased velocities in other areas. A calculation model for determining shielding has been developed (Refs 8 and 12).

The calculation procedure for checking the platform against global collapse is done using a quasi-static procedure. This is a reasonable approximation for a North Sea platform in shallow water because the dynamic amplification is small. A load corresponding to the wave position shown in Fig. 7 is applied to the structural model. The wave crest is then in time steps moved towards the platform. The length of the time step is not constant, but is determined from the following criteria:

1) The absorbed potential energy in the platform must not exceed the energy absorbed in the first time step.

2) The change in potential energy does not exceed 4% of the total potential energy.

3) The change in sectional forces in a plastificated node must not exceed 10% of the total plastic capacity.

After each time step the structure is checked against collapse due to the dead load, which is applied only in the first time step. The structure is also checked against punching shear capacity in each node. If the capacity is exceeded the specific beam end is disconnected from the node in the next and following time steps.

WELLHEAD PLATFORM

In order to demonstrate the effect of shielding the ultimate wave load carrying capacity of a typical wellhead platform for Danish water has been calculated.

In Fig. 8 the computer model of the platform is shown. The conductor layout is shown in Fig. 9. The conductor array consists of a 3x4 array with a spacing of 7'6" between the 24" conductors. In the computer model the conductor array modelled as one member and also the skirt-piles are simplified.

The modelling of the 12 supporting piles is made by non-linear springs with an initial stiffness equal to the secant stiffness for the 50 yr load level.

The platform which is sited at 40m water depth is designed in accordance with the Danish Code of Practice (Ref 5). Shielding effects are included in the design. As previously mentioned the effect of shielding depends on the wave height and the wave period. For the present platform the calculation of the shielding effect is carried out for several wave conditions.

In Table 1, the shielding is presented for the design wave (with 50 yrs return period) and for the ultimate, near breaking 27m high wave. The results using wave kinematics determined from stream function theory are shown in form of total reduction in overturning moment for the platform. The table is valid for waves coming from north, for other directions the shielding is varying as shown in Fig. 10.

WAVE CLIMATE

A previous hindcast analysis has shown that the probability distribution of ultimate waves in the North Sea is best described with a Weibull distribution. This fact has been found by Chi-square tests, Kolmogorov-Smirnov tests and by visual inspection of the results of the above investigations. In all these tests the Weibull distribution came out best when compared with the Gumbel distribution and the truncated Log-normal distribution (Ref 4).

The cumulative probability function for the Weibull distribution is given by:

$$F(H,\alpha,\beta,\gamma) = 1 - \exp\left(-\left(\frac{H-\gamma}{\beta-\gamma}\right)^{\alpha}\right) \qquad (5)$$

in which α, β, and γ are parameters. A maximum likelihood estimate gives that the T-year estimate for the wave height is, (Ref 4):

$$H_T = \hat{\gamma} + (\hat{\beta} - \hat{\gamma})\{\ln(\hat{\lambda} T)\}^{1/\hat{\alpha}} \qquad (6)$$

in which $\hat{\alpha} = 1.591$, $\hat{\beta} = 13.27$, and $\hat{\gamma} = 9.80$,. $\hat{\lambda}$ is the average number of severe storms per year, $\hat{\lambda} = 2.0$ fo the Danish continental shelf.

In Table 2, the estimated T years waves are presen ted for the selected site (40m water depth). The ultimate near breaking highest wave which can exist in this water depth is 27.0m corresponding to a 170.000 year return period to to a frequency of $6 \cdot 10^{-6}$.

ANALYSIS PRECEDURE

Let us assume that the wave causing collapse frequency which will be acceptable for collapse of platform as high as $2 \cdot 10^{-4}$ per year. The deformation of the platform is therefore determined when exposed to waves of this frequency (H = 23.80m).

In order to compare the waves giving the same deformations (both instantaneous and permanent deformations) with and without shielding the following procedure is applied:

1. As a bench mark determine the amount of damage to the platform applying a wave with a 5000 year return period. In the analysis the effect of shieldin is not included.

2. Next determine the wave which gives the same amount of damage as under 1. When shielding <u>is</u> taken into account.

3. Compare the probabilities of occurrence between 1. and 2. The ratio will indicate the factor for reser ve strength towards wave causing collapse.

RESULTS

A standard designed platform not taking shielding into account can easily sustain a wave with a frequency of occurrence of $2 \cdot 10^{-4}$ (23.80m) without collapsing. Th platform will sustain minor deformation in cross bracings but will be fully functional after the passage of the wave. In Fig. 11 the deformation of the topside as a function of time is shown, the wave crest is placed at t = 0. In Fig. 12 the maximum platform deflection is shown. On this figure the members which have been damaged are marked. Member no. 77 is separated from the platform leg due to punching shear fracture and member no. 58 is slightly globally buckled due to axial overload. The platform will not for this wave go into globa collapse, only the two listed members will be damaged.

It has further been investigated which effect ther will be of several passages of high waves. Assuming th the 23.8m wave is followed by one more 23.8m wave the deformations are increased, but the platform maintains its integrity, Fig. 13.

When the effect of shielding is taken into account in the analysis, the platform can sustain a higher wave It was found that a wave with a frequency of occurrence of $6 \cdot 10^{-6}$ (H = 27.0 m) will give the same deformations as in the case of no shielding. This results in an increase in safety level against collapse with a factor 34.

The 27m high wave is on the breaking limit and is the highest wave which can exist in the 40m of water. Since the platform is still functional after the passag of this wave, it is not waves which govern the ultimate stability of the platform (under the assumption that stream function theory can be used for wave kinematics under these conditions).

CONCLUSIONS

The following conclusions can be drawn:

1. The normal safety systems used for design of plat-

forms for instance the Danish partial coefficient system for design practice provides sufficient safety against structural collapse for steel jacket wellhead platforms provided the stream function theory is sufficiently accurate to describe near breaking waves.

2. The shielding effect on a typical shallow water wellhead platform gives an important contribution to the safety against wave causing collapse. For a typical Danish wellhead platform it can increase the safety against wave causing collapse with a factor 34 when taken into account.

3. In view of 2. more optimal designs for platforms are possible. In Fig. 15 favourable effects are shown. Including the shielding effect can for a given structure lead to reduction in number or piles and/or increase in number of wells.

ACKNOWLEDGEMENTS

Mærsk Olie og Gas A/S, Denmark, has contributed with help concerning design details of their wellhead platforms and background material from their design basis for environmental loads. The help is gratefully acknowledged.

Statoil, Norway, has released data concerning shielding on wellhead platforms. The help of Dr. Ove Gudmestad is gratefully acknowledged.

REFERENCES

1. Archer, J.S.: "Consistent Matrix Formulations for Structural Analysis using Finite-Element Techniques". AIAA-Journal, Vol. 3, No. 10, 1965, pp. 1910-1918.

2. Bergan, P.G.; T.H. Søreide: "Solution of Large Displacement and Instability Problems using the Current Stiffness Parameter". Finite Elements in Non-Linear Mechanics, Tapir 1977, pp. 647-670.

3. Brink-Kjær, O., J. Knudsen, G. Rodenhuis and M. Rugbjerg, 1984: "Extreme Wave Conditions in the North Sea". Offshore Technology Conference, Houston 1984.

4. Brink-Kjær, O., B. Lyngby and J.B. Nielsen, 1983: "Direct Assessment of Environmental Forces from Hindcast Time Series". I+P Forum on Environmental Parameters, Subcommittee C. Meeting on Physical Oceanography and Meteorology, London, November 1985.

5. Danish Engineering Association, 1983: "Code of Practice for Pile Supported Offshore Steel Structures". DS 449, Part 1+2, 1. Edition 1983. Translated to English, September 1984.

6. Heideman, J.C. and T. Sarpkaya, 1985: "Hydrodynamic Forces on Dense Arrays of Cylinders". Proceedings of the 17'th Annual Offshore Technology Conference OTC Paper 5008, Houston, Texas, 1985.

7. Kongsberg Våpenfabrikk A/S, 1982: "Production Riser Development Project", Reports nos. 1 and 2, JIP-Development Project, sponsored by AGIP, ARCO, Conoco, Chevron, Elf, Getty, Mobil, Norsk Hydro, Statoil and Texaco. Norway 1982.

8. LICengineering, 1985: "Hydrodynamic Forces on Well Conductor Arrays", Vol. I-III, JIP-Development Project, sponsored by Mobil, Mærsk, Norsk Hydro, Statoil and Texaco. Denmark 1985.

9. Meek, J.L., Tan, H.S.: "Geometrically Non-Linear Analysis of Space Frames by an Incremental Iterative Technique". Computer Methods in Applied Mechanics and Engineering 47, 1984, pp. 261-282.

10. Moan, T., J. Amdahl, A.G. Engsets, T. Granli: "Collapse Behaviour of Trusswork Steel Platforms". BOSS'85, Delft 1985.

11. Nedergaard, H., P.T. Pedersen.: "Analysis Procedure for Space Frames with Material and Geometrical Non-Linearities". Proc. Europe US Symposium, Finite Element Methods for Non-Linear Problems, Trondheim, Norway, 1985.

12. Ottesen Hansen, N.-E. and P. Justesen, 1987: "Shielding in Pipe Arrays in Waves and Current". OMAE 1987, Houston, Texas, Paper OMAE-87-726.

13. Reissmann, C.: "Grundlagen der Nichtlinearen Festkorpermechanik - eine methodische Einführung". Technische Mechanik 5, Heft 1, 1984, pp. 19-30.

14. Saran, M.: "On the Influence of the Discretization Density in the Non-Linear Analysis of Frames". Computer Methods in Applied Mechanics and Engineering 43, 1984, pp. 173-180.

15. Ueda, Y., T. Yamakawa, M. Matsiushi: " A new Theory on Elastic Plastic Analysis of Framed Structures". Technology Reports of the Osaka University, Vol. 19 No. 875, 1969, pp. 263-276.

16. Ueda, Y., S.M.H. Rashed, K. Nakacho: "New Efficient and Accurate Method of Non-Linear Analysis of Offshore Tubular Frames (the idealized structural Unit Method)". 3rd. Int. Offshore Mechanics and Arctic Engineering Symposium, New Orleans, Luisiana 1984, pp. 260-267.

17. Williams, F.W.: "An Approach to the Non-Linear Behaviour of the Members of a Rigid Jointed Plane Framework with Finite Deflections". Quart. Journ. Mech. and Applied Math., Vol. 17, Pt. 4, 1964, pp. 451-469.

18. Wood, R.D., O.C. Zienkiewicz: "Geometrically Non-Linear Finite Element Analysis of Beams, Frames, Arches and Axisymmetric Shells". Computers and Structures, Vol. 7, 1977, pp. 725-735.

Wave	Reduction in overturning moment due to shielding
Height 19.7m Period 13.8s	10%
Height 27.0m Period 16.2s	16%

Table 1. Reduction in Overturning moment due to shielding for waves from North.

Return Periods Years	T-Year Wave m
10	16.72
100	19.70
1000	22.22
10000	24.46
100000	26.52
1000000	28.44

Table 2. T-Year estimate for highest wave.

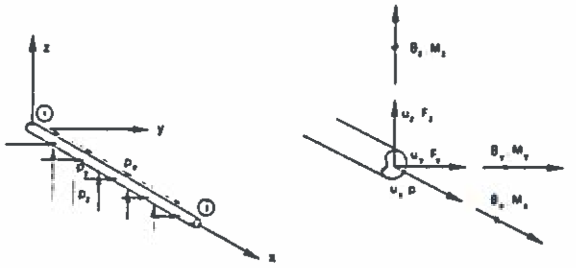

Fig. 1 Prismatic beam element.

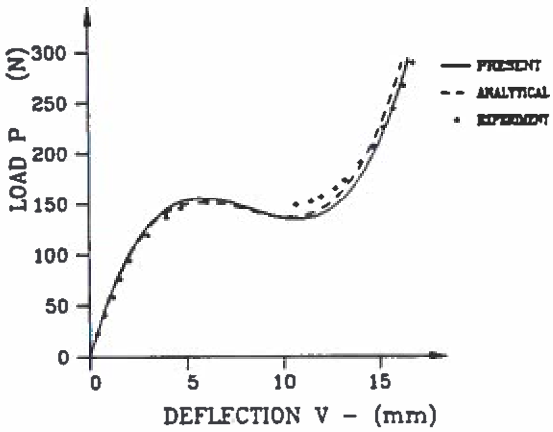

Fig. 4 Load deflection for Williams toogle frame. Ref. 17.

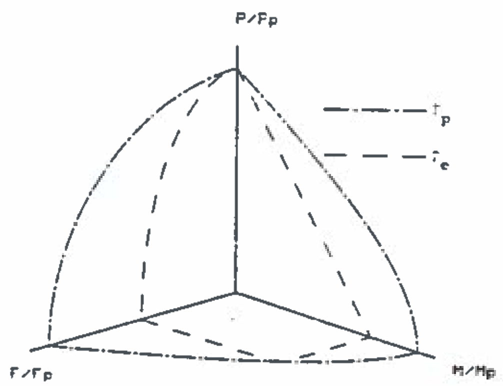

Fig. 2 Yield surface Γ_p and initial yield surface Γ_e for a hollow circular cross section.

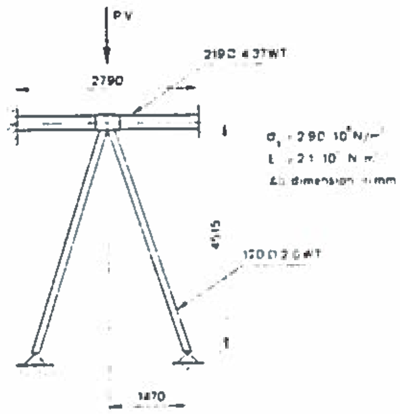

Fig. 5 Geometry of the K-brace.

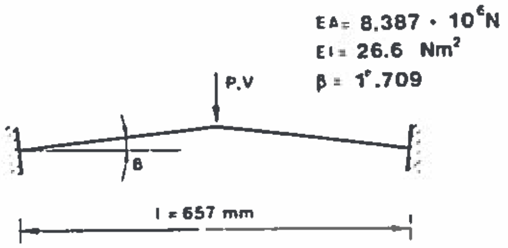

Fig. 3 Williams toogle frame, Ref. 17.

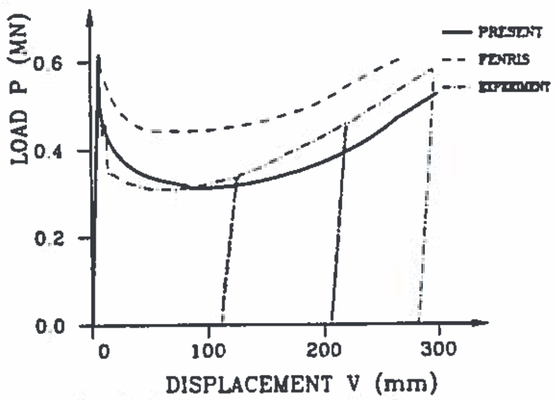

Fig. 6. Load-displacement for the K-brace.

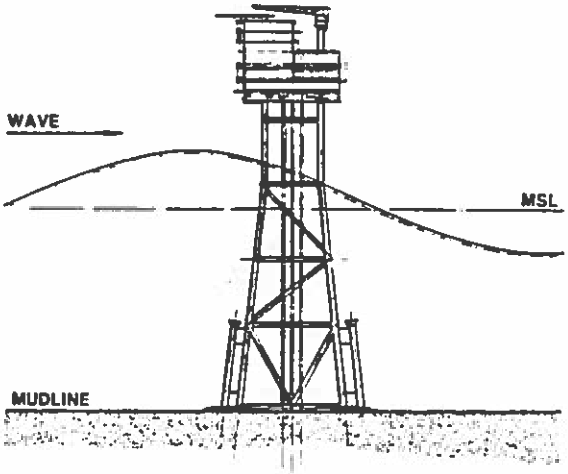

Fig. 7. Position of wave at the start of calculation.

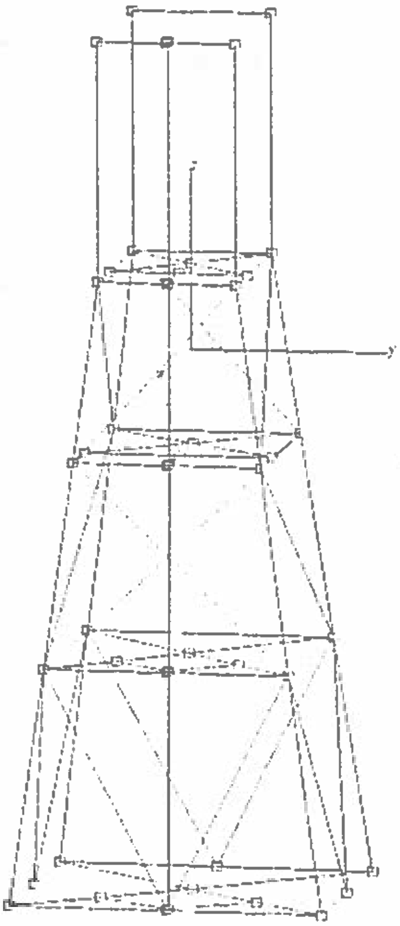

Fig. 8. Computer model of the platform.

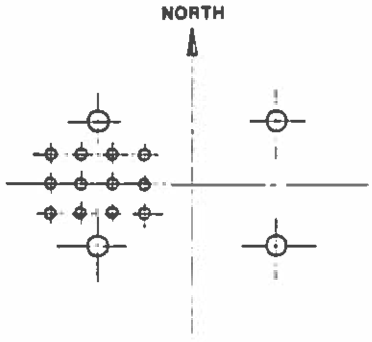

Fig. 9. Orientation of the platform and conductor layout.

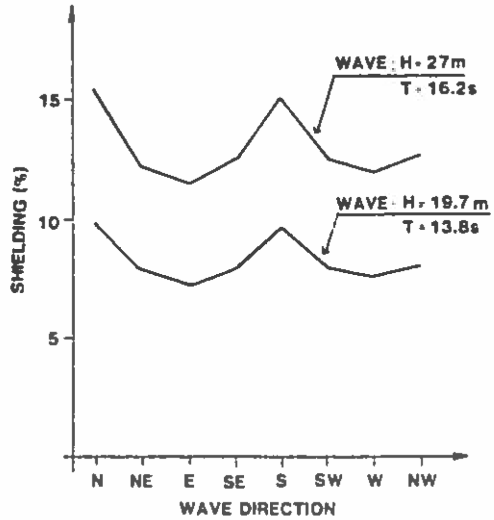

Fig. 10. Reduction in overturning moment due to shielding.

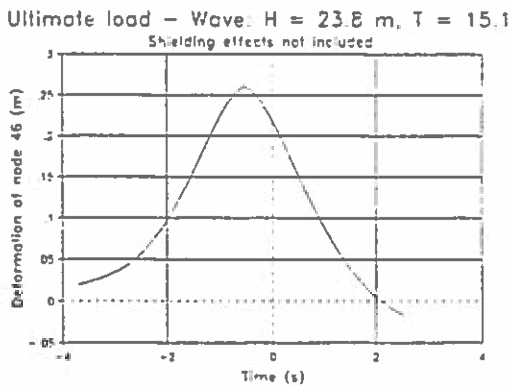

Fig. 11. Deflection of topside in wave: H=23.8, T=15.1s. Shielding effects not included.

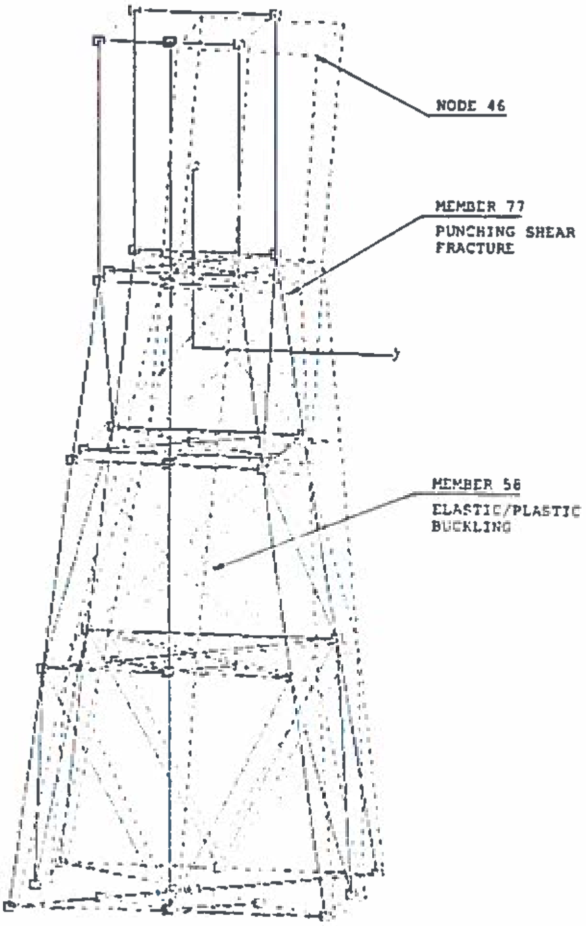

Fig. 12. Max. deflection of jacket multiplied by 20 wave: H=23.8m, T=15.1s. Shielding effects not included.

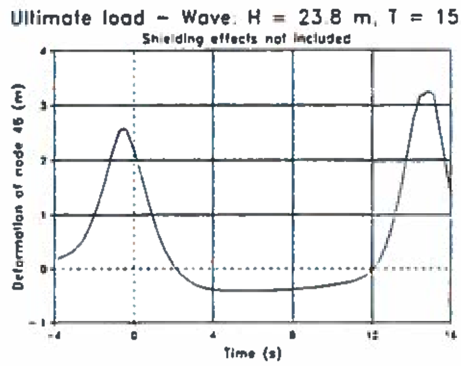

Fig. 13. Deformation of platform during two passages of 23.8m waves (shielding not included).

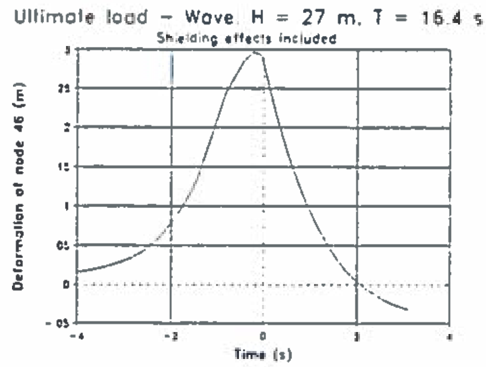

Fig. 14. Deflection of topside in wave: H=27m, T=16.4s shielding effects included.

a)

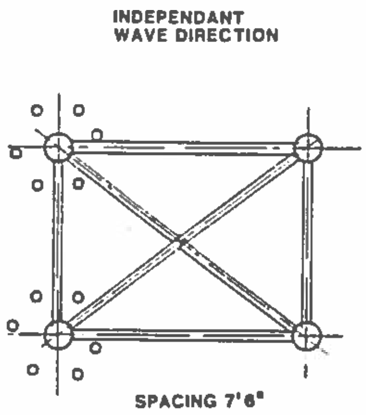

b)

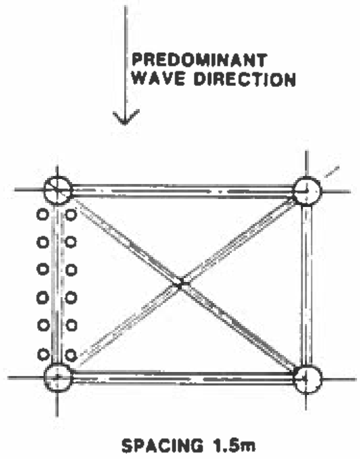

c)

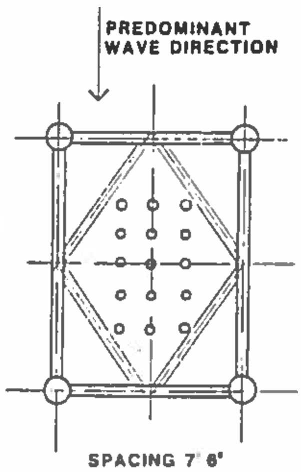

d)

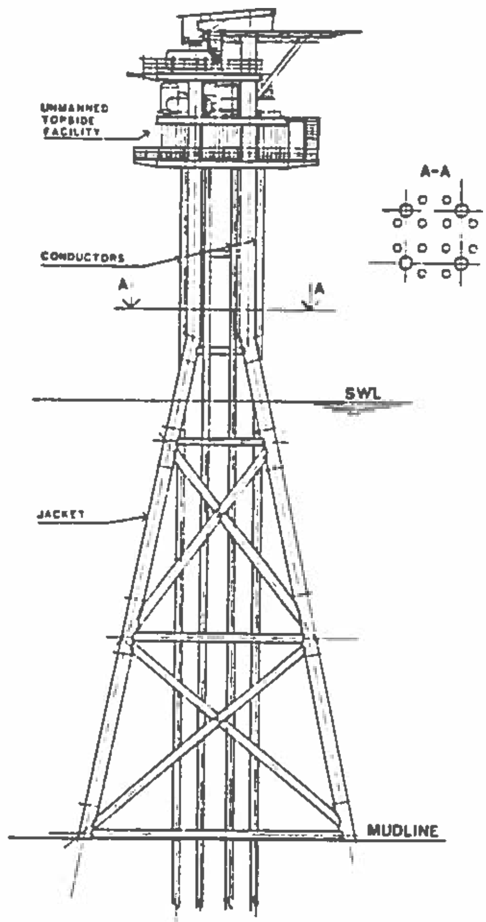

Fig. 15. Layouts favourable for utilizing the shielding effect (in principle).

a) Design wave equal for all directions.
b) Design wave different for the directions.
c) Conductor array isolated from interference with legs.
d) Integrated conductor/platform layout.

NUMERICAL HYDRODYNAMICS

BY

PER MADSEN, DANISH HYDRAULIC INSTITUTE

AND

JOHN CHRISTOFFERSEN, DANISH MARITIME INSTITUTE

NUMERICAL HYDRODYNAMICS

PER MADSEN
CHC

1. INTRODUCTION

A joint research project between DMI & DHI was started in 1986 financed partly by FTU and partly by IHS. The objective of the project has been to develop a general numerical modelling system for the computation of the hydrodynamic wave impact on floating structures and of the resulting motions.

Typical applications of this modelling system are

a) Unprotected installations in deep water.
b) Unprotected terminals and installations in shallow water (i.e. shoaling and refraction effects are included).
c) Protected terminals in harbours (i.e. diffraction and partial reflection effects are included).

The project has covered the following main problems:

a) Description of the wave field in protected and unprotected waters of arbitrary depth
b) Description of the ship generated wave motions.
c) Description of the wave induced motions of moored ships.

Each of these topics introduce a number of specific problems characterized by the water depth, the wave climate and protected or unprotected installations. Therefore it has been decided not to attempt to develop one single model which can take care of all the problems, but alternatively to develop model tools which should be used for specific purposes.

Three different model tools will be discussed in the following:

1) System 21 MK8 & MK11 based on the Boussinesq equations.
2) System 21 MK10 based on the Mild slope equations.
3) BEMSHIP based on the Laplace equation.

2. WAVE MODELLING BASED ON THE BOUSSINESQ EQUATIONS

Mathematical short wave models are being more and more extensively applied in engineering practice to determine the evolution and transformation of waves travelling from offshore to coastal protected waters and to provide an assessment of the wave conditions in harbours and coastal regions. Models based on the Boussinesq equations (System 21 MK8) have been shown to be capable of reproducing the combined effects of most of the wave phenomena of interest to the coastal engineer for a relatively low cost: Shoaling, refraction, diffraction and partial reflection of directional irregular wave trains can be simulated and nonlinear wave-interactions taken into account. However, the application of models based on the Boussinesq equations is generally restricted to relatively shallow water: When the ratio of water depth to deep water wave length (h/L0) increases a rapidly increasing error will be introduced in the celerity and group velocity.

The simulation of important phenomena like refraction and diffraction strongly relies on a correct representation of the dispersion relation i.e. on the celerity of the wave. The group velocity on the other hand will influence the propagation of irregular wave trains and the rate at which energy propagates through the model.

2.1 Extension of Boussinesq Eq. to Deep Water

Recently a new form of the Boussinesq equations, which makes it possible to extend the application area to deeper water, has been developed at DHI. This extension is considered to be a major breakthrough in numerical short wave modelling. For the first time it is now possible to simulate the evolution of irregular wave trains travelling from deep water (say h/L0=0.6) to shallow water. In the range of 0.20< h/L0 <0.60 the model will perform as Stokes 1.order theory, while in more shallow water the wave profile and the celerity will be affected by the nonlinearities known from cnoidal wave theory.

The new equations lead to a dramatic improvement of the linear dispersion performance of the model. As an examble consider a regular wave with a period of 5 s on a water depth of 17m. In this case the standard form of the Boussinesq equations leads to a celerity error of -48% and a group velocity error of -90%, while the new form of the equations leads to an error of -3% for the celerity as well as for the group velocity.

In 1988 a one-dimensional version of the model was established and very good results were obtained. Since August 1988 we have been working on extending this model to two horizontal dimensions (SYSTEM 21 MK10). This work has still not been completed and has so far only been partly successfull. Unexpected problems with the numerical scheme have appeared and it turns out that the time-centering of the higher order gradient terms is essential in order to avoid artificial damping of the wave field. However it is expected that this work will completed by the end of this year.

2.2 Internal Generation of Waves

Recently the internal wave generation has been improved significantly. So far it has not been possible to obtain the correct amplitude of the generated waves in S21 MK8. The amplitudes have turned out to be larger than expected and the surface profiles have been distorted. The reason for these problems have now been identified to the Boussinesq terms P_{xxt} and Q_{xyt}. In order to give the input wave the correct propagation speed these terms need to operate on the correct wave profile. However the input waves will propagate symmetrically away from both sides of the generation line, creating a discontinuity in the surface slope

(S_x or P_x) at the line. This discontinuity will strongly influence the P_{xxt} and Q_{xyt} terms creating a distortion of the incoming wave profiles. The Boussinesq terms have now been corrected for the case of two parallel generation lines and the result is most satisfactory.

2.3 Directional Wave Input

Recently a new service program has been developed for the specification of random directional wave input to the Boussinesq model. The input spectrum can be chosen as Jonswap or Pierson-Moscowitz and the spreading relative to the mean incoming wave direction can be chosen as Normal, rectangular or $\cos^{2S}$ distributions. In every single grid point along the internal generation lines the time series of incoming waves will be determined. System 21 MK8 will read these data as a transfer file.

2.4 Sub- and Super Harmonics

Due to nonlinear wave-wave interaction a train of irregular waves will generate sub- and super harmonics. In fact this phenomena is related to the mechanism generating radiation stress and longshore currents in the surf zone (chapter 4). It is well known that these phenomena are very important for drift forces on floating structures in shallow and intermediate water depths. The classical theories for describing these complicated processes are based on the Laplace equation. Recently the theoretical solution based on the Boussinesq equations has been derived at DHI. It is the intension to verify System 21 against these solutions.

3. WAVE MODELLING BASED ON THE MILD SLOPE EQUATION

In the period 1986-1987 the first version of the numerical wave model SYSTEM 21 MK10 was developed.
This model solves the mild-slope equations using a very fast and

efficient algorithm based on implicit finite difference techniques.

The mild slope equations, which were originally derived by Berkhoff(1972), describe the transformation of monochromatic waves moving over a weakly sloping bottom. Shoaling, refraction, diffraction and partial reflection is included and the equations can be applied to any combination of wave period and water depth. The only limitation is that all nonlinear effects are disregarded. This means that the wave celerity depends only on the local water depth and the wave period.

The classical way to solve the mild slope equations is to apply the finite element method. However , this method rapidly becomes expensive and eventually impossible for increasing model sizes. Alternatively DHI has applied an iterative implicit finite difference method. In order to do so the original equations have been reformulated into a system of first order differential equations, which are equivalent to the classical continuity and momentum equations, describing tidal flow. This has made it possible to use the very efficient and economical algorithms established for classical tidal flow simulations. By extracting the timeharmonic part of the solution and using a varying time step in the iterations the computational time is reduced greatly as compared with previous techniques.

Typical applications of the System 21 MK10 are harbour resonance and seiching studies. Used for this purpose to model is from 5 to 30 times faster than System 21 MK8.

Recently the model has been extended to include empirical wave breaking criteria. A Rayleigh distribution of wave heights is assumed and the local energy dissipation will be a function of the peak period and significant wave height only. This leads to a realistic spreading of the surf zone although the model basically is a monochromatic wave model. The output from the model will be maps of wave heights and of the corresponding radiation stress.

The radiation stress which are formulated to take crossing wave trains into account can be used as input to System 21 MK8 which will then compute the corresponding long-shore current distribution.

4. COMBINED WAVE & SHIP MODELLING BASED ON THE LAPLACE EQUATION

A new hydrodynamic model, BEMSHIP is under development at DHI for the purpose of computing the wave induced motion of moored unprotected floating structures. In its final form this model will be able to compute the fully non-linear wave body interaction incl the effects of diffraction of nonlinear directional irregular wave trains. So far a linearized version of the model has been developed and verified against measurements. Simulations of heave,sway,roll yaw,pitch and surge can be made very accurately. The theoretical basis for the model is a solution of the Laplace equation using a boundary integral equation method directly in the timedomain.

5. COMBINED WAVE & SHIP MODELLING BASED ON THE BOUSSINESQ EQUATIONS

A short wave model, SYSTEM 21 MK11 is under development at DHI for the purpose of computing the wave induced motion of moored vessels in protected waters i.e. diffraction and reflection from piers and breakwaters will be taken into account. The model is based on the Boussinesq equations which are modified to allow for the ship motion. A simple body mask has been developed i.e. a geometric code which transforms a description of the ship from a coordinate system moving with the ship to a coordinate system which is fixed relative to the harbour. The impact of the waves on the ship is determined by integrating the local excess pressure over the ship hull to obtain the hydrodynamic forces and moments. The momentum impact of the ship on the waves is determined by integrating the local body velocity over the ship hull.

This yields the net wave flux generated by the motion of the ship. The waves are generated internally by using source terms in the continuity equation. So far a linearized version of the model has been developed. Simulations of heave,sway,roll,yaw,pitch and surge can be made with reasonable accuracy in the shallow water area. Further refinement of the model still has to be made in order to improve the accuracy of the first order ship motions. The next step will be to extend the model to include drift motions.

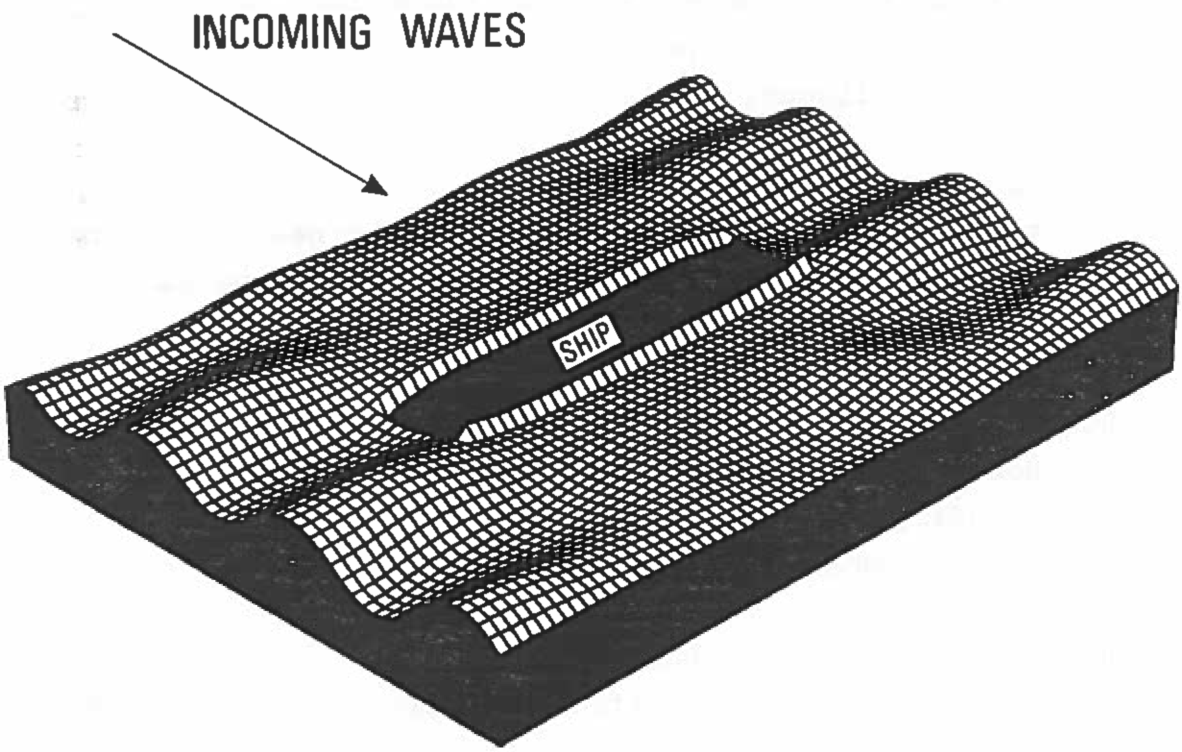

Fig. 1 Moored ship in beam sea waves. Simulation with System 21 MK11. T = 8 sec., h = 14 m, DX = 5 m, DT = 0.1 s.

REFERENCES:

01) M.Brorsen (1989)
Driftforces simulated with the boundary integral equation method.
To be published.

02) Madsen,P.A. and Murray,R. (1989)
An improved form of the Boussinesq equations.
PART 1: Linear dispersion characteristics.
To be published.

03) Madsen,P.A. (1989)
An improved form of the Boussinesq equations.
PART 2: Weakly non-linear solutions for mono- and bichromatic waves.
To be published.

04) Madsen,P.A. (1988)
Fourier series solutions to the Boussinesq equations considering monochromatic and bichromatic waves.
Internal report.

05) M.Brorsen & J.Larsen (1987)
Source generation of nonlinear gravity waves with the boundary integral equation method.
Coastal Engineering 11, 1987.

06) Madsen,P.A. and J.Larsen (1987)
An efficient finite-difference approach to the mild-slope equation.
Coastal Eng., vol 11 pp 329-351.

07) P.A.Madsen, R.Deigaard & M.Hebsgaard (1987)
A Coastal protection study based on physical and mathematical modelling.
Conference on Coastal & Port Engineering in Developing Countries, September 1987, Beijing , China.

08) I.B.Hedegaard, P.Girolamo, R.Deigaard, P.A.Madsen & O.H.Andersen (1987)
Model for Morphological Changes under waves and current.
Abstract for IAHR Symposium, Copenhagen, may/june 1988.

09) Bundgaard,H.I. (1987)
BEMSHIP.
A time domain hydrodynamic model for calculating ship movements, using the boundary element method.
Internal report.

1006-1/chcr71
1989-03-07
PRM/lkn/C

NUMERICAL HYDRODYNAMICS

John Christoffersen

Danish Maritime Institute

1. INTRODUCTION

In the joint industry project between DHI and DMI, Per Madsen from CHC has reported DHI's part of the project and also explained about the background for the project. Here DMI's part of the project is explained. It has been concentrated about two different model tools:

1) FSFLOW for calculation of the wave resistance of ships.

2) OCEAN for description of the wave-induced motions of moored structures.

2. SHIP WAVE RESISTANCE

2.1 Purpose

Since the start of NUMERICAL HYDRODYNAMIC a model has been developed for determination of ships' wave resistance when sailing in calm seas with constant speed on a straight course. The knowledge about wave resistance is very important, as the most energy economical ship among alternatives can be choosen already at the project stage. Except for the wave resistance the model will give results which can be used for mounting side skegs, bilge keels and other appendages. Placing of these parallels to the streamlines gives the least energy consumption which is necessary for the propulsion. The model will in this way substitute some kind of wind tunnel and tank tests. By continuing refinement of the model still smaller differences in form can be quantified with respect to propulsion.

2.2 Method

By disregarding viscous effects, which mainly are dominating around the aft ship, potential theory can be used. Within the potential theory the problem can be converted from having unknown in the total fluid to just having unknown on the boundaries, which limit the fluid. Thus the dimension of the problem is reduced by one - in this case from three to two. The equations, which have to be solved, thereby become integral equations. The equations are non-linear, which only can be solved by an iterative method. Great difficulties are found in obtaining convergency of the iteration process.

2.3 Status

Since the start of the project a total linear model (one iteration step) has been extended such that the governing non-linear equations are solved twice (two iteration steps). The two iteration steps appears by linearizing the non-linear equations in two rates, first suggested by Dawson (1977). For many ship types this gives applicable results.

For the slender Wigley-hull, which is the first test example used worldwide, satisfactory results have been obtained. It should also be noted, that the two iteration steps represents 'the-state-of-the-art".

Worldwide, research is carried out in order to achieve solutions for further iteration steps. The problems around the difficult iterative process has only been slightly touched, as have other. The necessary radiation condition is treated according to a method developed by Jensen (1987).

Furthermore, the work during the last years has implied the possibility to include a link in the linearization which is not used by similar models. A report covering this recognition and the presentation of the latest results are intended at the coming Office of Naval Research Conference in Haag, 1988.

The EDP program, which solves the mathematical model, is implemented in a form well suited for a vector processor which results in large savings of computer time.

Parallel with the development of the calculation model itself the pre- and post-processors have been improved. The pre-processor performs the necessary element generation from data stored from DMI's normal hull data base. The post-processor undertakes plots of the results, e.g. wave shapes, velocities and streamlines. These data are, just like the wave resistance, important in order to be able to judge the quality of a hull form's propulsion or lack of it.

2.4 Applications

1. The model has been used for placing the side skeg parallel to the streamlines.

   a) As an internal tool in connection with model tests, where tests with different placings of side skegs could not be performed owing to economical limitations.

   b) Models are with regard to this point verified by comparison with model test results from the "Optimal Aft Ship" project. A status report is under preparation.

2. The model has recently been used for mounting of bilge keels on a trawler.

3. WAVE-INDUCED MOTIONS OF MOORED STRUCTURES

3.1 Purpose

The purpose is to develop a software package, which is able to predict how 3-dimensional structures of arbitrary form behave in the sea at arbitrary water depth, when they are influenced by wave action.

3.2 Method

Since offshore structures and ships are complex 3-dimensional floating bodies, which demand many elements in order to get reasonable accuracy, DMI has chosen to build its software package on the basis of a so-called Boundary Integral Element Model (BIEM) formulated in the frequency domain and limited to linear wave theory.

This choice has many advantages, i.e.:

1. By limiting oneself to linear wave theory, it is only necessary to discretisize the floating and/or fixed bodies; but not the water surface or the sea bed. This gives very large savings in CPU-requirements and storage.

2. By formulation of the model in the frequency domain, one can once and for all run the BIEM program for 20-30 frequencies, i.e. independent of the solution of the equations of motions. They hereby found frequency dependent coefficients can thereafter be transformed into the time domain by the Fourier transform, and the equations of motions can thereafter be integrated independently of the more time demanding BIEM program.

3. Results are obtained in both the frequency domain and in the time domain.

Even though that the model principally is limited to linear wave theory, it has been shown that it is possible to include the most important 2nd order wave effects as for example the slowly varying drift forces.

It has further been possible to include slowly speed effects in this kind of models. These effects are important for structures, which move slowly in their moorings.

Wind, current, non-linear moorings and fender configurations can also be dealt with.

The drawbacks with this kind of method are first of all that the wave effects are limited to 1st and 2nd order wave theory, i.e. to waves of limited height.

This kind of model has for the last 5-10 years proved its applicability round the world due to its accuracy and speed, and will also in the future be among the most applied model types for practical calculations.

DMI has therefore chosen further to develop such a model based on a program from the Technical University of Athens.

3.3 Status

3.3.1 Frequency domain BIEM program

At the arrival from the Technical University of Athens the program was able to predict added mass, damping, 1st order exciting forces and phases, motions, constant 2nd order drift forces, section forces in the bodies, and the whole wave field around one or more floating or fixed structures on finite water depth.

The program functioned reasonably satisfactory, but had certain disadvantages:

a. A relatively large CPU-consumption.
b. Lacking accuracy for ships with small keel clearance.
c. Problems in deep water.
d. Non-modulized internal structure, and not too good input/output facilities.

At DMI the program has been tested on a diving support vessel and a semi-submersible, where DMI earlier had performed towing tank experiments, with absolute satisfying results.

Normally, one uses approximately 100-200 elements per ship, and this required approximately 4 h CPU-time per frequency on DMI's Micro VAX II. DMI has therefore optimized the program, so that the computer time is now approximately 15 minutes per frequency, and so that structures on deep water can be handled now.

The program's internal structure has further been improved by modulization. The running of the program is further dividted into to "sweeps" such that the time consuming computation of the potentials and the velocities can be performed once and for all. Afterwards, running of the rest of the program can be done quickly.

The program has also been adjusted to DMI's SLAFO-data base for storing of test results, such that the results from the program can be presented and compared with i.e. test results by use of existing analyses and plotting programs. The results from the frequency-domain are in this way easier to transmit to the time domain.

The new implementations are all documented and tested. The model is therefore ready for practical use in the frequency-domain and has already been included in national as well as international project proposals.

3.2.2 Time Domain Motion Program

Software has been developed which, based on the Fourier transformation, transform frequency dependent "added mass" and damping into a frequency independent "constant added mass' and time dependent memory function. This is done for six degrees of freedom. This transformation has been tested using related analytical damping functions and memory functions with very satisfactory result.

Due to the memory effects, convolutions integrals appear in the equations of motions. Therefore, a routine for integration of the equations of motions in time, with memory effects present, has been developed. This routine has been thoroughly tested for one degree of freedom on three examples with analytical solutions, giving a very fine result.

In the light of the above-mentioned a linear time domain motion program in 6 degrees of freedom is under development, such that the response of a floating structure due to wave action can be found. This time domain program is expected to be working at the end of 1987 for simple linear wave action.

4. RESULTS

The results from DMI's ship wave model FS-FLOW and DMI's model for floating bodies' motions in the ocean OMEGA are shown in the following:

First, a selection of runs with the boundary element program FS-FLOW are given for:

a. A Twin Screw Merchant Vessel.
b. A Trawler.
c. A 5.5 m Sailing-Boat.
d. The Wigley Hull.

Subsequently, the result from a run with the frequency domain boundary-element program OMEGA on a semisubmersible with complicated three-dimensional structure, modelled with 535 elements, is shown.

On Figures 1-3 is shown a comparison between calculated values from OMEGA and test results from DMI's towing tank. Here the 6 motions (surge, sway, heave, roll, pitch and yaw) are shown, when the waves are oblique from ahead (bow quartering sea). The agreement is very good, especially when one takes into account that the viscous effects have not been modelled in OMEGA.

COMPUTER AIDED HYDRODYNAMIC DESIGN

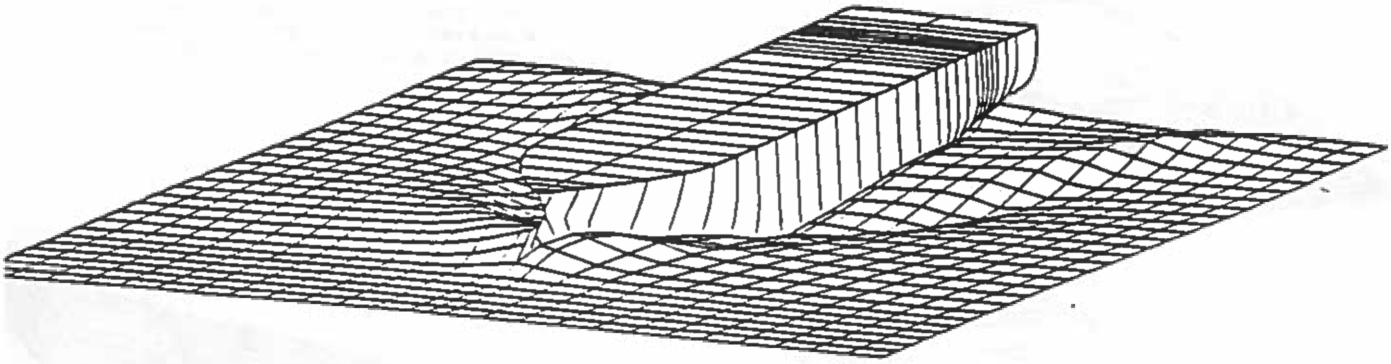

STATIONARY FREE SURFACE FLOW

FS-FLOW

- WAVE RESISTANCE
- PRESSURE
- WAVE PATTERN

- TRAWLERS
- YACHTS
- MERCHANT SHIPS

THE FS-FLOW SYSTEM

The hull designers basic needs

Hull form designers must among a lot of subjects also consider hydrodynamic design criteria. For allmost every ship a optimum propulsion performance when the ship is sailing in calm water, on a straight course and at constant speed is an important design criteria. The wave-resitance is a major factor for the propulsion efficiency.

Using ordinary physical model testing techniques makes it very expensive to reach a optimum condition because a lot models must be build and testet. Numerical flow models is therefor an attractive alternative when a minimum waveresitance hull shall be found.

As a bi-product it has been shown that usefull imformation also can be gained from the present flow model when skegs and appendices are to be alligned with the flow.

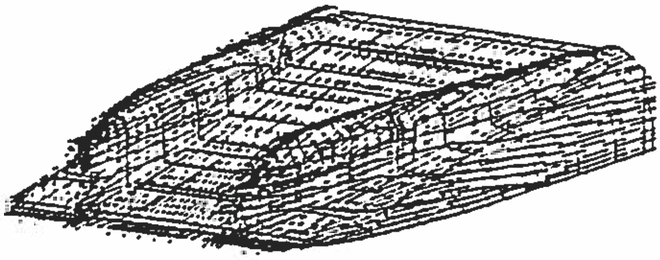

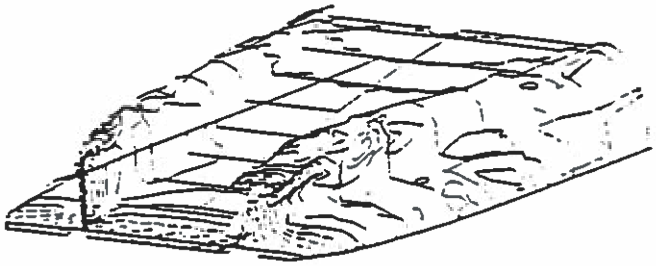

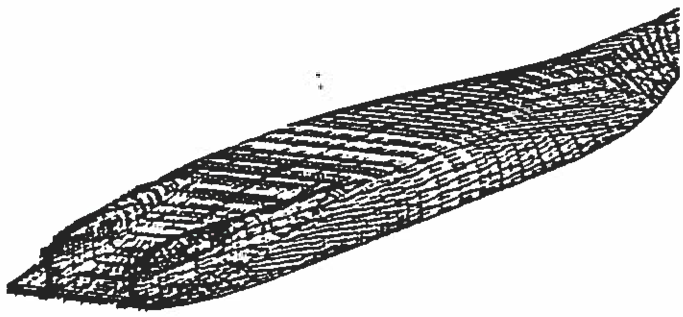

The model input - hull geometry definition

When a ship is defined in DMI's hull database it is very easy to make a numerical flow calculation for the ship sailing in calm water at constant speed and on a straight course. Compared to physical modeling this means very small model expenditures.

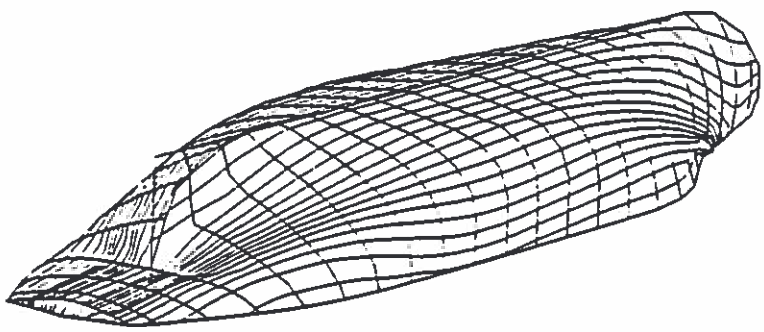

The model output - flow pattern

The result of the numerical flow calculation can be used in various situation as a suplement to results obtained from physical model tests.

The main results from the calculations are:

- wave resistance
- wave pattern
- fluid velocities as arrows
  streamlines
  presure coefficients

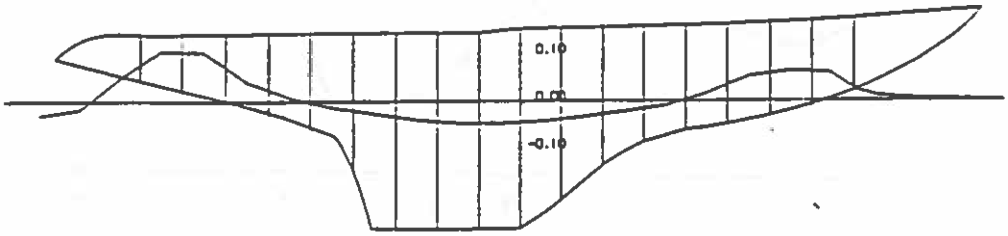

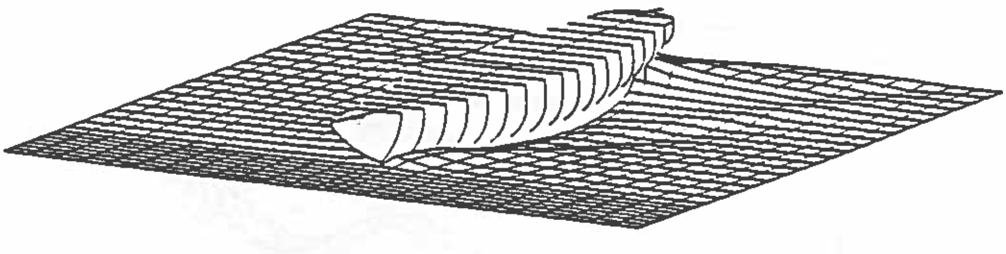

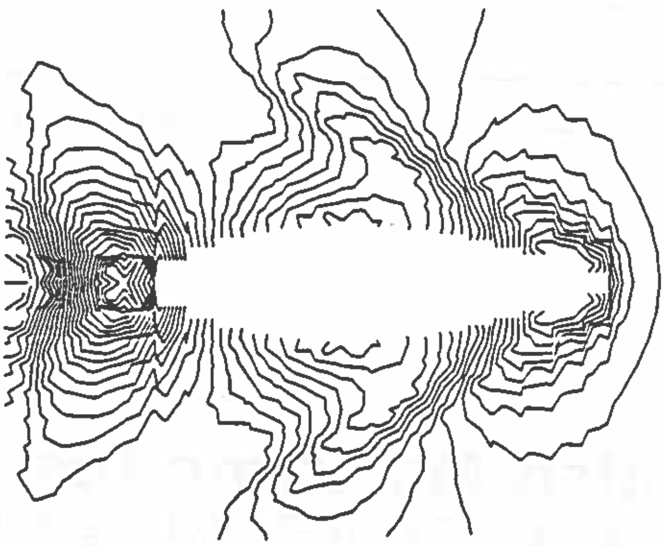

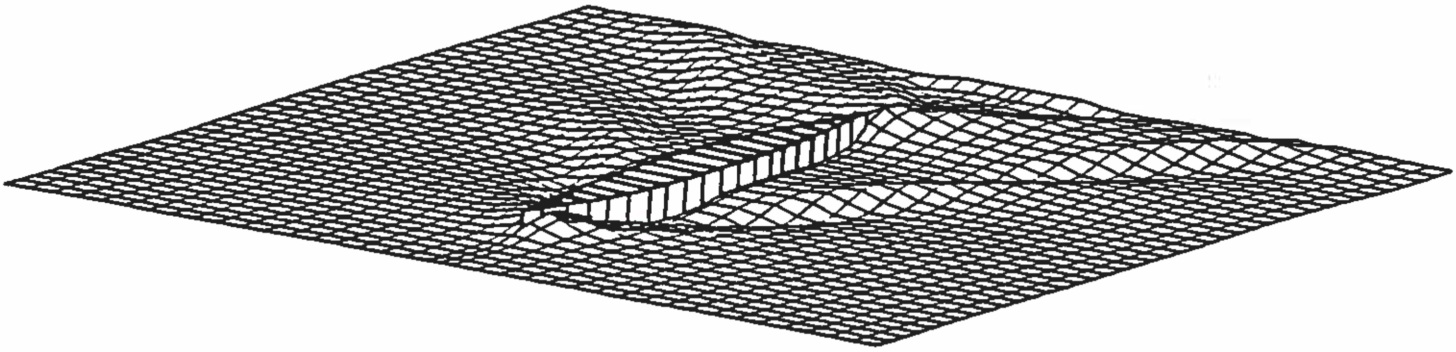

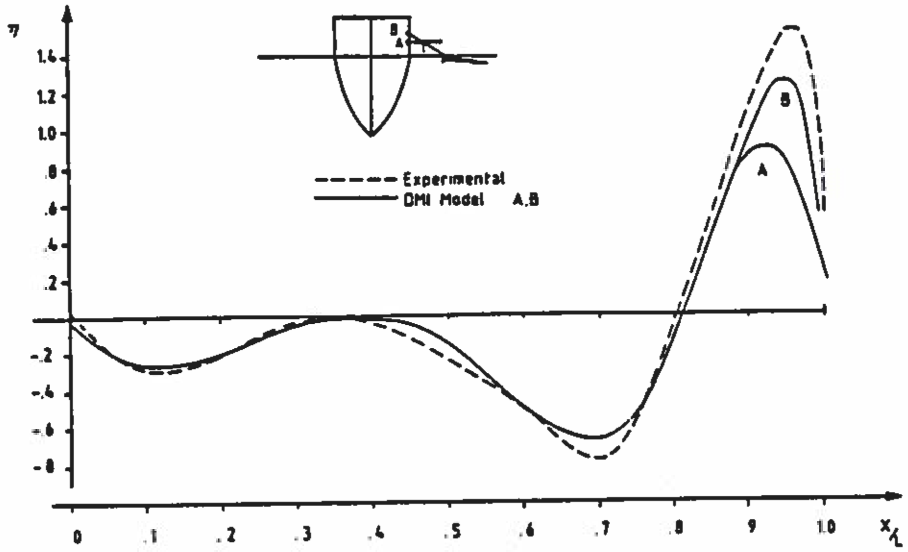

F_n = .313

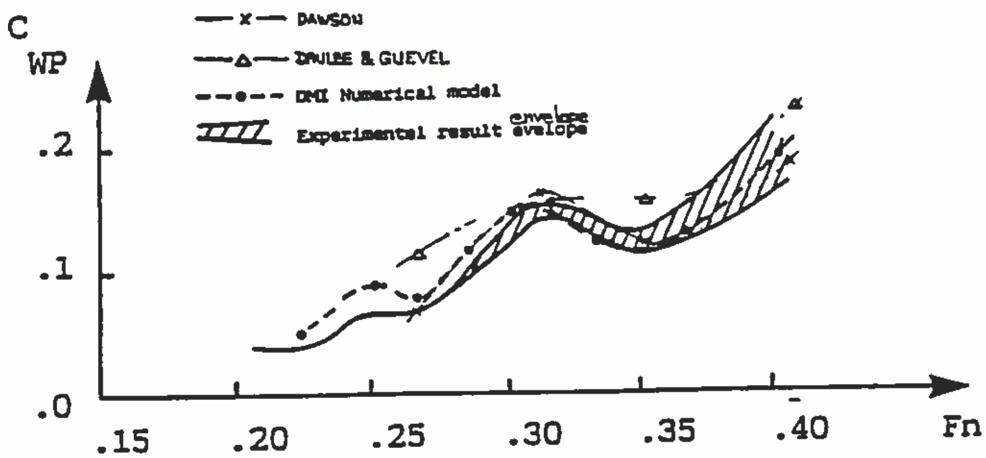

Danish Maritime Institute

Hjortekærsvej 99, DK-2800 Lyngby, Denmark

telephone: 02 87 93 25
telex: 37223 shilab dk

telefax: 02 87 93 33
cables: SHIPLABORATORY

STATIONARY FREE SURFACE FLOW

FS-FLOW

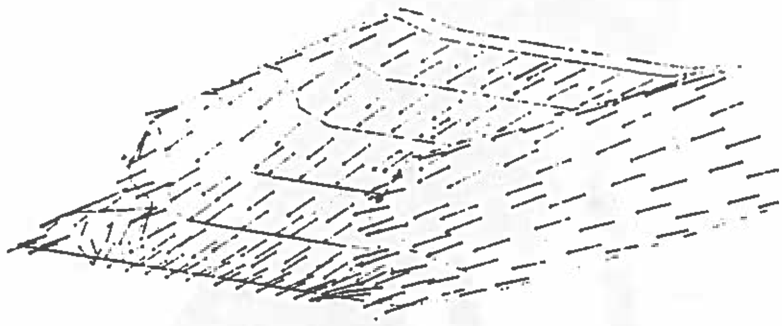

Computer-generated streamlines on a twin-skeg aftbody (CB = 0.614).

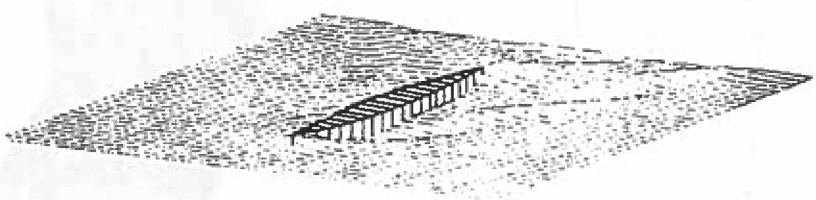

The three-dimensional wave pattern around the Wigley hull for Froude number 0.316 is shown in this computer generated drawing.

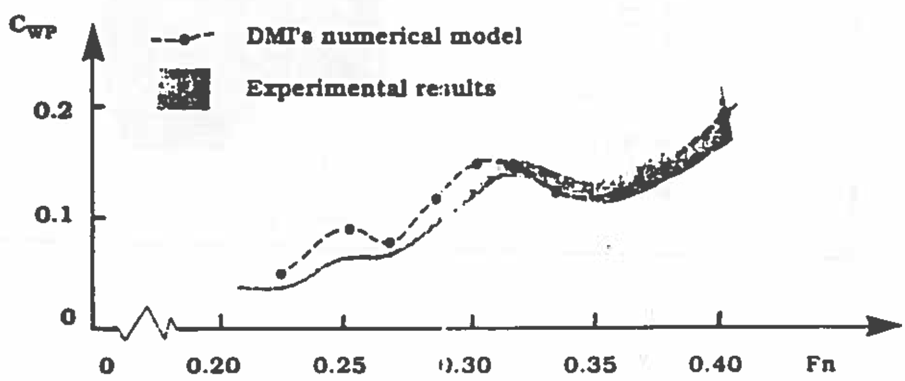

The slender Wigley hull is normally the first hull used for verification of a wave resistance program. In this illustration, the red line shows the wave resistance calculated by DMI's numerical model, and the green area indicates the scatter of experimental data. As shown by the illustration, good correlation was found between the two methods.

MOTION OF FLOATING BODIES IN THE SEA

OMEGA

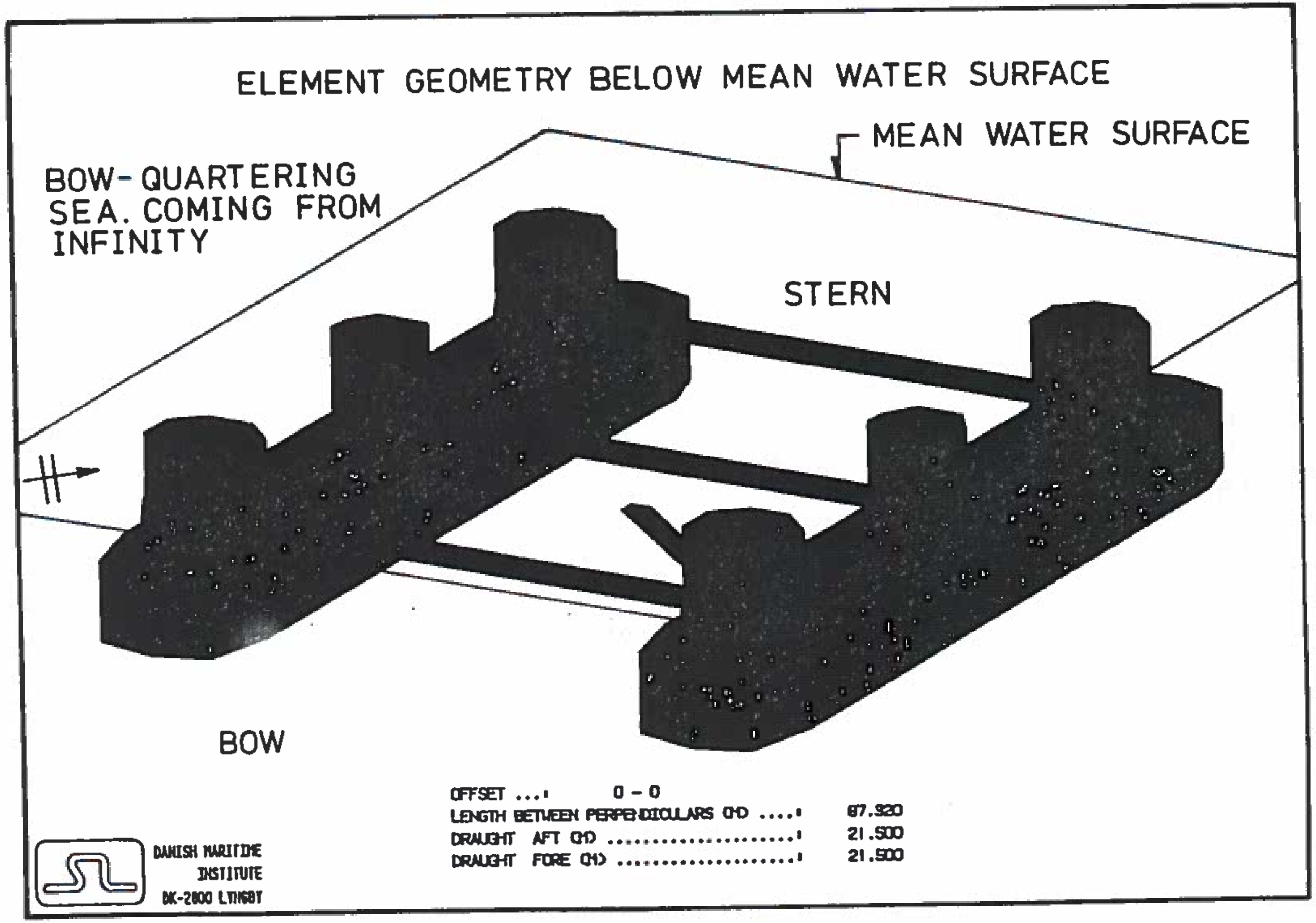

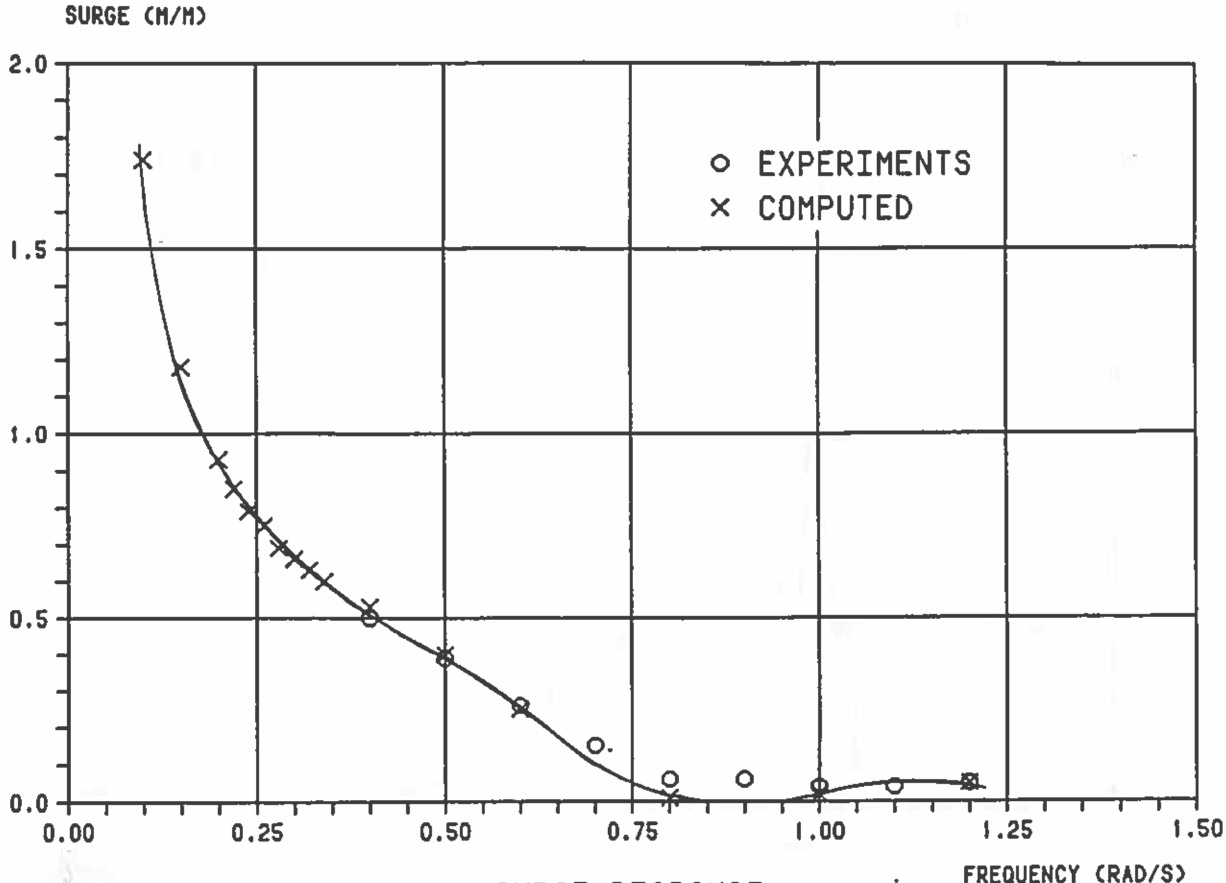

SURGE RESPONSE

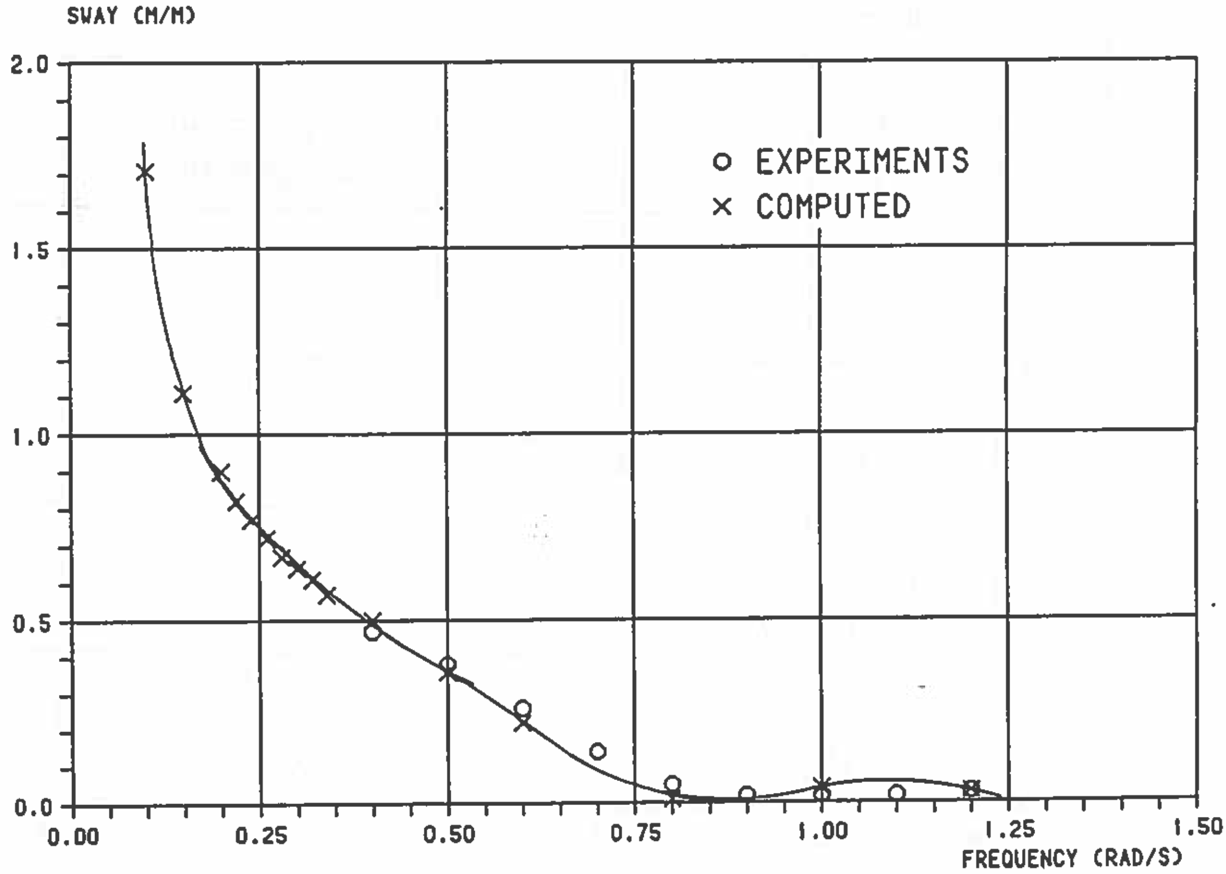

SWAY RESPONSE

AGJ-3

DANISH MARITIME INSTITUTE
LYNGBY DENMARK

SEMISUBMERSIBLE
BOW-QUARTERING-SEA
FIG 1

ORDER 0
DATE 871029

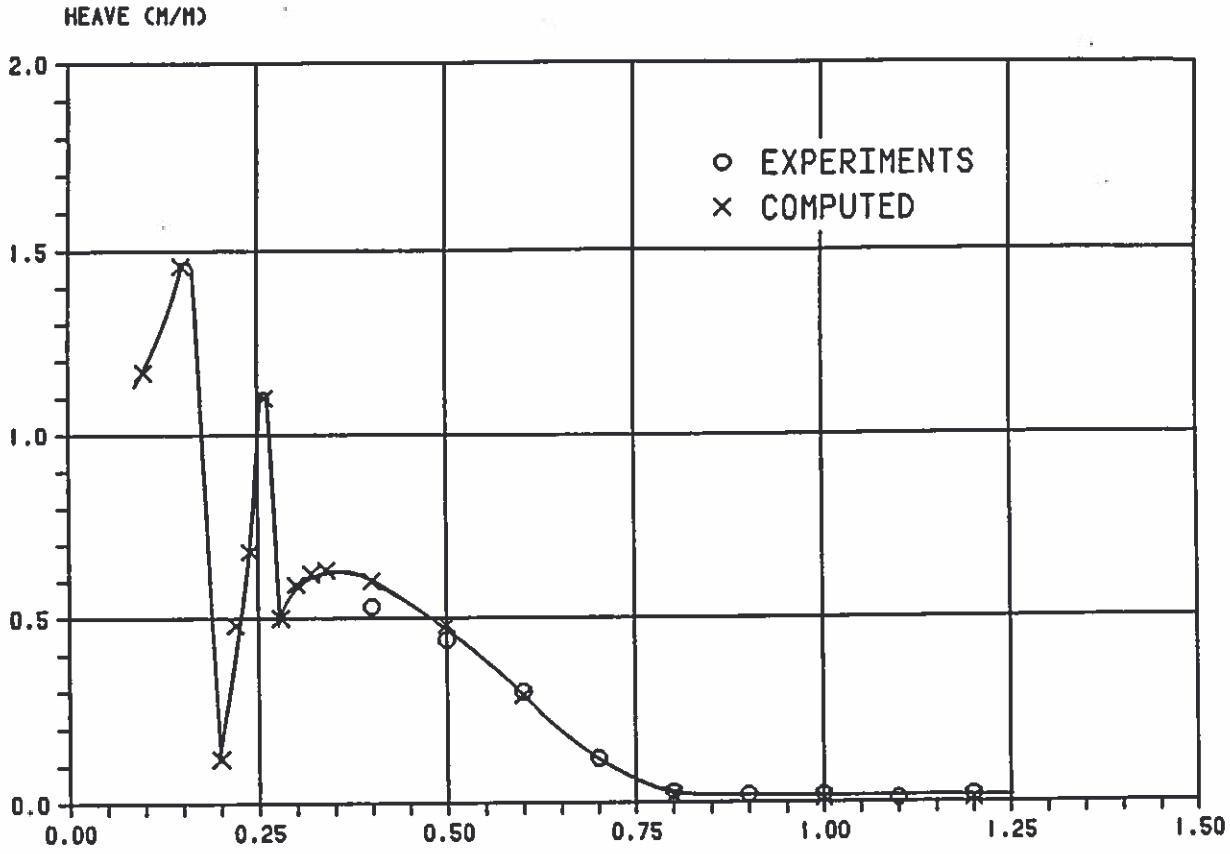

HEAVE RESPONSE

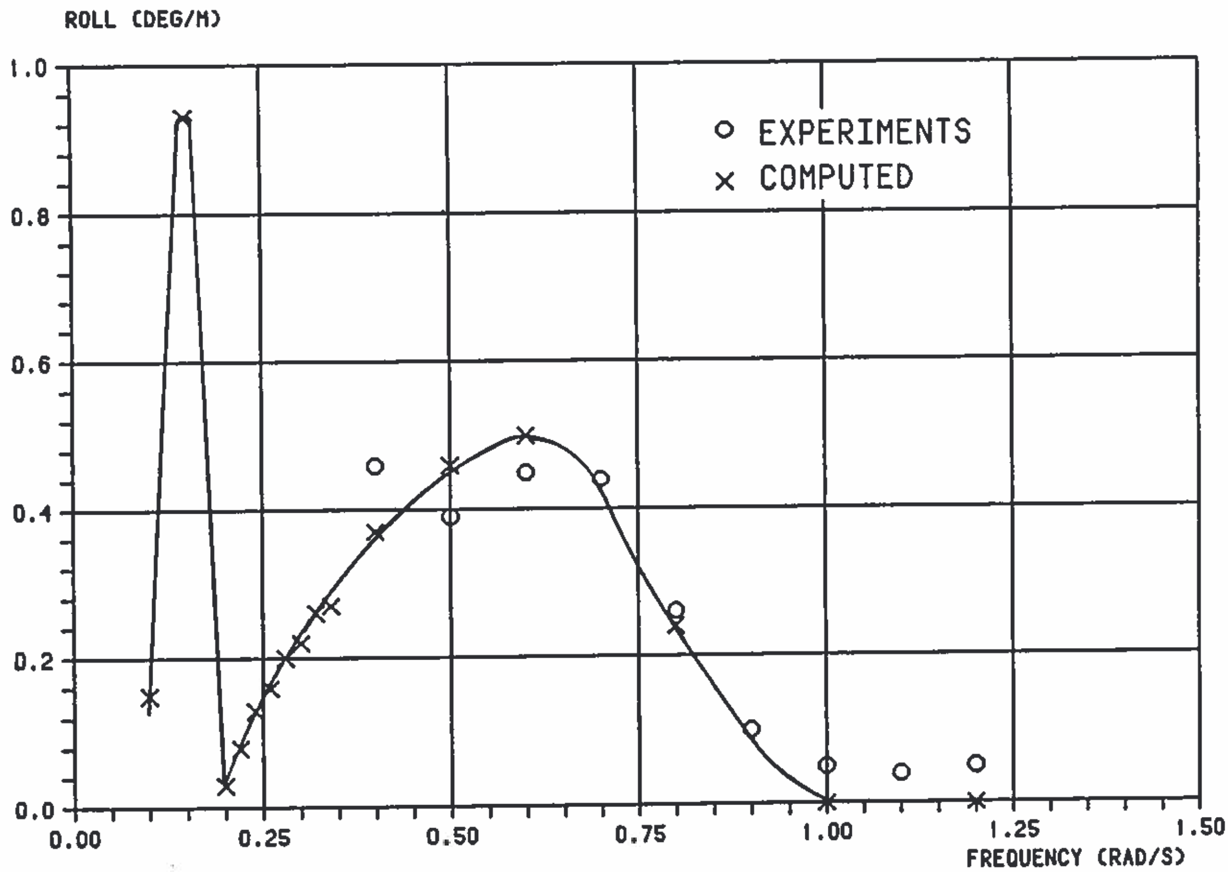

ROLL RESPONSE

AGJ-3

DANISH MARITIME INSTITUTE

LYNGBY DENMARK

SEMISUBMERSIBLE

BOW-QUARTERING-SEA

FIG 2

ORDER

DATE 87

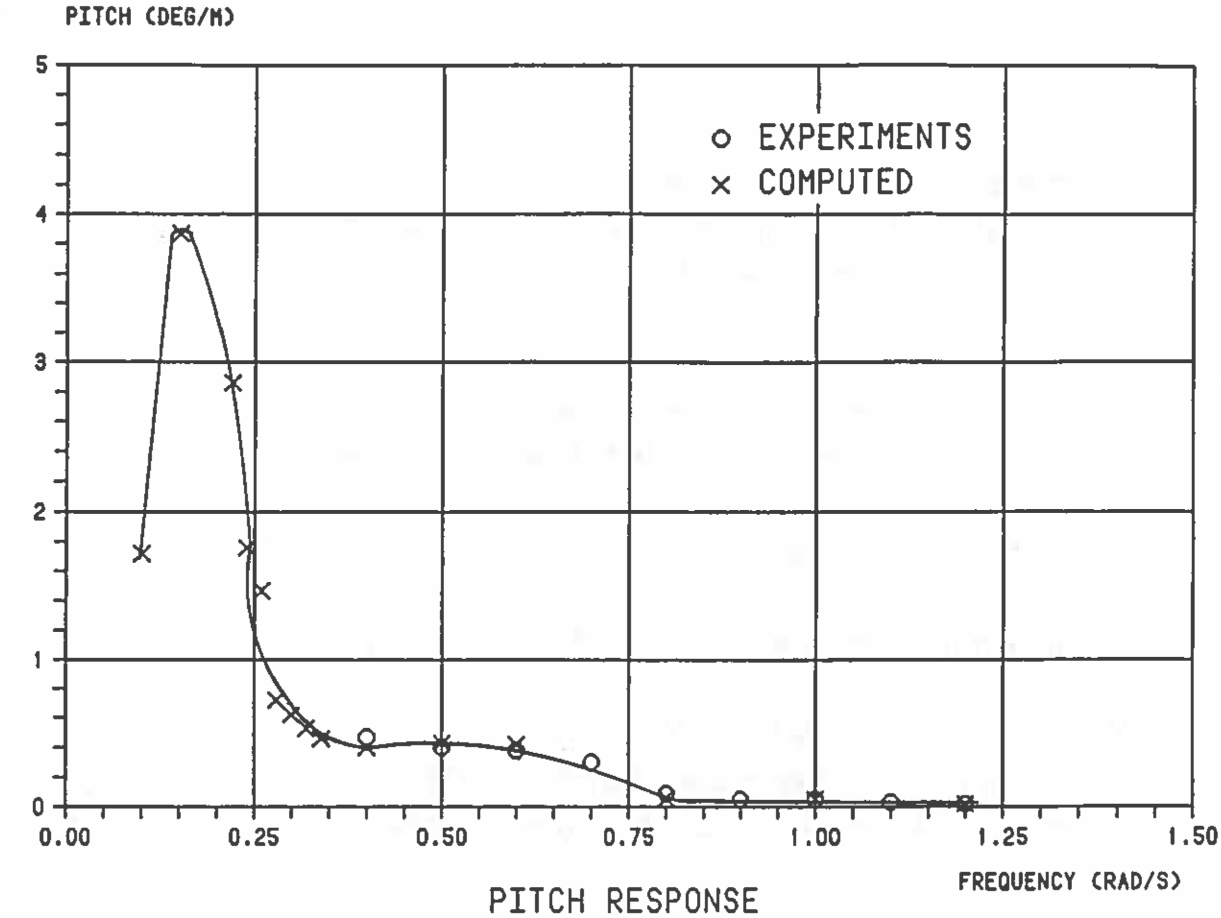

PITCH RESPONSE

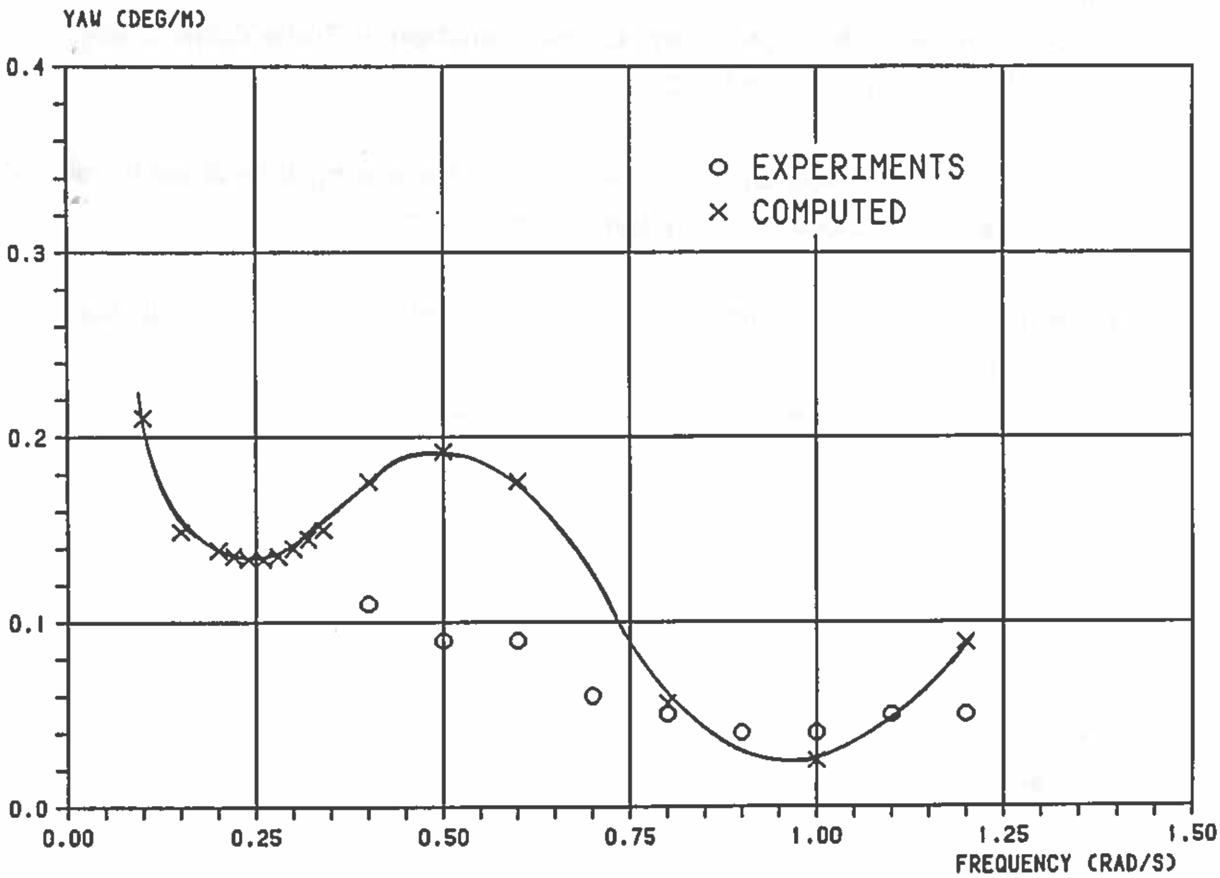

YAW RESPONSE

DANISH MARITIME INSTITUTE
LYNGBY DENMARK

SEMISUBMERSIBLE
BOW-QUARTERING-SEA

FIG 3

ORDER 0
DATE 871029

AGJ-3

REFERENCES

Christoffersen, J.B., and J.E. Larsen (1987).
"Evaluation of the Frequency-Dependent Function on Finite Water Depth".
In Preparation and based on the following internal reports:

Christoffersen, J.B. (1986):
"The Deep Water Green Function GRADIF".
The Danish Maritime Institute, DMI-Report, December.

Christoffersen, J.B. (1987):
"The John's Series".
The Danish Maritime Institute, DMI-Report, January.

Christoffersen, J.B. (1987):
"The Finite Water Depth Green Function FINITE".
The Danish Maritime Institute, DMI-Report, February.

Larsen, J.E. (1986):
"Calculation of the Free-Surface Green's Function on Finite Water Depth".
Match-Tech, on contract for DMI.

Dawson, C.W.: "A Practical Computer Method for Solving Ship-Wave Problems".
Proc. Second Int. Conf. on Ship Hydrodynamics, 1977.

Jensen, P.S.: "On the Numerical Radiation Condition in the Steady State Ship Wave Problem".
Journal of Ship Research, Vol. 31. No. 1, March 1987.

1989-04-27
JOC/ak-D2013

STATUS AND TRENDS IN DESIGN OF FLOATING PRODUCTION SYSTEMS

Tor Naess
Aker Engineering a.s., Oslo - Norway

TN001/1/eke

CONTENTS

1. INTRODUCTION

This paper addresses the current status and development trends within floating production systems in relation to the various phases of a field development. Further, challenges in design and analysis of such systems are briefly discussed.

2. DEFINITIONS

In general floating production may be applicable in the following phases or modes of a field development:

- Extended Well Testing
- Early Production
- Permanent Production

The functional requirements to the floating production system for these modes will vary. When discussing floating production facilities it is therefore important to relate the discussion to the mode in which the systems shall operate.

Extended Well Testing is normally carried out from one well. During extended well testing the gas is burned, but the oil is produced and shipped to shore. Extended well testing will in this way contribute with an early cash flow and provide valuable information of the reservoir characteristics.

An extended well testing system will typically be on location from 6 to 18 months. Monohulls and semi-submersibles are potential candidates for extended well testing.

An Early Production System may also be a one well production system, but usually more than one well are tied back to the floater. The subsea scenario may consist of single well completions or a template completion. The early production system will normally be replaced by a permanent production system. In the same way as for the extended well testing an early production system will give early cash flow and provide reservoir information prior to final commitment of any major capital expenditure.

Typically an early production system will be in operation from 2 to 6 years. Monohulls and semi-submersibles are platform candidates for early production.

Permanent Production Systems are characterized by higher production rates, an increased number of wells and stationary service over the entire field life. Heavy duty semi-submersibles, monohulls and tension leg platforms (TLP) are potential floater alternatives.

3. CURRENT STATUS

It is generally accepted within the industry that floating production facilities offer a number of attractive features such as:

- modest fabrication costs
- early cash flow
- short fabrication schedule
- high degree of fabrication flexibility
- short fabrication time
- low installation cost
- proven technology for structural design
- favourable with respect to inspection, maintenance and repair
- virtually insensitive to soil conditions
- possible to relocate
- low abandonment cost at expiration of field life

Despite these attractive features only 25-30 floating production systems are in operation around the world and another 5-10 systems are likely to be installed within the next one to two years. In the North Sea the first floating production system was installed in 1975 at the Argyll field and five floating production systems are in operation today. Such systems account for 5 % of the oil production in this area.

The reluctance towards floating production platforms was mainly due to three reasons:

- the operators general hesitation to deviate from traditional and well proven solutions
- the high oil prices experienced until end of 1985 have not given any real incentives for more cost effective technology.
- the subsea and in particular the riser system have not been fully accepted as proven technology.

The dramatic drop in oil prices in 1985/1986 has however, made it necessary for the oil companies to look for more cost effective solutions and this has boosted the interest for floating production systems considerably. At the same time progress has been made in development of riser and subsea systems and operational experience with such systems are being accumulated. In particular the advances made and the experience now becoming available on flexible risers have increased the confidence and attractiveness of floating production systems. Today such systems have reached technical maturity and are being accepted as viable alternatives to fixed platforms.

4. TRENDS IN DEVELOPMENT OF FLOATING PRODUCTION SYSTEM

<u>Monohull Vessels</u>

A monohull is supposed to exhibit the following attractive features

- high carrying capacity
- large available deck area
- oil storage capacity
- moderate investment costs

Drawbacks for a monohull are considered to be:

- complex system for transfer of the wellstream from the riser termination to the processing facilities.
- limited possibilities for workover of the wells.

In 1986 the Norwegian contractor Golar Nor Offshore commissioned the "Petrojarl" production vessel at the Oseberg field. This vessel is operating in an extended well testing mode and is producing from one well through a flexible riser. "Petrojarl" has in all respect functioned up to or above expectations. The experienced production regularity has been in the order of 90-95 % whereas the planned regularity was estimated to less than 80%.

Up to now, monohull production systems have primarily been considered for mild environment conditions. The success of Petrojarl should demonstrate that such units also can be utilized in North Sea weather conditions for specific applications.

The monohulls will first of all be seen in conjunction with extended well testing and possibly as early production systems. Unless substantial improvements in the turret design and the transfer system are made, allowing for more risers to be tied back to the vessel, the monohull will primarily have its potential for moderate production rates.

<u>Semi-Submersible Production Systems</u>

As opposed to a monohull the semi-submersible is assumed to have the following attractive features:

- favourable motion characteristics.
- longstanding operational track record from the North Sea.
- relatively easy tie in of risers.
- possibilities for work-over operations.

The greatest drawback for a semi-submersible is the rather limited possibilities for oil storage in case a pipeline is not available.

Semi-submersible production platforms may be classified in three categories:

1. generation - Conversion of existing platforms
2. generation - Newbuild based on existing designs
3. generation - Newbuild tailor-made for production purposes.

Conversion of existing semi-submersibles to floating production platforms is considered to be a low cost and short schedule alternative. Due to the topside carrying capacity limitations of an existing semi-submersibles the most likely application of converted semi-submersible will be in an early production mode or for moderate size fields. For the early production systems a trend is seen towards a modularized approach. If sufficient load carrying capacity is available the drilling outfit can be kept intact and the processing facilities located in self-contained modules. In this way stripping of equipment and interface with existing platform systems can be kept to a minimum. If required the rig can later be converted back to a drilling mode with relatively moderate efforts.

The design of the floating production vessel will heavily depend on the well completion scenario. For a permanent floating production system the wells can be completed subsea or the wellheads elevated above the sea level by means of a separate structure. Traditionally floating production systems have been based on subsea completed wells, but lately the elevated wellhead concepts have received considerable interest. For both scenarios a newbuilt platform or a converted semi-submersible may be used.

So far only one new-built floating production vessel has been installed i.e. at the Balmoral Field in the British Sector of the North Sea. For this field operator Sun Oil decided to use an existing drilling rig design and adapt it to suit specific production requirements. Within the industry it is, however, believed that the next new-built production semi-submersible will be a tailormade design i.e. a 3rd generation production semi-submersible.

A tailormade production semi-submersible will be based on established and proven design principles and should be developed to incorporate design requirements and features such as:

- stationary service over the entire field life
- deck configuration to satisfy safe area segregation
- high degree of integration of equipment in the deck and hull

- simplified vessel systems fully integrated with platform utility systems
- simple and clean layout of structural configuration such that fatigue stresses are reduced to a minimum
- acceptable motions and airgap to operate the platform in all conditions and at constant draft
- easy access to vital structural components for inspection and maintenance
- structural redundancy in compliance with acceptable safety requirements
- high availability
- flexibility w.r.t. fabrication.

For a floating production system incorporating subsea completed wells, the subsea and riser costs very often turns out to be a significant portion of the total capital expenditure. For a multiwell development, say 15-20 wells, the subsea and riser costs may account for 50% or more of the total capital expenditure. A 15-20 well development also implies a fairly complex riser system if no subsea commingling or subsea manifolding are accepted.

In order to eliminate the complex riser system and obtain dry access to the wellheads the elevated wellhead concept has been proposed. Statoil decided to install such a system for their Veslefrikk field. The floating production system for Veslefrikk is scheduled to be on stream late 1989. This concept consists of a fixed wellhead platform to which 24 wells are tied back and a converted semi-submersible carrying all the production facilities. The semi-submersible is moored close to the wellhead platform. The wellstream is manifolded on the wellhead platform and transferred through flexible hoses over to the floater for processing. The stabilised crude is then transferred back to the wellhead platform and further pumped into the export line. The two platforms are connected with a telescopic gangway bridge.

By splitting the topside facilities on two platforms, it will be possible to design a slim and lightweight fixed structure and utilize a converted drilling rig. In the Veslefrikk case a last generation heavy duty drilling rig will be used. The advantage of using a converted rig is first of all to obtain a short lead time from project start to first oil on deck.

For the elevated wellhead floating production concept special attention must be paid to interface between the two platforms. This will affect the station keeping requirements, catenary transfer lines interference control and operation of the gangway bridge.

The hybrid concept will in general have the same limitations to water depth as a fixed structure. However, due to lighter topside it might be possible to use a compliant structure as wellhead platform and in this way extend the use of this concept to water depths beyond what is normally considered to be the limit for a fixed platform.

Tension Leg Platforms

For a tension leg platform the heave, roll and pitch motions are virtually eliminated. Consequently it is possible to tie back the wells to the TLP deck and use conventional well completion. Subsea installations are thereby kept to a minimum. Compared to a semi-submersible, these factors are considered to be the TLP's greatest advantage.

However, the TLP is much more expensive than a semi-submersible platform. The extra cost are basically found in a more costly mooring system, but also in the fact that over 20% of the total platform's displacement is used to carry the tethers and provide adequate pretension in the mooring lines.

The TLP will first of all have it's potential for greater production rates as many risers more easily can be tied back to the platform. The TLP may also be the concept having the greatest potential for deep waters, down to 1000 meters.

Recently one has seen trends towards using the TLP as a wellhead platform. In such a scenario the wells are typically tied back to a TLP located in deep water. The wellstream are then stabilized (if necessary) and manifolded on the TLP and the wellstream pumped to an existing processing unit.

Such a scenario is chosen for Conoco's Green Canyon Joliet Field in the Gulf of Mexico. A wellhead TLP will be installed in 535 metres water depth and the well stream exported to a nearby production platform located in more shallow water.

In the North Sea, Saga Petroleum has decided to use a TLP for their Snorre Field. This platform will be installed in 310 metres of water and produce at a rate of 240.000 BOPD. A total of 72 wells will be tied back to the platform - 48 located beneath the platform and the remaining 24 tied back via flexible risers from subsea templates. The Joilet and Snorre TLP's both have a four column hull configuration with ring pontoons and no bracings. Neutrally buoyant large diameter tethers will be used as opposed to the heavy wall tubulars for the Hutton TLP.

Operational experience obtained from the Hutton TLP and design and development work now being carried out on the Joilet and Snorre TLP's will with no doubt contribute to an enhanced confidence in the TLP concept.

5. DESIGN AND ANALYTICAL CHALLENGES

The challenges in design of a floating production system probably lie more in development of certain hardware elements than in analytical methods and tools.

Over the last years the design methods and analytical computer programs have been developed to an advanced stage. With these tools the platform behaviour can be predicted with a good confidence. But there are still room for enhancements and certain effects are still not fully appreciated and conceived.

From a designers point of view further attention should be paid to:

Platform Response

- Slowly varying dynamics due to wind and wavedrift in the presence of current i.e.

  * better formulation of the wind spectrum
  * more precise estimation of wavedrift
  * better assessment of damping

Mooring Systems

- Dynamics and damping of catenary lines
- Effect of TLP tether fatigue due to ringing and vortex shedding

Flexible Risers

- Dynamics due to out of plane waves and current
- Fatigue assessment
- Emergency disconnect simulation
- Correlation between predicted and full scale behaviour

Global Analysis of Structural Strength

- Make a representative, but at the same time conceivable model that take due account for important effects.

A close corporation between the research institutions and the designers will be required in order to further develop appropriate methods and analytical tools.

6. CONCLUSIONS

The dramatic drop in oil prices in late 1985/86 has boosted the interest for floating production systems and cost effective systems in general.

In view of this perspective the status and outlook for floating production systems may be concluded as follows:

- Floating production systems have reached technical maturity and are accepted to be a viable alternative to fixed platforms.

- In a short term perspective, the most likely application of floating production systems will be:

  * as extended well testing systems
  * as early production systems
  * for reservoirs that can be drained from a limited number of wells
  * in combination with fixed platforms
  * for deepwater fields

- Advances in design of fixed platforms imply, however, that these platforms will still maintain a strong position.

Until now floating production systems have in general experienced a lack of confidence among the oil companies and have been unduly penalized in comparison with fixed platforms. The mistrust has first of all been directed towards the riser and subsea systems. As experience now are accumulated on floating structures in general and, on the riser and subsea systems in particular, it is believed that a floating production system and a fixed platform will be evaluated on a more equal confidence basis and that an increasing number of floating production systems will be seen in the future.

NOTAT OM

3rd International Conference on
THE WAY FORWARD FOR FLOATING PRODUCTION SYSTEMS

udarbejdet af

Jens Kirkegaard, Danish Offshore Laboratories

Danish Offshore Laboratories
c/o dansk hydraulisk institut, Agern Alle 5, 2970 Hørsholm
Telefon 02 86 80 33 - Telefax 02 86 79 51 - Telex 37402 dhicph dk

19. januar 1988
JKJ/BE
88801.00/DOL2

Notat om
3rd International Conference on
THE WAY FORWARD FOR FLOATING PRODUCTION SYSTEMS
London, 15.-16. December 1987.
Arrangør: IBC Technical Services Ltd.

Udarbejdet af: Jens Kirkegaard, Danish Offshore Laboratories.

----

1. INDLEDNING

Konferencen blev afholdt i en optimistisk stemning, som udtrykt i det officielle programs indledningsord:

- "The era of the floating production system (FPS) has arrived in the North Sea. No producer can afford huge fixed platform developments with the current price scenario, and the trend is definitely towards floating production for other than very large fields. Early question marks over this new technology and its economic projections held the industry back, but now that the concept is technically mature this confidence, combined with the availability of low cost rigs for conversion, has provided the final impetus to their more general adoption. North Sea operators are having to look at smaller, more marginal fields, which require cheaper and simpler production systems for their development. Virtually every operator with a proposed field development has a floating production system under consideration. Not all these projects will employ a floater in the end, but many operators do feel these systems to be a real 'Way Forward."

Danish Offshore Laboratories

Som ved tidligere konferencer i denne serie var præsentationerne kommercielt prægede denne gang med kraftig deltagelse fra norsk side.

Af de 230 registrerede deltagere var halvdelen englændere, en tredjedel nordmænd og de resterende fordelte sig med 1-6 deltagere fra hvert af 12 lande. Fra Danmark deltog Jesper Perge fra J. Lauritzen og undertegnede.

På konferencen blev præsenteret 16 foredrag, der kan opdeles i fire grupper:

1. Konceptbeskrivelser og konceptvalg. Foredragene spændte fra generelle analyser af flydende kontra faststående konstruktioner over diskussioner af forskellige flydende koncepters relative fordele og til præsentationer af enkelte typiske koncepter og deres designgrundlag. Af speciel interesse var her en præsentation om det første driftårs erfaringer med "Petrojarl 1".

2. Beskrivelser af de enkelte komponenter som indgår i flydende produktionssystemer. Her drejede det sig specielt om fortøjningsliner, flexible stigrør og kontrolsystemer. Desuden blev beregningsmetoder for flydende legemers bevægelser i bølger behandlet i et foredrag.

3. Finansieringsaspektet blev gennemgået i et foredrag, og mulighederne for omkostningsreduktion i offshore sektoren blev beskrevet på grundlag af et norsk forskningsprojekt.

4. Endelig gennemgik medarbejdere fra det Norske Teknisk-Naturvidenskabelige Forskningsråd hovedpunkterne i de norske forskningsprogrammer for flydende produktionsanlæg.

I det følgende vil jeg kort gennemgå indholdet af disse foredrag. Det noget begrænsede omfang af præsentationer umuliggør en detaljeret State-of-Art vurdering på baggrund af konferencen, men det er alligevel mit håb, at den følgende omtale vil belyse mulighederne i flydende produktionsanlæg.

Det skal understreges, at der ikke i beskrivelserne søges en speciel dansk synsvinkel. Flydende produktionsanlæg giver imidlertid mulighed for en mere international orientering end opbygningen af stationære anlæg, og det bør derfor overvejes, om bygning af flydende produktionsanlæg kan være grundlag for udvikling af en dansk offshore virksomhed ud over de danske felter i Nordsøen.

2. RESUME

De væsentligste indtryk af foredragene kan resumeres således:

- Flydende produktionsanlæg (FPS) betragtes nu som gennemprøvet teknologi selv under ekstreme miljøbetingelser. Fig. 1 giver en oversigt over koncepter.

- Forøgede krav til forhåndsviden om felter før planlægning af permanente produktionsanlæg vil forøge markedet for FPS i fremtiden.

- Fremtidige oliefund vil i højere grad være marginale, hvilket indebærer behov for flexible og genanvendelige udbygningskoncepter.

- Der er talrige FPS-koncepter. Konceptvalget for en given lokalitet afhænger af en lang række faktorer, heraf ikke mindst den eksisterende infrastruktur for transport af olie og gas i området.

- Koncepter bestående af en kombination af en FPS og en let wellhead platform er lovende og bør videreudvikles. Norsk anbefaling!

- Der er stort behov for udvikling af metoder til nyttiggørelse af associeret gas.

- Påligeligheden af FPS kan øges ved anvendelse af effektive datematbaserede kontrol- og overvågningssystemer.

- Fortøjningssystemer og dynamisk positionering (DP) kan udformes med stor pålidelighed, men der er stadig muligheder for forbedringer.

- Flexible risere giver flere frihedsgrader med hensyn til konceptvalg. Forbindelsen mellem risersystemer og FPS kan forbedres.

- Norge har omfattende planer for F&U-aktiviteter indenfor flydende produktion. Indholdet af disse planer blev præsenteret på konferencen.

3. FOREDRAGENES INDHOLD

3.1 Konceptvalg og konceptbeskrivelser

I sit foredrag "Economic and Operating Implications of FP Systems" siger D.M. Fishman fra Energy Research Consultants i en historisk oversigt, at interessen for nye udviklingskoncepter skyldes - at nye store fund, der kan begrunde konventionel udbygning, bliver færre, - at der nu er en infrastruktur, som gør alternative udbygninger mulig, - at der er mange eksempler på budgetoverskridelser ved tidligere feltudbygninger og endelig - at der er sket store teknologiske fremskridt med hensyn til undervands- og flydende systemer. Ved anvendelse af FP-systemer til 'Extended Well Testing' og 'Early Production' kan opnås et forbedret grundlag for feltudbygninger. Dette forhold er en nyorientering i forhold til for 10 år siden. De væsentligste faktorer for valg af udviklingskoncept omtales: Udbygningsomkostninger, operationsomkostninger, fjernelse og genanvendelse af komponenter (hvor FP har særlige fordele) og flexibilitet. Også betydningen af beskatningsregler omtales. Et regneeksempel viser fordele ved at gennemføre feltudbygning med 'early production', bl.a. som følge af beskatningsreglerne, selvom de samlede udviklingsomkostninger er større.

"Aspects of Development in the Design of Low Cost Tanker-based FPSO'S". I.M. Barrett fra BP Shipping beskriver forskellen mellem semi-submersibles (SSB) og skibsbaserede flydende produktionsanlæg (FPSO). Specielt har skibe mere plads til procesanlæg, og de kan anvendes som lagerfacilitet. Desuden har de større mobilitet. BP har gode erfaringer med Dynamisk Positionering (DP), og med fremtidig positionsbestemmelse ved hjælp af satellit bliver mulighederne for udnyttelse af DP forbedret. Artiklen omtaler modelforsøgsresultater til optimering af DP-styrestrategi. Desuden beskrives et nyt ophængingssystem for flexible risere, Heliflex. BP Shipping har foretaget en markedsundersøgelse, der konkluderer, at det ikke er relevant at bygge på et enkelt FPSO design på grund af de mange forskellige design forudsætninger rundt om i verden, fig. 2. Der er et synligt marked for FPSO's, der fastholdes ved DP alene, fig. 3. Anvendelse af flexible i stedet for stive risere gør det muligt at flytte riserforbindelsen væk fra midten af skibet, således at skibet bedre orienterer sig mod bølgerne.

"An Integrated Floating System for Production, Drilling and Offloading". Heri beskriver G.J. Schepman fra Marine Structure Consultants, Holland et koncept studie, der fører frem til en "kombination" af fordelene ved SSB og skibe, i form af en 75.000 t SSB med indbygget lagerkapacitet, se fig. 4.

Udviklingen af SSB produktions-platforme blev beskrevet i et foredrag af U.S. Henriksen fra Aker Engineering, Norge. Henriksen gennemgår indledningsvis fordelene ved anvendelse af en fase-opdelt feltudbygning, d.v.s. "Extended Well Testing", 'Early Production' og 'Permanent Production'. Som eksempel nævnes planerne for udbygning af Heidrun feltet i den norske sektor. Udformningen af topside på SSB's beskrives som modul-opbyggede eller integrerede i dækket, fig. 5 og 6. Førstnævnte fører til større vægt og større påvirkninger, specielt fra vind, men med fordele ved evt. senere ombygning. De designmæssige overvejelser vedr. riserens forbindelse til platformen samt placering af wellhead. I denne forbindelse omtales det nye koncept til Veslefrikk feltet, hvor man benytter en kombination af en fast letvægtsplatform og en SSB process platform, fig. 7 og 8.

Direktør S. Fjeld, Norwegian Contractors, gennemgik i sit foredrag planerne for produktionsfaciliteter baseret på flydende betonplatforme.

NC har udarbejdet planer for både SSB-typer og Tension Leg Platforme (TLP). Der redegøres ikke specifikt for omkostningerne, men disse platforme påstås at være billigere end flydende stålplatforme fabrikeret i det fjerne østen.

Produktionsfaciliteter på tankskibe blev beskrevet med et eksempel fra Middelhavet og et fra Bohaibugten i Kina. L. de Fresco og G. Frigerio fra Snamprogetti beskrev Nilde projektet, der består af den ombyggede 138.000 DWT Agip Firenze, der er fortøjet på 100 m's vanddybde ved en "turret" i stævnen, se fig. 9. Designbølgehøjden er H_{max} = 18 m. Fortøjningskæderne bæres dermed af skibet selv, og det har været muligt at udforme en beskyttet forbindelse mellem de to risere og skibets rørsystem. Produktionskapaciteten er 15.000 BOPD.

Det kinesiske projekt er endnu under udarbejdelse og K.J. Stovell's foredrag beskrev konceptstudiet for udbygning af faciliteterne til en produktionskapacitet på 20.000 BOPD. Studiet er udført af Global Engineering i samarbejde med japanske og kinesiske partnere. Vanddybden på feltet er 19 m, havbunden består af blød leret silt og bølge-, strøm- og vindforhold er som i den sydlige del af Nordsøen. Desuden må der tages hensyn til at der hvert 5. år optræder fuldt isdække.

På grund af den geografiske placering og afstanden til andre faciliteter er det besluttet at udbygge med et specialbygget 68000 DWT tankskib fortøjet ved et pendularrangement til et tårn, der samtidig er det centrale samlingspunkt for flowlines og fordelingscenter for vand- og gasinjection, se fig. 10. Det anses ikke for økonomisk at fastholde skibet i tilfælde af helt isdække, og anlægget kan derfor frakobles under sådanne ekstreme situationer.

L. Wikholm fra Wärtsilä Marine Industries præsenterede planerne for et Floating Production Supply Vessel (FPSV). Wärtsilä konkluderer, at det er muligt at benytte en supply båd til produktion fra 1-2 brønde med op til 10-15000 BOPD, se fig. 11, på indtil 150 m's vanddybde. Man foreslår denne type produktionsskib til Extended Well Testing, marginal feltudbygning og midlertidig produktion i tilfælde af uheld med permanente installationer. Analyser af operationstiden i væsentlige offshore områder (dog ikke Nordsøen) viser, at systemet vil være operationelt i 95-98% af tiden. Artiklen beskriver økonomiske overvejelser, fig. 12, og restriktioner ved anvendelsen.

Erfaringerne med det første års operationer med "Petrojarl 1" på Oseberg feltet blev beskrevet af K. Gisvold fra Golar-Nor Offshore og O. Rønning fra Norsk Hydro. "Petrojarl 1" er det første produktionsskib, der har opereret i Nordsøen. Dets opbygning ses på fig. 13. Skibet er fortøjet med 8 kæder fastgjort til en drejeskive (turret) lidt foran midtskibs. Under operationerne det første år blev der benyttet både stiv og fleksibel riser. Skibet er udover normal fremdrivning udstyret med tværpropeller for og agter og er dermed i stand til at sikre en optimal orientering og position i forhold til bølgerne.

"Petrojarl 1" har et deplacement på 51000 t og procesfaciliteter med en kapacitet på 30.000 BOPD.

Skibet har i det første år produceret i 92% af tiden, og man regner med at kunne opnå mere end 95%. Hovedårsagen til afbrydelse af produktionen har været testing og problemer med kontrolsystemet, som gradvist er blevet justeret. Egentlig vejr-downtime har været under 1%.

Kun 10-15% af den associerede gas er brugt ombord, mens resten måtte brændes af. Man betragter derfor en mere fuldstændig anvendelse af gassen som en udfordring for fremtidigt udviklingsarbejde.

Artiklen gennemgår fortøjningssystemets funktioner og fastslår at selv under ekstreme storme har fortøjningskraften været under 25% af brudlasten som følge af DP-systemets effektivitet.

Økonomien under denne "Extended Well Test" har været god, idet operationsomkostningerne og andelen af investeringerne er dækket ved en oliepris på USD 14,5/bbl. Der er ialt produceret 5,96 mill. bbls i perioden.

3.2 De enkelte komponenter af FPS

Når påliddeligheden af et FPS skal vurderes, vil man i første række se på de hydrodynamiske påvirkninger på platformen, på fortøjnings- og risersystemer samt på kontrol- og overvågningssystemerne ombord.

Prof. Eatock Taylor fra University College gennemgik "Recent Advances in Hydrodynmaic Prediction Techniques for Design of Floating Production Systems". Dette paper behandlede specielt numeriske beregninger af hydrodynamiske påvirkninger på SSB og TLP konstruktioner. Prof. Taylor beskriver i korte træk de væsentlige hydrodynamiske fænomener, som virker på disse fartøjer, men som iøvrigt er lige så væsentlige for FPSO systemer: Bølgedriftkræfter og de deraf genererede lavfrekvente bølgekræfter samt ikke-lineære højfrekvente bølgekræfter. (Disse fænomener er iøvrigt også centrale i F&U-arbejdet ved danske forskningsinstitutioner). Yderligere beskrives betydningen af bølgernes deformation mellem søjlerne i en kompleks konstruktion, deformationer, der kan medføre væsentligt højere bølgetoppe end i det uforstyrrede bølgefelt.

Fortøjningsliner af stålwire beskrives i en artikel af Dr. C.R. Chaplin fra University of Reading. Artiklen handler specielt om muligheden for forudsigelse af fortøjningernes levetid. Traditionelt benyttes visuel inspektion til afgørelse af, om en fortøjning bør udskiftes. Dr. Chaplin mener imidlertid, at en holdbarhedsanalyse baseret på S-N kurver for forskellige påvirkningstyper kombineret med data fra en belastningsregistering og moderne inspektionsudstyr (NDT) vil kunne forøge brugstiden og dermed forbedre økonomien, fig. 14. Der er et behov for udvikling af pålideligt inspektionsudstyr. Foruden træthed i materialet omtales korrosion, og der henvises til nye studier om dette emne.

Flexible risere udvikles af en lang række fabrikanter. Coflexip, der var først på markedet, har præsenteret sine produkter ved tidligere konferencer i denne serie. Denne gang var det Dunlop Armaline, der blev præsenteret. Riserens opbygning og anvendelser blev gennemgået, og der blev givet eksempler på designberegninger både med statistiske og dynamiske beregningsmetoder, fig. 15 og 16. Dunlop Armaline konkluderer, at det er af største vigtighed at gennemføre designanalyser for hver enkelt anvendelse, således at belastningerne på forbindelserne såvel til den flydende enhed som til havbundskonstruktioner kan forudsiges.

"Integrated Constrol Systems for Floating Production Vessels" blev præsenteret i en artikel af Monro og Daniel fra Honeywell Aerospace and Defence Ltd. Det meget omfattende overvågnings- og styresystem på Balmoral feltet blev beskrevet, fig. 17. Systemet foretager produktionsrapportering, overvågning og styring af stabilitet og fortøjningssystemer, styrer elforsyning samt analyserer måledata, rapporterer alarmer m.v.

Alle funktioner omtales i artiklen, og det konkluderes, at anvendelse af de pålidelige integrerede overvågnings- og styreanlæg, (der i adskillige år har været anvendt på landjorden), er vejen frem for flydende produktionsanlæg.

3.3 Finansiering af FPS og mulighederne for omkostningsreduktioner ved feltudbygning

R.A. Cranwell fra Barclays Bank omtalte i sit indlæg, at FPS væsentligst vil blive benyttet på marginale felter med deraf følgende stor risiko. Den indledende produktionsfase vil ofte give den fornødne sikkerhed med hensyn til feltets reserver og finansieringen kan derfor indrettes, således at en projektrelateret finansiering først etableres, efter at produktionen er påbegyndt. Leasing arrangementer kan være attraktive, dels af skattemæssige årsager og dels fordi investeringen i et FPS derved kan fordeles på flere projekter. Desuden omtales skibsfinansieringsordninger og finansiering gennem den Europæiske Investeringsbank (EIB).

I Norge overvejes omkostningsniveauet i forbindelse med feltudbygning. Specielt udbygningen af mindre felter vil nødvendiggøre en ændring af de herskende forhold. På denne baggrund har Norges Teknisk-Naturvidenskabelige Forskningsråd (NTNF) med deltagelse fra Petroleum Direktoratet, Industrirådet og det Norske Metalarbejderforbund gennemført et projekt med henblik på at finde muligheder for reduktion af omkostningerne ved feltudbygning. Projektets resultater blev præsenteret af J. Ulltveit-Moe fra Knutsen OAS Shipping.

Man havde forventet, at der ville være tale om et teknologisk problem, men analyserne viste, at forhindringerne i høj grad skyldes organisationsstrukturen og reglerne. Der arbejdes uflexibelt og i store organisationer. Omkostningsreduktioner kan opnås ved enklere organisation, nye kontraktformer samt ved genanvendelse af nøglekomponenter. I projektet fandt man, at det ville være muligt at producere for USD 10,8 pr. barrel. Der foreslås en ny organisationsform, kaldet "Project Collaboration". Modellen sigter mod forenkling af de kontraktlige forhold og tilsynsfunktionerne, se fig. 18.

3.4 Forskning og udvikling i relation til FPS

Milch og Tegelsrud fra Norges Teknisk-Videnskabelige Forskningsråd (NTNF) præsenterede den norske offentlige F&U planlægning.

På grundlag af White Paper 46 er der udpeget en "Task Force" til at undersøge behovet for offentlig støtte til F&U i relation til FP-koncepter. Denne Task Force har foreslået et NOK 100 mio. forskningsprogram, hvoraf en tredjedel finansieres af det offentlige.

De væsentligste udviklingsområder er:

a. FP-koncepter kombineret med en let platform.

b. Forbedrede riser koncepter - specielt flexible.

c. Ankringssystemer og dynamisk positionering. Påliddeligheden skal forbedres.

d. Udvikling af nye kæde- og wiretyper og dertil hørende håndteringsgrej til dybt vand og ekstreme miljøforhold.

e. Nye materialer i FPS (lette, større styrke og med gode korrosionsegenskaber).

f. Behandling af associeret gas.

Man skønner potentielle besparelser på 500 mio. NOK pr. installation efter gennemførelse af disse aktiviteter. I kølvandet på dette udviklingsarbejde kommer behovet for nye regler, og man ser muligheder for et større omfang af turn-key produktion for offshore konstruktionsvirksomheder.

Danish Offshore Laboratories

Den offentlige støtte vil blive koncentreret om forskningsinstitutter og universiteter samt til små virksomheder. Støtten gives til et koordineret program, hvis indhold i høj grad defineres af målgruppen for at sikre en "marketing approach". Yderligere understreger man betydningen af olieselskabernes medvirken for tilførsel af know-how.

Projektforslag of rapporter under dette program skal vurderes af en programkommittee, der refererer til NTNF.

Jens Kirkegaard

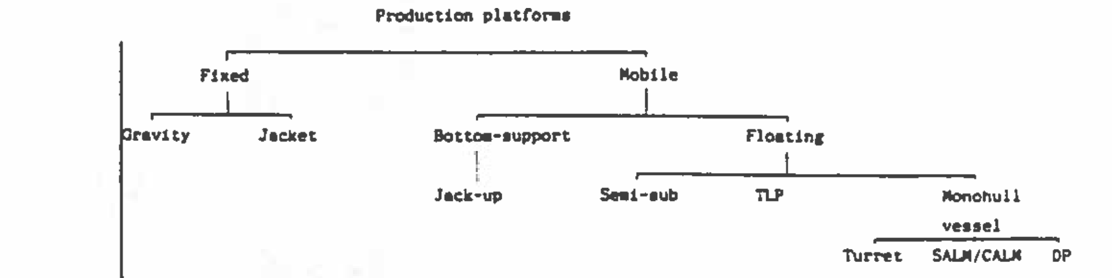

	Gravity	Jacket	Jack-up	Semi-sub	TLP	Turret	SALM/CALM	DP
Storage	yes	no	no	no	no	yes	yes	yes
Drilling/ work over	yes	yes	yes	yes	yes	yes	no	yes
Production eq.	yes	yes	yes	yes	yes	yes	yes	yes
Offloading	pipeline	pipeline	pipeline SBM	pipeline SBM	pipeline SBM	direct	direct	direct
Waterdepth (North Sea environment)	< 250	< 200	< 100	< 600	< 600	< 200	< 200	< 600
Type of well compl.	surface	surface	surface	subsea	subsea	subsea	subsea	subsea

Figure 1.: Platform concepts and areas of application

FPSO FUNDAMENTAL DESIGN CONSIDERATIONS

- Water depth
- Wave height, wind and currents
- Operational environmental conditions
- Sea-bed and soil conditions
- Vessel size
- Installation philosophy
- Maintenance strategy and life
- Oil and gas properties, volume rate
- Secondary recovery requirements
- Mobility from one field to another

GENERAL COMPARISON OF SYSTEM COSTS

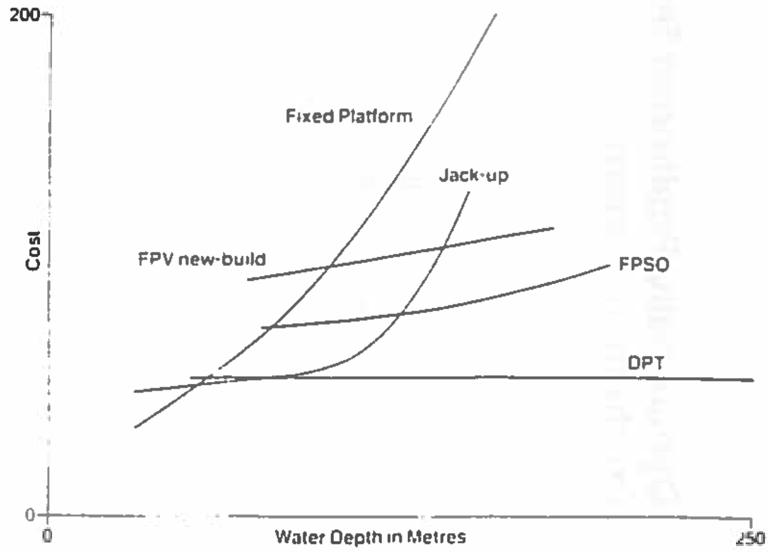

Fig.2

Dynamically-Positioned Tanker Production System

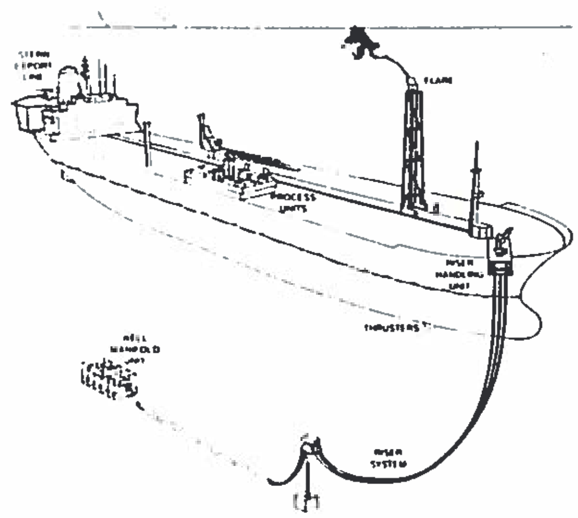

DP Simulation of Bow Movement

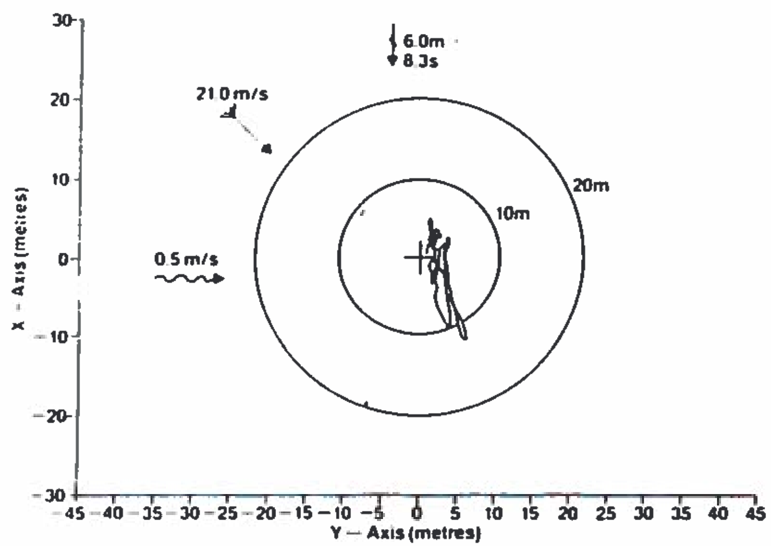

Fig. 3

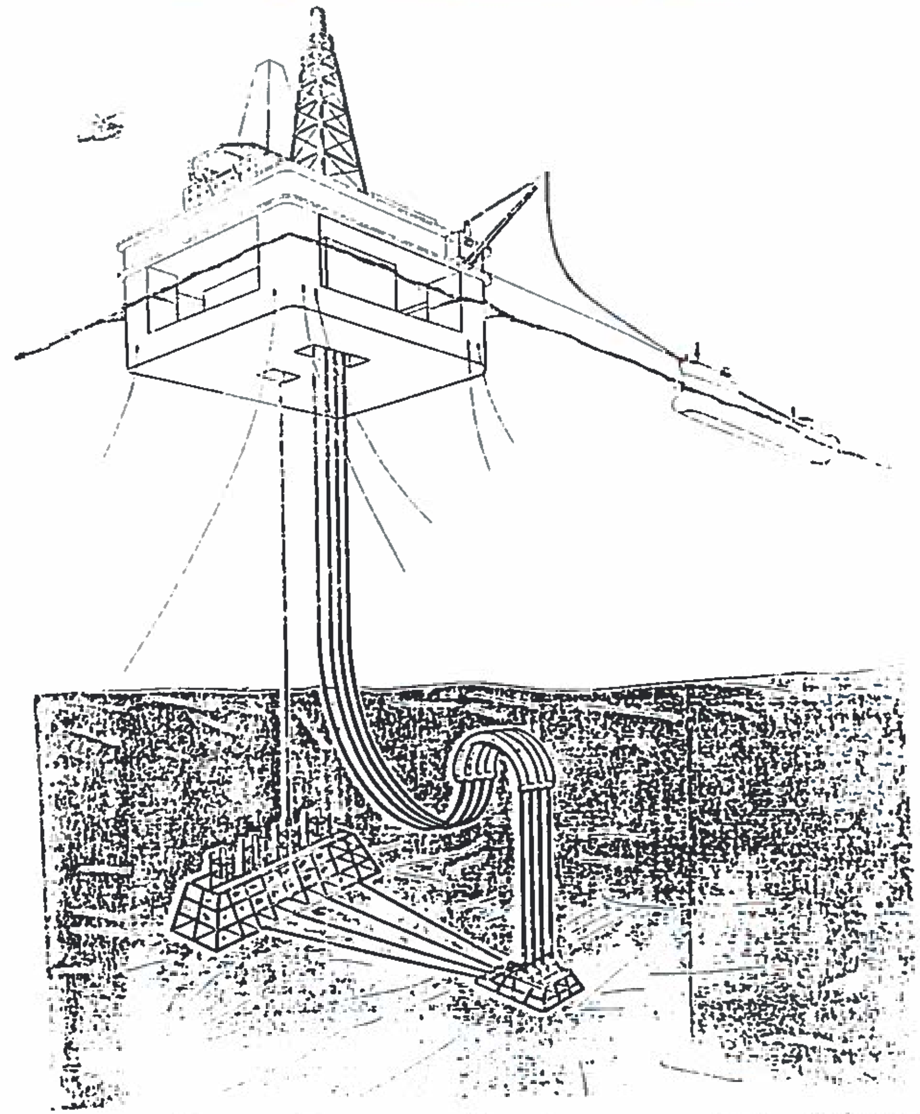

Figure ... Floating Drilling Offloading Production Storage ...
(FDPS)

Fig. 4

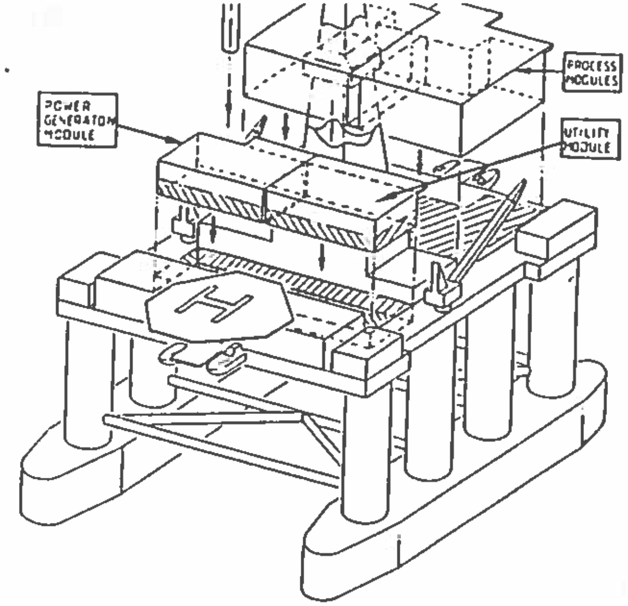

MODULARISED EARLY PRODUCTION PLATFORM
FIG. 5

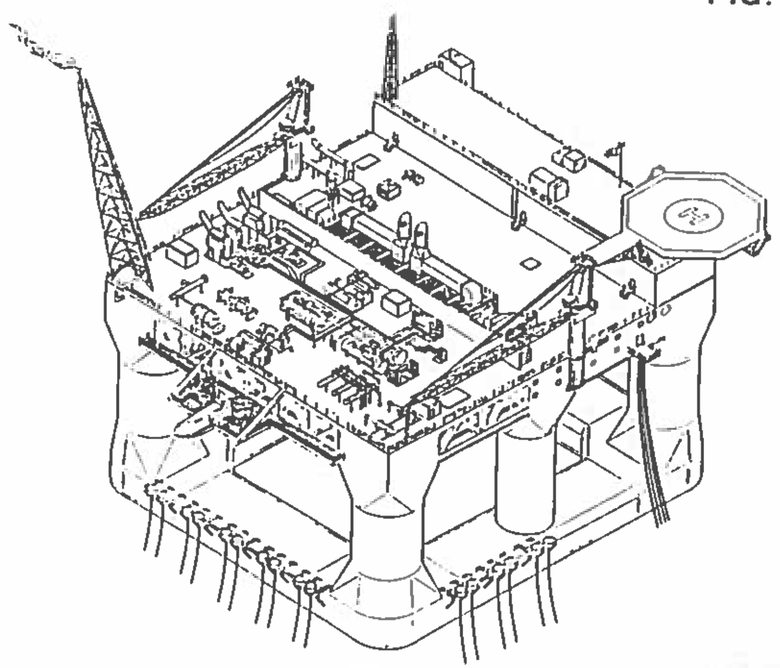

AKER PS-9 PRODUCTION PLATFORM
FIG. 6

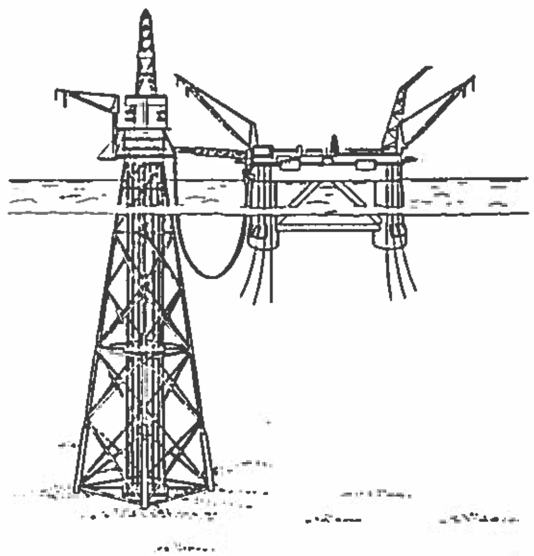

FLOATING PRODUCTION UNIT AND
A FIXED LIGHTWEIGHT WELLHEAD PLATFORM
FIG. 7

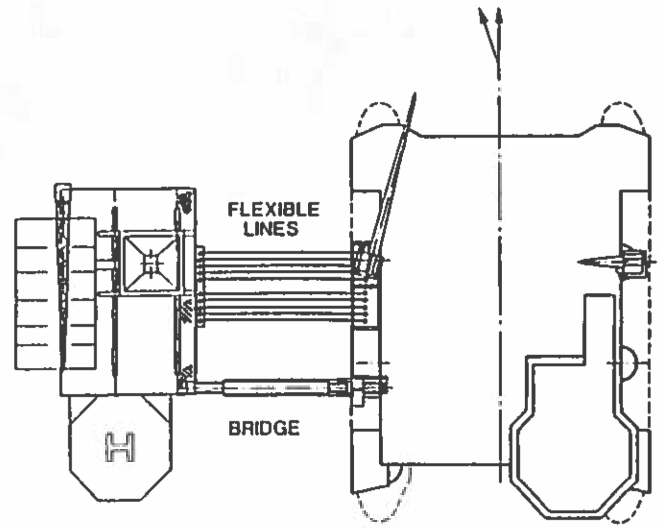

FLOATER - WELLHEAD PLATFORM INTERFACE
FIG. 8

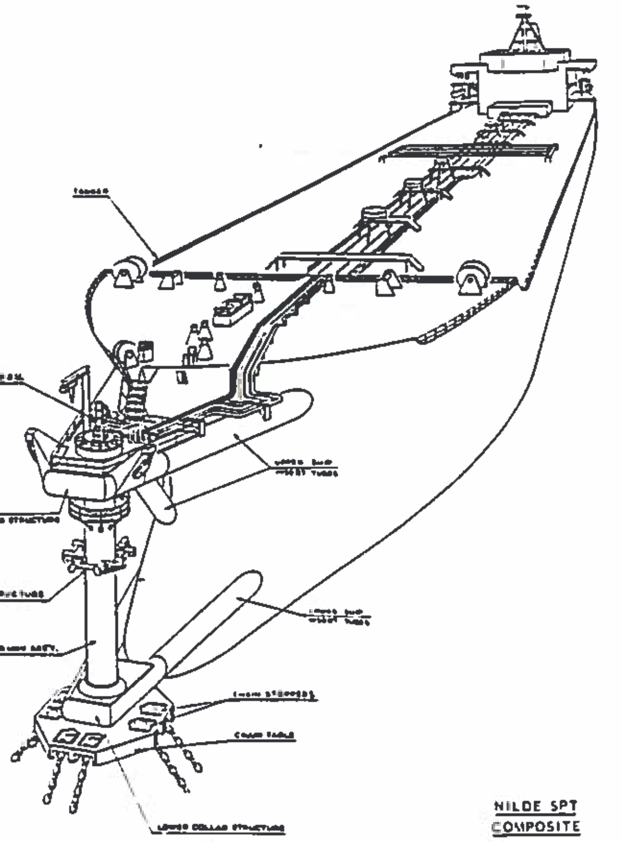
NILDE SPT
COMPOSITE

Fig. 9

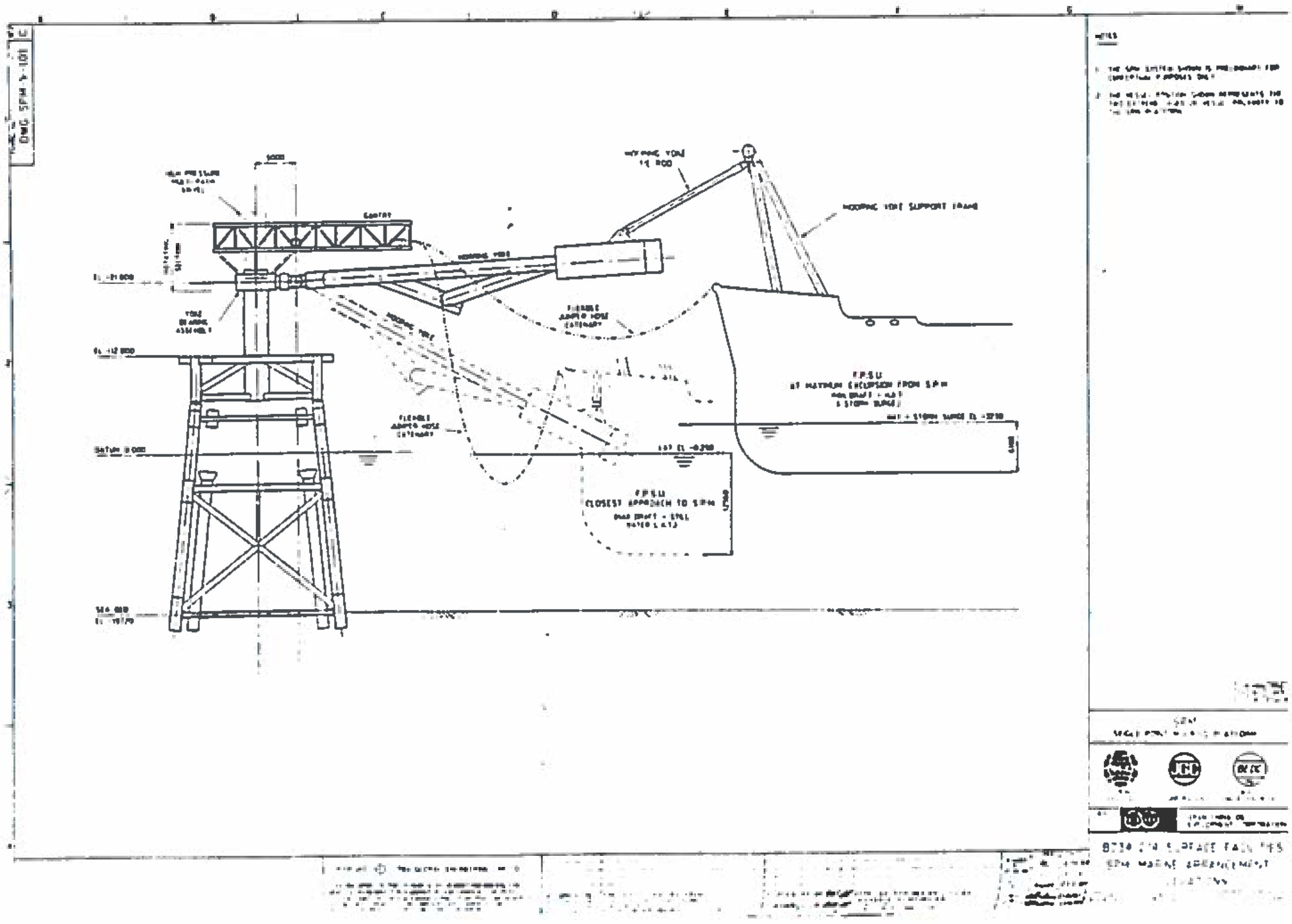
DWG SPM-V-101
F.P.S.U.
CLOSEST APPROACH TO S.P.M.
MOORING YOKE SUPPORT FRAME
SPM
SINGLE POINT MOORING PLATFORM

Fig. 10

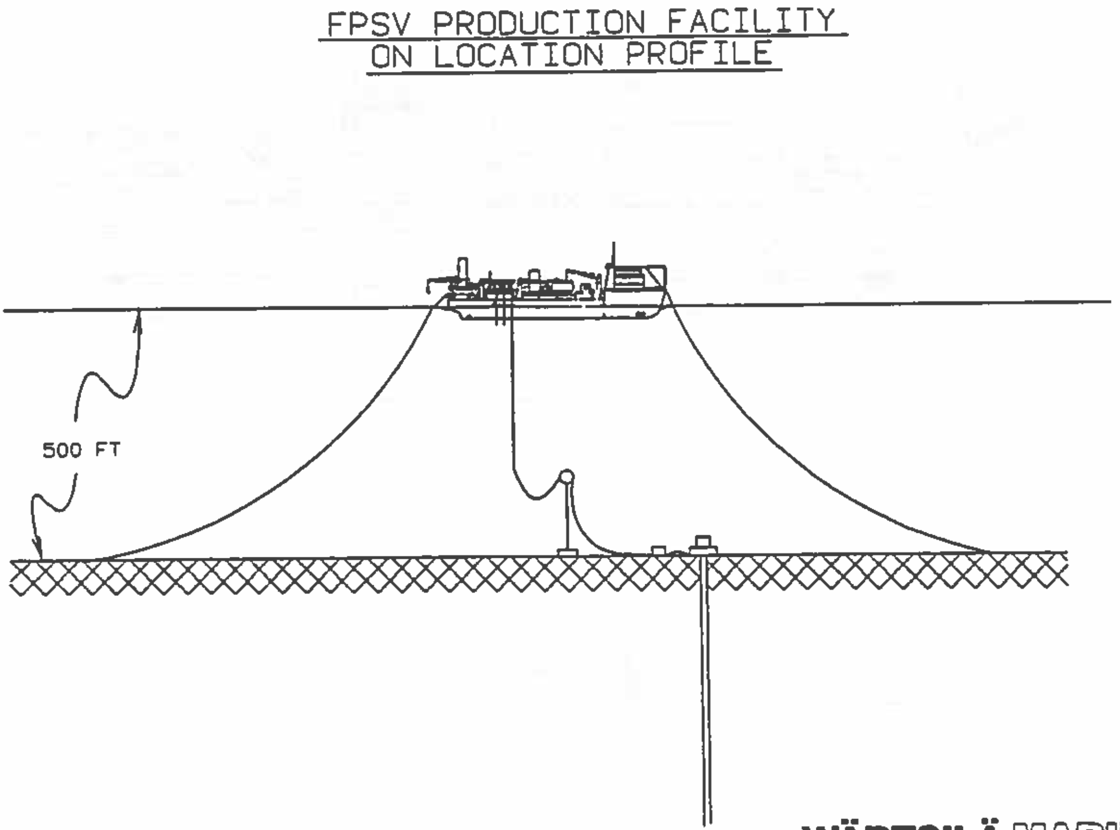

Fig. 11

WÄRTSILÄ MARINE

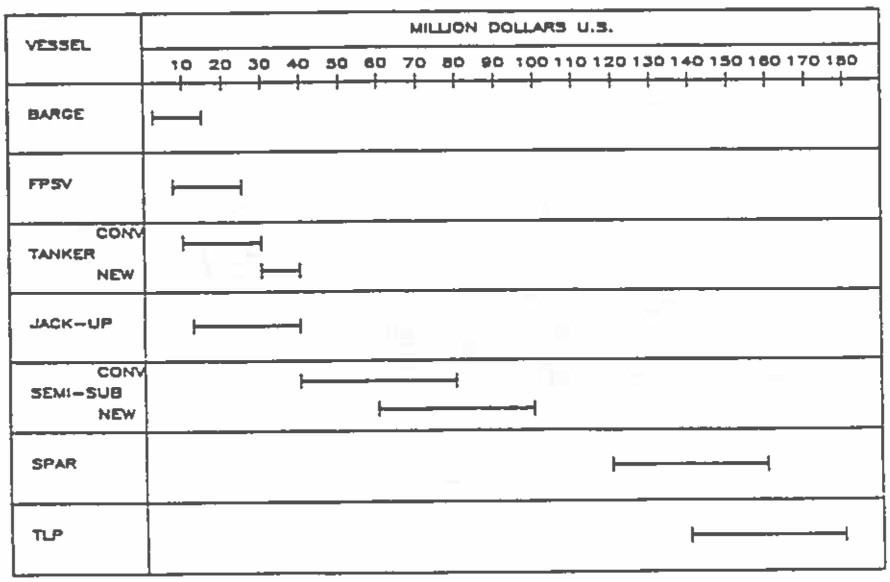

Fig.12 Typical Cost Range of Production Vessel

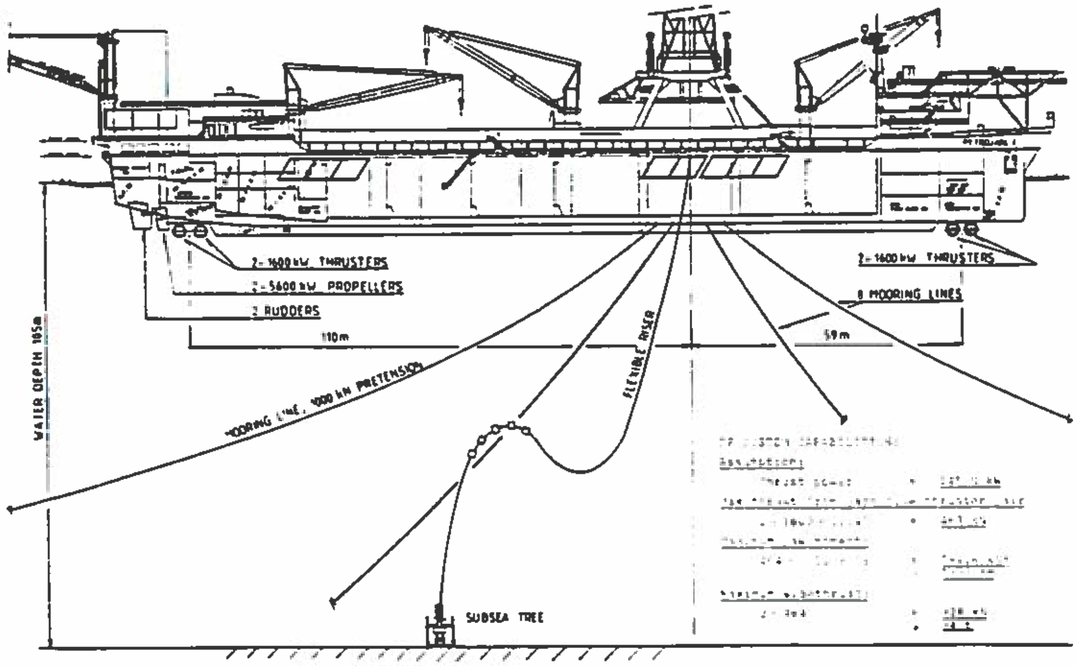

PETROJARL RISER AND MOORING SPREAD

Fig. 13

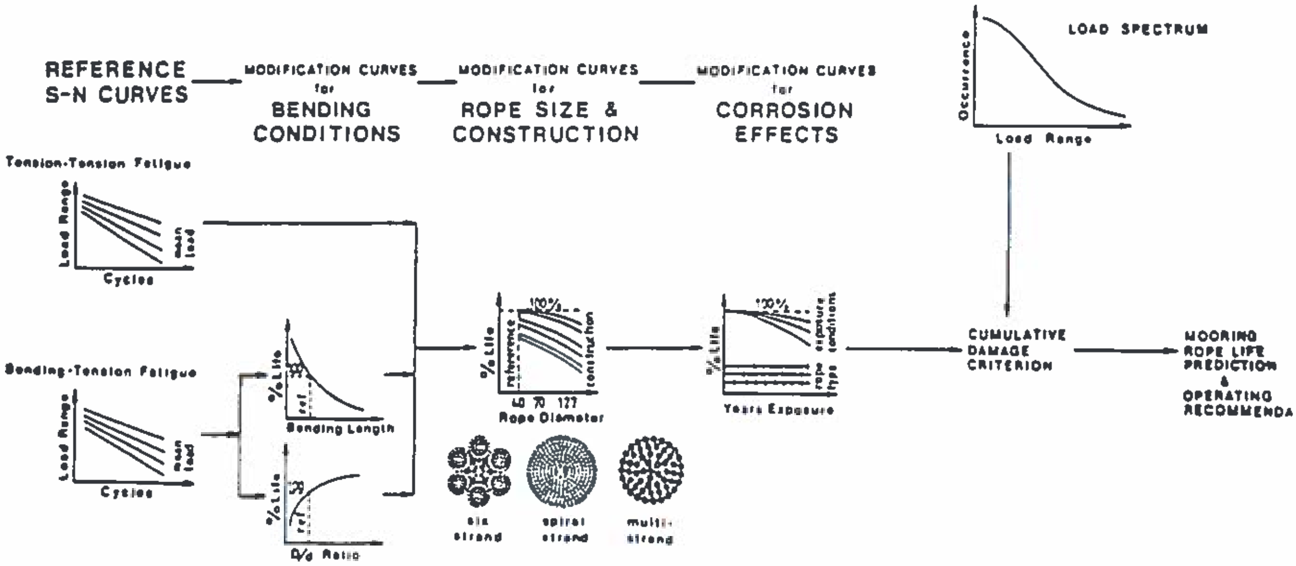

Fig. 14

Schematic representation of the endurance prediction method proposed for the joint industry study on the fatigue life of mooring ropes for offshore structures.
From Potts and Chaplin (1985).

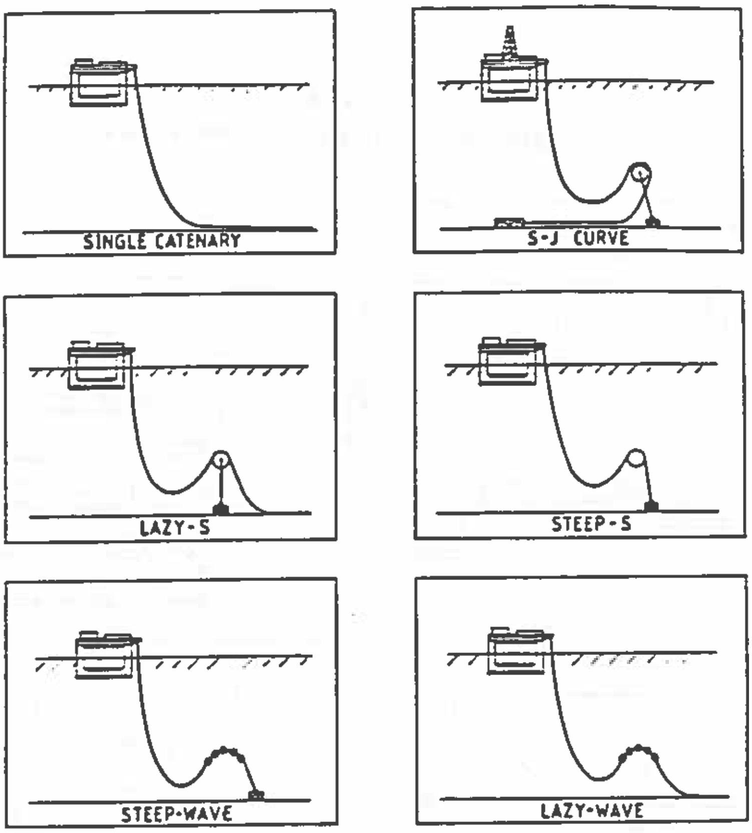

Fig. 15 FLEXIBLE DYNAMIC RISER SYSTEMS

TYPICAL CONFIGURATIONS

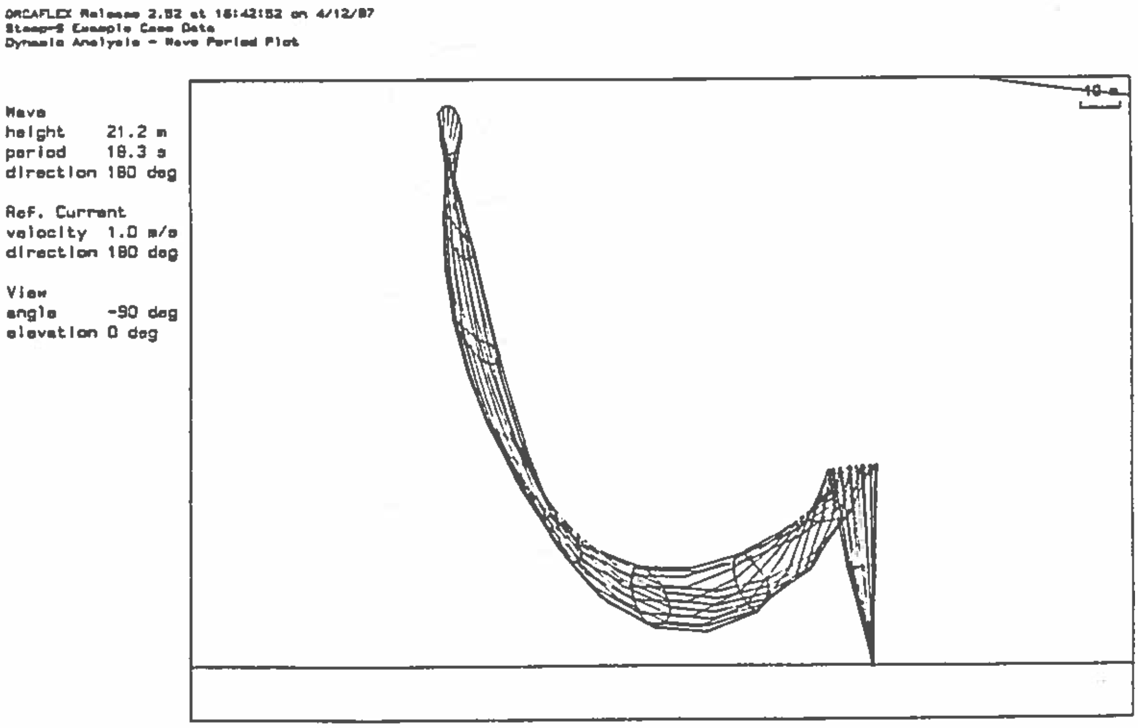

Fig. 16

BALMORAL

OFFSHORE DISTRIBUTED MANAGEMENT SYSTEM

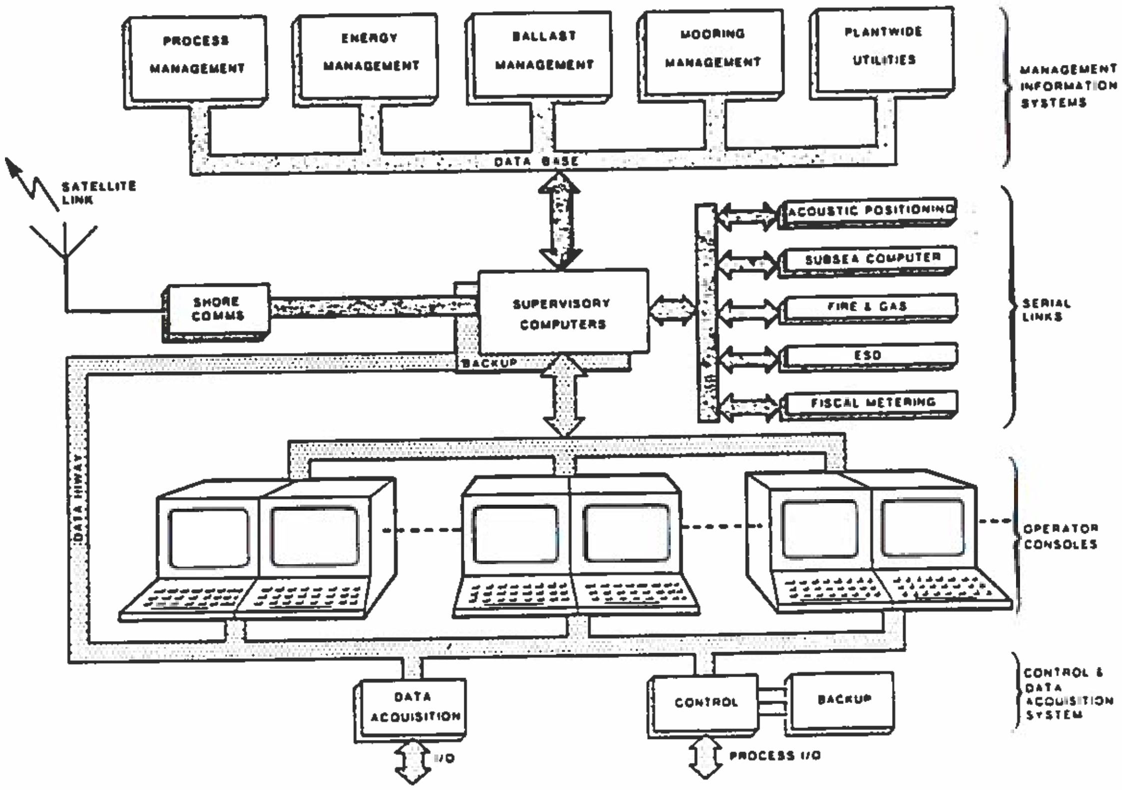

Fig. 17

NEW ORGANIZATION DEVELOPED

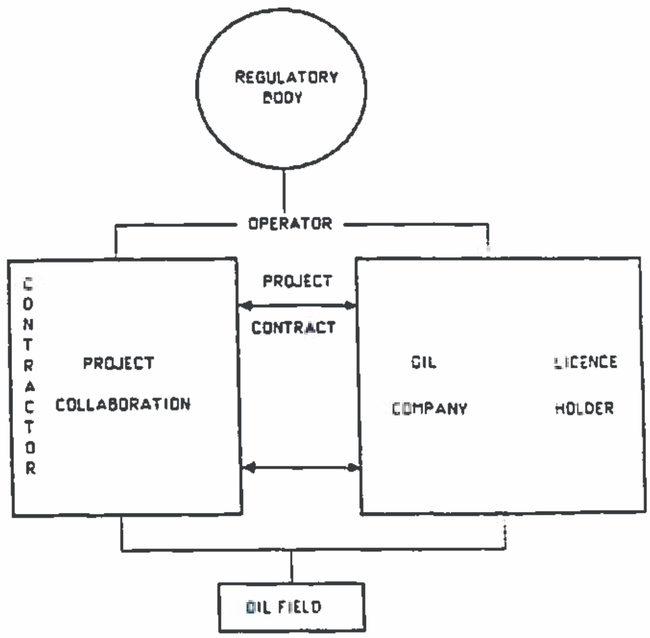

Fig. 18 - CONTRACTORS COLLABORATE IN ONE GROUP
- PROJECT CONTRACT SIMPLIFIES RELATIONSHIP TO OIL COMPANY
- REGULATORY BODY WORKS DIRECTLY WITH CONTRACTOR

JACK-UP USED FOR DRILLING AND PRODUCTION

by

Stig E. Sand

March 1989

1. INTRODUCTION

The jack-up is very well known as a drilling rig. In fact 60% of the world's exploration drilling is carried out by jack-ups. In total 440 units are on the market, and that is double the number of semisubmersibles plus drillships.

The jack-up has some very favourable combined advantages. First of all the mobility, i.e. the rather easy installation and removal, and still the desirable rigidity required for drilling and workover purposes. Furthermore the cantilever type gives flexibility of the horizontal position and of the elevation of the drill floor when operating over fixed platforms.

The first jack-up appeared in 1955. It had 14 legs and was designed for 26 m water depth in the Gulf of Mexico. As late as 1975 only 38 rigs claimed to be able to work in 90 - 107 m water depths, and the extreme wave height was only about 18 m. Thus the first generation of jack-up's has been said to cover the years 1955 to 1975.

The second generation from 1975 to 1985 is capable of operating in up to 122 m of water and the design wave height reaches 20 to 31 m. Variable deck load has been increased and automatic drilling tools are now optional.

Since 1985 the third generation jack-up's has aimed at extreme wave heights of 31 to 34 m, and operational maximum depths of still 122 m. Again variable deck load has increased (now about 3000 t), the BOP maximum pressure is 15000 psi, and automatic drilling tools are compulsory.

The growing of the jack-up rigs has not been without problems. When designing for deeper water the increased leg size requires a larger hull and jacks to withstand the loads. When nearly everything gets larger - the weight goes up. When the weight increases the leg strength has to go up - thus creating a spiral of increasing elements. This has to be managed in combination with requirements of stability, fatigue and e.g. afloat stability requirements with legs fully elevated.

However, the great advantages of the jack-up concept have in recent years made operators seriously consider the potential in either converting or purpose-building jack-up's for production tasks. Fast on-stream schemes and cost effective production of marginal fields by means of jack-up's have been obtained in a.o. the Persian Gulf, Gulf of Mexico, Gulf of Thailand, off Western Australia and off the Ivory Coast. The latter is amongst other represented by the Espoir field operated by Philips, who used the Lauritzen Dan Duke rig for production/testing at 86 m of water, cf. Fig. 1. In Gulf of Thailand, Thai Shell had the Mærsk Drilling rig Maersk Voyager converted for production. The time schedule was as fast as follows: discovery of field spring 1987, declaration of commerciality (Thai Shell) August 1987, field on stream with Maersk Voyager January 1988, cf. Fig.2.

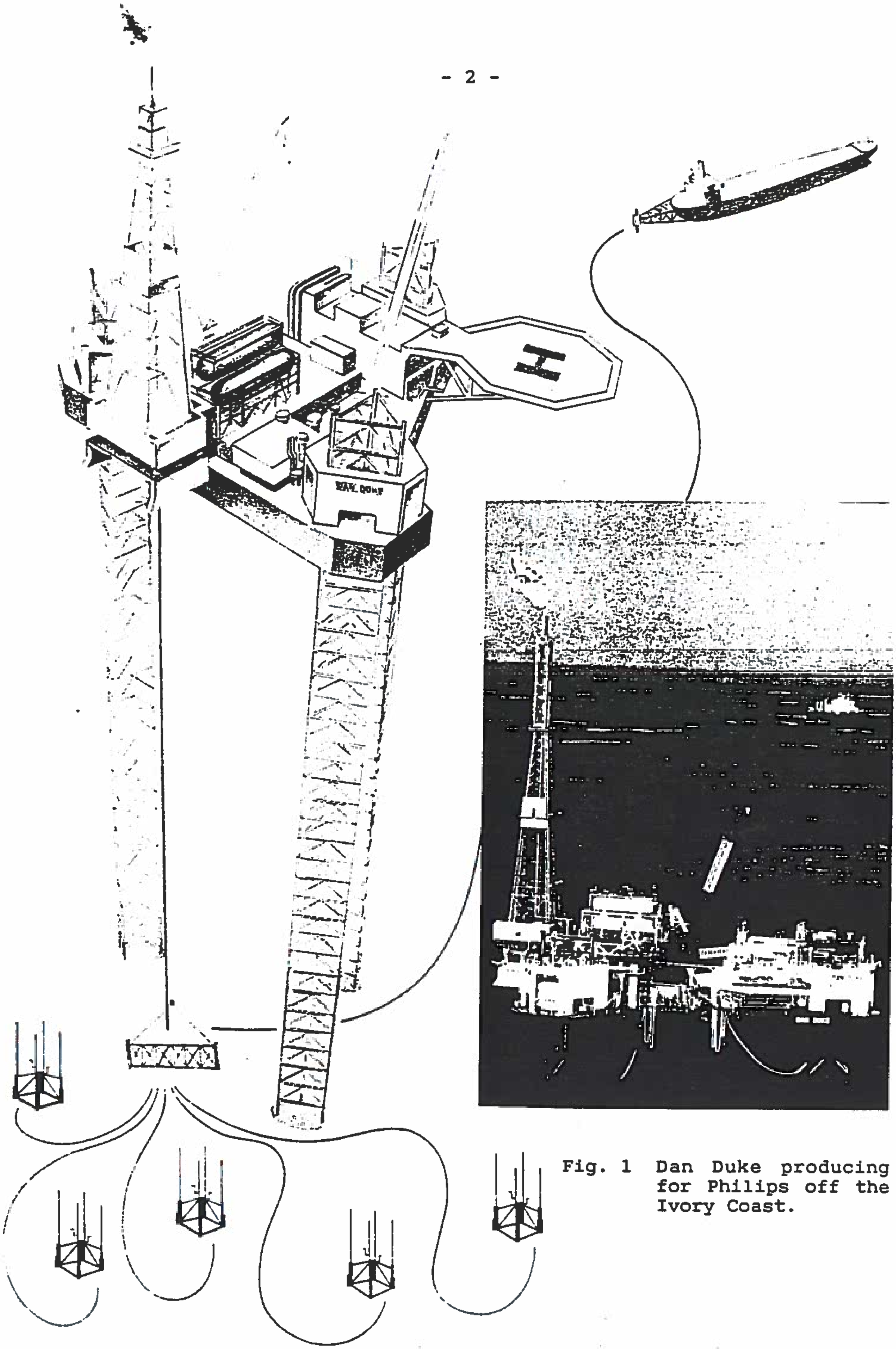

Fig. 1 Dan Duke producing for Philips off the Ivory Coast.

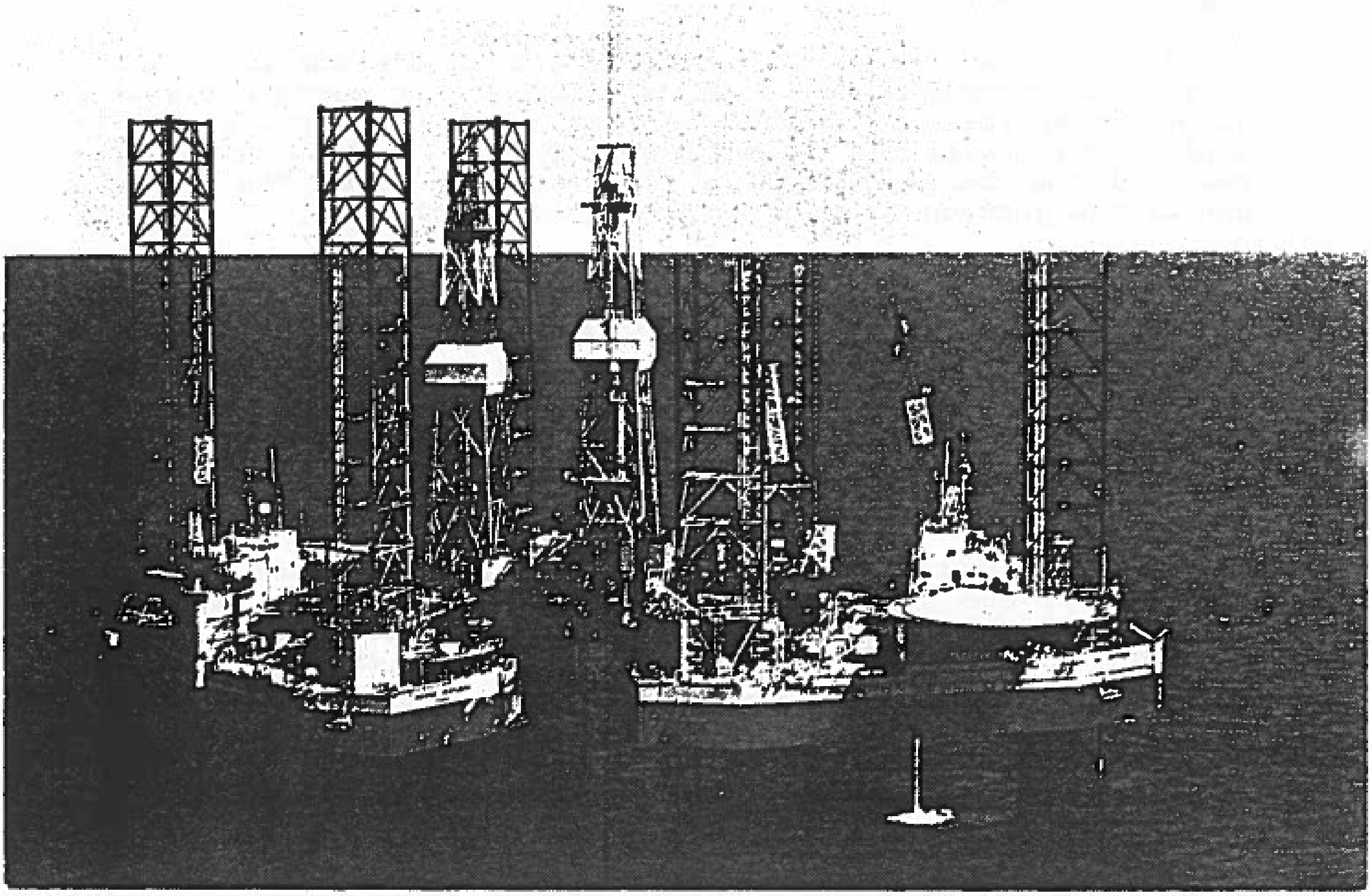

Fig. 2 The Mærsk Voyager equipped with production modules takes over from the drilling rig Mærsk Venturer in the Gulf of Thailand.

2. JACK-UP'S AS PRODUCTION/TESTING UNITS

A possible utilization of jack-up's for production purposes could pertain to Danish marginal fields with a rather short lifetime, i.e. in the order of 3 to 5 years.

In this case an overall advantage could be the mobility. Thus, instead of constructing satellite platforms or perhaps planning subsea completions, different areas of the reservoir may be depleted by moving the rig successively to a location outside the reach of the deviated wells of the former location. The detailed use of the jack-up concept would then be as follows:

- exploration drilling
- appraisal drilling
- production drilling (over template)
- tow to yard for conversion
- tow to field for production
- production (3 - 5 years)
- tow to yard for conversion or replacement/maintenance of production equipment
- new task (drilling or production)

There are of course numerous variations of this scheme. An illustration of one possible sequence with the use of a converted jack-up for production is given in Fig. 3. In this case the converted one is supported by a standard jack-up from the drilling (contract) market. It is important to note the great advantage of being able to install modules at a yard rather than offshore. Very limited lifts are required since modules can be skidded on the deck. Further it reduces the actual offshore hook-up to a minimum.

It is not unrealistic to operate with topside capacities today of 5,000 - 10,000 tons for a modern jack-up (even 16,000 tons for the TPG 500 concept). Compared to a jacket structure the advantage of the jack-up is that less structural steel (module support frames) is necessary as shown in Fig. 4. In other words, for a jacket only about 50% of the topside weight will be equipment and bulk, whereas it will be 73% for the jack-up. This will also have obvious economical consequences.

There is no doubt that a very early production is possible with the jack-up concept. It is easy to install and to remove. It can be contracted and converted or purpose built dependent on the actual market conditions.

EARLY PRODUCTION - MARGINAL FIELDS

FIELD A Standard jack-up (contract) Template drilling	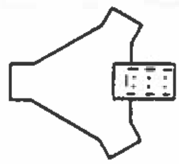
Converted jack-up arrives for production Standard jack-up drills further production wells over template.	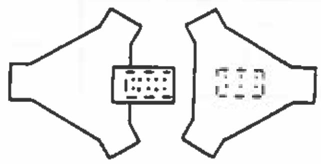
Cantilever mounted on production jack-up for Xmas-tree Skids installed for work-over derrick (wireline/tubing)	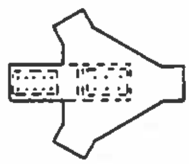
FIELD A-1 Production drilling Subsequent conversion to production unit	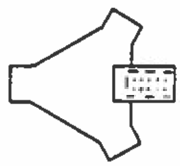

Fig. 3 Early production scheme illustrated by a standard and a converted jack-up.

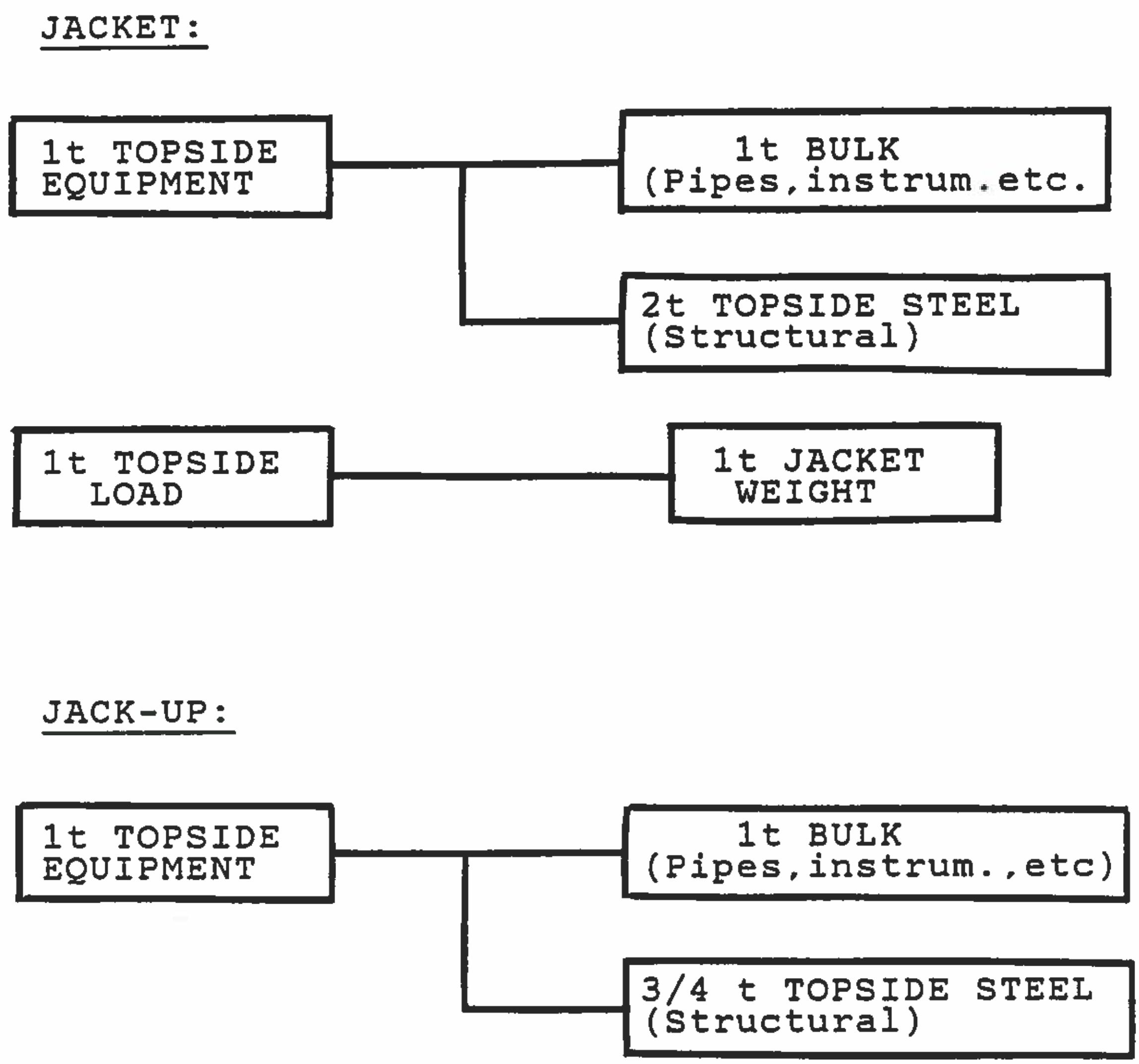

Fig. 4 Comparison of topside capacities for a conventional jacket and a converted jack-up.

3. AREAS OF RESEARCH

Although the jack-up concept seems to possess an economical potential in connection to certain marginal fields it definitely has limitations. These are - for converted units - things like space, number of possible conductors, strength, fatigue, etc.

To fully investigate the economical and technical aspects of the jack-up as production unit in general, the following items are among those which seem to require further research:

- foundation fixity (Noble Denton zero, Lloyds limited)
- scour development/protection
- marine growth
- jacking/locking system
- overall stability and strength
- conductor forces
- dynamic analyses (depth larger than 75 m)
- fatigue analyses
- material requirements
- safety and hazard study

Joint studies should be set up with a.o. the Danish Energy Agency (DEA) especially in the area of safety. This should provide a further technical basis for comparing topside safety philosophy and risks for jacket and jack-up solutions, and in turn support official guidelines and regulations.

The Statoil-group (including Danop) is launching a research project on economic feasibility and safety aspects in one part and a more technical study as a second part of a jack-up investigation to be performed during 1989/1990.

So far the only Danish example of the use of jack-up's (apart from pure drilling purposes) is the water injection project at Skjold, where the Mærsk Explorer has for some years now been used for water injection purposes (on dispensation from the DEA).

SES/lkj
31.03.1989

THE TRIPOD PROJECT

BY

G. BUSETTO, TECNOMARE S.p.A. (Italy)

THE TRIPOD PROJECT

by G. Busetto
Tecnomare S.p.A. (Italy)

1. INTRODUCTION

Since the beginning of the seventies Tecnomare, a Company specialized in research and development activities in the field of marine technologies, dedicated an important part of its resources to the study of viable solutions to deep water production.

The technological benefits resulting from these projects can be combined to obtain various exploitation alternatives, and the suitability of a concept can be ascertained by thoroughly evaluating merits and risks with respect to the environment and the production scheme.

The alternatives that have been developed spread from steel gravity platforms with integral storage, suitable for shallow to average water depths (up to 300 m), to floating production systems, like the tension leg platforms (up to 1000 m w.d.).

Within this branch of activities, the Tripod Project deserves a certain interest and presents innovative aspects.

Chronologically, the project started back in 1984 and completion is planned for the middle of the current year.

Overall objective is the investigation and definition of procedures for construction, assembling, transportation and installation of a tripod configuration of steel fixed platform, suitable for water depths of about 350 m.

This task requires a complete analysis of the basic problems associated with the components to be used and of the operations to be carried out on land, in sheltered water area and at open sea.

The research study is conducted with the financial support of the Economic European Community and of Istituto Mobiliare Italiano, other sponsors being Saipem, Snamprogetti, Micoperi and Tecnomare.

2. DESIGN CRITERIA

The northern sector of the North Sea, i.e. the Norwegian Trench (Troll East Field) has been identified as a possible installation area.

The characteristic environmental conditions are:

- Water depth	350.0 m
- Maximum wave height	29.5 m
- Associated wave period	16.8 s
- Maximum current speed (surface)	2.5 m/s
- Wind velocity (1 minute sustained)	45.0 m/s

A total topside weight of 30,000 tonnes has been assumed, including the deck structure contribution.

3. DEVELOPMENT OF THE PROJECT

According to the project requirements, four successive stages have planned, reflecting for a certain extent the natural sequence of development of a research study. They can be summarized as:

- an investigation of the basic aspects for the design of structures intended for deep water applications;
- a basic study of construction and assembling techniques;
- analyses and procedures for the selected concepts;

- time and cost evaluations for fabrication and installation.

Each of the above stages has been subdivided in tasks, whose qualifying aspects can be detailed as follows:

- development of a computer programme to analyse the behaviour of a multibody system in floating condition;
- investigation of the possible solutions for cylindrical shells subjected to external pressure;
- study of behaviour and characteristics of the materials to be employed in the construction of the platform in order to investigate the possibility of a significant weight reduction;
- study of the structural inspection and monitoring system during operative life to detect any evidence of damage and to check the adequacy of the prevention systems;
- identification of a procedure to evaluate the upending with the contemporary use of the two cranes of an S.S.C.V. (Semi Submersible Crane Vessel);
- study of temporary and permanent connections between structural components;
- analysis of alternative concepts to evaluate a site assembling procedure, i.e. of the behaviour, during installation, of a very long structural component (leg), hinged at the bottom and free to oscillate at the upper end;
- execution of a programme of model tests in order to verify the most critical marine operations in comparison with the calculated results;
- development of a computer programme suitable to evaluate construction time and costs for alternative configurations;
- investigations to verify the field of application and the validity of the selected concepts.

4. SELECTION OF THE CONFIGURATION

The most important task of the second stage of the project was the definition, analysis and evaluation of five possible tripod configurations, designated as tripod A, C, D, F and S, respectively (see Fig. 1).

The evaluation criteria have covered many aspects:

- sub-assembly construction;
- transportation of the components to a deep water site;
- assembling;
- transportation to the installation site;
- installation;
- operational life.

Particular importance has been attributed to the assembling phase, which appears to be the most critical for the feasibility of the concept.

From the evaluation of the various configurations, the following was concluded:

- tripods A and S are the two concepts that match the project requirements best;
- tripod D presents drawbacks related to the fabrication and erection of the main sub-assemblies;
- tripods F and C turn out to be the most complex as far as the marine operations for assembling are concerned.

Consideration of additional advantages of the tripod A with respect to S (i.e. possibility of performing the assembling operation directly at the installation site in the presence of a sufficient weather window and a better behaviour in operative conditions, owing to the symmetry of the configuration) has led to the selection of the tripod A as basic configuration to be further developed.

The tripod A is a symmetric lattice structure, consisting of three legs, a star shaped base frame and a conductor tower (Fig. 2).
The legs have a square section and are placed each other at 120 deg. orientation.
The three arms of the base frame have rectangular section and are coincident with the projection of the legs.
The legs are inclined of about 18 deg. with respect to the vertical axis and interconnected at the top.
The leg top connection creates the nine point support of the deck and a triangular shaped support of the conductor tower.
The conductor tower has triangular section and is fitted with 17 guide frames.
The tripod foundations are installed and piled prior to towing the assembled structure.
The star shaped base frame is temporarily connected to the bottom of the legs by hinges.

The main characteristics of the tripod A are the following:

- Overall height of the structure		378.0 m
- Distance between leg centers at the base level		204.5 m
- Distance between corner columns of the legs		28.0 m
- Distance between columns of the conductor tower		21.0 m
- O. diameter of the leg columns		4.0 m
- O. diameter of the cond. tower columns		2.5 m
- Weight of the structure	(about)	68,000 tonnes
- Weight of cathodic protection, appurtenances, miscellanea and contingency	(about)	13,800 tonnes
- Weight of piles	(about)	14,600 tonnes

Main features of the selected configuration are:

- reliability of transportation of the sub-assemblies
- reliability of the permanent connections
- good structural behaviour in operational conditions.

5. CONSTRUCTION, ASSEMBLING AND INSTALLATION PROCEDURES

5.1 Construction of the Sub-Assemblies

The fabrication and erection of the sub-assemblies do not require any innovative technology, although special attention has to be paid to the fabrication tolerances to ensure that no mis-match occurs at the assembly stage.

The following sub-assemblies will be realized with conventional yard techniques as usually developed for medium size jackets:

- base frame
- foundation bases
- legs (each in two halves)
- conductor tower (in two halves)
- template for the wells.

5.2 Installation of the Foundation Bases and Template (Fig. 3)

After load-out onto a suitable barge, the base will be towed in a sheltered water area, together with the template and the three foundation bases.

Following launching, the base will be temporarily connected to foundation bases and template. With the aid of an S.S.C.V. it will then be lowered down at the installation site. Levelling and piling will be performed and the temporary connections will then be released. The base frame will be raised to the surface and towed back to the deep water assembly site (Langenuen Fjord, near Stord Island).

5.3 Assembling of the Legs and Conductor Tower (Fig. 4)

The halves of the legs and of the conductor tower shall be towed onto a barge to the deep water site, launched and connected each other.

By means of a controlled water ballast sequence the lower end of each leg will be hinged to the corresponding base arm.

Then the structure will be progressively ballasted down until the legs become vertical. In the meantime, the conductor tower will be launched, uprighted and brought alongside the S.S.C.V.

Whilst being controlled by the hoisting wire and tugger liner from the S.S.C.V., the tower will be progressively lowered and placed in its final position onto the base. Pinning and grouting will render the connection permanent.

The folding operation of the legs towards the tower will be carried out by acting skid mounted winches, while tugs provide some restraint.

A temporary mechanical system will block the legs one each other and against the conductor tower.

The permanent connection between legs and conductor tower will be realized by welding the splices of the leg tops and additional beams to match the geometry of the space frame.

Final connection between legs and base will consist of pinning and grouting the bottom of the legs to the base frame by means of pins lodged inside the legs.

The completed structure will eventually be refloated to the towing draught and towed to the installation site.

Then it will be lowered on the pre-installed bases and template, ready to receive deck and topsides.

6. ALTERNATIVE CONCEPTS

With the purpose of minimizing the overall time for completion of the programme and making the tripod economically more competitive, two alternative concepts have been investigated, i.e.

- The elimination of the conductor tower
- The assembling of the platform directly on the installation site.

6.1 Elimination of the Conductor Tower

The first objective can be pursued either by tensioning each conductor, let without intermediate support or by locating the conductors inside one leg.

In the latter case, at the lower end the conductors shall be bent to make a vertical connection with the template while at the upper end they shall be let inclined.

The elimination of the conductor tower involves a weight saving of about 5,500 tonnes, while both solutions will allow the early production scheme (use of sub sea drilling template and tripod installation onto predrilled wells).

6.2 Assembly at the Installation Site (Fig. 5)

The use of three independent foundation bases fitted with spherical hinges is featuring the concept.

The bases shall be lowered by an S.S.C.V. while they are kept connected by a light positioning structure.

Each leg will be towed to the location, upended with the use of ballast and lowered with the aid of an S.S.C.V.

Then its lower end will engage the spherical hinge section on the base and deballasting of the leg will be performed.

After folding of the legs, a capping piece will be fitted, thus realizing the permanent joint.

The use of this configuration allows a weight saving in the range of 8,000 tonnes.

7. MODEL TESTS

As anticipated, a comprehensive model testing programme has been planned with the attention focused on selected stages of the assembling sequence, in order to verify the feasibility of the marine operations, to collect experimental data on the dynamic behaviour exhibited by the structure during assembling, and to provide experimental support to the design procedures for the prediction of motions and loads of multibody systems.

The tests are at present under execution at the Danish Offshore Laboratories and will be completed in a three-week period.

They will cover:

- launching operation of the base frame
- assembling of the legs to the floating base
- upending of the legs
- conductor tower installation
- leg folding.

A separate set of test runs will be utilized to verify the feasibility of the alternative regarding assembly at the installation site.

8. CONCLUSIONS

As it has been seen above, the selection of a basic configuration called tripod A required a widespread investigation of various concepts and problems of multidisciplinar nature.

At present, the solution to be pursued is a platform that includes both the innovating concepts, i.e. the elimination of the conductor tower and the assembly on site.

Besides the considerable weight saving (about 13,500 tonnes), this choice will allow a simpler assembly and installation procedure in addition to a significant reduction of the completion time, further to the possibility to plan an early production scheme.

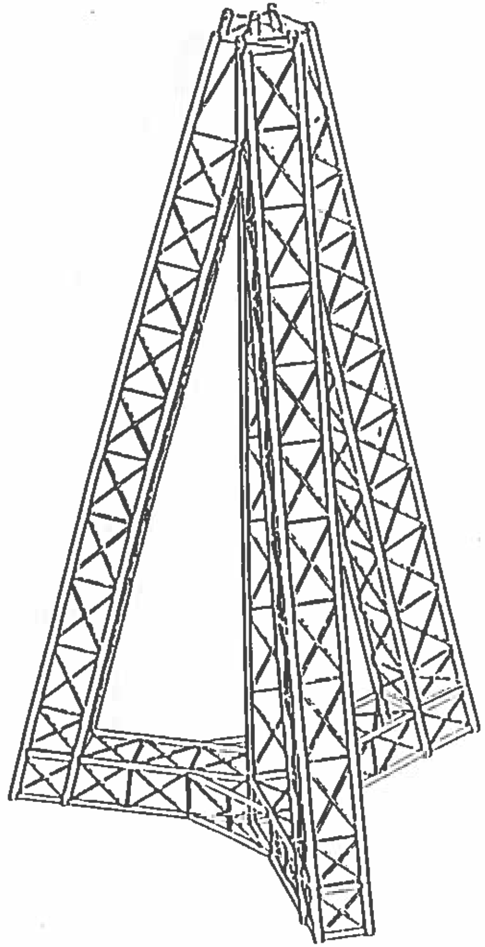

1.1 - Tripod A

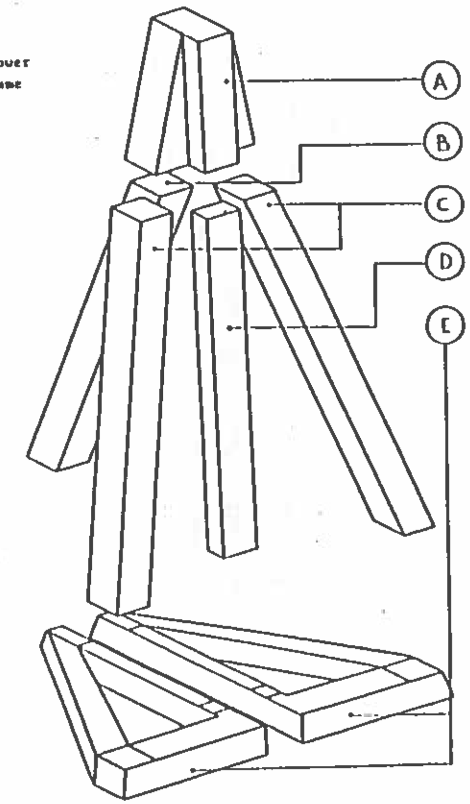

1.2 - Tripod C

FIG. 1 - Tripod concepts analysed

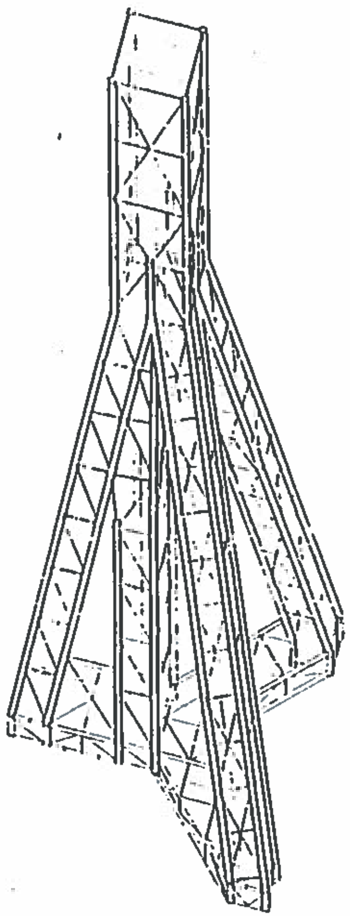

1.3 - Tripod D

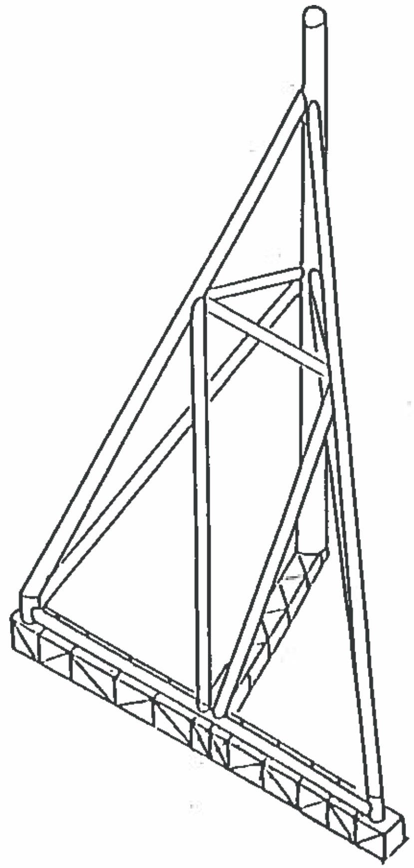

1.4 - Tripod F

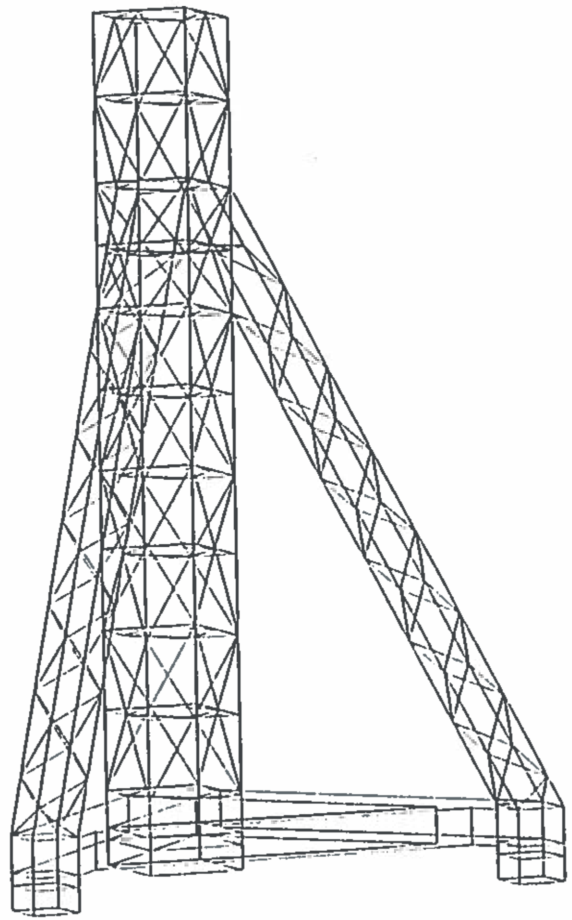

1.5 - Tripod S

FIG. 1 (continued) - Tripod concepts analysed

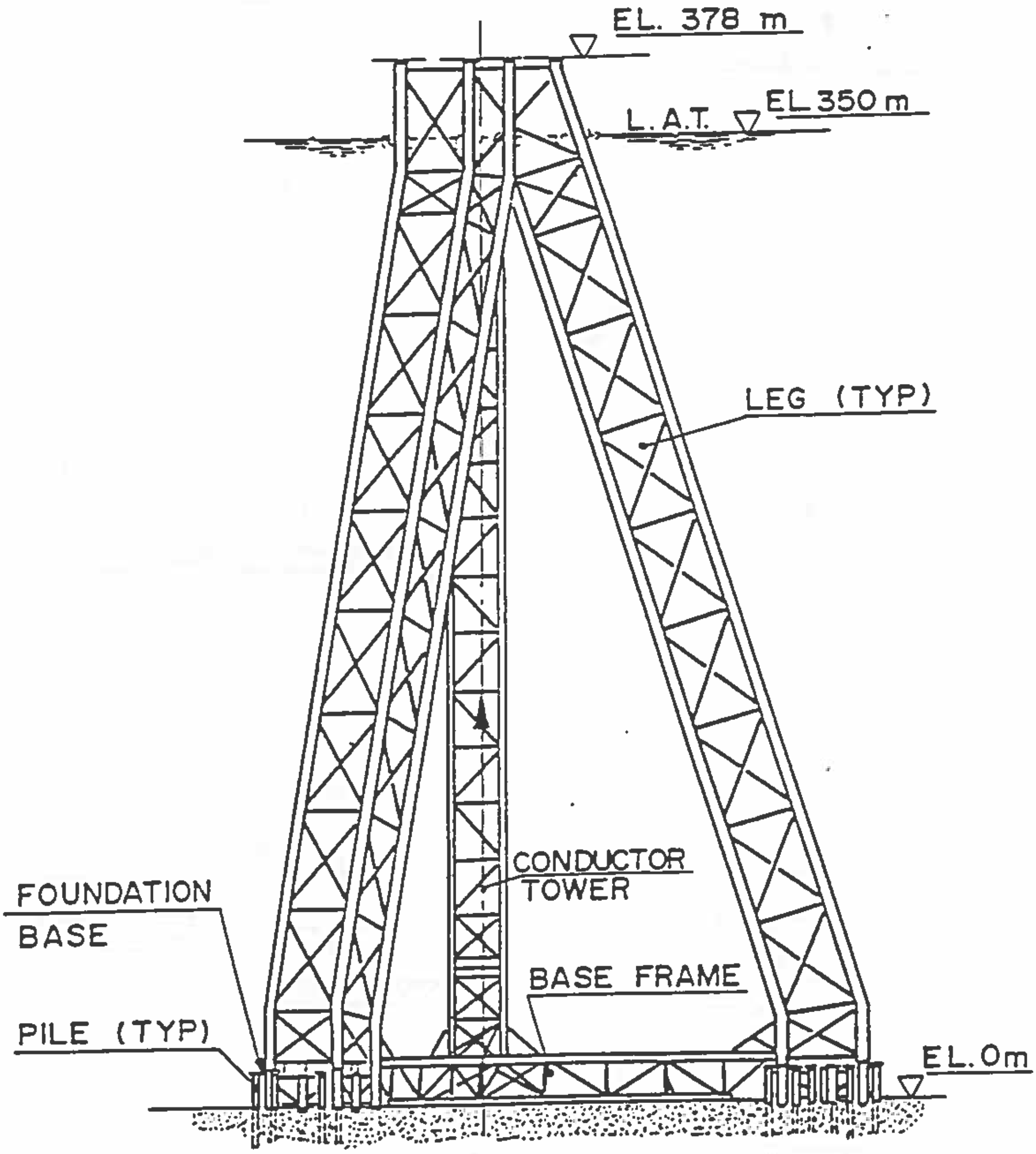

FIG. 2 - Tripod A assembly

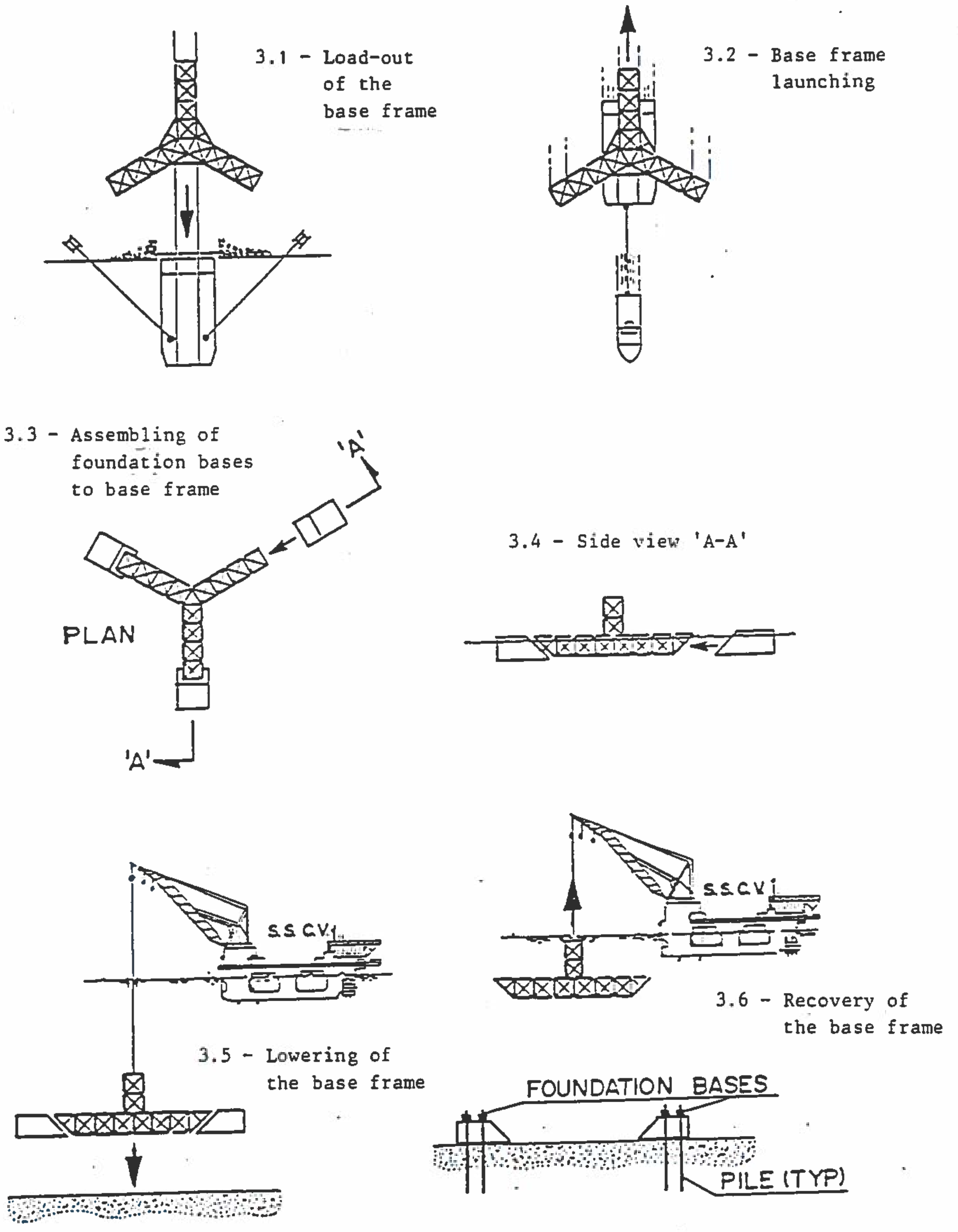

FIG. 3 - Installation of the Foundation bases and Template

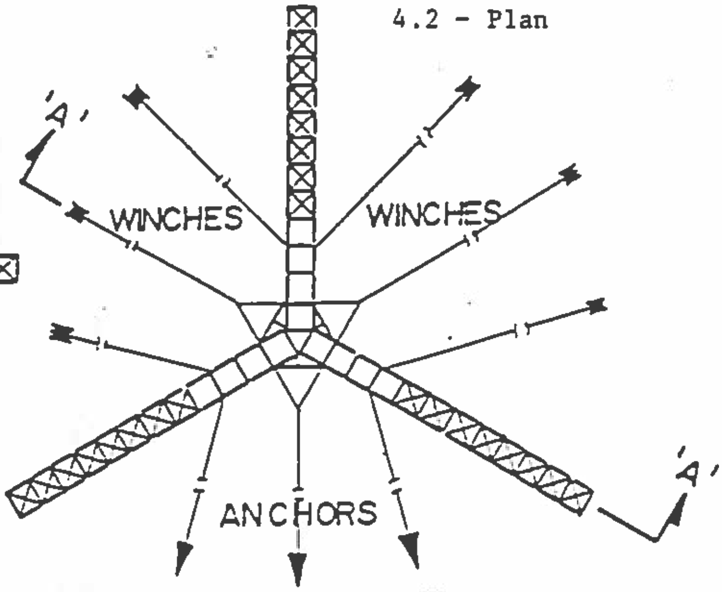

4.2 - Plan

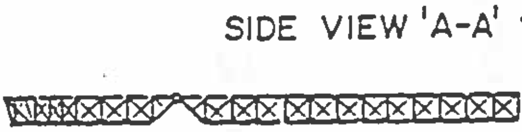

4.1 - Leg connection
to base frame

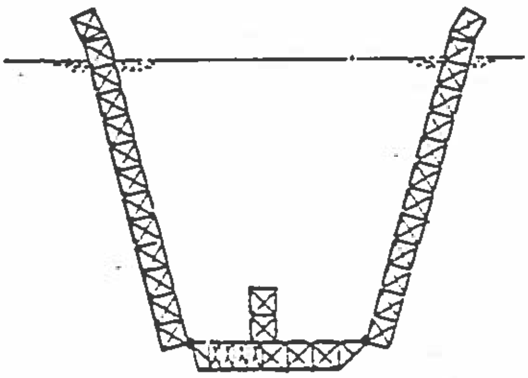

4.3 - Legs up-righting by
base frame ballasting

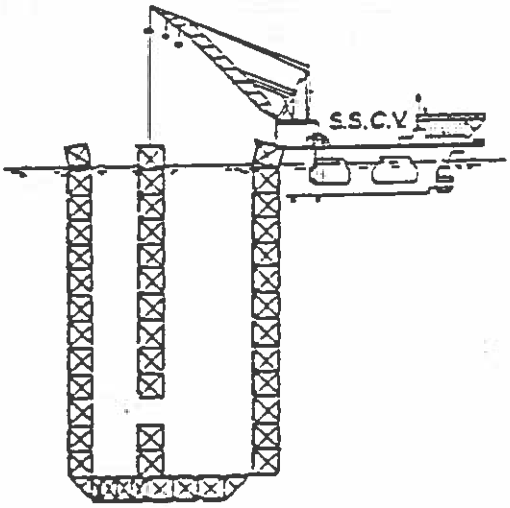

4.4 - Conductor tower
installation

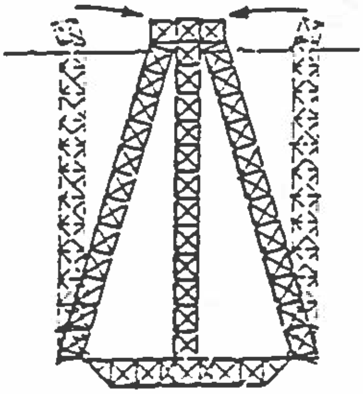

4.5 - Top connection among
legs and conductor tower

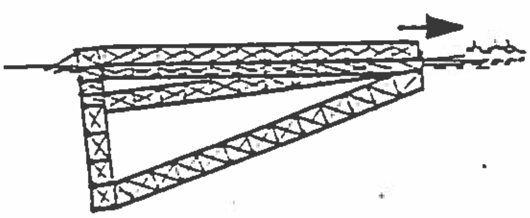

4.6 - Towing of the assembled
tripod to the installation site

FIG. 4 - Assembling of the legs and Conductor Tower

5.1 - Legs hinged to
base frame

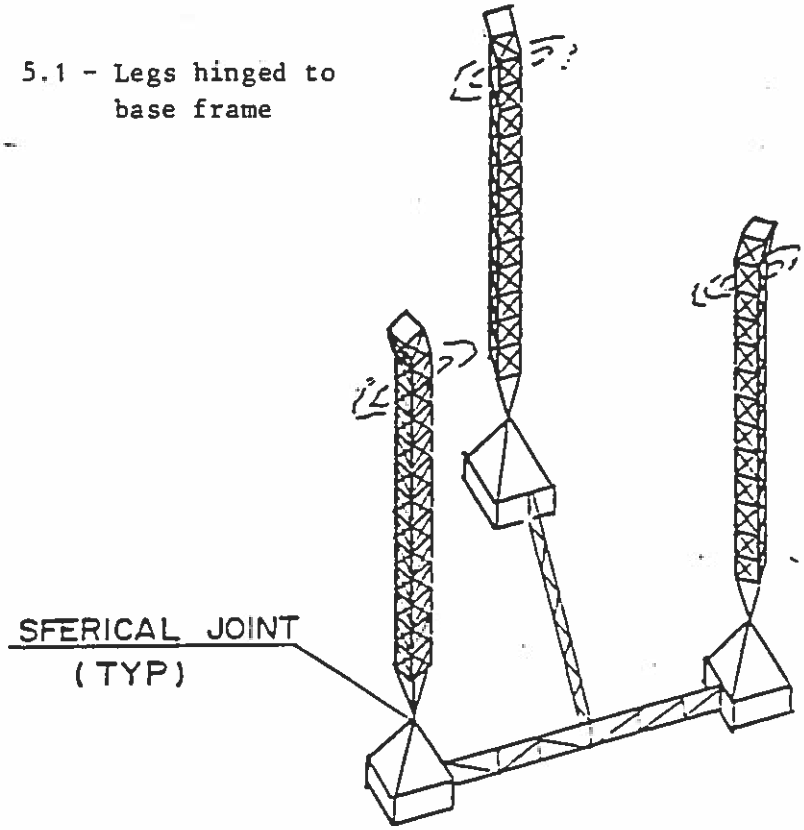

5.2 - Top connection
of the leg with
a capping structure

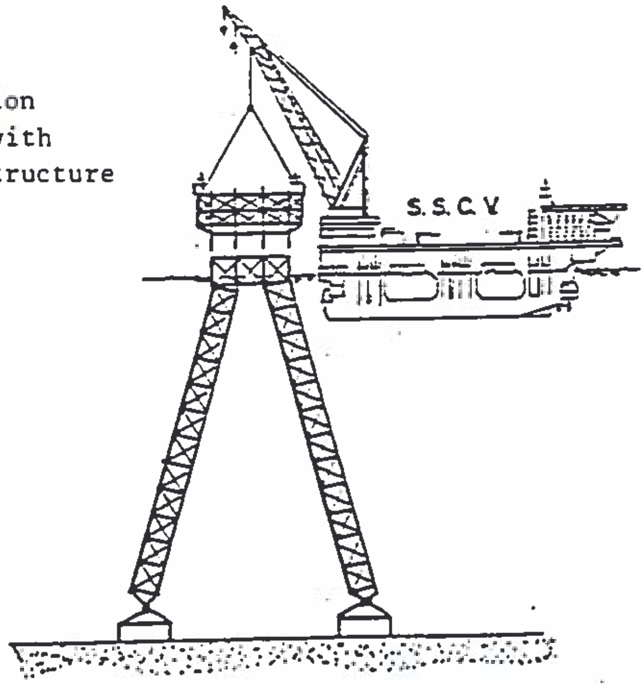

FIG. 5 - Site assembly alternative

THE TECHNICAL AND ECONOMIC FEASIBILITY OF PLATFORM SYSTEMS

IN

ICEBERG INFESTED AREAS

BY

KAI B. OLSEN AND JOHN WAEGTER, RAMBØLL & HANNEMANN

To be presented at the 10th International Conference on Port and Ocean Engineering under Arctic Conditions, Luleå, Sweden June 12-16, 1989

THE TECHNICAL AND ECONOMIC FEASIBILITY OF PLATFORM SYSTEMS IN ICEBERG INFESTED AREAS

Kai B. Olsen	Rambøll & Hannemann
John Wægter	Consulting Engineers and Planners A/S, Denmark

ABSTRACT

The design premises for the conceptual development of platform systems along the west coast of Greenland has been described. Three different concepts: Floating Production Systems, Rock Islands and Detachable Platforms together with their offloading systems have been identified as technically feasible. For intermediate water depths, the detachable platform seems most beneficial and a preliminary economic evaluation demonstrates a promising economy for oil prices as low as 20 US $ a barrel.

INTRODUCTION

Being Danes, with a close relationship to Greenland, it is natural to consider the problems of oil production in Greenland and other similar arctic areas. A particular challenge is to develop cost effective production systems in areas which cannot be exploited with conventional platforms. The area under consideration in this study has been the west coast of Greenland, characterized by having generally open water, but with a flow of very large icebergs. The icebergs are so large that conventional platforms cannot sustain an impact and the iceberg load is therefore the dominant environmental load.

The particular area has been chosen because it is feasible with present technology to explore the area, e.g. by drilling in the summer time. Areas where the depths and ice conditions make exploration impossible with present technology, e.g. along the east coast of Greenland, will not represent realistic goals in the immediate future.

EVALUATION OF DESIGN PREMISES

General

Design assumptions have been established for two sites: Holsteinsborg, 120 km west of the town of Holsteinsborg, (Sisimiut), and Sukkertoppen, 70 km west of the town of Sukkertoppen (Maniitsoq), Fig. 1. The water depth of the former site is 200 m while it is 81 m for the latter. Both areas are characterized by having generally open water, but with icebergs. Only occasionally, the packice from the Disko Bay will drift south to cover the sites.

Waves, Wind & Current

The wave climate is milder than in the North Sea with 50 year wave heights of 15.9 m for Holsteinsborg and 16.2 m for Sukkertoppen.

As regards operational conditions, the significant wave height H_s is less than 2 m 70% of the time at Holsteinsborg and 60% of the time at Sukkertoppen.

Wind and current velocities do not differ much from standard North Sea conditions and will not be dealt with further.

Soils

A typical soil profile on the West Greenland continental shelf consisting of moraine and tertiary sediments with properties according to Tab. 1 has been assumed.

Depth below Sea Floor (m)	Type	[illegible] (kN/m^3)	c_u (kN/m^2)	Φ_{tr} (deg)
0-2	Mud	4	0	0
2-22	Moraine	8	0	31
22-	Clay	9	90	0

Tab. 1 Characteristic soil parameters

Ice Cover

The ice off the west coast of Greenland consists of first year ice. Normally, it has reached its maximum extent at the end of March, where the ice covers nearly all the Davis Strait and the Baffin Bay. In late summer, both areas are free of ice. The following values for the extreme ice condition have been assumed:

Holsteinsborg	:	1.0 m first year ice
Sukkertoppen	:	0.5 m first year ice
Chrushing strength	:	3.8 MPa

Icebergs

Icebergs are produced from glaciers along the coast of Greenland. The large icebergs are produced along the entire length of the east coast and at some locations along the west coast such as the Disko Bay and the Umanak Bay, Fig. 2.

The drift of the icebergs is influenced by winds and in particular by currents. Therefore, icebergs produced at the east coast drift southwards along the coast, around Kap Farvel and northwards along the west coast of Greenland. Icebergs produced in the Disko Bay at the west coast will drift to the southwest or follow an anti clockwise current circulation northwards to the Baffin Bay and eventually drift southwards along the Canadian east coast.

Design Philosophy

Based on information about iceberg density, mass, draft and drift velocities, Refs. 1 and 2, a statistical model for the kinetic energy in the drifting icebergs has been developed. The probability of a collision between the platform and an iceberg has been determined and especially the probability of a collision with icebergs approaching with a kinetic energy which may be critical for the platform. The platform can only sustain iceberg collisions with kinetic energies below a certain level, for higher energies it is disconnected and removed when an iceberg is within a critical distance, Refs. 3 and 4.

An assumption for these calculations has been that the data for icebergs collected during the summer period are valid for the winter period too. For a conceptual study, this is considered acceptable. However, in case of an actual project, more comprehensive data will have to be collected.

CONCEPT EVALUATION

The present study has been limited to 3 different types of structures:

- Floating Production Systems;
- Rock Islands;
- Detachable Platforms.

Floating Production Systems

The choice of floating production systems seems obvious in deep waters not confined in ice all year round. The systems are well proven and can be reinforced to sustain the first year ice. However, when dealing with icebergs, special problems arise. It will not be feasible to design the structure to withstand large iceberg loads, thus the structure has to be emergency removed during the passing of the largest icebergs.

The main problem areas are the conductors and the anchor lines.

The concept presented in this project, Fig. 3 is based on a continuous production of oil during the passing of icebergs, by means of flexible risers. The deeper the water, the more feasible the floating production system, because the radius of manoeuvrability increases.

Rock Islands

In shallow waters a rock island is an attractive alternative, capable of withstanding the largest icebergs. Rock islands can be built relatively cheap, but the problem is the long construction time for increasing water depths. Our conclusion is, surprisingly, that for water depths up to nearly 100 m, the concept, Fig. 4, may be competitive, depending on the distance to rock materials.

Detachable Platforms

Between the two extremes, floating production systems and rock islands, platforms which are designed to be regularly removed during passing of the iceberg seem to be even more beneficial.

The system consists of a detachable upper part and a permanent subsea base, Fig. 5. The upper part, the hull, is a steel structure holding all production and service facilities. Locally, the platform has been designed to resist small icebergs, in order to keep the detachments at a low level.

It has been a design premise to maintain the oil production as long as possible, hence a quick release system for the hull has been developed. The system is based on a simple suction principle, enabling the detachment to take place as a last minute operation. The subsea base is built in concrete and serves as foundation for the hull. Further, it comprises the well system with the subsea Christmas trees. The base is surrounded by a subsea breakwater, which protects against impact of icebergs.

OIL TRANSPORTATION

Loading

The loading system is the same for all three types of developments considered. The crude oil is pumped from a storage tank via a flexible hose to the tanker. The hose can either be floated from the platform to the tanker when there is no surface ice, or it can be suspended above the water supported by a cradle extended from one of the platform service cranes.

Tanker Routing

The distance to the nearest available refinery from the platform location is a major consideration when equating the ultimate tanker size and turn around time.

It is proposed that two tankers work a rotation to and from the platform location delivering the crude to Saint Johns, New Brunswick or Glasgow, U.K.

ECONOMIC EVALUATION

General

A preliminary economic evaluation has so far only been made for the detachable platform concept. Based on assumptions concerning the future oil production, cost estimates and future oil prices, inflation, exchange rates and taxes, the net present value is calculated.

Cost Estimates

The following costs were used in the evaluation of the economic feasibility:

COST	Base mio. DKK	Hull & Deck mio. DKK	Total mio. DKK
Concrete	3,440	-	3,440
Steel	315	3,500	3,815
Ballast	69	73	142
Mechanical equip.	20	-	20
Process equip.		10,000	10,000
Total	3,844	13,573	17,417

Tab. 2 Construction costs of base and platform

Base Protection 360 mio. DKK

Transportation and Installation Tugs 40 mio. DKK

Year 1:	4,715
Year 2:	4,354
Year 3:	4,354
Year 4:	4,394

Tab. 3 Investment cost per year mio. DKK

Abandonment costs are assumed to be negligible.

Mio. DKK	0-4 years	Rest of production period
Manpower	650	260
Equipment cost	200	200
1 ice breaker	20	20
4 tugs/supply vessels	40	40
Total	910	520

Tab. 4 Operation costs

Yearly Transportation Costs

Rental of four 50,000 tons tankers at 10,000 dollars/day: 102 mio. DKK.

Downtime

Average yearly downtime due to false alarms, disconnections, maintenance and system failures is estimated at 32 days/year.

Production

The production profile, Tab. 5, is based on 26 production wells each having a peak production of 6500 bbls per day after allowing for downtime. The 26 wells are assumed drilled and put into production during the first 3½ years.

Year	One well mio. bbls/year	Total production mio. bbls/year
1	2,4	10,7
2	2,4	26,1
3	2,4	45,1
4	2,4	60,5
5	2,4	61,7
6	2,4	61,7
7	2,4	61,7
8	2,4	61,3
9	2,0	59,6
10	1,7	55,9
11	1,4	49,8
12	1,2	42,2
13	0,9	35,5
14	0,8	29,2
15	0,7	23,8
16	0,5	19,5
17	0,5	16,4
18	0,4	13,8
19	0,3	11,8
20	0,3	9,7
Total	29,7	756,0

Tab. 5 Production profile

Economic Assumptions

Oil price: 35$/bbl

US$ exchange rate: 7 DKK/$

Inflation: 3% p.a.

Financing: 100% equity

Real discount rate: 6% p.a.

Calculations are in fixed 1988 prices.

Taxation

For this illustration and evaluation purpose, the present Danish royalty and tax regime is used. The system consists of a 50% corporation tax and a 70% hydrocarbon tax.

Results

The net present value of the field was calculated, and in addition, a sensitivity analysis considering changes in the oil price,-production volume and costs was carried out, Tab. 6.

	BASE CASE	SENSITIVITIES		
		Oil Price 25$/bbl	Production - 25%	Costs + 25%
NPV before tax	55	33	36	50
NPV after tax	22	15	16	21
IRR after tax	21%	16%	17%	18%
Pay out year	8	9	9	9

Tab. 6 Net present values in billion DKK (fixed 1988 DKK)

The project seems highly profitable with a net present value of 22 billion DKK and an internal real rate of return of 21%, provided the oil price is as high as 35 US $ a barrel.

The sensitivity analysis shows a good robustness with respect to cost overruns, lower oil prices and reduced production. However, it is estimated that the crude price shall have a level of around US $ 20 per barrel before the internal rate of return is acceptable.

ACKNOWLEDGMENT

The authors gratefully acknowledge the permission to publish the results from the group of companies participating in the project. The companies are Rambøll & Hannemann (Project Coordinator), LICengineering, Danyard, ISVA/DTH, Nunaoil all from Denmark, Gøtaverken Arendal AB from Sweden, SINTEF and Bjarne Instanes from Norway. The project work is supervised by an Advisory Committee holding members from BP Exploration Ltd., Statoil, D.O.N.G., the Danish Energy Agency, Grønlands Energiforsyning and GTO.

The project is partly supported by Nordisk Industrifond, Teknologirådet, Denmark, STU and SIND, Sweden, and partly by the participating companies.

The environmental data have kindly been supplied by the Greenland Technical Organization (GTO).

REFERENCES

/1/ Danish Hydraulic Institute: "Environmental Conditions Offshore West Greenland", prepared for Greenland Technical Organization, December 1979.

Vol. 1 Summary
Vol. 2 Wind and Waves
Vol. 3 Currents
Vol. 4 Icebergs

/2/ Danish Hydraulic Institute: "Environmental Studies Offshore East Greenland 1981", prepared for Greenland Technical Organization 1982.

/3/ Wægter J., Madsen A.H., Olsen K.B.: "Design Loads for Detachable Platforms subjected to Iceberg Impact Loads". POLARTECH' 88, Proceedings from the International Conference on Technology for Polar Areas, Trondheim, June 1988.

/4/ Wægter J., Madsen A.H., Olsen K.B.: "Design Procedures for Detachable Platforms located in Iceberg Infested Areas". IAHR, Proceedings of the 9th International Symposium on Ice, August 23-27, 1988, Sapporo.

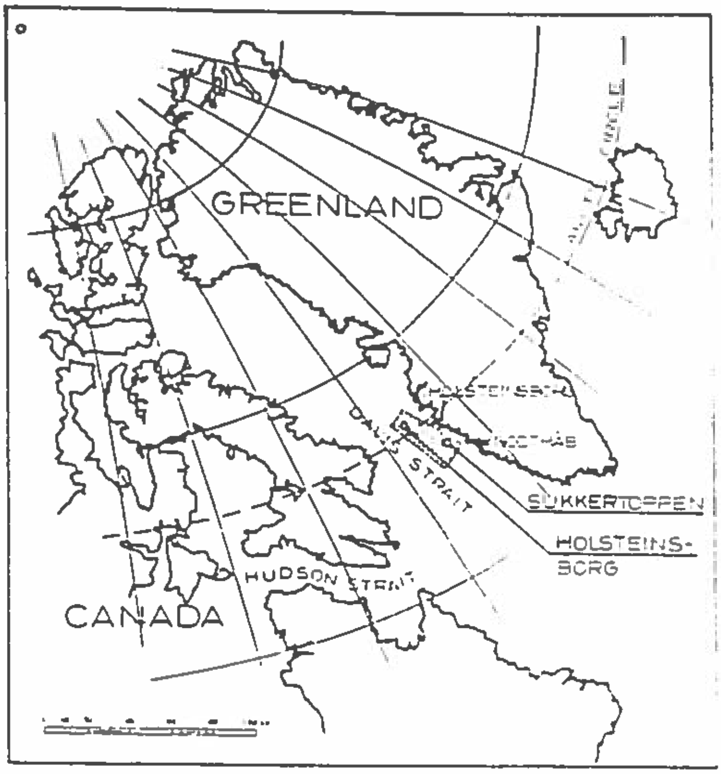

Fig. 1 Study area, Sukkertoppen and Holsteinsborg

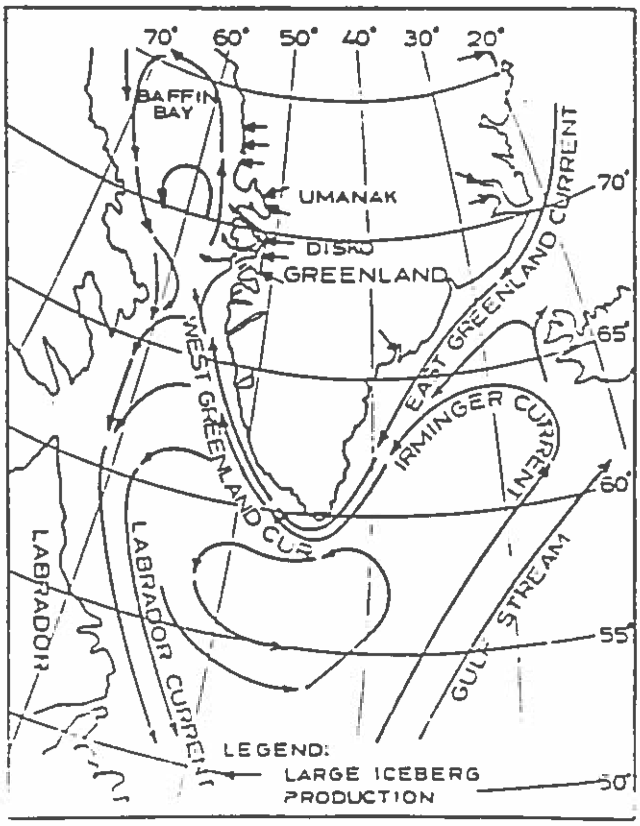

Fig. 2 Iceberg production and current circulation

B400893.art
1989.01.24

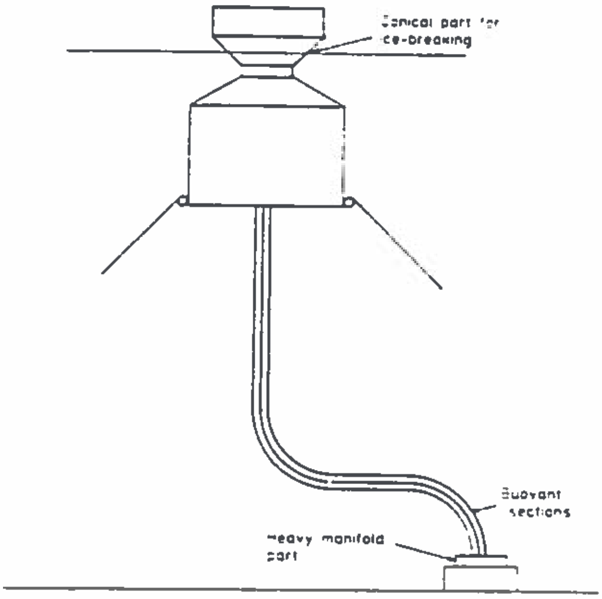

Fig. 3 Floating production system

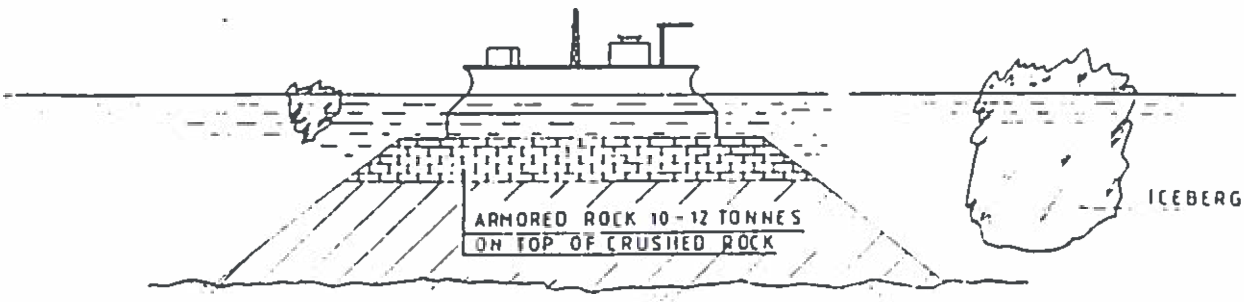

Fig. 4 Rock island

8400893.art
1989.01.24

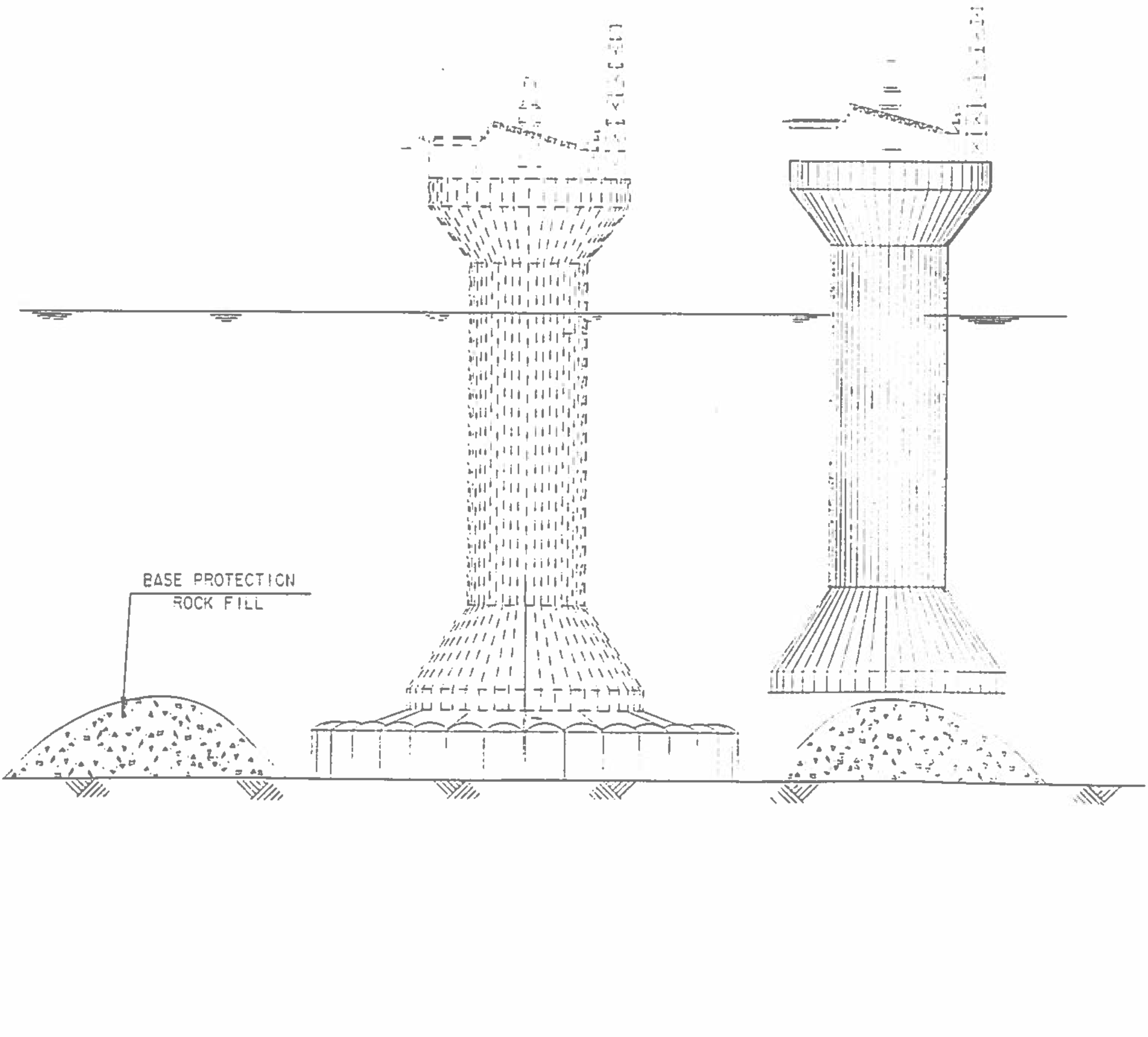

Fig. 6 Detachable platform

6400893.art
1989.01.24